Application of Statistical Mechanics to a model Neuron

William Joseph ELLIS, B. Sc. (Hons)

A thesis submitted in accordance with the
requirements for the Degree of Doctor of Philosphy

E-Mail:wellis@adelphi.physics.adelaide.edu.au
Department of Physics
and Mathematical Physics,
University of Adelaide,
South Australia.

March 1993

To Fleagle, Bingo, Snorky and Drooper

Contents

1 Introduction **1**

1.1 Description and function of neurons 1

1.1.1 Structure of a neuron 1

1.1.2 Ion transport through cell membranes 1

1.2 Electrical Double Layer (EDL) 7

1.2.1 Description of the EDL 7

1.2.2 "Primitive" Models of the EDL 7

1.2.3 "Civilised" Models of the EDL 14

1.3 Hydration of ions 15

1.4 Description of Model 16

1.5 Outline of Thesis 18

2 Equilibrium Statistical Mechanics **25**

2.1 Grand partition function 25

2.2 Distribution functions and the BBGKY hierarchies 27

2.3 Electrostatic potential conditions 32

2.4 Number densities 38

2.4.1 Hard-Sphere system 38

2.4.2 Point system 43

2.5 Indirect correlation functions 44

2.5.1 Hard-Sphere system 44

2.5.2 Point system 50

3 Two Membrane Point Model Neuron **53**

3.1 Mean electrostatic potential 54

3.1.1 One membrane limiting form 57

3.1.2 Two semi-infinite membrane limiting form 59

3.2 Transverse Hankel transform mean electrostatic fluctuation potential 60

3.2.1 Case 1:$-\infty < z_2 \leq -[L+D]$ 66

3.2.2 Asymptotic transverse Hankel transform mean electrostatic fluctuation potential 71

3.2.3 Limiting forms of the transverse Hankel transform mean electrostatic fluctuation potential 82

3.2.4 Case 2:$-D \leq z_2 \leq D$ 85

3.2.5 Asymptotic transverse Hankel transform mean electrostatic fluctuation potential 89

3.2.6 Limiting forms of the transverse Hankel transform mean electrostatic fluctuation potential 92

4 Ionic Hydration Numbers **97**

4.1 Mean electrostatic fluctuation potential 97

4.1.1 Extracellular mean electrostatic fluctuation potential 97

4.1.2 Intracellular mean electrostatic fluctuation potential 103

4.2 Calculation of ionic hydration numbers 107

5 Conclusion **113**

A Molecular Potentials **118**

A.1 One body potential 118

A.2 Two body potential 120

B One Membrane Point Model Neuron **126**

B.1 Mean electrostatic potential 126

B.2 Transverse Hankel transform mean electrostatic fluctuation potential 127

B.2.1 $\zeta_E > 0$ . . . 129
B.2.2 $\zeta_E < 0$ . . . 130
B.2.3 Asymptotic transverse Hankel transform mean electrostatic fluctuation potential . . . 131
B.2.4 Limiting forms of the transverse Hankel transform mean electrostatic fluctuation potential . . . 138

C Two Semi-infinite Membrane Point Model Neuron **144**
C.1 Mean electrostatic potential . . . 144
C.2 Transverse Hankel transform mean electrostatic fluctuation potential . . . 146

D Mathematical Identities **149**
D.1 Bessel functions . . . 149
D.1.1 Uniform asymptotic expansions for large order . . . 149
D.1.2 Small argument expansions . . . 150
D.2 Modified Bessel functions . . . 150
D.2.1 Uniform asymptotic expansions for large order . . . 150
D.2.2 Small argument expansions . . . 151
D.3 Bessel integrals . . . 151
D.4 Exponential integral . . . 151
D.4.1 Definition . . . 151
D.4.2 Asymptotic expansion . . . 152
D.5 Hydration integrals . . . 152

List of Figures

1.1 Schematic representation of the distribution of molecules near a negatively surface charged membrane wall showing the IHP and OHP. 8

1.2 Schematic representation of a two membrane model geometry showing the various regions and the associated inverse Debye lengths, dielectric constants and surface charge densities. 21

1.3 Schematic representation of two semi-infinite membrane model geometry various regions and the associated inverse Debye lengths, dielectric constants and surface charge densities. 23

1.4 Schematic representation of a one membrane model geometry showing the various regions and the associated inverse Debye lengths, dielectric constants and surface charge densities. 24

2.1 Schematic representation of the ion-dipole exclusion planes relative to a membrane wall. 33

2.2 Interfacial wall geometry 34

3.1 Mean electrostatic potential for a two membrane point model system. . . . 56

3.2 Dielectric Function 58

3.3 Exact and approximate mean electrostatic potential in the intracellular fluid between the membranes. 63

3.4 Effective Schroedinger potential of the transverse Hankel transform mean electrostatic fluctuation potential for the two membrane system. 67

3.5 Comparison of the numerical and asymptotic solution for the transverse Hankel transform mean electrostatic fluctuation potential at the source point in the extracellular fluid of a two membrane system vs distance from the membrane wall for k=0.001. 78

3.6 Comparison of the numerical and asymptotic solution for the transverse Hankel transform mean electrostatic fluctuation potential at the source point in the extracellular fluid of a two membrane system vs distance from the membrane wall for k=0.01. 79

3.7 Comparison of the numerical and asymptotic solution for the transverse Hankel transform mean electrostatic fluctuation potential at the source point in the extracellular fluid of a two membrane system vs distance from the membrane wall for k=0.1. 80

3.8 Comparison of the numerical and asymptotic solution for the transverse Hankel transform mean electrostatic fluctuation potential at the source point in the extracellular fluid of a two membrane system vs distance from the membrane wall for k=1. 81

3.9 Comparison of $-\bar{\Delta}_1 \frac{J_{2\nu_E}[2\zeta_E^{\frac{1}{2}}]}{Y_{2\nu_E}[2\zeta_E^{\frac{1}{2}}]}$ and $-\bar{\Delta}_2 \frac{J_{2\nu_E}[2\zeta_E^{\frac{1}{2}}]}{Y_{2\nu_E}[2\zeta_E^{\frac{1}{2}}]}$ in the extracellular fluid vs k. 83

3.10 Comparison of the numerical and asymptotic solution for the transverse Hankel transform mean electrostatic fluctuation potential at the source point in the intracellular fluid of a two membrane system vs distance from the membrane wall for k=0.001. 93

3.11 Comparison of the numerical and asymptotic solution for the transverse Hankel transform mean electrostatic fluctuation potential at the source point in the intracellular fluid of a two membrane system vs distance from the membrane wall for k=0.01. 94

3.12 Comparison of the numerical and asymptotic solution for the transverse Hankel transform mean electrostatic fluctuation potential at the source point in the intracellular fluid of a two membrane system vs distance from the membrane wall for k=0.1. 95

3.13 Comparison of the numerical and asymptotic solution for the transverse Hankel transform mean electrostatic fluctuation potential at the source point in the intracellular fluid of a two membrane system vs distance from the membrane wall for k=1. 96

4.1 Numerical solution for the extracellular mean electrostatic fluctuation potential in the normal direction for a one membrane point model system for various values with the source and field points in the transverse direction to the membrane coinciding i.e. $\rho = 0$. Normal distances are measured from the membrane wall. 101

4.2 Numerical solution for the extracellular mean electrostatic fluctuation potential in the transverse direction for a one membrane point model system for various values with the source and field points in the normal direction to the membrane coinciding i.e. $z_2 = z_1$. Normal distances are measured from the membrane wall. 102

4.3 Numerical solution for the intracellular mean electrostatic fluctuation potential in the normal direction for a one membrane point model system for various values with the source and field points in the transverse direction to the membrane coinciding i.e. $\rho = 0$. Normal distances are measured from the membrane wall. 104

4.4 Numerical solution for the intracellular mean electrostatic fluctuation potential in the transverse direction for a one membrane point model system for various values with the source and field points in the normal direction to the membrane coinciding i.e. $z_2 = z_1$. Normal distances are measured from the membrane wall. 105

4.5 Schematic representation of the region of integration for the calculation of ionic hydration numbers. 109

A.1 Schematic representation of a two membrane model geometry showing the various regions and the associated dielectric constant, inverse Debye length and surface charge density. 119

B.1 Mean electrostatic potential for a one membrane point model system. . . . 128

B.2 Comparison of the numerical and asymptotic solution for the transverse Hankel transform mean electrostatic fluctuation potential at the source point in the extracellular fluid of a one membrane system vs distance from the membrane wall for k=0.001. 134

B.3 Comparison of the numerical and asymptotic solution for the transverse Hankel transform mean electrostatic fluctuation potential at the source point in the extracellular fluid of a one membrane system vs distance from the membrane wall for k=0.01. 135

B.4 Comparison of the numerical and asymptotic solution for the transverse Hankel transform mean electrostatic fluctuation potential at the source point in the extracellular fluid of a one membrane system vs distance from the membrane wall for k=0.1. 136

B.5 Comparison of the numerical and asymptotic solution for the transverse Hankel transform mean electrostatic fluctuation potential at the source point in the extracellular fluid of a one membrane system vs distance from the membrane wall for k=1. 137

B.6 Comparison of the numerical and asymptotic solution for the transverse Hankel transform mean electrostatic fluctuation potential at the source point in the intracellular fluid of a one membrane system vs distance from the membrane wall for k=0.001. 139

B.7 Comparison of the numerical and asymptotic solution for the transverse Hankel transform mean electrostatic fluctuation potential at the source point in the intracellular fluid of a one membrane system vs distance from the membrane wall for k=0.01. 140

B.8 Comparison of the numerical and asymptotic solution for the transverse Hankel transform mean electrostatic fluctuation potential at the source point in the intracellular fluid of a one membrane system vs distance from the membrane wall for k=0.1. 141

B.9 Comparison of the numerical and asymptotic solution for the transverse Hankel transform mean electrostatic fluctuation potential at the source point in the intracellular fluid of a one membrane system vs distance from the membrane wall for k=1. 142

C.1 Mean electrostatic potential for a two semi-infinite membrane point model system. 145

List of Tables

1.1 Concentrations (mM) of the major mobile ionic constituents of the intracellular and extracellular fluid for a neuron 4

1.2 Molecular hard sphere radii and hydration numbers. 17

1.3 Typical values of the parameters for the two membrane model. 22

3.1 Table of κ, ϵ, ζ and ν values in the extracellular and intracellular fluid regions for the two membrane point model. 65

3.2 Table of ζ_E and ζ_I values for various membrane thickness values of the one and two membrane systems. 74

4.1 Table of $\kappa\nu(0)$ values in the extracellular and intracellular fluid regions for the one membrane point model. 106

B.1 Table of κ, ϵ, ζ and ν values in the extracellular and intracellular fluid regions for the one membrane point model. 129

Abstract

Structure and movement of molecules in the Debye layers of a neuron is of fundamental importance to the function of a neuron. This thesis is an investigation into the hydration and distribution of mobile ionic species adjacent to the membrane walls of a model neuron using electrical double layer theory.

The model neuron considered has two separated planar membranes thus creating the intra/extra cellular fluid regions. The membranes are modelled as a continuum with an associated dielectric constant and surface charge density. One and two semi-infinite membrane geometries are also considered as limiting forms. The fluid regions are modelled as a hard sphere ion-dipole system with the dipoles creating the solvent structure through the angular dependent potentials. The limiting form of a point ion-dipole system is also considered for the fluid regions.

The BBGKY hierarchy of partial differential equations for the correlation functions are truncated with Loeb's closure relation to determine expressions for the number densities and pair correlation functions of the ionic species and dipoles. The results obtained for the pair correlation function indicate a shielding both in the normal and transverse directions. The shielding in the transverse direction occurs because the charge on the opposite side of the membrane is able to redistribute itself, screening the potential between molecules. Comparison of the two membrane point model system (at large separation) and the one membrane point system plus the effect of membrane thickness are investigated. Calculation of hydration numbers for the mobile ionic species are also presented.

Acknowledgements

The work for the following thesis was carried out during the years 1986-1993 under the supervision of Emeritus Professor H.S. Green in the Department of Physics and Mathematical Physics. I would like to express my gratitude to Bert Green for his time, advice and guidance over the last few years. I'm also grateful to Professor C.A. Hurst and Dr. L.R. Dodd for their time in helpful discussions and the administration of my candidature. Also thanks goes to my fellow students, especially Alex, Amanda, Andy, Janice, Don, Peter, Geoff and the Honours Class of 92 in Mathematics for keeping my sanity in the Sun Room.

Thanks also goes to the Australian-American Educational Foundation for providing a Fulbright Postgraduate Scholarship to enable a research programme at the University of Arizona (1987-1989). For that time, a special thanks to Dr. Terry Triffet and his family plus the College of Engineering and Mines for their hospitality and support during my stay in Tucson.

I wish to thank the Commonwealth Government for providing an APRA. Also thanks to the Department of Physics and Mathematical Physics and the Department of Applied Mathematics for providing tutorial and lecturing experience throughout my candidature.

To Roy Slaven and H.G. Nelson thanks for making me laugh (a lot) on Sat arvos through the years.

To Jamie, Sue and Jacob thankyou for keeping my sanity and my herbal lifestyle.

To my family, especially my father who had the patience to watch my floundering attempts at solving problems, thanks.

Final thanks goes to Katrina, for drawing some of the pictures, but more importantly, for making writing up over the last few months a bearable experience.

Declaration

I, William Joseph ELLIS, certify that this thesis contains no material which has been accepted for the award of any other degree or diploma in any University, and that, to my best knowledge and belief, the thesis contains no material previously published or written by any other person, except where reference is made of in the text of the thesis.

I give consent to this copy of my thesis, when deposited in the University Library, being available for loan and photocopying.

William Joseph ELLIS

March 10, 1993

Chapter 1

Introduction

The structure and distribution of mobile ionic species in a solvent medium (predominantly water) is of fundamental importancé to the function of a neuron. Together with the structural and electrostatic properties of the membrane these factors determine the strength and duration of the nerve signals. Of critical importance is the structure of the fluid adjacent to a membrane wall. Electrical Double Layer (EDL) theory will be used to model this region of fluid.

1.1 Description and function of neurons

1.1.1 Structure of a neuron

The gross anatomy of the neuron cell of most animals is as follows. The *soma* (cell body) contains the nucleus and *cytoplasm* (intracellular fluid). Attached to the soma is a tube-like structure called the *axon* which is the medium for the propagation of the nerve signal. At the base of the axon is the *axon hillock* which is the site for the initiation of the nerve signal. The nerve signal reaches the terminal branches called *synapses* which form the connections with the *dendrites* which receive the nerve signals to the soma [1]. In primitive animals (such as the leech [2]) the distinction (in function) between axon and dendrites tends to disappear.

1.1.2 Ion transport through cell membranes

Though the nerve signal or *action potential* travels longitudinally to the axon it is transmitted due to voltage differences across the membrane (width $\approx 50 - 100\mathring{A}$) of the axon.

The voltage difference is due to a variation in the concentration of the mobile ionic species in the intracellular and extracellular fluid and differences in the fixed charge associated with protein at the membrane surfaces and in the cellular fluid regions. The most important mobile ionic species being Na^+, K^+, Cl^- and Ca^{++} ions. The Na^+ and Cl^- ions constitute more than 90% of the ionic species in the extracellular fluid but less than 10% in the intracellular fluid. In the intracellular fluid the dominant ionic species are K^+ ions and negatively charged organic molecules. In general the membrane is impermeable to negatively charged organic molecules. As a result in the *resting state*, when the membrane is polarized and the concentrations of the ionic species is stable, there is a potential difference of about $90mV$ with the intracellular fluid negative relative to the extracellular fluid. See Table 1.1. The membrane is called an *excitable membrane* since the permeability decreases with an increase in the potential difference across the membrane [3], [4], [5]. It should be noted that even in the resting state there maybe some *leakage* of potassium ions across the membrane if the concentrates are not in chemical equilibrium [6]. During the *depolarization* and then *repolarization* stages of the action potential, the concentration of the ionic species varies due to diffusion across the membrane.

The membrane wall or *lipid bilayer* consists of protein molecules embedded in lipids. Transport through this bilayer is either via interstices in the lipids which act as channels and by a "pumping" mechanism associated with enzymes in the membrane. The relative impermeability of ions through the lipid bilayer occurs mainly because

1. most of the ions are hydrated (see below) which greatly increases their size and therefore reduces the movement through channels in the lipid bilayer, and
2. electrical charge of an ion interacts with the charges of the lipid bilayer and causes a repulsive force between the charged species.

The relative importance of these factors depends of structural properties of the channels and the state of the neuron [6].

The enzymes or *transport proteins* act selectively to the type(s) of mobile ionic species which can be transported across the membrane due to channel's size, shape and the amount

of electrical charge along its surfaces. Diffusion through these channels is by the process of *simple diffusion* — due to the kinetic movement of the molecules and is in the direction of the *electrochemical gradient* caused by variations in concentration, electrical potential and pressure between the intracellular and extracellular fluids. *Active transport* of ionic species is against the electrochemical gradient and thus energy must be imparted to the diffusing ions. The active transport of sodium into the extracellular fluid and potassium into the intracellular by the *sodium-potassium pump* mechanism with energy derived from metabolic processes. The carrier proteins are distinguished by their ATPase which can cleave ATP (to form ADP or AMP) with the release of energy by breaking the phosphate bonds. The mechanism that then imparts this energy to the diffusing ions is still unclear [6].

The sodium transport protein selective to sodium ions is mainly characterized by the high amount of negative charge along its inner surface. These charges attract sodium ions in preference to other ions due to the electrical "bareness" (only one set of orbital electrons) of the sodium ion. Once inside the channel these ions diffuse due to their kinetic motion. Whereas, the potassium transport protein is slightly smaller than the sodium transport protein and does not posses the high amount of negative charge. Thus its selectivity to potassium ions is not due to Coulomb forces but rather the smaller size of the hydrated potassium ion.

An important difference between Na^+ and K^+ mobile ions is the binding of the water molecules in their primary hydration shell. For the Na^+ ions, the water molecules are more strongly held than for the K^+ ions, such that the K^+ ions more easily exchanges water molecules while moving through the fluid resulting in a faster transport rate than for the Na^+ ions. Transport rate of the divalent ion Ca^{++} is lower than for the monovalent ions Na^+ and K^+ due to its larger hydration number and hence size [7]. See Table 1.2. Thus the hydration of the ionic species is an important phenomena in the transport through the fluid regions and membrane. In general the Cl^- and K^+ ions are more permeable than the Na^+ ion.

To gain a further understanding of the relationship between the concentration of the

Molecule	Intracellular	Extracellular
Na^+	10	142
K^+	140	4
Ca^{++}	10^{-4}	0.1
Cl^-	4	103

Table 1.1: Concentrations (mM) of the major mobile ionic constituents of the intracellular and extracellular fluid for a neuron

various ionic species and the electrical and chemical potentials, macroscopic models have been proposed including the pioneering Hodgkin-Huxley model [8], [9], [10], [11]. More recently, Green and Triffet [12], [13], [14], [15], [16], [17], [18], [19] and their associates Vaccaro [20], [21] and Sherwood [22], have had considerable success (e.g. explaining the role of calcium in the action potential) by predicting changes in the chemical and electrical potentials due to variations in the concentrations of the mobile ionic species not only in the intracellular and extracellular fluid but within the membrane itself. As a result, the Green-Triffet model is an advance on and helps to explain the empirical success of the Hodgkin-Huxley model.

The Green-Triffet model essentially combines the equations of continuity and the Boltzmann distribution for the number density of the ionic species to yield

$$\gamma_i \frac{\partial \phi_i}{\partial t} = \nabla^2(\phi_i - \phi) \ , \tag{1.1}$$

where ϕ_i is the chemical potential and γ_i the inverse diffusion coefficients associated with the *ith* type of ionic species with ϕ as the mean electrostatic potential. This equation can be closed by the use of Poisson's equation for the mean electrostatic potential, resulting in

$$\gamma_i \frac{\partial \phi_i}{\partial t} = \nabla^2 \phi_i + \frac{4\pi}{\epsilon} \sum_k e_k n_k^0 \Big[\exp[-\beta e_k \phi_k] - 1 \Big] \ , \tag{1.2}$$

where e_k is the charge, n_k^0 is the number density of the kth type of ion in the bulk of the electrolyte and ϵ is the dielectric constant. The inverse diffusion coefficients used in this equation are determined by experimental techniques. As noted above, hydration of the ionic species is an important factor in determining the transport rate (rate of diffusion) through the intracellular and extracellular fluid regions and membrane. Even though the diffusion coefficients for the mobile ionic species do not exhibit a large variation, a theoretical model to determine these coefficients would be advantageous in discussing the possible solutions of Eq. (1.2). This is our motivation for developing a model to determine the hydration of the ionic species in the intracellular and extracellular fluid regions with particular emphasis on the structure near a membrane wall.

The theoretical framework for the determination of the diffusion coefficients is through statistical mechanics. The importance of such a molecular description to support the empirical relations of the Hodgkin-Huxley model was recognized by Agin [23]. He showed the connection of such solutions with the ensemble average of statistical mechanics. A detailed statistical mechanical description of the action potential in terms of the one and two body distribution functions was first presented by Vaidhyanathan and Phillips [24]. However, the resulting equations were only solved in the Debye-Huckel approximation. In both these and subsequent papers by Agin [25] and Arndt, Bond and Roper [26], the importance of an electroneutrality condition in regards to the type of solutions for the electrodiffusion equation is discussed. The two types of electroneutrality considered are

1. microscopic electroneutrality, $\sum_i e_i n_i = 0$, where all ionic charges add to zero at every point in both of the fluid regions and membrane, and
2. macroscopic electroneutrality, $\int dz \sum_i e_i n_i = 0$, such that the total ionic charges integrated over the fluid regions and membrane (in one dimension) is zero.

In the case of no concentration gradients, macroscopic electroneutrality is equivalent to microscopic electroneutrality. Microscopic electroneutrality, in the context of constructing solutions to the electrodiffusion equation, provides a mathematical simplification. This is a valid approximation for an aqueous electrolyte solution but is not applicable to a

biological membrane [25]. The criteria for determining the applicability of the microscopic electroneutrality condition in the membrane is the ratio of the Debye length in the membrane to the membrane thickness being $\ll 1$ [27].

A related electroneutrality condition is that of electroneutrality in the bulk electrolyte solution such that all ionic charges in the fluid regions where the membrane wall(s) have negligible effect, i.e. in the far normal distance limit, add to zero. The bulk electroneutrality condition is given by

$$\sum_i e_i n_i^0 = 0 \ . \tag{1.3}$$

This particular electroneutrality condition is used in most physiological text books, for example [1], [2], as a simplifying assumption for the discussion of electrical and chemical concentration gradients even though the condition is not satisfied in a neuron. It should be noted that all these definitions do not include the prescence of surface charges (protein molecules) on the membrane walls. The correct electroneutrality condition for a biological membrane system is macroscopic electroneutrality that includes the prescence of surface charges i.e.

$$\int dz \sum_i e_i n_i + \sigma = 0 \ , \tag{1.4}$$

where σ is the surface charge density and the region of integration is over the fluid regions including the membrane.

The determination of the electrostatic potentials is simplified by the cylindrical geometry of the neuronal cell. The natural length scale of the system is determined by the Debye screening length which for physiological concentrations has a value of about $5\mathring{A}$ in the resting state. However, this value is appreciably less than the diameter of the smallest mammalian nerve fibres ($\approx 1000\mathring{A}$). Thus we will neglect the curvature of the membrane since we are mainly interested in properties near the membrane wall and consider rather the simpler geometry of planar membranes. But it should be noted that in the dynamical phase of the action potential the concentrations vary such that the effective Debye length becomes much larger than in the resting state and possibly comparable to the membrane thickness [14].

1.2 Electrical Double Layer (EDL)

1.2.1 Description of the EDL

Under equilibrium conditions, the time average forces are the same in all directions and at all points in the bulk of the intracellular and extracellular fluids (the system is isotropic and homogeneous). Forces acting on molecules near a membrane wall are anisotropic (different from bulk electrolyte forces). These different forces at the membrane wall effect the distribution of solvent molecules (water) and charged solute molecules. Thus there is a net orientation of the dipoles (associated with the water molecules) and excess charge in the fluid region adjacent to the membrane wall. Once the extracellular and/or intracellular fluid acquires an excess charge an electric field is detected across the membrane wall. The term electrical double layer is used to describe the distribution of the solvent and solute molecules near a membrane wall.

In general, if the membrane has an excess charge density, the distribution of the molecules is as follows. The first layer from the membrane wall is mainly occupied by solvent molecules. This layer is referred to as the hydration sheath of the membrane wall. The next layer is mainly occupied by hydrated charged solute molecules. The locus of centres of these hydrated ions is called the Outer Helmholtz plane (OHP). Although the hydration sheath of the membrane wall is mainly occupied by water, there are some charged solute molecules in the same layer. The locus of the centres of these charged solute molecules is called the Inner Helmholtz plane (IHP). It is important to note that these charged solute molecules in the IHP are unhydrated. Such charged solute molecules in the IHP are in contact absorption with the charged wall [28], [29], [30], [31]. It should be noted that the above description of the EDL is a time average view of a dynamical system. See Figure 1.1.

1.2.2 "Primitive" Models of the EDL

The historical development of the theoretical explanation for the EDL phenomena can be traced back to von Helmholtz [32]. He proposed that the membrane wall and the IHP could be considered as plates in a capacitor thus creating a potential difference between

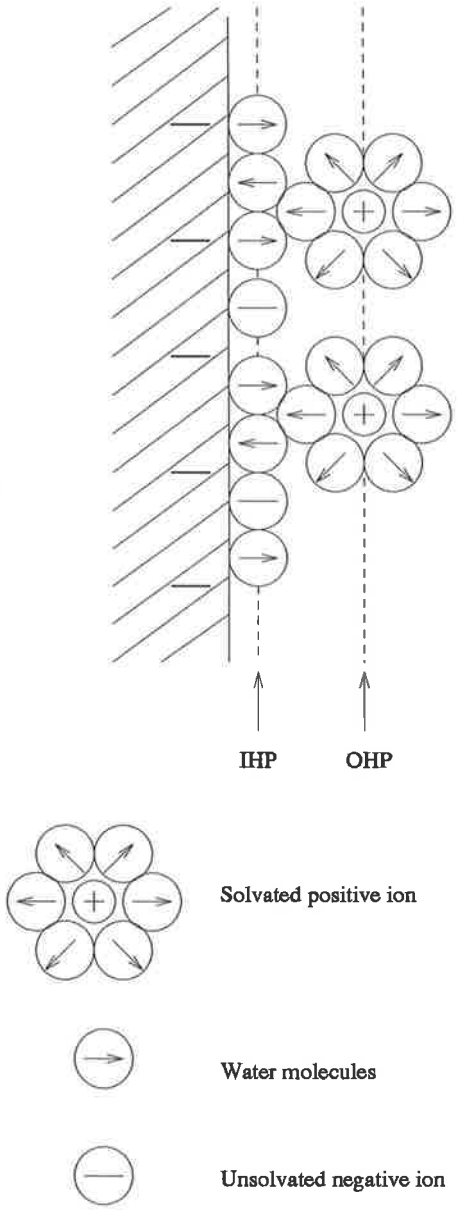

Figure 1.1: Schematic representation of the distribution of molecules near a negatively surface charged membrane wall showing the IHP and OHP.

the planes. The major assumption being that all the charged solute molecules on the time average remain in the IHP. Also the charged solute molecules are point molecules and thus no effects due to their size was considered. The solvent molecules were modelled as a dielectric continuum with an associated dielectric constant. Thus, as in a capacitor, the potential between the planes has a linear variation with distance. This model is simplistic but does exhibit some properties of the EDL.

The next major development was independently proposed by Gouy [33] and Chapman [34] and is known today as the Gouy-Chapman (GC) theory. They suggested that the charged solute molecules are not constrained to the IHP but are free to move. Thus the charged solute molecules experience the field produced by the membrane wall and the thermal motion of the other charged solute molecules. Equilibrium will be achieved by a balance of these forces and a theoretical distribution of the charged solute molecules in the region near the membrane wall can be derived. The derivation of the distribution essentially comprises of equating the charge density $\rho(z)$ as predicted by Poisson's equation and that predicted by Boltzmann and then linearizing the equation

$$\rho(z) = -\kappa^2 \psi(z) \ , \tag{1.5}$$

where $\psi(z)$ is the potential between a plane at distance z from the membrane wall and the bulk of the electrolyte. Explicitly the potential is given by

$$\psi(z) = \psi^0 e^{-\kappa z} \ , \tag{1.6}$$

such that ψ^0 is the potential at the membrane wall. The constant κ (inverse Debye length) is defined by

$$\kappa^2 = \frac{4\pi\beta}{\epsilon} \sum_i n_i^0 e_i^2 \ . \tag{1.7}$$

This model is in general agreement with experimental data only at low concentrations i.e.$< 0.01M$ [30].

The major criticisms of the GC theory have been

1. the "intuitive" coupling of Poisson's equation (electrostatics) and the Boltzmann equation (statistical mechanics) rather than a rigorous development from

the equations of statistical mechanics,

2. the applicability only at low concentrations since the Boltzmann equation neglects the interaction between charged solute molecules, and
3. the molecules are point molecules and thus effects due to their exclusion volume are neglected.

It is interesting to note that the Gouy-Chapman theory was proposed a decade earlier than the Debye-Huckel theory for electrolytes [35].

In the year after the development of the Debye-Huckel theory, Wagner [36] proposed a model that included the effect of "image" forces due to the differences in the dielectric permittivity of the fluid region and membrane. This model was subsequently generalized by Onsager and Samaras [37] and thus today is known as the Wagner-Onsager-Samaras model. It also incorporates the effect of the distortion of the "Debye sphere" surrounding a charged solute molecule near a membrane wall. One advantage of this model over the GC theory is the incorporation of the effect of the interaction between the charged solute molecules. Though in the original model the interaction between the charged solute molecules and the surface charges was neglected and the equations were derived again in an intuitive way by combining the Poisson and Boltzmann equations.

A combination of both the von Helmholtz and GC models was proposed by Stern [38]. In his model the charged solute molecules have a distance of closest approach to the membrane wall. At this distance there is a plane of charged solute molecules. Thus the effect of

1. the finite size of the charged solute molecules in relation to the membrane wall, and
2. the contact absorption of charged solute molecules,

have been incorporated by introducing the "Stern" layer. The potential varies linearly between the membrane wall and the distance of closest approach and past this plane (in the bulk of the electrolyte) it has an exponential variation as predicted by the GC theory.

Grahame [39] suggested that the charged solute molecules in contact absorption lie in the IHP and the other charged solute molecules in the OHP. These two planes were introduced to model the phenomena that some charged solute molecules that are unhydrated can move into the IHP from the bulk region and others which are hydrated can only approach up to the OHP. In the limit that the IHP and OHP coincide, we obtain the Stern model.

All these early phenomenological models provide some insight into the theoretical description of the EDL but neglect, to varying extents, some important physical features such as solvent structure, exclusion volume effects and the interaction between molecules. The only consistent way of providing a theoretical description of the EDL is via the exact equations of statistical mechanics, first considered by Buff and Stillinger [40]. Approximations are made in this formulation to the Hamiltonian that describes the EDL and the bulk electrolyte and in solving the resulting equations for the distribution functions. This type of theoretical formulation and refinements thereof form the basis of most research into the EDL for the last thirty years [41].

The simplest formulation is called the Primitive Model (PM). The Hamiltonian in the PM consists of the separation and orientation of only the charged solute molecular coordinates. Effects of the solvent are neglected as a first approximation. The charged solute molecules are considered to be hard spheres with an embedded point charge. The membrane wall is modelled as a smooth, polarizable wall with uniform surface charge density. Also included are the image charge effects in the Hamiltonian [42], [43].

Since the intermolecular potentials and equations in the above theories are approximate, it is impossible to compare the accuracy of any theory to experimental data. Rather, a comparison can be made of a theory with a computer simulation using the approximate intermolecular potentials as inputs and then the properties of the system computed for a few thousand molecules. The simulation techniques that can be used are

1. Monte Carlo (MC) - an equilibrium ensemble is generated from a random walk algorithm, and

2. Molecular Dynamics (MD) - the equations of motion are solved simultaneously.

For a charged hard sphere PM system, the MD technique cannot be used since the intermolecular Coulombic forces are both singular and long ranged—although the MC technique has been implemented by Torrie [44], [45], it does possess some inherent difficulties due to the long range nature of the Coulombic forces [46].

The success of integral equations and the various closure relations for the correlation functions (compared with computer simulations) in the region of the bulk electrolyte, excluding membrane wall effects, [47], [48], [49], [50], has prompted their use in the theoretical description of the diffuse part of the EDL. The two major integral equations are the Ornstein-Zernicke (OZ) [51] and the BBGKY hierarchy, named after its authors, Bogolyubov [52], Born and Green [53], Kirkwood [54] and Yvon [55].

The OZ integral equation defines a relationship between the direct and indirect correlation functions. This has to be supplemented with a closure relation for the direct correlation function so that the OZ integral equation can be solved. In the theory of bulk electrolytes the most accurate closure relation is the Hypernetted Chain (HNC) [49]. However, the HNC gives a poor approximation for the exclusion volume of the molecules near the membrane wall and is not a good approximation for the EDL at low concentrations and surface charge density. Improvement with computer simulation is noted if the Mean Spherical Approximation is used rather than the HNC [56]. The OZ integral equation with the HNC closure relation is seriously flawed in its inability to handle image interactions due to differences in the dielectric permittivity. This stems from the fact that the Hamiltonian, that includes image interactions, has its translational invariance violated and thus the derivation of the OZ integral equation via density functional techniques is no longer valid [41].

An interesting method, presented in a series of papers by Kjellander and Marcelja [57], [58], [59], [60], [61], [62], [63], is to transform a three dimensional inhomogeneous system between charged walls into a two dimensional homogeneous system. This two dimensional homogeneous system can then be numerically evaluated using the HNC closure with the

OZ integral equation. The advantage of this method is its ability to handle the image interactions since there is no violation of the translation invariance in the lateral direction for the new system. The numerical solutions show excellent agreement with computer simulations.

The BBGKY hierarchy are a set of coupled integro-differential equations that relate the n body distribution function to the n+1 distribution function. In addition, a closure relation that gives an approximate expression for the n+1 distribution function in terms of lower order distribution functions is necessary to close the set of equations at the nth level of the hierarchy. The major advantage of this set of equations over the OZ integral equations is the possibility of including image interactions although this is computationally intensive due to the evaluation of multiple integrals. Numerical solutions show good agreement with computer simulations [64], [65], [41].

In parallel development with the integral equation theories has been the emergence of Modified Poisson-Boltzmann (MPB) theories. The GC idea of combining Poisson's and Boltzmann's equation is further exploited but features such as the exclusion volume effect, correlations between molecules and image effects are not neglected. Outhwaite, Levine and Bhuiyan [66], [67], [68], [69], [70], [71], [72], [73] have presented a whole series of related theories called MPB1, MPB2, ..., MPB5 which improve on these various effects. The numerical solutions are very good compared with numerical simulations provided the surface charge density is low. If this is not the case then excluded volume effects become dominant and the theory fails. Also possible are analytic solutions for the potentials in certain geometries [74]. Improved credibility of the MPB theories has been obtained by their derivation from the BBGKY hierarchy by Outhwaite [75].

Another method of improving the GC theory is to assume a smooth variation of the dielectric permittivity from the bulk region, across the diffuse layer into the membrane. Various forms for the variation have been considered by Perram and Barber [76] and Buff, Goel and Clay [77], [78], [79], [80]. The major criteria for these forms have been the correct limiting values in the bulk and membrane regions, sufficient differentiability and the ability to calculate analytic solutions from Poisson's equation. These solutions are in

close agreement with the predictions of the GC theory.

Despite its deficiencies, the PM of charged hard spheres near a charged hard wall, embedded in a dielectric continuum, is by far the most studied and well understood model of the EDL. As quoted from Blum [81]

> The primitive model should not be considered as a working model for the interpretation of experimental data, but rather a learning model for the theoretician.

1.2.3 "Civilised" Models of the EDL

In the above models of the EDL, the solvent has been considered to be a dielectric continuum. Any structure of the solvent has been neglected. Theories that describe the whole transition from the diffuse region near the membrane wall to the bulk electrolyte and include the solvent structure have emerged over recent years with particular emphasis in putting the solvent molecules on equal footing with the charged solute molecules. Such models are called "civilised" models.

As a first attempt to introduce solvent structure, models for the solvent molecules in the IHP exist [82], [83]. Though outside the IHP, in the diffuse layer, the fluid structure is a continuum. Also there are no charged solute molecules in the IHP. These models give an insight into the dielectric properties near a membrane wall but fail to account for interactions between solvent and charged solute molecules in the diffuse layer with the solvent molecules in the IHP.

Numerical models for dipoles alone (water molecules) near hard walls have been developed by Isbister, Rasaiah and Eggebrecht [84], [85], [86], [87], by using the HNC closure relation for the OZ integral equation. An important feature is the dielectric function decreases as the distance of approach to the wall decreases. This is due to the ordering of the dipoles in a minimum energy arrangement adjacent to the wall compared with the random orientation in the bulk region. Such models are important in the verification of models that include charged hard sphere molecules (e.g. Torrie, Kusalik and Patey [88], [89], [90], [91]) in the limit of zero density for the ionic species. It should be noted, as in

the PM, these theories neglect the effect of image forces.

Outhwaite has presented in a series of papers [92], [93], [94], [95], an extension of the MPB theory for the PM to the hard sphere ion-dipole system. Analytic solutions are obtained for the linearized version of the equations for the potentials and thus the distribution functions. The solutions exhibit a damped oscillatory behaviour in qualitative agreement with computer simulations. As for the PM, the MPB for the hard sphere ion-dipole system has the advantage of incorporating image effects and analytic solutions are obtainable for the linearized theory in the point ion limit. Though, it should be noted that the dielectric constant derived from the linearized theory is only applicable to a low density dipolar system.

1.3 Hydration of ions

The ionic hydration number is defined by the number of water molecules "attached" to an ion [7]. This definition is ambiguous due to the inherent difficulty in defining the term "attached" in a quantitative manner. The spirit of the definition is to differentiate between water molecules that are chemically and/or electrically attached to the ion and those that are in the bulk of the fluid on the time average.

Bockris' view [96] of hydration and thus hydration number is a refinement of the above definition. He proposed that a certain number of water molecules (dipoles) are orientated by the field produced by an ion and form an immobile sheath of water relative to the ion. They are strongly bound by this ionic field and experience negligible influence from the other molecules in the fluid. The size of the region should only be a few angstroms due to Debye shielding of the ionic field. This region is called the *primary hydration sheath* and the number of water molecules in it called the primary hydration number. The region between the primary hydration sheath and the bulk fluid is called the *secondary hydration sheath* and the number of water molecules in this region is called the secondary hydration number. Again this is an ambiguous definition but the ambiguity is now localized to the secondary hydration sheath. In this region, the field due to the ion is tending to orient the water molecules parallel to the field and the other water molecules in the sheath are tending

to align the water molecules into the bulk region arrangement. The picture proposed by Bockris is of an ion with a immobile sheath of water moving through the fluid and the water molecules in the second hydration sheath becoming attached and unattached and being replaced by other water molecules as the ion moves. Typical range of values for the hydration number for various ionic species are presented in Table 1.2. The numbers in the table are an average of the different numbers obtained from the variety of experiments to determine them [7].

Even though the size of the second hydration sheath is ambiguous, a precise definition by Azzam [97] can be given for the primary hydration sheath in terms of the pair correlation function $g(r)$. The hydration number is based on the number of nearest neighbour water molecules to the ion by the following relation

$$n_i^H = 4\pi n_d^0 \int_{R_i^{HS}}^{R_{max}} dr r^2 g(r) \ , \tag{1.8}$$

where n_d^0 is the number density of the water molecules in the bulk, R_i^{HS} is the hard sphere radius of the ion and R_{max} is the first minimum in the pair correlation function between the ion and water molecules. The first minimum defines the most probable location of the hydrated sheath. However, this definition is only useful in the bulk region where the fluid is isotropic and homogeneous. For our particular application, the number density and the pair correlation function will have functional dependence on the normal distance from the membrane walls and angular dependence on the orientation of the dipole (water molecule). A modified integral expression for the hydration number is presented in Chapter 4.

1.4 Description of Model

The model discussed in this thesis is developed to investigate the structure of water molecules in the vicinity of an ion, adjacent to a membrane, by the application of EDL theory. Let us restrict our attention to hydration effects in the intracellular and extracellular fluid regions only. We will not consider the effects of hydration in the membrane. Also we will consider the neuron to be in the resting state and thus assume there is no net transport across the membrane. The ion-dipole system of Chan, Mitchell, Ninham and

Molecule	Radius $\mathring{A}$	Hydration No.
Na^+	0.95	5 ± 1
K^+	1.33	4 ± 2
Ca^{++}	0.99	12 ± 2
Mg^{++}	1.00	14 ± 2
Cl^-	1.81	1 ± 1
H_2O	1.38	-

Table 1.2: Molecular hard sphere radii and hydration numbers.

Carnie [98], [99] and Outhwaite [93], [94], [95], will be used to model the extracellular and intracellular fluids of the neuron.

Since protein molecules are the major component of the negative organic charge and a constituent of the membrane it does not seem unreasonable to assume that a percentage of the protein molecules can be modelled as a membrane surface charge density. The charge balance is restored by including the contribution from the membrane surface charge density and relating fixed charges associated with protein in the electrolyte. Thus the model is as follows.

The electrolyte solution consists of mobile and fixed ionic species with hard sphere diameters R_i, electric charge e_i, bulk number density n_i^0 (i=1,..., M:M=no. of different ionic species) and point dipoles with hard sphere diameter R_d, number density n_d and dipole moment $\mathbf{m}(\omega_1)$ such that ω_1 describes the orientation of the dipole. The point dipoles are introduced to model the solvent structure. The electrolyte is contained in three regions which are separated by two membranes (of finite thickness L and separated by distance $2D$) and uniform surface charge density. The uniform surface charge densities

model the negatively charged protein molecules protruding from the membrane walls which create a negative potential. Also a constant negative background potential models the fixed protein molecules in the electrolyte. The membranes are modelled as a continuum with an associated dielectric constant. See Figure 1.2. We shall refer to this geometry as the two membrane model. Typical values of the parameters from [3], [4], for the two membrane model are presented in Table 1.3.

We also consider a limiting form of the above model by setting the surface charge density and number densities in the extracellular region to zero and then taking the limit as the membrane thickness tends to infinity. See Figure 1.3. This is called the two semi-infinite membrane model. The two semi-infinite membrane model geometry is introduced to test the solutions for two membrane model. The one membrane model is introduced to investigate the effect of the presence of a second membrane in the two membrane model. See Figure 1.4.

1.5 Outline of Thesis

In Chapter 2 we present a derivation of the potential formulation of the distribution functions from the BBGKY hierarchy in a similar manner to Outhwaite's derivation [75] for the PM. The method essentially involves the closure of the equation for the mean electrostatic potential with the first of the BBGKY hierarchy for the number density (in terms of the mean electrostatic potential) and neglecting the integral terms which are first order in the indirect correlation function. A similar process is involved in the determination of the mean electrostatic fluctuation potential by its closure with the second of the BBGKY hierarchy for the two body correlation function and truncating the resulting equation using Loeb's approximation. In addition for our derivation, we do not assume bulk electroneutrality but rather a linearized version (in the mean electrostatic potential) of the macroscopic electroneutrality condition for the interfacial regions. The differential equations in our derivation reduce to Outhwaite's equations [94], [95], if bulk electroneutrality is assumed. The point model systems are considered by letting the hard sphere diameters of the molecules tend to zero. These equations are also consistent with previous results by

Carnie and Chan [74]. Due to the cylindrical geometry, we perform a Hankel transform in the transverse distance variable which reduces the partial differential equation for the mean electrostatic fluctuation potential for the point model systems to a second order ordinary differential equation in the normal distance variable. The Hankel transform of the mean electrostatic fluctuation potential is called the transverse Hankel transform mean electrostatic fluctuation potential. The inhomogeneous term in the ordinary differential equation for the transverse Hankel transform mean electrostatic fluctuation potential is a Delta function in the relative distance between the source and field point. Thus the differential equation defines a Green's function problem which can be solved by the standard technique of variation of parameters [100].

In Chapter 3 explicit solutions for the mean electrostatic potential and the transverse Hankel transform mean electrostatic fluctuation potential for the two membrane point model system are derived by applying boundary conditions at each of the membrane walls. For the transverse Hankel transform mean electrostatic fluctuation potential, both cases for the position of the source point are considered i.e. when the source is in the extracellular and intracellular fluid regions. The solution to these ordinary differential equations is written in terms of either Bessel or modified Bessel functions depending on a charge asymmetry parameter that is introduced. Asymptotic expansions of the transverse Hankel transform mean electrostatic fluctuation potential for both cases are presented and show excellent agreement with a numerical solution of the differential equations for the specialized case of the source and field point coinciding. Due to the complicated nature of the expressions for the solutions, for each of the cases, consistency of the these solutions with relevant limiting forms, presented in the Appendices and the one wall system considered by Carnie and Chan [74], are verified. The limiting forms considered are

- large behaviour in the transform variable,
- $D \to 0$, thus creating a system with one membrane and extracellular fluid on either side,
- $L \to \infty$, reducing to the two semi-infinite membrane model system,

- $\epsilon_M \to 0$, the membranes are perfect insulators, and
- $\epsilon_M \to \infty$, the membranes are perfect conductors.

Comparison of the two membrane point model system solution for the transverse Hankel transform mean electrostatic fluctuation potential, in each region, with that of the one membrane point model system shows negligible difference in the region adjacent to the membrane walls for typical values of the parameters as in Table 1.3. The effect of the second membrane is negligible due to the large distance between the membranes $2D$ compared with the Debye length. Provided the ratio of the Debye length to the distance between the membranes is $\ll 1$, then the effect of the second wall is negligible. For the purposes of calculating the indirect and pair correlation functions it is only necessary to evaluate the transform inversion for the transverse Hankel transform mean electrostatic fluctuation potential, in each region, for the one membrane point model system.

In Chapter 4 we present the calculation of the ionic hydration number for various ionic species in both the extracellular and intracellular fluid regions. To obtain the ionic hydration number, we first calculate the inverse transverse Hankel transform mean electrostatic fluctuation potential, in each region, for the one membrane point model system. Since we are interested in the structure in the vicinity of the ion, which corresponds to large values in the transform variable, the asymptotic form for large values of the transform variable is inverted in closed form. Comparison of this analytic expression with a numerical integration of the transverse Hankel transform mean electrostatic fluctuation potential shows excellent agreement. Thus this analytic form for the mean electrostatic fluctuation potential is used in our proposed definition of the ionic hydration number which accounts for the orientation of the dipoles (water molecules). Due to the inherent difficulties in integrating functions that have both a normal and transverse dependence over a spherical region, we propose to take the region of integration for the ionic hydration number not as a sphere (as in Azzam's definition) but rather as a cylinder. Thus the cylindrical region of integration is a simplification though the volume of the region will be similar to those of Azzam's spherical region.

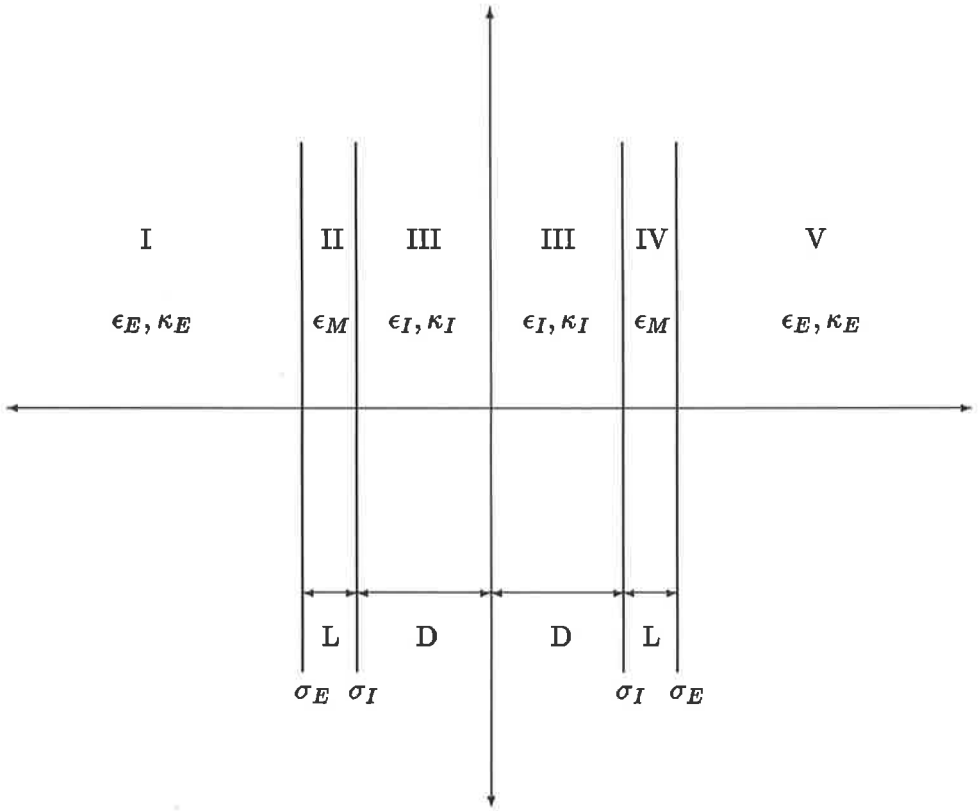

Figure 1.2: Schematic representation of a two membrane model geometry showing the various regions and the associated inverse Debye lengths, dielectric constants and surface charge densities.

Quantity	Value
L	$50\,\mathring{A}$
D	$100\,\mathring{A}$
σ_E	$-0.53406E-22\,C\mathring{A}^{-2}$
σ_I	$-0.53406E-22\,C\mathring{A}^{-2}$
ψ_E^B	$-7\,mV$
ψ_I^B	$-92\,mV$
$\frac{\epsilon_M}{4\pi\epsilon_0}$	3

Table 1.3: Typical values of the parameters for the two membrane model.

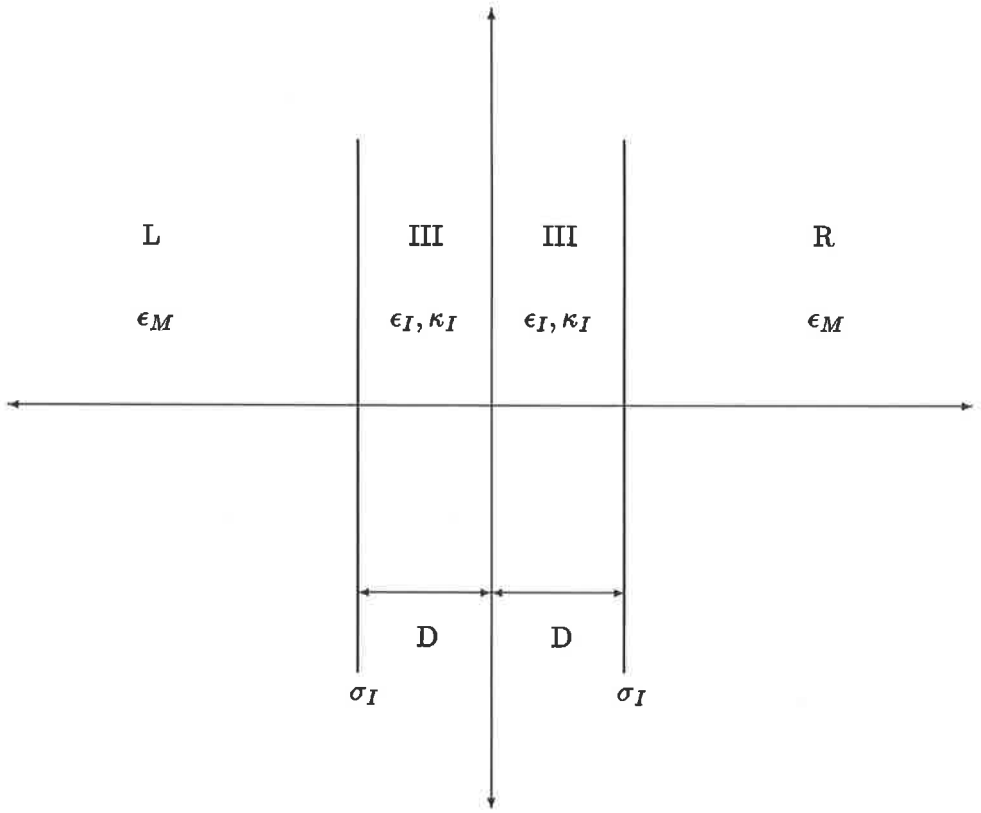

Figure 1.3: Schematic representation of two semi-infinite membrane model geometry various regions and the associated inverse Debye lengths, dielectric constants and surface charge densities.

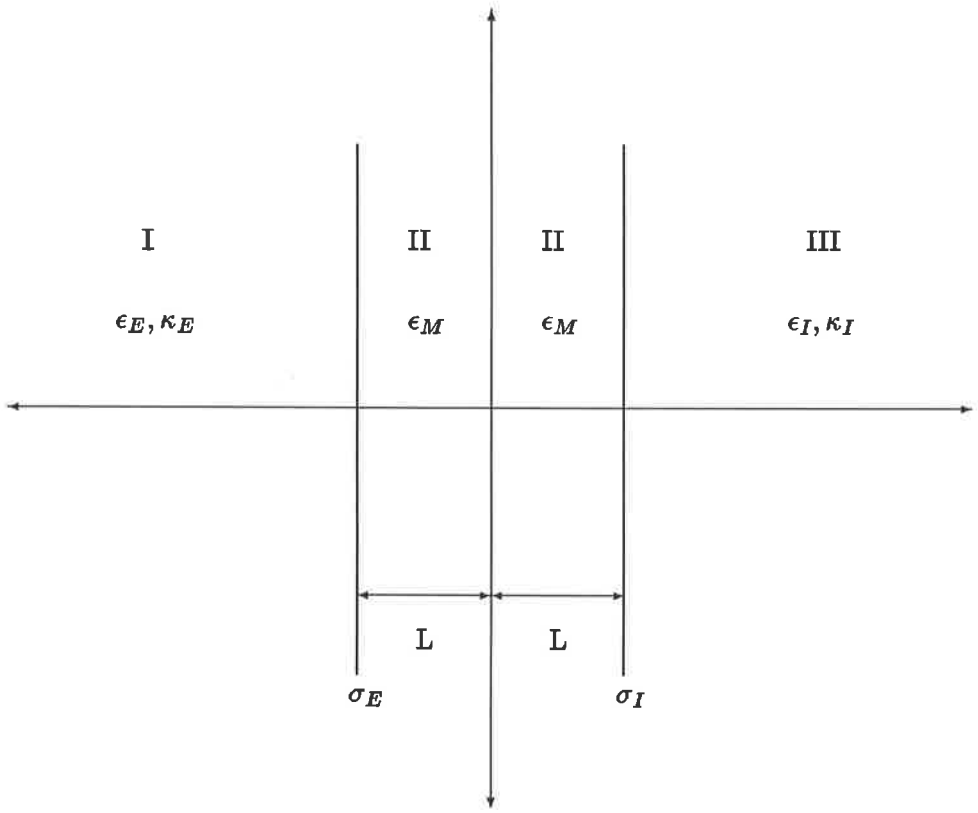

Figure 1.4: Schematic representation of a one membrane model geometry showing the various regions and the associated inverse Debye lengths, dielectric constants and surface charge densities.

Chapter 2

Equilibrium Statistical Mechanics

In this chapter we will consider in general the statistical mechanics of the electrical double layer. Since the relative orientation of ions and water molecules is important, but rarely considered in other contents, we briefly derive the fundamental equations and exact conditions on various quantities of the EDL including the number density, pair and indirect correlation functions from first principles. Then approximations to determine these quantities will be introduced and their validity discussed.

2.1 Grand partition function

In statistical mechanics we construct an ensemble of the system (in particular a fluid for our application) to be studied. An ensemble consists of an infinite number of identical systems with the same macroscopic parameters but occupying different microscopic states with the particles having different positions, momenta and possibly orientations. From the distribution of the corresponding points in phase-space we construct the probability density function. We wish to consider an ensemble of systems which can exchange both heat and matter with a heat reservoir. Such an ensemble is called the grand canonical ensemble.

The state of a system is determined by the following macroscopic (or extensive) parameters. They are

1. energy in a region of thermal contact (i.e. exchange of heat or energy is possible),

2. momentum and angular momentum in a region of mechanical contact,

3. number of particles in a region of chemical contact (i.e. particle transfer is allowed to and from the region), and

4. volume of a region of mechanical contact.

With these quantities there is an associated conservation law and each of them is defined by a constant of motion C_α. These are the

1. C_1=H=Hamiltonian or energy of the particles in volume V,

2. C_2, C_3, C_4=**P**= total momentum of the particles,

3. C_5, C_6, C_7=**L**= total angular momentum of the particles,

4. C_8=N_1=total number of particles of type one, and

5. C_9=N_2=total number of particles of type two....etc.

For convenience, the set of the constants of motion is denoted by $\mathbf{C} = (C_1, C_2, C_3, ...)$.

We introduce $P(\mathbf{C})$, the probability that the constants of motion **C** have the value **C** in the ensemble. From the laws of probability, we have the normalization condition

$$\sum_{\mathbf{C}} P(\mathbf{C}) = 1 \ , \tag{2.1}$$

where the summation is over all possible values of **C** in the ensemble. Also the average of **C** is defined by

$$\langle \mathbf{C} \rangle = \sum_{\mathbf{C}} \mathbf{C} P(\mathbf{C}) \ . \tag{2.2}$$

Note that the functional dependence of the probability function is in actual fact

$$P(\mathbf{C}) = P(\mathbf{C}, \langle \mathbf{C} \rangle, V) \ . \tag{2.3}$$

Together with the fact that the constants of motion **C** are additive we have the usual form for the probability function [101]

$$P(\mathbf{C}) = P_0(\mathbf{C}, V) \exp\left[- \sum_\alpha \lambda_\alpha C_\alpha - \int_V d\mathbf{x} h(\mathbf{x}) \right] \ , \tag{2.4}$$

where $P_0(\mathbf{C}, V)$ is a constant determined by the high temperature limit and the λ_α's are parameters which are determined by the state of the system. The function $h(\mathbf{x})$ is a function of $\mathbf{x}$ and due to the normalization condition, Eq. (2.1), is dependent on the set of intensive (volume independent) quantities which can be expressed as functions of $\boldsymbol{\lambda} = (\lambda_1, \lambda_2, \lambda_3, ...)$. In turn, $\boldsymbol{\lambda} = (\lambda_1, \lambda_2, \lambda_3, ...)$ are functions of the volume and the other extensive parameters $\langle \mathbf{C} \rangle$ and it can be shown by thermodynamical arguments that $h(\mathbf{x})$ is proportional to the hydrostatic pressure at $\mathbf{x}$ [102].

Now we define the grand partition function Ξ, in terms of $\boldsymbol{\lambda}$ and the constants of motion $\mathbf{C}$, by

$$\begin{aligned} \Xi &= \sum_{\mathbf{C}} P_0(\mathbf{C}, V) \exp[-\boldsymbol{\lambda}\cdot\mathbf{C}] \\ &= \exp[\int_V d\mathbf{x} h(\mathbf{x})] \ . \end{aligned} \tag{2.5}$$

A variation in Ξ with respect to $\boldsymbol{\lambda}$ yields

$$\begin{aligned} \delta\Xi &= \sum_{\mathbf{C}} P_0(\mathbf{C}, V)[-\delta\boldsymbol{\lambda}\cdot\mathbf{C}] \exp[-\boldsymbol{\lambda}\cdot\mathbf{C}] \\ &= \delta\boldsymbol{\lambda}\cdot\langle\mathbf{C}\rangle\Xi \ . \end{aligned} \tag{2.6}$$

Hence

$$\begin{aligned} \langle\mathbf{C}\rangle &= -\frac{1}{\Xi}\frac{\delta\Xi}{\delta\boldsymbol{\lambda}} \\ &= -\int_V d\mathbf{x}\frac{\delta h}{\delta\boldsymbol{\lambda}} \ . \end{aligned} \tag{2.7}$$

Thus a knowledge of the dependence of the grand partition function on the parameters $\boldsymbol{\lambda}$ determines the average values of the constants of motion.

2.2 Distribution functions and the BBGKY hierarchies

We can now define the classical mechanical grand canonical phase-space distribution function from Eq. (2.4) as

$$\frac{P(\mathbf{C})}{P_0(\mathbf{C}, V)} = F_{\mathbf{N}}(\mathbf{x}_1, \ldots, \mathbf{x}_N; \mathbf{p}_1, \ldots, \mathbf{p}_N; \boldsymbol{\omega}_1, \ldots, \boldsymbol{\omega}_N) \ . \tag{2.8}$$

A quantal analogue is due to Wigner [103], and at ordinary temperatures approximates very closely the classical function (except when free electrons are involved). For convenience, we use the concise notation

$$F_{\mathbf{N}}(\mathbf{x};\mathbf{p};\boldsymbol{\omega}) \equiv F_{\mathbf{N}}(\mathbf{x}_1,\ldots,\mathbf{x}_N;\mathbf{p}_1,\ldots,\mathbf{p}_N;\boldsymbol{\omega}_1,\ldots,\boldsymbol{\omega}_N) \ . \tag{2.9}$$

The quantity

$$F_{\mathbf{N}}(\mathbf{x};\mathbf{p};\boldsymbol{\omega}) \prod_{i=1}^{N} d\mathbf{x}_i d\mathbf{p}_i d\boldsymbol{\omega}_i \ , \tag{2.10}$$

defines the probability that the volume elements $d\mathbf{x}_1,\ldots,d\mathbf{x}_{N_1}$ are occupied by particles of the first kind with orientations $d\boldsymbol{\omega}_1,\ldots,d\boldsymbol{\omega}_{N_1}$ and momenta in the ranges $d\mathbf{p}_1,\ldots,d\mathbf{p}_{N_1}$ and the volume elements $d\mathbf{x}_{N_1+1},\ldots,d\mathbf{x}_{N_1+N_2}$ are occupied by particles of the second kind with orientations $d\boldsymbol{\omega}_{N_1+1},\ldots,d\boldsymbol{\omega}_{N_1+N_2}$ and momenta in the ranges $d\mathbf{p}_{N_1+1},\ldots,d\mathbf{p}_{N_1+N_2}$ and etc.. The orientation vector $\boldsymbol{\omega}$ is described by the angular co-ordinates (θ,ϕ) such that $\int d\boldsymbol{\omega}_1 = 4\pi$.

Thus the probability that the volume V consists of N_1 particles of the first kind, N_2 particles of the second kind etc., is given by

$$P_{\mathbf{N}} = \frac{1}{N_1!N_2!\ldots N_M!}\int\ldots\int F_{\mathbf{N}}(\mathbf{x};\mathbf{p};\boldsymbol{\omega}) \prod_{i=1}^{N} d\mathbf{x}_i d\mathbf{p}_i d\boldsymbol{\omega}_i \ , \tag{2.11}$$

such that the normalization of $F_{\mathbf{N}}$ required by Eq. (2.1) is satisfied. That is

$$\sum_{\mathbf{N}} P_{\mathbf{N}} = \sum_{\mathbf{N}} \int F_{\mathbf{N}}(\mathbf{x};\mathbf{p};\boldsymbol{\omega}) d\Omega_N = 1 \ , \tag{2.12}$$

where

$$\begin{aligned} \sum_{\mathbf{N}} &= \sum_{N_1=0}^{\infty}\sum_{N_2=0}^{\infty}\cdots\sum_{N_M=0}^{\infty} \ , \\ d\Omega_N &= \prod_{a=1}^{M}\frac{1}{N_a!}\prod_{i=1}^{N} d\mathbf{x}_i d\mathbf{p}_i d\boldsymbol{\omega}_i \ , \\ M &= \text{no. of species of particles.} \end{aligned}$$

It should be noted that the grand canonical phase-space distribution function is related to the grand partition function via Eq. (2.4), Eq. (2.5) and Eq. (2.8) by

$$\ln F_{\mathbf{N}}(\mathbf{x};\mathbf{p};\boldsymbol{\omega}) = -\ln \Xi - \boldsymbol{\lambda}\cdot\mathbf{C} \ . \tag{2.13}$$

Thus substituting this relationship for the grand canonical phase-space distribution function into the normalization condition, Eq. (2.12), yields

$$\Xi = \sum_{\mathbf{N}} \int \exp\Big[-\boldsymbol{\lambda}\cdot\mathbf{C}\Big] d\Omega_N \ . \tag{2.14}$$

Finally we can write the ensemble average of some quantity G, as defined in Eq. (2.2), as

$$\begin{aligned} \langle G \rangle &= \sum_{\mathbf{N}} \int G F_{\mathbf{N}}(\mathbf{x};\mathbf{p};\boldsymbol{\omega}) d\Omega_N \\ &= \frac{1}{\Xi} \sum_{\mathbf{N}} \int G \exp\Big[-\boldsymbol{\lambda}\cdot\mathbf{C}\Big] d\Omega_N \ . \end{aligned} \tag{2.15}$$

The number density n_a or the one body distribution function for molecules of the ath kind, is defined by

$$n_a(\mathbf{x},\boldsymbol{\omega}|V) = \langle \sum_i \delta_{ia}\delta(\mathbf{x}-\mathbf{x}_i)\delta(\boldsymbol{\omega}-\boldsymbol{\omega}_i)\rangle \ . \tag{2.16}$$

Similarly the two particle correlation function n_{ab} or the two body distribution function is defined by

$$n_{ab}(\mathbf{x},\boldsymbol{\omega};\mathbf{x}',\boldsymbol{\omega}'|V) = \langle \sum_i \delta_{ia}\delta(\mathbf{x}-\mathbf{x}_i)\delta(\boldsymbol{\omega}-\boldsymbol{\omega}_i) \sum_j{}' \delta_{jb}\delta(\mathbf{x}'-\mathbf{x}_j)\delta(\boldsymbol{\omega}'-\boldsymbol{\omega}_j)\rangle \ , \tag{2.17}$$

where $\sum_j{}'$ indicates the value i=j is excluded from the summation. These two quantities are important for describing most of the features of the molecular structure of the fluid system. Quantities related to the two body correlation function are the pair distribution function $g_{ab}(\mathbf{x},\boldsymbol{\omega};\mathbf{x}',\boldsymbol{\omega}'|V)$ defined by

$$g_{ab}(\mathbf{x},\boldsymbol{\omega};\mathbf{x}',\boldsymbol{\omega}'|V) = \frac{n_{ab}(\mathbf{x},\boldsymbol{\omega};\mathbf{x}',\boldsymbol{\omega}'|V)}{n_a(\mathbf{x},\boldsymbol{\omega}|V) n_b(\mathbf{x}',\boldsymbol{\omega}'|V)} \ , \tag{2.18}$$

and the indirect correlation function $h_{ab}(\mathbf{x},\boldsymbol{\omega};\mathbf{x}',\boldsymbol{\omega}'|V)$ defined by

$$h_{ab}(\mathbf{x},\boldsymbol{\omega};\mathbf{x}',\boldsymbol{\omega}'|V) = g_{ab}(\mathbf{x},\boldsymbol{\omega};\mathbf{x}',\boldsymbol{\omega}'|V) - 1 \ . \tag{2.19}$$

The notation $|V$ is used to show explicitly that an external potential V_a is acting on the system. If the external potential is equivalently set to zero, the number density and the two particle correlation functions reduce to their homogeneous values [104].

The general fluid system we wish to consider consists of particles which interact via a potential that is dependent not only on the particles position but their orientation. The

Hamiltonian of our model system has the form

$$H = \sum_{i=1}^{N}\sum_{a=1}^{M}\delta_{ia}\frac{p_i^2}{2m_i} + \frac{1}{2}\sum_{i=1}^{N}\sum_{j=1}^{N}\sum_{a=1}^{M}\sum_{b=1}^{M}\delta_{ia}\delta_{jb}\Phi_{ab}(\mathbf{x}_i,\boldsymbol{\omega}_i;\mathbf{x}_j,\boldsymbol{\omega}_j) + \sum_{i=1}^{N}\sum_{a=1}^{M}\delta_{ia}V_a(\mathbf{x}_i,\boldsymbol{\omega}_i) \ , \tag{2.20}$$

where p_a is the momenta of a particle of the ath kind. $\Phi_{ab}(\mathbf{x}_i,\boldsymbol{\omega}_i;\mathbf{x}_j,\boldsymbol{\omega}_j)$ represents the mutual potential energy of two molecules of the ath and bth kind, if their mass centres and orientations are at $(\mathbf{x}_i,\boldsymbol{\omega}_i)$ and $(\mathbf{x}_j,\boldsymbol{\omega}_j)$ respectively. Define δ_{ia} to be equal to 1 if the molecule at $\mathbf{x}_i$ with orientation $\boldsymbol{\omega}_i$ is of the ath kind and zero otherwise. $V_a(\mathbf{x}_i,\boldsymbol{\omega}_i)$ denotes the potential energy of the ath kind of molecule at $(\mathbf{x}_i,\boldsymbol{\omega}_i)$ due to the external field.

The grand partition function can be written in the form

$$\Xi = \sum_{\mathbf{N}}\int \exp\Big[\sum_{i=1}^{N}\sum_{a=1}^{M}\delta_{ia}\gamma_a(\mathbf{x}_i,\boldsymbol{\omega}_i) - \frac{\beta}{2}\Phi\Big]d\Omega_N \ , \tag{2.21}$$

and

$$\beta = (k_BT)^{-1} \ , \tag{2.22}$$

$$\tau_a = \frac{3}{2}\ln[\frac{2\pi m_a}{\beta h^2}] \ , \tag{2.23}$$

$$\gamma_a(\mathbf{x}_i,\boldsymbol{\omega}_i) = \tau_a + \beta\mu_a(\mathbf{x}_i,\boldsymbol{\omega}_i) - \beta V_a(\mathbf{x}_i,\boldsymbol{\omega}_i) \ , \tag{2.24}$$

$$\Phi = \sum_{i=1}^{N}\sum_{j=1}^{N}\sum_{a=1}^{M}\sum_{b=1}^{M}\delta_{ia}\delta_{jb}\Phi_{ab}(\mathbf{x}_i,\boldsymbol{\omega}_i;\mathbf{x}_j,\boldsymbol{\omega}_j) \ , \tag{2.25}$$

where k_B is Boltzmann's constant, $\mu_a(\mathbf{x}_i,\boldsymbol{\omega}_i)$ the chemical potential associated with the ath kind of molecule at $(\mathbf{x}_i,\boldsymbol{\omega}_i)$. The expression for τ_a is derived from the integration over the momenta coordinates. Thus the ensemble average of G, Eq. (2.15), can be explicitly written as

$$\langle G\rangle = \frac{1}{\Xi}\sum_{\mathbf{N}}\int G\exp\Big[\sum_{i=1}^{N}\sum_{a=1}^{M}\delta_{ia}\gamma_a(\mathbf{x}_i,\boldsymbol{\omega}_i) - \frac{\beta}{2}\Phi\Big]d\Omega_N \ , \tag{2.26}$$

provided the function G does not have an explicit dependence upon the momenta.

From the definition of the grand canonical phase-space distribution function it is possible to derive a set of coupled integro-differential equations relating the n body distribution

function to the n+1 body distribution function. The resulting set of equations are known as the BBGKY hierarchy.

The grand canonical phase-space distribution function $F_{\mathbf{N}}(\mathbf{x};\mathbf{p};\omega)$ satisfies Liouville's equation

$$DF_{\mathbf{N}}(\mathbf{x};\mathbf{p};\omega) = \frac{\partial F_{\mathbf{N}}(\mathbf{x};\mathbf{p};\omega)}{\partial t} + \{F_{\mathbf{N}}(\mathbf{x};\mathbf{p};\omega), H\} = 0 \ , \tag{2.27}$$

where D is the Liouville operator and $\{\}$ is the Poisson bracket [102]. For the Hamiltonian of our system, Eq. (2.20), the Poisson bracket can be evaluated to give the explicit form for the Liouville operator which is then substituted into Eq. (2.27), to yield

$$\begin{aligned} DF_{\mathbf{N}}(\mathbf{x};\mathbf{p};\omega) = & \frac{\partial F_{\mathbf{N}}}{\partial t} + \sum_{i=1}^{N}\sum_{a=1}^{M} \delta_{ia}\frac{\mathbf{p}_a}{m_a}\cdot\frac{\partial F_{\mathbf{N}}}{\partial \mathbf{x}_i} - \sum_{i=1}^{N}\sum_{a=1}^{M}\delta_{ia}\frac{\partial V_a(\mathbf{x}_i,\omega_i)}{\partial \mathbf{x}_i}\cdot\frac{\partial F_{\mathbf{N}}}{\partial \mathbf{p}_i} \\ & - \frac{1}{2}\sum_{i=1}^{N}\sum_{j=1}^{N}\sum_{a=1}^{M}\sum_{b}^{M}\delta_{ia}\delta_{jb}\frac{\partial \Phi_{ab}(\mathbf{x}_i,\omega_i;\mathbf{x}_j,\omega_j)}{\partial \mathbf{x}_i}\cdot\frac{\partial F_{\mathbf{N}}}{\partial \mathbf{p}_i} \\ = & \ 0 \ . \end{aligned} \tag{2.28}$$

To obtain the first equation in the BBGKY hierarchy, we multiply Eq. (2.28) by $\delta_{ia}\delta(\mathbf{x}-\mathbf{x}_i)\delta(\mathbf{p}-\mathbf{p}_i)\delta(\omega-\omega_i)$, sum over i, integrate over the phase-space of the N particles with the weight factor $\prod_{a=1}^{M}\frac{1}{\mathbf{N}_a!}$, and then sum over $\mathbf{N}$ to obtain

$$\begin{aligned} \frac{\partial f_a(\mathbf{x},\mathbf{p},\omega|V)}{\partial t} + & \frac{\mathbf{p}}{m_a}\cdot\frac{\partial f_a}{\partial \mathbf{x}} - \frac{\partial V_a(\mathbf{x},\omega)}{\partial \mathbf{x}}\cdot\frac{\partial f_a}{\partial \mathbf{p}} \\ & = \sum_{b}\int \frac{\partial \Phi_{ab}(\mathbf{x},\omega;\mathbf{x}',\omega')}{\partial \mathbf{x}}\cdot\frac{\partial f_{ab}(\mathbf{x},\mathbf{p},\omega;\mathbf{x}',\mathbf{p}',\omega'|V)}{\partial \mathbf{p}} d\mathbf{x}' d\mathbf{p}' d\omega' \ , \end{aligned} \tag{2.29}$$

where the quantities $f_a(\mathbf{x},\mathbf{p},\omega|V)$ and $f_{ab}(\mathbf{x},\mathbf{p},\omega;\mathbf{x}',\mathbf{p}',\omega'|V)$ are the velocity and pair velocity distribution functions which are defined by

$$f_a(\mathbf{x},\mathbf{p},\omega|V) = \langle \sum_i \delta_{ia}\delta(\mathbf{x}-\mathbf{x}_i)\delta(\mathbf{p}-\mathbf{p}_i)\delta(\omega-\omega_i)\rangle \ , \tag{2.30}$$

$$\begin{aligned} f_{ab}(\mathbf{x},\mathbf{p},\omega;\mathbf{x}',\mathbf{p}',\omega'|V) = & \langle \sum_i \delta_{ia}\delta(\mathbf{x}-\mathbf{x}_i)\delta(\mathbf{p}-\mathbf{p}_i)\delta(\omega-\omega_i) \\ & \times \sum_j{}' \delta_{jb}\delta(\mathbf{x}'-\mathbf{x}_j)\delta(\mathbf{p}'-\mathbf{p}_j)\delta(\omega'-\omega_j)\rangle \ . \end{aligned} \tag{2.31}$$

These quantities are related to the number density and the two particle correlation functions by

$$f_a(\mathbf{x},\mathbf{p},\omega|V) = \mathcal{P}_a(\mathbf{p}) n_a(\mathbf{x},\omega|V) \ , \tag{2.32}$$

$$f_{ab}(\mathbf{x},\mathbf{p},\boldsymbol{\omega};\mathbf{x}',\mathbf{p}',\boldsymbol{\omega}'|V) = \mathcal{P}_{ab}(\mathbf{p};\mathbf{p}')n_{ab}(\mathbf{x},\boldsymbol{\omega};\mathbf{x}',\boldsymbol{\omega}'|V) \ , \tag{2.33}$$

where $\mathcal{P}_a$ and $\mathcal{P}_{ab}$ are the Maxwellian distribution of velocities normalized to unity [105]. Using the definition of the ensemble average, Eq. (2.15), the partial derivatives with respect to the momenta yield

$$\frac{\partial f_a(\mathbf{x},\mathbf{p},\boldsymbol{\omega}|V)}{\partial \mathbf{p}} = -\frac{\beta}{m_a}\mathbf{p} f_a(\mathbf{x},\mathbf{p},\boldsymbol{\omega}|V) \ , \tag{2.34}$$

$$\frac{\partial f_{ab}(\mathbf{x},\mathbf{p},\boldsymbol{\omega};\mathbf{x}',\mathbf{p}',\boldsymbol{\omega}'|V)}{\partial \mathbf{p}} = -\frac{\beta}{m_a}\mathbf{p} f_{ab}(\mathbf{x},\mathbf{p},\boldsymbol{\omega};\mathbf{x}',\mathbf{p}',\boldsymbol{\omega}'|V) \ . \tag{2.35}$$

Since the fluid is assumed to be in equilibrium there is no explicit time dependence of the distribution functions thus the partial derivatives with respect to t are zero. Substituting these results into Eq. (2.29) and integrating over the momenta $\mathbf{p}'$ yields

$$\begin{aligned}\frac{\mathbf{p}}{m_a}\cdot\left[\frac{\partial}{\partial \mathbf{x}} + \beta\frac{\partial V_a(\mathbf{x},\boldsymbol{\omega})}{\partial \mathbf{x}}\right] n_a(\mathbf{x},\boldsymbol{\omega}|V) \\ = -\beta\frac{\mathbf{p}}{m_a}\cdot\sum_b \int \frac{\partial \Phi_{ab}(\mathbf{x},\boldsymbol{\omega};\mathbf{x}',\boldsymbol{\omega}')}{\partial \mathbf{x}} n_{ab}(\mathbf{x},\boldsymbol{\omega};\mathbf{x}',\boldsymbol{\omega}'|V)d\mathbf{x}'d\boldsymbol{\omega}' \ .\end{aligned} \tag{2.36}$$

Since the momenta $\mathbf{p}$ is arbitrary, the equation can be rearranged to yield the first of the BBGKY hierarchy

$$\begin{aligned}\nabla \ln n_a(\mathbf{x},\boldsymbol{\omega}|V) = &- \beta\nabla V_a(\mathbf{x},\boldsymbol{\omega}) \\ &- \beta\sum_b \int d\mathbf{x}_1 d\boldsymbol{\omega}_1 \nabla\Phi_{ab}(\mathbf{x},\boldsymbol{\omega};\mathbf{x}_1,\boldsymbol{\omega}_1)\frac{n_{ba}(\mathbf{x}_1,\boldsymbol{\omega}_1;\mathbf{x},\boldsymbol{\omega}|V)}{n_a(\mathbf{x},\boldsymbol{\omega}|V)} \ .\end{aligned} \tag{2.37}$$

Similarly, this process can be repeated to obtain the second of the BBGKY hierarchy

$$\begin{aligned}\nabla \ln n_{ab}(\mathbf{x},\boldsymbol{\omega};\mathbf{x}',\boldsymbol{\omega}'|V) = &- \beta\nabla V_a(\mathbf{x},\boldsymbol{\omega}) - \beta\nabla\Phi_{ab}(\mathbf{x},\boldsymbol{\omega};\mathbf{x}',\boldsymbol{\omega}') \\ &- \beta\sum_c \int d\mathbf{x}_1 d\boldsymbol{\omega}_1 \nabla\Phi_{ac}(\mathbf{x},\boldsymbol{\omega};\mathbf{x}_1,\boldsymbol{\omega}_1) \\ &\times \frac{n_{cab}(\mathbf{x}_1,\boldsymbol{\omega}_1;\mathbf{x},\boldsymbol{\omega};\mathbf{x}',\boldsymbol{\omega}'|V)}{n_{ab}(\mathbf{x},\boldsymbol{\omega};\mathbf{x}',\boldsymbol{\omega}'|V)} \ .\end{aligned} \tag{2.38}$$

2.3 Electrostatic potential conditions

The one body potentials, $V_a(\mathbf{x}_1,\boldsymbol{\omega}_1)$, are written in the form

$$V_a(\mathbf{x}_1,\boldsymbol{\omega}_1) = V_a^S + V_a^E \ , \tag{2.39}$$

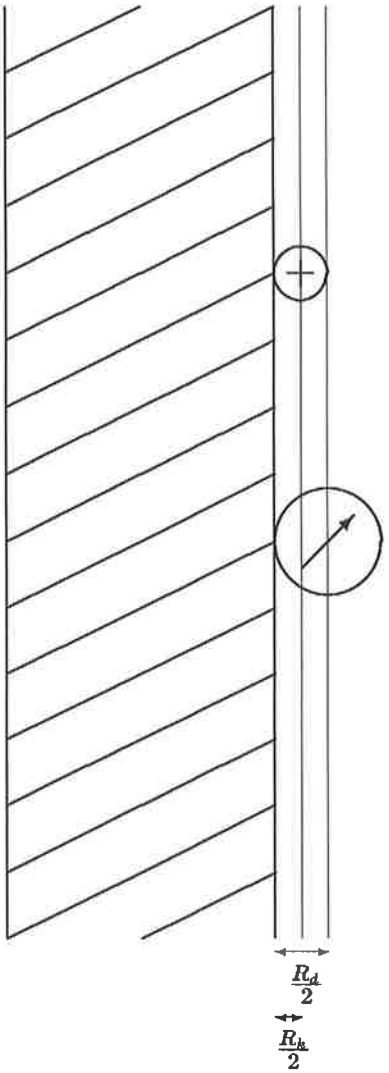

Figure 2.1: Schematic representation of the ion-dipole exclusion planes relative to a membrane wall.

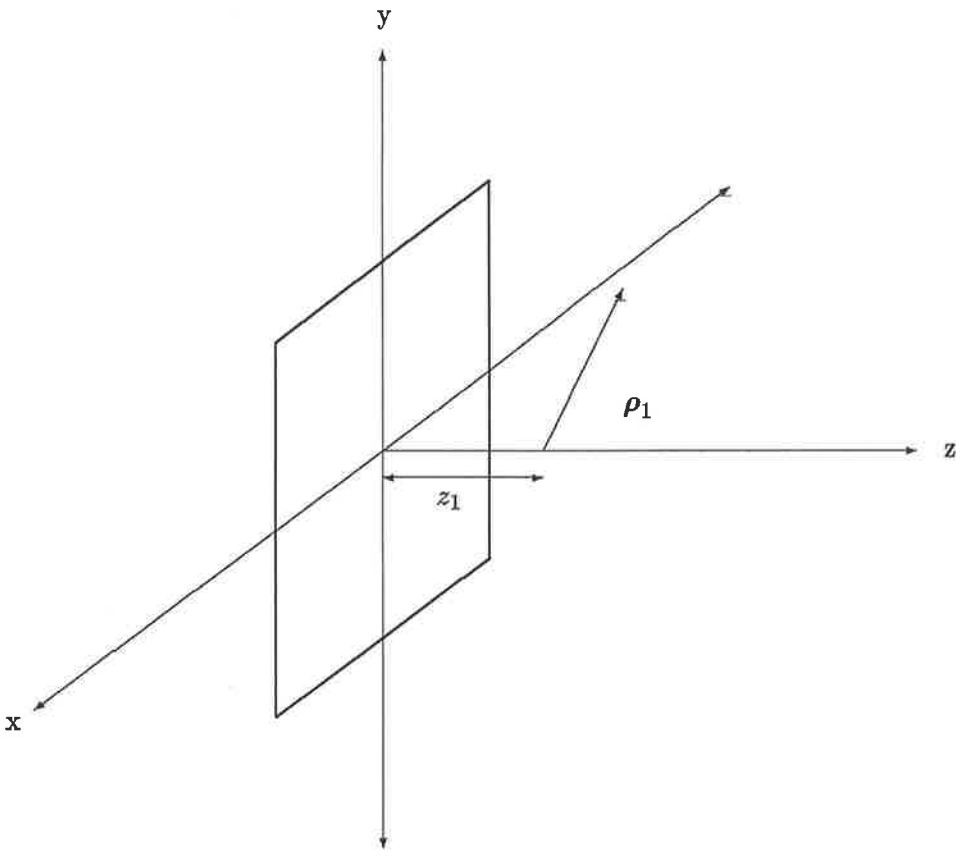

Figure 2.2: Interfacial wall geometry

where V_a^S is the short range contribution to the one body potential which models the exclusion of molecules from a region adjacent to the membrane wall. See Figure 2.1. The short range potential, V_a^S, is given by

$$V_a^S(\mathbf{x}_1, \boldsymbol{\omega}_1) = \begin{cases} \infty & \mid z_1 \mid < \frac{R_a}{2} \\ 0 & \mid z_1 \mid > \frac{R_a}{2} \end{cases} , \tag{2.40}$$

where z_1 is defined as the perpendicular distance from the membrane wall and R_a is the hard sphere diameter for the ath type of molecule. See Figure 2.2. The term V_a^E is the electrostatic contribution to the one body potential.

The two body (intermolecular) potentials, $\Phi_{ab}(\mathbf{x}_1, \boldsymbol{\omega}_1; \mathbf{x}_2, \boldsymbol{\omega}_2)$, are also written in the form

$$\Phi_{ab}(\mathbf{x}_1, \boldsymbol{\omega}_1; \mathbf{x}_2, \boldsymbol{\omega}_2) = \Phi_{ab}^S + \Phi_{ab}^E \ , \tag{2.41}$$

where Φ_{ab}^S is the short range contribution to the two body potential and is given by

$$\Phi_{ab}^S(\mathbf{x}_1, \boldsymbol{\omega}_1; \mathbf{x}_2, \boldsymbol{\omega}_2) \ = \ \begin{cases} \infty & r < R_{ab} \\ 0 & r > R_{ab} \end{cases} , \tag{2.42}$$

such that

$$R_{ab} = \frac{1}{2}(R_a + R_b) \ . \tag{2.43}$$

The other term, Φ_{ab}^E, is the electrostatic contribution which is defined by

$$\Phi_{ab}^E(\mathbf{x}_1, \boldsymbol{\omega}_1; \mathbf{x}_2, \boldsymbol{\omega}_2) = \Phi_{ab}^C + \Phi_{ab}^I \ , \tag{2.44}$$

where Φ_{ab}^I is the image potential due to the discontinuities in the dielectric tensor at the membrane walls and Φ_{ab}^C is the Coulombic potential. The one and two body potentials are derived and explicitly shown, for our model system(s), in Appendix A.

For the rest of the thesis let the subscripts i, j, k refer to the various ionic species and d to the dipoles with a, b, c referring to general molecules.

The mean electrostatic potential $\psi(\mathbf{x}_1)$ is defined by

$$\begin{aligned} e_i\psi(\mathbf{x}_1) = \quad & V_i^E(\mathbf{x}_1) + \sum_k \int d\mathbf{x}_3 \Phi_{ik}^E(\mathbf{x}_1, \mathbf{x}_3) n_k(\mathbf{x}_3 | V) \\ + \quad & \int d\boldsymbol{\omega}_3 d\mathbf{x}_3 \Phi_{id}^E(\mathbf{x}_1; \mathbf{x}_3, \boldsymbol{\omega}_3) n_d(\mathbf{x}_3, \boldsymbol{\omega}_3 | V) \ , \end{aligned} \tag{2.45}$$

where the first term is due to the external potential $V_i^E(\mathbf{x}_1)$ and the integral terms are the potential due to the distribution of molecules in the region. Related quantities are the mean electric field $\mathbf{E}(\mathbf{x}_1)$, which is defined by

$$\mathbf{E}(\mathbf{x}_1) = -\nabla_1 \psi(\mathbf{x}_1) \ , \tag{2.46}$$

and the polarization vector $\mathbf{P}(\mathbf{x}_1)$, defined by

$$\mathbf{P}(\mathbf{x}_1) = \int d\boldsymbol{\omega}_1 \mathbf{m}(\boldsymbol{\omega}_1) n_d(\mathbf{x}_1, \boldsymbol{\omega}_1 | V) \ . \tag{2.47}$$

The displacement vector $\mathbf{D}(\mathbf{x}_1)$ is then defined by

$$\mathbf{D}(\mathbf{x}_1) = 4\pi \mathbf{P}(\mathbf{x}_1) + \mathbf{E}(\mathbf{x}_1) \ . \tag{2.48}$$

Application of the Laplacian operator ∇_1^2 to Eq. (2.45) yields Poisson's equation

$$\nabla_1^2 \psi(\mathbf{x}_1) = -4\pi \sum_k e_k n_k(\mathbf{x}_1 | V) + 4\pi \nabla_1 \cdot \mathbf{P}(\mathbf{x}_1) \ . \tag{2.49}$$

From the expressions for the one and two body potentials for our model system(s) in Appendix A, the mean electrostatic potential (which is a function of the normal distance from the membrane wall) can be written, as derived by Outhwaite [93], in the form

$$\begin{aligned} \psi(z_1) = \ & - \ 4\pi \sum_k e_k \int_{max(\frac{R_k}{2}, z_1)} dz_3 (z_3 - z_1) n_k(z_3 | V) \\ & - \ 4\pi \int_{max(\frac{R_d}{2}, z_1)} dz_3 P(z_3) \ , \end{aligned} \tag{2.50}$$

such that

$$P(z_1) = \hat{\mathbf{z}} \cdot \mathbf{P}(\mathbf{x}_1) \ , \tag{2.51}$$

where $\hat{\mathbf{z}}$ is an unit vector, normal to the membrane wall. Differentiating this expression w.r.t. z_1 yields

$$\begin{aligned} \psi'(z_1) = \ & 4\pi \sum_k e_k \int_{max(\frac{R_k}{2}, z_1)} dz_3 n_k(z_3 | V) \\ & + \ 4\pi H(z_1 - \frac{R_d}{2}) P(z_1) \ , \end{aligned} \tag{2.52}$$

where $H(z_1)$ is the Heaviside (unit step) function. Thus the normal derivative of the mean electrostatic potential is discontinuous at the distance of closest approach of the dipoles to the walls. At $\frac{R_d}{2}$, the point of discontinuity, we have the following condition

$$\psi^{'}(z_1) \mid_{\frac{R_d^+}{2}} - \psi^{'}(z_1) \mid_{\frac{R_d^-}{2}} = 4\pi P(\frac{R_d}{2}) \ . \tag{2.53}$$

Outhwaite [94] has noted the difficulty in defining the dielectric tensor $\epsilon(\mathbf{x}_1)$. The dielectric tensor is usually defined by the macroscopic relationship between the mean electric field vector $\mathbf{E}(\mathbf{x}_1)$ and the polarization vector $\mathbf{P}(\mathbf{x}_1)$ such that

$$\begin{aligned} \mathbf{D}(\mathbf{x}_1) &= 4\pi\mathbf{P}(\mathbf{x}_1) + \mathbf{E}(\mathbf{x}_1) \\ &= \epsilon(\mathbf{x}_1) \cdot \mathbf{E}(\mathbf{x}_1) \ . \end{aligned} \tag{2.54}$$

This definition is only correct if the mean electric field is non zero. However, we see from Eq. (2.52), that the mean electric field and the polarization do not necessarily vanish simultaneously.

The surface charge density is related to the number density through

$$\sum_k \int dz_1 e_k n_k(z_1|V) = -\sigma \ , \tag{2.55}$$

which is the condition of electroneutrality over the interfacial regions.

We also define the mean electrostatic potential $\psi_b(\mathbf{x}_1; \mathbf{x}_2, \boldsymbol{\omega}_2)$ at $\mathbf{x}_1$, given a molecule of type b is fixed at $(\mathbf{x}_2, \boldsymbol{\omega}_2)$, by

$$\begin{aligned} e_i\psi_b(\mathbf{x}_1; \mathbf{x}_2, \boldsymbol{\omega}_2) = \quad & V_i^E(\mathbf{x}_1) + \Phi_{ib}^E(\mathbf{x}_1; \mathbf{x}_2, \boldsymbol{\omega}_2) \\ + \quad & \sum_k \int d\mathbf{x}_3 \Phi_{ik}^E(\mathbf{x}_1, \mathbf{x}_3) n_k(\mathbf{x}_3|V) g_{kb}(\mathbf{x}_3; \mathbf{x}_2, \boldsymbol{\omega}_2|V) \\ + \quad & \int d\boldsymbol{\omega}_3 d\mathbf{x}_3 \Phi_{id}^E(\mathbf{x}_1; \mathbf{x}_3, \boldsymbol{\omega}_3) n_d(\mathbf{x}_3, \boldsymbol{\omega}_3|V) g_{db}(\mathbf{x}_3, \boldsymbol{\omega}_3; \mathbf{x}_2, \boldsymbol{\omega}_2|V) \ , \end{aligned} \tag{2.56}$$

and the polarization vector $\mathbf{P}_b(\mathbf{x}_1; \mathbf{x}_2, \boldsymbol{\omega}_2)$, is defined by

$$\mathbf{P}_b(\mathbf{x}_1; \mathbf{x}_2, \boldsymbol{\omega}_2) = \int d\boldsymbol{\omega}_1 \mathbf{m}(\boldsymbol{\omega}_1) n_{db}(\mathbf{x}_1, \boldsymbol{\omega}_1; \mathbf{x}_2, \boldsymbol{\omega}_2|V) \ . \tag{2.57}$$

Thus the displacement vector $\mathbf{D}_b(\mathbf{x}_1;\mathbf{x}_2,\boldsymbol{\omega}_2)$ at $\mathbf{x}_1$, given a molecule of type b is fixed at $(\mathbf{x}_2,\boldsymbol{\omega}_2)$, is given by

$$\mathbf{D}_b(\mathbf{x}_1;\mathbf{x}_2,\boldsymbol{\omega}_2) = 4\pi\mathbf{P}_b(\mathbf{x}_1;\mathbf{x}_2,\boldsymbol{\omega}_2) - \nabla_1\psi_b(\mathbf{x}_1;\mathbf{x}_2,\boldsymbol{\omega}_2) \ . \tag{2.58}$$

The difference between $\psi_b(\mathbf{x}_1;\mathbf{x}_2,\boldsymbol{\omega}_2)$ and $\psi(\mathbf{x}_1)$ is defined to be the mean electrostatic fluctuation potential $\bar{\psi}_b(\mathbf{x}_1;\mathbf{x}_2,\boldsymbol{\omega}_2)$:

$$\begin{aligned} e_i\bar{\psi}_b(\mathbf{x}_1;\mathbf{x}_2,\boldsymbol{\omega}_2) \equiv & \quad e_i\psi_b(\mathbf{x}_1;\mathbf{x}_2,\boldsymbol{\omega}_2) - e_i\psi(\mathbf{x}_1) \\ = & \quad \Phi^E_{ib}(\mathbf{x}_1;\mathbf{x}_2,\boldsymbol{\omega}_2) \\ & + \sum_k \int d\mathbf{x}_3 \Phi^E_{ik}(\mathbf{x}_1,\mathbf{x}_3) n_k(\mathbf{x}_3|V) h_{kb}(\mathbf{x}_3;\mathbf{x}_2,\boldsymbol{\omega}_2|V) \\ & + \int d\boldsymbol{\omega}_3 d\mathbf{x}_3 \Phi^E_{id}(\mathbf{x}_1;\mathbf{x}_3,\boldsymbol{\omega}_3) n_d(\mathbf{x}_3,\boldsymbol{\omega}_3|V) h_{db}(\mathbf{x}_3,\boldsymbol{\omega}_3;\mathbf{x}_2,\boldsymbol{\omega}_2|V) \ . \end{aligned} \tag{2.59}$$

The boundary conditions that must be satisfied by the mean electrostatic potential and the mean electrostatic fluctuation potential will be discussed in Section 2.4, for the relevant cases of point and the more general hard sphere ion-dipole system.

2.4 Number densities

In this section we evaluate, with the help of Loeb's closure, from the BBGKY hierarchy the number densities for the hard sphere and point ion-dipole model systems from the potentials defined in the previous section.

2.4.1 Hard-Sphere system

The first of the BBGKY hierarchy, Eq. (2.37), can be written as

$$\begin{aligned} \nabla_1 \ln n_a(\mathbf{x}_1,\boldsymbol{\omega}_1|V) = & \ - \ \beta\nabla_1 V_a(\mathbf{x}_1,\boldsymbol{\omega}_1) \\ & - \ \beta \sum_c \int d\mathbf{x}_3 d\boldsymbol{\omega}_3 \nabla_1 \Phi_{ac}(\mathbf{x}_1,\boldsymbol{\omega}_1;\mathbf{x}_3,\boldsymbol{\omega}_3) \\ & \times \ n_c(\mathbf{x}_3,\boldsymbol{\omega}_3|V) g_{ca}(\mathbf{x}_3,\boldsymbol{\omega}_3;\mathbf{x}_1,\boldsymbol{\omega}_1|V) \ . \end{aligned} \tag{2.60}$$

Application of the operator $-\beta\nabla_1$ to the mean electrostatic potential, Eq. (2.45), yields

$$-\beta\nabla_1 e_i\psi(\mathbf{x}_1) = \ - \ \beta\nabla_1 V_i^E(\mathbf{x}_1)$$

$$- \beta \sum_c \int d\boldsymbol{\omega}_3 d\mathbf{x}_3 \nabla_1 \Phi^E_{ic}(\mathbf{x}_1; \mathbf{x}_3, \boldsymbol{\omega}_3) n_c(\mathbf{x}_3, \boldsymbol{\omega}_3 | V) \ . \qquad (2.61)$$

Setting molecule a to be an ion in Eq. (2.60) and subtracting Eq. (2.61) from Eq. (2.60) results in

$$\begin{aligned} \nabla_1 \ln n_i(\mathbf{x}_1|V) = & - \beta \nabla_1 e_i \psi(\mathbf{x}_1) - \beta \nabla_1 V_i^S(\mathbf{x}_1) - \nabla_1 \ln \tau_i \\ & - \beta \sum_c \int d\mathbf{x}_3 d\boldsymbol{\omega}_3 \nabla_1 \Phi^E_{ic}(\mathbf{x}_1; \mathbf{x}_3, \boldsymbol{\omega}_3) n_c(\mathbf{x}_3, \boldsymbol{\omega}_3 | V) h_{ci}(\mathbf{x}_3, \boldsymbol{\omega}_3; \mathbf{x}_1 | V) \ , \end{aligned} \qquad (2.62)$$

where

$$\nabla_1 \ln \tau_a = -\beta \sum_c \int d\mathbf{x}_3 d\boldsymbol{\omega}_3 \nabla_1 \Phi^S_{ac}(\mathbf{x}_1, \boldsymbol{\omega}_1; \mathbf{x}_3, \boldsymbol{\omega}_3) n_c(\mathbf{x}_3, \boldsymbol{\omega}_3 | V) g_{ca}(\mathbf{x}_3, \boldsymbol{\omega}_3; \mathbf{x}_1, \boldsymbol{\omega}_1 | V) \ , \qquad (2.63)$$

is an exclusion volume type term as it contains the short range contribution from the two body potentials [93], [92].

Application of the operator $-\beta \nabla_1 \frac{1}{e_i} \mathbf{m}(\boldsymbol{\omega}_1) \cdot \nabla_1$ to the mean electrostatic potential, Eq. (2.45), yields

$$\begin{aligned} -\beta \nabla_1 \mathbf{m}(\boldsymbol{\omega}_1) \cdot \nabla_1 \psi(\mathbf{x}_1) = & - \beta \nabla_1 V_d^E(\mathbf{x}_1, \boldsymbol{\omega}_1) \\ & - \beta \sum_c \int d\boldsymbol{\omega}_3 d\mathbf{x}_3 \nabla_1 \Phi^E_{ic}(\mathbf{x}_1; \mathbf{x}_3, \boldsymbol{\omega}_3) n_c(\mathbf{x}_3, \boldsymbol{\omega}_3 | V) \ . \end{aligned} \qquad (2.64)$$

Setting molecule a to be an dipole in Eq. (2.60) and subtracting Eq. (2.64) from Eq. (2.60) results in

$$\begin{aligned} \nabla_1 \ln n_d(\mathbf{x}_1, \boldsymbol{\omega}_1 | V) = & - \beta \nabla_1 \mathbf{m}(\boldsymbol{\omega}_1) \cdot \nabla_1 \psi(\mathbf{x}_1) - \beta \nabla_1 V_d^S(\mathbf{x}_1) - \nabla_1 \ln \tau_d \\ & - \beta \sum_c \int d\mathbf{x}_3 d\boldsymbol{\omega}_3 \nabla_1 \Phi^E_{dc}(\mathbf{x}_1, \boldsymbol{\omega}_1; \mathbf{x}_3, \boldsymbol{\omega}_3) \\ & \times \ n_c(\mathbf{x}_3, \boldsymbol{\omega}_3 | V) h_{cd}(\mathbf{x}_3, \boldsymbol{\omega}_3; \mathbf{x}_1, \boldsymbol{\omega}_1 | V) \ . \end{aligned} \qquad (2.65)$$

Eq. (2.62) and Eq. (2.65) are exact equations. However, we need some ansatz for the indirect correlation functions h_{cb} to close this set of equations. In the limit that the external field approaches zero, both the number density and indirect correlation functions

reduce to their homogeneous (zero field) values, i.e. as $V \rightarrow 0$

$$n_a(\mathbf{x}_1, \boldsymbol{\omega}_1|V) \rightarrow n_a(\mathbf{x}_1, \boldsymbol{\omega}_1|0) \ , \tag{2.66}$$

$$h_{ab}(\mathbf{x}_1, \boldsymbol{\omega}_1; \mathbf{x}_2, \boldsymbol{\omega}_2|V) \rightarrow h_{ab}(\mathbf{x}_1, \boldsymbol{\omega}_1; \mathbf{x}_2, \boldsymbol{\omega}_2|0) \ , \tag{2.67}$$

provided the distance between the membrane walls is large compared with the Debye length [106]. In a neuron this is the case. Thus, a first approximation is to assume that the indirect correlation function takes the homogeneous (bulk) values for the entire region that the fluid occupies. Since the homogeneous indirect correlation function is only a function of the relative distance of the field point to the source point, there is no dependence in the indirect correlation function on the relative distance of the source and field point to the membrane wall(s). Obviously, the approximation deviates more from the actual distribution as the source and/or field point approaches a membrane wall (i.e within one to two Debye lengths). Despite this limitation, the approximation has the correct limiting value for large distances away from the membrane wall(s) and can be used to start an iterative procedure to determine a more accurate approximation for the indirect correlation function [94].

Since the homogeneous values are spherically symmetric, the angular integrals in the right hand side of Eq. (2.62) and Eq. (2.65) will vanish. Thus

$$\nabla_1[\ln n_i(\mathbf{x}_1|V) + \beta e_i \psi(\mathbf{x}_1)] = -\beta \nabla_1 V_i^S(\mathbf{x}_1) \ , \tag{2.68}$$

$$\nabla_1[\ln n_d(\mathbf{x}_1, \boldsymbol{\omega}_1|V) + \beta \mathbf{m}(\boldsymbol{\omega}_1) \cdot \nabla_1 \psi(\mathbf{x}_1)] = -\beta \nabla_1 V_d^S(\mathbf{x}_1, \boldsymbol{\omega}_1) \ . \tag{2.69}$$

Use of the boundary condition that the number densities must approach their homogeneous value for large distances from the membrane wall i.e.

$$n_i(\mathbf{x}_1|V) \rightarrow n_i^0 \text{ as } |\, z_1 \,| \rightarrow \infty \ , \tag{2.70}$$

$$n_d(\mathbf{x}_1, \boldsymbol{\omega}_1|V) \rightarrow \frac{n_d^0}{4\pi} \text{ as } |\, z_1 \,| \rightarrow \infty \ , \tag{2.71}$$

which is consistent with setting the external potential equivalently to zero. Thus Eq. (2.68) and Eq. (2.69) integrate to

$$n_i(\mathbf{x}_1|V) = n_i^0 H(z_1 - \frac{R_i}{2}) \exp\Big[-\beta e_i[\psi(\mathbf{x}_1) - \psi^B]\Big] \ , \tag{2.72}$$

$$n_d(\mathbf{x}_1,\boldsymbol{\omega}_1|V) \;=\; \frac{n_d^0}{4\pi}H(z_1-\frac{R_d}{2})\exp\Big[-\beta\mathbf{m}(\boldsymbol{\omega}_1)\cdot\nabla_1[\psi(\mathbf{x}_1)-\psi^B]\Big]\;, \qquad (2.73)$$

where ψ^B is the constant background potential. The functions $n_i^0 H(z_1-\frac{R_i}{2})$ and $\frac{n_d^0}{4\pi}H(z_1-\frac{R_d}{2})$ are approximates to the exclusion volume term when the indirect correlation function has its bulk value [93], [92].

These results for the number densities can now be substituted into Poisson's equation, Eq. (2.49), the angular integration performed by the expansion of the exponential terms to first order in the mean electrostatic potential and use of the fact that the external potential is only a function of the normal distance z_1 to yield

$$\begin{aligned}\Big[1+H(z_1-\frac{R_d}{2})3y\Big]\psi''(z_1) = \;&-\; 4\pi\sum_k H(z_1-\frac{R_k}{2})n_k^0 e_k\exp[\beta e_k\psi^B]\\ &+\; 4\pi\beta\sum_k H(z_1-\frac{R_k}{2})n_k^0 e_k^2\exp[\beta e_k\psi^B]\psi(z_1)\;, \qquad (2.74)\end{aligned}$$

where

$$y=\frac{4\pi}{9}\beta m^2 n_d^0\;. \qquad (2.75)$$

The mean electrostatic potential boundary conditions for the hard sphere system are

$$\psi(\mathbf{x}_1)\;\text{ continuous}, \qquad (2.76)$$

$$\psi(\mathbf{x}_1)\to\psi^B \;\text{ as }\; |\,z_1\,|\to\infty\;, \qquad (2.77)$$

$$\mathbf{D}(\mathbf{x}_1)\cdot\hat{\mathbf{z}}\,|_{z_1^+} \;-\; \mathbf{D}(\mathbf{x}_1)\cdot\hat{\mathbf{z}}\,|_{z_1^-}=4\pi\sigma \qquad (2.78)$$

at the membrane walls, and

$$\psi'(z_1)\,|_{\frac{R_d^+}{2}} - \psi'(z_1)\,|_{\frac{R_d^-}{2}} = P(\frac{R_d}{2}) \qquad (2.79)$$

at distance $\frac{R_d}{2}$ from the membrane walls.

The first three boundary conditions are the usual conditions associated with the mean electrostatic potential for a point system. The last condition, Eq. (2.79), was derived in the previous section, Eq. (2.53), and is particular to a hard sphere system [93].

For the last boundary condition, we calculate the polarization in the normal direction at the dipole exclusion plane in the following manner. Substitution of the dipole number

density, in terms of the mean electrostatic potential, Eq. (2.73), into the definition for the polarization vector, Eq. (2.47), we obtain

$$\mathbf{P}(\mathbf{x}_1) = \frac{n_d^0}{4\pi} H(z_1 - \frac{R_d}{2}) \int d\boldsymbol{\omega}_1 \mathbf{m}(\boldsymbol{\omega}_1) \exp\Big[-\beta \mathbf{m}(\boldsymbol{\omega}_1) \cdot \nabla_1 [\psi(\mathbf{x}_1) - \psi^B]\Big] \ . \tag{2.80}$$

Only the normal component will contribute to the polarization. Thus the angular integral is of the form $I = 2\pi \int_0^\pi d\theta_1 \sin\theta_1 m \cos\theta_1 \exp[-\beta m \cos\theta_1 \psi'(z_1)]$. This integral can be evaluated to yield

$$\begin{aligned} I &= -\frac{4\pi}{\beta m \psi'(z_1)} \frac{d}{d\beta} \left[\frac{\sinh[\beta m \psi'(z_1)]}{\beta m \psi'(z_1)}\right] \\ &\approx -\frac{4\pi}{3} \beta m^2 \psi'(z_1) \ . \end{aligned} \tag{2.81}$$

This linear approximation to the angular integral is substituted into Eq. (2.80), to yield

$$4\pi \mathbf{P}(\mathbf{x}_1) \cdot \hat{\mathbf{z}} = -H(z_1 - \frac{R_d}{2})[\epsilon - 1]\psi'(z_1) \ . \tag{2.82}$$

We define the inverse Debye length κ as

$$\begin{aligned} \kappa^2 &= \frac{4\pi\beta}{\epsilon} \sum_k e_k^2 n_k^0 \exp[\beta e_k \psi^B] \\ &\approx \frac{4\pi\beta}{\epsilon} \sum_k e_k^2 n_k^0 \ , \end{aligned} \tag{2.83}$$

and the background potential ψ^B by

$$\begin{aligned} \psi^B &= \frac{4\pi}{\epsilon\kappa^2} \sum_k e_k n_k^0 \exp[\beta e_k \psi^B] \\ &\approx \frac{4\pi}{\epsilon\kappa^2} \sum_k e_k n_k^0 \ , \end{aligned} \tag{2.84}$$

where we have assumed $\mid \beta e_k \psi^B \mid \ll 1$ and for convenience we define the dielectric constant in the usual form

$$\epsilon \equiv [1 + 3y] \ . \tag{2.85}$$

It should be noted that the summation for ψ^B is over all the ionic species (mobile and fixed) whereas the summation for the inverse Debye length κ is restricted to the mobile ionic species. To simplify the model we assume that all the ionic species have the same hard sphere diameter R_i.

Thus the differential equation for the mean electrostatic potential for a hard sphere system is given by

$$\Big[1+H(z_1-\frac{R_d}{2})3y\Big]\psi^{''}(z_1)-\epsilon\kappa^2H(z_1-\frac{R_i}{2})\psi(z_1)=-\kappa^2\epsilon H(z_1-\frac{R_i}{2})\psi^B \quad . \tag{2.86}$$

This differential equation reduces to the usual linearized GC differential equation for the mean electrostatic potential, [93], when the bulk electroneutrality condition is satisfied i.e. $\sum_k e_k n_k^0 = 0$.

2.4.2 Point system

The equations for the number densities and the mean electrostatic potential in the point system, can be obtained by setting the hard sphere diameters to zero for all molecules. Thus the relationships between the number densities and the mean electrostatic potential are given by

$$n_i(\mathbf{x}_1|V) = n_i^0 \exp\Big[-\beta e_i[\psi(\mathbf{x}_1)-\psi^B]\Big] \ , \tag{2.87}$$

$$n_d(\mathbf{x}_1,\boldsymbol{\omega}_1|V) = \frac{n_d^0}{4\pi}\exp\Big[-\beta\mathbf{m}(\boldsymbol{\omega}_1)\cdot\nabla_1[\psi(\mathbf{x}_1)-\psi^B]\Big] \ , \tag{2.88}$$

and the differential equation satisfied by the mean electrostatic potential is given by

$$\psi^{''}(z_1)-\kappa^2\psi(z_1)=-\kappa^2\psi^B \quad . \tag{2.89}$$

The mean electrostatic potential for the point system has the usual boundary conditions [93] of

$$\psi(\mathbf{x}_1) \ \text{ continuous}, \tag{2.90}$$

$$\psi(\mathbf{x}_1)\rightarrow\psi^B \quad \text{as} \quad |\,z_1\,|\rightarrow\infty, \tag{2.91}$$

and

$$\mathbf{D}(\mathbf{x}_1)\cdot\hat{\mathbf{z}}\,|_{z_1^+} - \mathbf{D}(\mathbf{x}_1)\cdot\hat{\mathbf{z}}\,|_{z_1^-} = 4\pi\sigma \tag{2.92}$$

at the membrane walls.

2.5 Indirect correlation functions

In this section we evaluate, with the help of Loeb's closure, from the BBGKY hierarchy the indirect correlation functions for the hard sphere and point ion-dipole model systems from the potentials defined in Section 2.3.

2.5.1 Hard-Sphere system

The second of the BBGKY hierarchy, Eq. (2.38), can be written as

$$\begin{aligned}\nabla_1 \ln n_{ab}(\mathbf{x}_1,\boldsymbol{\omega}_1;\mathbf{x}_2,\boldsymbol{\omega}_2|V) = & - \beta\nabla_1 V_a(\mathbf{x}_1,\boldsymbol{\omega}_1) - \beta\nabla_1\Phi_{ab}(\mathbf{x}_1,\boldsymbol{\omega}_1;\mathbf{x}_2,\boldsymbol{\omega}_2) \\ & - \beta\sum_c \int d\mathbf{x}_3 d\boldsymbol{\omega}_3 \nabla_1\Phi_{ac}(\mathbf{x}_1,\boldsymbol{\omega}_1;\mathbf{x}_3,\boldsymbol{\omega}_3) \\ & \times \frac{n_{cab}(\mathbf{x}_1,\boldsymbol{\omega}_1;\mathbf{x}_3,\boldsymbol{\omega}_3;\mathbf{x}_2,\boldsymbol{\omega}_2|V)}{n_{ab}(\mathbf{x}_1,\boldsymbol{\omega}_1;\mathbf{x}_2,\boldsymbol{\omega}_2|V)} \ . \end{aligned} \tag{2.93}$$

This equation is closed by using the Kirkwood superposition approximation

$$\begin{aligned}\frac{n_{cab}(\mathbf{x}_1,\boldsymbol{\omega}_1;\mathbf{x}_3,\boldsymbol{\omega}_3;\mathbf{x}_2,\boldsymbol{\omega}_2|V)}{n_{ab}(\mathbf{x}_1,\boldsymbol{\omega}_1;\mathbf{x}_2,\boldsymbol{\omega}_2|V)} = & \quad n_c(\mathbf{x}_3,\boldsymbol{\omega}_3|V) g_{ac}(\mathbf{x}_1,\boldsymbol{\omega}_1;\mathbf{x}_3,\boldsymbol{\omega}_3|V) \\ & \times \ g_{cb}(\mathbf{x}_3,\boldsymbol{\omega}_3;\mathbf{x}_2,\boldsymbol{\omega}_2|V) \ , \end{aligned} \tag{2.94}$$

which is substituted into, Eq. (2.93), to yield

$$\begin{aligned}\nabla_1 \ln n_{ab} = & - \beta\nabla_1 V_a(\mathbf{x}_1,\boldsymbol{\omega}_1) - \beta\nabla_1\Phi_{ab}(\mathbf{x}_1,\boldsymbol{\omega}_1;\mathbf{x}_2,\boldsymbol{\omega}_2) \\ & - \beta\sum_c \int d\mathbf{x}_3 d\boldsymbol{\omega}_3 \nabla_1\Phi_{ac}(\mathbf{x}_1,\boldsymbol{\omega}_1;\mathbf{x}_3,\boldsymbol{\omega}_3) n_c(\mathbf{x}_3,\boldsymbol{\omega}_3|V) \\ & \times \ g_{ac}(\mathbf{x}_1,\boldsymbol{\omega}_1;\mathbf{x}_3,\boldsymbol{\omega}_3|V) g_{cb}(\mathbf{x}_3,\boldsymbol{\omega}_3;\mathbf{x}_2,\boldsymbol{\omega}_2|V) \ . \end{aligned} \tag{2.95}$$

Also the left hand side of Eq. (2.95) can be written in terms of the pair correlation function and the number density resulting in

$$\begin{aligned}\nabla_1 \ln n_{ab}(\mathbf{x}_1,\boldsymbol{\omega}_1;\mathbf{x}_2,\boldsymbol{\omega}_2|V) &= \nabla_1 \ln\Big[n_a(\mathbf{x}_1,\boldsymbol{\omega}_1|V) n_b(\mathbf{x}_2,\boldsymbol{\omega}_2|V) g_{ab}(\mathbf{x}_1,\boldsymbol{\omega}_1;\mathbf{x}_2,\boldsymbol{\omega}_2|V)\Big] \\ &= \nabla_1 \ln n_a(\mathbf{x}_1,\boldsymbol{\omega}_1|V) + \nabla_1 \ln g_{ab}(\mathbf{x}_1,\boldsymbol{\omega}_1;\mathbf{x}_2,\boldsymbol{\omega}_2|V) \ , \end{aligned} \tag{2.96}$$

and then Eq. (2.60) can be substituted for the number density to yield

$$\begin{aligned}\nabla_1 \ln g_{ab} = & - \beta\nabla_1\Phi_{ab}(\mathbf{x}_1,\boldsymbol{\omega}_1;\mathbf{x}_2,\boldsymbol{\omega}_2) \\ & - \beta\sum_c \int d\mathbf{x}_3 d\boldsymbol{\omega}_3 \nabla_1\Phi_{ac}(\mathbf{x}_1,\boldsymbol{\omega}_1;\mathbf{x}_3,\boldsymbol{\omega}_3) n_c(\mathbf{x}_3,\boldsymbol{\omega}_3|V) \\ & \times \ g_{ac}(\mathbf{x}_1,\boldsymbol{\omega}_1;\mathbf{x}_3,\boldsymbol{\omega}_3|V) h_{cb}(\mathbf{x}_3,\boldsymbol{\omega}_3;\mathbf{x}_2,\boldsymbol{\omega}_2|V) \ . \end{aligned} \tag{2.97}$$

Setting the molecule a to be an ion and a dipole respectively in Eq. (2.97) and substituting for the electrostatic component of the intermolecular potential Φ^E using Eq. (2.59), yields

$$\begin{aligned}
\nabla_1 \ln g_{ib} = & - \beta\nabla_1\Phi^S_{ib}(\mathbf{x}_1;\mathbf{x}_2,\boldsymbol{\omega}_2) - \beta\nabla_1 e_i\bar{\psi}_b(\mathbf{x}_1;\mathbf{x}_2,\boldsymbol{\omega}_2) \\
& - \beta\sum_c \int d\mathbf{x}_3 d\boldsymbol{\omega}_3 \nabla_1\Phi^S_{ic}(\mathbf{x}_1;\mathbf{x}_3,\boldsymbol{\omega}_3) n_c(\mathbf{x}_3,\boldsymbol{\omega}_3|V) \\
& \times g_{ic}(\mathbf{x}_1;\mathbf{x}_3,\boldsymbol{\omega}_3|V) h_{cb}(\mathbf{x}_3,\boldsymbol{\omega}_3;\mathbf{x}_2,\boldsymbol{\omega}_2|V) \\
& - \beta\sum_c \int d\mathbf{x}_3 d\boldsymbol{\omega}_3 \nabla_1\Phi^E_{ic}(\mathbf{x}_1;\mathbf{x}_3,\boldsymbol{\omega}_3) n_c(\mathbf{x}_3,\boldsymbol{\omega}_3|V) \\
& \times h_{ic}(\mathbf{x}_1;\mathbf{x}_3,\boldsymbol{\omega}_3|V) h_{cb}(\mathbf{x}_3,\boldsymbol{\omega}_3;\mathbf{x}_2,\boldsymbol{\omega}_2|V) \ , \qquad (2.98)
\end{aligned}$$

and

$$\begin{aligned}
\nabla_1 \ln g_{db} = & - \beta\nabla_1\Phi^S_{dc}(\mathbf{x}_1,\boldsymbol{\omega}_1;\mathbf{x}_3,\boldsymbol{\omega}_3) - \beta\nabla_1\mathbf{m}(\boldsymbol{\omega}_1)\cdot\nabla_1\bar{\psi}_b(\mathbf{x}_1;\mathbf{x}_2,\boldsymbol{\omega}_2) \\
& - \beta\sum_c \int d\mathbf{x}_3 d\boldsymbol{\omega}_3 \nabla_1\Phi^S_{dc}(\mathbf{x}_1,\boldsymbol{\omega}_1;\mathbf{x}_3,\boldsymbol{\omega}_3) n_c(\mathbf{x}_3,\boldsymbol{\omega}_3|V) \\
& \times g_{dc}(\mathbf{x}_1,\boldsymbol{\omega}_1;\mathbf{x}_3,\boldsymbol{\omega}_3|V) h_{cb}(\mathbf{x}_3,\boldsymbol{\omega}_3;\mathbf{x}_2,\boldsymbol{\omega}_2|V) \\
& - \beta\sum_c \int d\mathbf{x}_3 d\boldsymbol{\omega}_3 \nabla_1\Phi^E_{dc}(\mathbf{x}_1,\boldsymbol{\omega}_1;\mathbf{x}_3,\boldsymbol{\omega}_3) n_c(\mathbf{x}_3,\boldsymbol{\omega}_3|V) \\
& \times h_{dc}(\mathbf{x}_1,\boldsymbol{\omega}_1;\mathbf{x}_3,\boldsymbol{\omega}_3|V) h_{cb}(\mathbf{x}_3,\boldsymbol{\omega}_3;\mathbf{x}_2,\boldsymbol{\omega}_2|V) \ . \qquad (2.99)
\end{aligned}$$

As a first approximation we use Loeb's closure [107], which neglects the integral terms in both Eq. (2.98) and Eq. (2.99), to upon integration

$$g_{ib} = H(r_{12} - \frac{R_{ib}}{2}) \exp[-\beta e_i\bar{\psi}_b(\mathbf{x}_1;\mathbf{x}_2,\boldsymbol{\omega}_2)] \ , \qquad (2.100)$$

$$g_{db} = H(r_{12} - \frac{R_{db}}{2}) \exp[-\beta\mathbf{m}(\boldsymbol{\omega}_1)\cdot\nabla_1\bar{\psi}_b(\mathbf{x}_1;\mathbf{x}_2,\boldsymbol{\omega}_2)] \ , \qquad (2.101)$$

where we have used the boundary condition that

$$\bar{\psi}_b(\mathbf{x}_1;\mathbf{x}_2,\boldsymbol{\omega}_2) \to 0 \ \text{ as } \ | z_1 | \to \infty \ . \qquad (2.102)$$

This closure approximates the exclusion volume term between the two molecules by the Heaviside function. Thus the indirect correlation functions are defined by

$$h_{ib} = H(r_{12} - \frac{R_{ib}}{2}) \exp[-\beta e_i\bar{\psi}_b(\mathbf{x}_1;\mathbf{x}_2,\boldsymbol{\omega}_2)] - 1 \ , \qquad (2.103)$$

$$h_{db} = H(r_{12} - \frac{R_{db}}{2}) \exp[-\beta\mathbf{m}(\boldsymbol{\omega}_1)\cdot\nabla_1\bar{\psi}_b(\mathbf{x}_1;\mathbf{x}_2,\boldsymbol{\omega}_2)] - 1 \ . \qquad (2.104)$$

These results are then substituted into Eq. (2.59) for the mean electrostatic fluctu. potential and the Laplacian operator ∇_1^2 applied to yield

$$\begin{aligned}
\nabla_1^2 e_i\bar{\psi}_b = \quad & \nabla_1^2\Phi_{ib}^E(\mathbf{x}_1;\mathbf{x}_2,\boldsymbol{\omega}_2) \\
- \quad & 4\pi e_i\sum_k e_k n_k(\mathbf{x}_1|V)\Big[H(r_{12}-\frac{R_{kb}}{2})\exp[-\beta e_k\bar{\psi}_b(\mathbf{x}_1;\mathbf{x}_2,\boldsymbol{\omega}_2)]-1\Big] \\
+ \quad & 4\pi e_i\nabla_1\cdot\int d\boldsymbol{\omega}_3\mathbf{m}(\boldsymbol{\omega}_3)n_d(\mathbf{x}_1,\boldsymbol{\omega}_3|V) \\
\times \quad & \Big[H(r_{12}-\frac{R_{db}}{2})\exp[-\beta\mathbf{m}(\boldsymbol{\omega}_3)\cdot\nabla_1\bar{\psi}_b(\mathbf{x}_1;\mathbf{x}_2,\boldsymbol{\omega}_2)]-1\Big] \ . \qquad (2.105)
\end{aligned}$$

To simplify Eq. (2.105) we expand to first order in the mean electrostatic fluctuation potential, substitute for the dipole number density and perform the angular integration over $\boldsymbol{\omega}_3$, to yield

$$\begin{aligned}
\nabla_1^2 e_i\bar{\psi}_b = \quad & \nabla_1^2\Phi_{ib}^E(\mathbf{x}_1;\mathbf{x}_2,\boldsymbol{\omega}_2) \\
- \quad & 4\pi e_i\sum_k e_k n_k(\mathbf{x}_1|V)\Big[H(r_{12}-\frac{R_{kb}}{2})-1\Big] \\
+ \quad & 4\pi\beta e_i\sum_k e_k^2 n_k(\mathbf{x}_1|V)H(r_{12}-\frac{R_{kb}}{2})\bar{\psi}_b(\mathbf{x}_1,\mathbf{x}_2) \\
+ \quad & e_i\chi_b(\mathbf{x}_1,\mathbf{x}_2)\frac{\partial\bar{\psi}_b(\mathbf{x}_1;\mathbf{x}_2,\boldsymbol{\omega}_2)}{\partial z_1}+e_i\xi_i(\mathbf{x}_1;\mathbf{x}_2,\boldsymbol{\omega}_2)\frac{\partial^2\bar{\psi}_b(\mathbf{x}_1;\mathbf{x}_2,\boldsymbol{\omega}_2)}{\partial z_1^2} \\
+ \quad & e_i\nu_b(\mathbf{x}_1,\mathbf{x}_2)-e_i\eta_b(\mathbf{x}_1,\mathbf{x}_2)\nabla_1^2\bar{\psi}_b(\mathbf{x}_1;\mathbf{x}_2,\boldsymbol{\omega}_2) \ , \qquad (2.106)
\end{aligned}$$

where, by letting $\theta=\beta m\frac{d\psi}{dz_1}$, we have

$$\begin{aligned}
\nu_b(\mathbf{x}_1,\mathbf{x}_2) = \quad & - \quad 4\pi\Big[H(r_{12}-\frac{R_{db}}{2})-1\Big]n_d^0H(z_1-\frac{R_d}{2})m\frac{d\theta}{dz_1} \\
& \times \quad \Big[\frac{\theta(\theta^2+2)\sinh\theta-2\theta^2\cosh\theta}{\theta^4}\Big] \\
= \quad & O(\frac{d\theta}{dz_1}) \ , \qquad (2.107)
\end{aligned}$$

$$\begin{aligned}
\chi_b(\mathbf{x}_1,\mathbf{x}_2) = \quad & - \quad 4\pi\beta H(r_{12}-\frac{R_{db}}{2})n_d^0H(z_1-\frac{R_d}{2})m^2\frac{d\theta}{dz_1} \\
& \times \quad \Big[\frac{\theta(\theta^2+6)\cosh\theta-3(\theta^2+2)\sinh\theta}{\theta^4}\Big] \\
= \quad & O(\theta\frac{d\theta}{dz_1}) \ , \qquad (2.108) \\
\eta_b(\mathbf{x}_1,\mathbf{x}_2) = \quad & 4\pi\beta H(r_{12}-\frac{R_{db}}{2})n_d^0H(z_1-\frac{R_d}{2})m^2\Big[\frac{\theta\cosh\theta-\sinh\theta}{\theta^2}\Big] \\
= \quad & 3yH(r_{12}-\frac{R_{db}}{2})H(z_1-\frac{R_d}{2})+O(\theta^2) \ , \qquad (2.109)
\end{aligned}$$

$$\begin{aligned}\xi_b(\mathbf{x}_1,\mathbf{x}_2) &= 3\eta_b(\mathbf{x}_1,\mathbf{x}_2) - 4\pi\beta H(r_{12}-\frac{R_{db}}{2})n_d^0 H(z_1-\frac{R_d}{2})m^2\Big[\frac{\sinh\theta}{\theta}\Big] \\ &= O(\theta^2)\ . \end{aligned} \tag{2.110}$$

Compared to the corresponding equation derived by Outhwaite [94], [95], Eq. (2.106) has additional terms due to the violation of the bulk electroneutrality condition i.e. $\sum_k e_k n_k^0 \neq 0$.

If the second order terms $\chi_b(\mathbf{x}_1,\mathbf{x}_2)$, $\xi_b(\mathbf{x}_1,\mathbf{x}_2)$ in θ are neglected and expanding the other terms to first order in the mean electrostatic potential with the added assumption, $\mid \beta e_k \psi^B \mid \ll 1$, Eq. (2.106) reduces to

$$\begin{aligned} e_i\Big[1 &+ 3yH(r_{12}-\frac{R_{db}}{2})H(z_1-\frac{R_d}{2})\Big]\nabla_1^2\bar{\psi}_b \\ &- 4\pi\beta e_i\sum_k H(r_{12}-\frac{R_{kb}}{2})H(z_1-\frac{R_k}{2})e_k^2 n_k^0\Big[1-\beta e_k\psi\Big]\bar{\psi}_b \\ = &\quad \nabla_1^2\Phi_{ib}^E(\mathbf{x}_1;\mathbf{x}_2,\omega_2) \\ &- 4\pi e_i\sum_k\Big[H(r_{12}-\frac{R_{kb}}{2})-1\Big]H(z_1-\frac{R_k}{2})e_k n_k^0\Big[1-\beta e_k\psi\Big] \\ &+ e_i 3y\Big[H(r_{12}-\frac{R_{db}}{2})-1\Big]H(z_1-\frac{R_d}{2})\frac{d^2\psi}{dz_1^2}\ . \end{aligned} \tag{2.111}$$

The boundary conditions associated with the differential equation for the mean electrostatic fluctuation potential are

$$\bar{\psi}_b(\mathbf{x}_1;\mathbf{x}_2,\omega_2) \to 0 \text{ as } \mid \mathbf{x}_2-\mathbf{x}_1 \mid \to \infty\ , \tag{2.112}$$

with $\bar{\psi}_b(\mathbf{x}_1;\mathbf{x}_2,\omega_2)$ continuous everywhere except for

$$e_i\bar{\psi}_b(\mathbf{x}_1;\mathbf{x}_2,\omega_2) \to \Phi_{ib}^E(\mathbf{x}_1;\mathbf{x}_2,\omega_2) \quad \text{as} \quad \mid \mathbf{x}_2-\mathbf{x}_1 \mid \to 0\ , \tag{2.113}$$

$$\epsilon(\mathbf{x}_1)\cdot\nabla_1\bar{\psi}_b(\mathbf{x}_1;\mathbf{x}_2,\omega_2)\cdot\hat{\mathbf{z}}\mid_{z_1^-} = \epsilon(\mathbf{x}_1)\cdot\nabla_1\bar{\psi}_b(\mathbf{x}_1;\mathbf{x}_2,\omega_2)\cdot\hat{\mathbf{z}}\mid_{z_1^+}\ , \tag{2.114}$$

at the membrane walls, and

$$-\hat{\mathbf{z}}\cdot\nabla_1\Big[\bar{\psi}_b(\mathbf{x}_1;\mathbf{x}_2,\omega_2)+\psi(\mathbf{x}_1)\Big]+4\pi\hat{\mathbf{z}}\cdot\mathbf{P}_b(\mathbf{x}_1;\mathbf{x}_2,\omega_2) \tag{2.115}$$

is continuous at the dipole exclusion plane (i.e at a distance $\frac{R_d}{2}$ from the membrane walls), and

$$-\hat{\mathbf{r}}_{12}\cdot\nabla_1\Big[\bar{\psi}_b(\mathbf{x}_1;\mathbf{x}_2,\omega_2)+\psi(\mathbf{x}_1)\Big]+4\pi\hat{\mathbf{r}}_{12}\cdot\mathbf{P}_b(\mathbf{x}_1;\mathbf{x}_2,\omega_2) \tag{2.116}$$

is continuous at the volume exclusion sphere boundary (i.e. at $r_{12} = R_{ab}$), where $\hat{\mathbf{r}}_{12}$ is an unit vector in the direction joining the centres of molecule 1 and 2. The first three boundary conditions are the usual conditions associated with the mean electrostatic fluctuation potential for a point system. The last two conditions are statements of the continuity of the generalized displacement vector $\mathbf{D}_b$, Eq. (2.58), and are in addition for a hard sphere system [94], [95].

Obviously the two cases to be investigated are when molecule b is an ion or a dipole. Also we assume that the ionic diameters are the same which is consistent with our assumption for the mean electrostatic potential. Thus the two equations to be considered are

$$\begin{aligned}
&\Big[1 \;+\; 3yH(r_{12}-\frac{R_{di}}{2})H(z_1-\frac{R_d}{2})\Big]\nabla_1^2\bar{\psi}_i \\
&\quad -\; 4\pi\beta H(r_{12}-R_i)H(z_1-\frac{R_i}{2})\sum_k e_k^2 n_k^0\Big[1-\beta e_k\psi\Big]\bar{\psi}_i \\
&= \;-\; 4\pi\delta(\mathbf{x}_2-\mathbf{x}_1) \\
&\quad -\; 4\pi\Big[H(r_{12}-R_i)-1\Big]H(z_1-\frac{R_i}{2})\sum_k e_k n_k^0\Big[1-\beta e_k\psi\Big] \\
&\quad +\; 3y\Big[H(r_{12}-\frac{R_{di}}{2})-1\Big]H(z_1-\frac{R_d}{2})\frac{d^2\psi}{dz_1^2}\;,
\end{aligned} \tag{2.117}$$

and

$$\begin{aligned}
&\Big[1 \;+\; 3yH(r_{12}-R_d)H(z_1-\frac{R_d}{2})\Big]\nabla_1^2\bar{\psi}_d \\
&\quad -\; 4\pi\beta H(r_{12}-\frac{R_{id}}{2})H(z_1-\frac{R_i}{2})\sum_k e_k^2 n_k^0\Big[1-\beta e_k\psi\Big]\bar{\psi}_d \\
&= \;-\; 4\pi\mathbf{m}(\boldsymbol{\omega}_2)\cdot\nabla_2\delta(\mathbf{x}_2-\mathbf{x}_1) \\
&\quad -\; 4\pi\Big[H(r_{12}-\frac{R_{id}}{2})-1\Big]H(z_1-\frac{R_i}{2})\sum_k e_k n_k^0\Big[1-\beta e_k\psi\Big] \\
&\quad +\; 3y\Big[H(r_{12}-R_d)-1\Big]H(z_1-\frac{R_d}{2})\frac{d^2\psi}{dz_1^2}\;.
\end{aligned} \tag{2.118}$$

A further simplification can be made by assuming that the diameters of all molecules are the same. The last two terms in both Eq. (2.117) and Eq. (2.118), are then simplified using Eq. (2.86) to

$$H(z_1-\frac{R}{2})\Big[4\pi\sum_k e_k n_k^0[1-\beta e_k\psi]-3y\frac{d^2\psi}{dz_1^2}\Big] \;=\; -H(z_1-\frac{R}{2})\frac{d^2\psi}{dz_1^2}$$

$$\equiv \quad -H(z_1 - \frac{R}{2})\nabla_1\psi(\mathbf{x}_1)\,. \quad (2.119)$$

Thus Eq. (2.111), for the case $r_{12} < R$ can be written in the form

$$e_i\nabla_1^2\Big[\bar{\psi}_b(\mathbf{x}_1;\mathbf{x}_2,\boldsymbol{\omega}_2) + H(z_1 - \tfrac{R}{2})\psi(\mathbf{x}_1)\Big] = \nabla_1^2\Phi_{ib}^E(\mathbf{x}_1;\mathbf{x}_2,\boldsymbol{\omega}_2)\,, \quad r_{12} < R \quad (2.120)$$

and for the case $r_{12} > R$ as

$$\Big[1 + 3yH(z_1 - \frac{R}{2})\Big]\nabla_1^2\bar{\psi}_b \quad - \quad 4\pi\beta H(z_1 - \frac{R}{2})\sum_k e_k^2 n_k^0\Big[1 - \beta e_k\psi\Big]\bar{\psi}_b$$
$$= 0\,, \quad r_{12} > R\,. \quad (2.121)$$

Eq. (2.120) and Eq. (2.121) have to be investigated when the field point is inside or outside the exclusion plane i.e. $z_1 < \frac{R}{2}$ or $z_1 > \frac{R}{2}$.

Case 1: $z_1 < \frac{R}{2}$

$$\nabla_1^2\bar{\psi}_b(\mathbf{x}_1;\mathbf{x}_2,\boldsymbol{\omega}_2) = 0 \quad \forall r_{12} \quad (2.122)$$

Case 2: $z_1 > \frac{R}{2}$

$$e_i\nabla_1^2\bar{\psi}_b = \begin{cases} \nabla_1^2\Phi_{ib}^E(\mathbf{x}_1;\mathbf{x}_2,\boldsymbol{\omega}_2) - e_i\nabla_1^2\psi(\mathbf{x}_1) & r_{12} < R \\ e_i 4\pi\beta\sum_k e_k^2 n_k^0[1 - \beta e_k\psi]\bar{\psi}_b & r_{12} > R \end{cases} \quad (2.123)$$

For the last two boundary conditions for the mean electrostatic fluctuation potential, Eq. (2.115) and Eq. (2.116), we calculate the polarization vector $\mathbf{P}_b$, explicitly in terms of the mean electrostatic potential $\psi(z_1)$ and mean electrostatic fluctuation potential $\bar{\psi}_b(\mathbf{x}_1;\mathbf{x}_2,\boldsymbol{\omega}_2)$ in the following manner. Substitution of the two body distribution function in terms of the one body distribution functions and the pair correlation function Eq. (2.18), into Eq. (2.57), yields

$$\mathbf{P}_b = n_b(\mathbf{x}_2,\boldsymbol{\omega}_2|V)\int d\boldsymbol{\omega}_1\mathbf{m}(\boldsymbol{\omega}_1)n_d(\mathbf{x}_1,\boldsymbol{\omega}_1|V)g_{db}(\mathbf{x}_1,\boldsymbol{\omega}_1;\mathbf{x}_2,\boldsymbol{\omega}_2|V)\,. \quad (2.124)$$

The expressions for the pair correlation function, Eq. (2.101), and the dipole number density, Eq. (2.73), in terms of the potentials are substituted into Eq. (2.124), such that

$$\mathbf{P}_b = \quad \frac{n_d^0}{4\pi}H(z_1 - \frac{R_b}{2})H(r_{12} - \frac{R_{db}}{2})n_b(\mathbf{x}_2,\boldsymbol{\omega}_2|V)$$
$$\times \quad \int d\boldsymbol{\omega}_1\mathbf{m}(\boldsymbol{\omega}_1)\exp\Big[-\beta\mathbf{m}(\boldsymbol{\omega}_1)\cdot\nabla_1[\bar{\psi}_b(\mathbf{x}_1;\mathbf{x}_2,\boldsymbol{\omega}_2) + \psi(z_1)]\Big]\,. \quad (2.125)$$

To be consistent with the approximations used in the derivation of the correlation functions in terms of the potentials, we must linearize Eq. (2.125) to first order in the mean electrostatic potential, to yield

$$\begin{aligned} 4\pi \mathbf{P}_b = & - 3yH(z_1 - \frac{R_d}{2})H(z_1 - \frac{R_b}{2})H(r_{12} - \frac{R_{db}}{2}) \\ & \times \nabla_1 \Big[\bar{\psi}_b(\mathbf{x}_1; \mathbf{x}_2, \boldsymbol{\omega}_2) + \psi(z_1)\Big] \ . \end{aligned} \tag{2.126}$$

Thus boundary condition Eq. (2.115) can be written, with the use of Eq. (2.53), as

$$\epsilon \hat{\mathbf{z}} \cdot \nabla_1 \bar{\psi}_b(\mathbf{x}_1; \mathbf{x}_2, \boldsymbol{\omega}_2) \mid_{\frac{R}{2}+} - \hat{\mathbf{z}} \cdot \nabla_1 \bar{\psi}_b(\mathbf{x}_1; \mathbf{x}_2, \boldsymbol{\omega}_2) \mid_{\frac{R}{2}-} = 0 \ . \tag{2.127}$$

Boundary condition Eq. (2.116), combined with the condition that the mean electrostatic potential is continuous across the exclusion volume sphere, has the form

$$\epsilon \hat{\mathbf{r}}_{12} \cdot \nabla_1 \bar{\psi}_b(\mathbf{x}_1; \mathbf{x}_2, \boldsymbol{\omega}_2) \mid_{R^+} - \hat{\mathbf{r}}_{12} \cdot \nabla_1 \bar{\psi}_b(\mathbf{x}_1; \mathbf{x}_2, \boldsymbol{\omega}_2) \mid_{R^-} = 0 \ . \tag{2.128}$$

2.5.2 Point system

The equations for the indirect correlations functions and the mean electrostatic fluctuation potential for the point ion-dipole system can be obtained by setting the hard sphere diameters to zero for all molecules. Thus the relationships between the indirect correlation functions and the mean electrostatic fluctuation potential are given by

$$h_{ib} = -\beta e_i \bar{\psi}_b(\mathbf{x}_1; \mathbf{x}_2, \boldsymbol{\omega}_2) \ , \tag{2.129}$$

$$h_{db} = -\beta \mathbf{m}(\boldsymbol{\omega}_1) \cdot \nabla_1 \bar{\psi}_b(\mathbf{x}_1; \mathbf{x}_2, \boldsymbol{\omega}_2) \ . \tag{2.130}$$

A simplification is made by noting the symmetry relation

$$\bar{\psi}_d(\mathbf{x}_1; \mathbf{x}_2, \boldsymbol{\omega}_2) = \frac{1}{e_j} \mathbf{m}(\boldsymbol{\omega}_2) \cdot \nabla_2 \bar{\psi}_j(\mathbf{x}_1, \mathbf{x}_2) \ , \tag{2.131}$$

and setting

$$\bar{\psi}_i(\mathbf{x}_1, \mathbf{x}_2) = e_i \bar{\psi}(\mathbf{x}_1, \mathbf{x}_2) \ . \tag{2.132}$$

Thus the differential equation satisfied by the mean electrostatic fluctuation potential, determined from Eq. (2.111), is given by

$$\Big[[1 + 3y]\nabla_1^2 - 4\pi\beta \sum_k n_k^0 e_k^2 [1 - \beta e_k \psi(\mathbf{x}_1)]\Big] \bar{\psi}(\mathbf{x}_1, \mathbf{x}_2) = -4\pi\delta(\mathbf{x}_2 - \mathbf{x}_1) \ . \tag{2.133}$$

The mean electrostatic fluctuation potential for the point system has the usual boundary conditions [95] of

$$\bar{\psi}(\mathbf{x}_1, \mathbf{x}_2) \rightarrow 0 \quad \text{as} \quad \mid \mathbf{x}_2 - \mathbf{x}_1 \mid \rightarrow \infty \ , \tag{2.134}$$

with $\bar{\psi}(\mathbf{x}_1, \mathbf{x}_2)$ continuous everywhere except for

$$\bar{\psi}(\mathbf{x}_1, \mathbf{x}_2) \rightarrow \frac{1}{\mid \mathbf{x}_2 - \mathbf{x}_1 \mid} \text{ as } \mid \mathbf{x}_2 - \mathbf{x}_1 \mid \rightarrow 0 \tag{2.135}$$

and

$$\epsilon(\mathbf{x}_1) \cdot \nabla_1 \bar{\psi}(\mathbf{x}_1, \mathbf{x}_2) \cdot \hat{\mathbf{z}} \mid_{z_1^-} = \epsilon(\mathbf{x}_1) \cdot \nabla_1 \bar{\psi}(\mathbf{x}_1, \mathbf{x}_2) \cdot \hat{\mathbf{z}} \mid_{z_1^+} \tag{2.136}$$

at the membrane walls.

An integral transform technique will be used to determined the mean electrostatic fluctuation potential [74], [108]. This reduces the problem from solving a partial differential equation to that of solving an ordinary differential equation and then performing the transform inversion. Defining the transverse Hankel transform by

$$\begin{aligned} \tilde{\bar{\psi}}(z_1, z_2, \mathbf{k}) &= \int d\boldsymbol{\rho} \exp[i\mathbf{k} \cdot \boldsymbol{\rho}] \bar{\psi}(z_1, z_2, \boldsymbol{\rho}) \\ &= 2\pi \int_0^\infty d\rho \rho J_0(k\rho) \bar{\psi}(z_1, z_2, \boldsymbol{\rho}) \ , \end{aligned} \tag{2.137}$$

where

$$\begin{aligned} \boldsymbol{\rho} &= (x_2 - x_1, y_2 - y_1) \ , \\ k &= \mid \mathbf{k} \mid \ , \end{aligned}$$

and applying it to Eq. (2.133) yields the following ordinary differential equation for the transverse Hankel transform mean electrostatic fluctuation potential $\tilde{\bar{\psi}}(z_1, z_2, \mathbf{k})$,

$$\left[\frac{d^2}{dz_1^2} - k^2 - \kappa^2 + \frac{4\pi\beta}{\epsilon} \sum_k n_k^0 e_k^3 \beta \psi(\mathbf{x}_1)\right] \tilde{\bar{\psi}}(z_1, z_2, \mathbf{k}) = -\frac{4\pi}{\epsilon} \delta(z_1 - z_2) \ . \tag{2.138}$$

Application of the transverse Hankel transform to the above boundary conditions yields the following boundary conditions for the transverse Hankel transform mean electrostatic fluctuation potential

$$\tilde{\bar{\psi}}(z_1, z_2, \mathbf{k}) \rightarrow 0 \text{ as } \mid z_1 \mid \rightarrow \infty \ , \tag{2.139}$$

with $\tilde{\psi}(z_1, z_2, \mathbf{k})$ continuous everywhere and

$$\epsilon(\mathbf{x}_1) \cdot \nabla_1 \tilde{\psi}(z_1, z_2, \mathbf{k}) \cdot \hat{\mathbf{z}} \mid_{z_1^-} = \epsilon(\mathbf{x}_1) \cdot \nabla_1 \tilde{\psi}(z_1, z_2, \mathbf{k}) \cdot \hat{\mathbf{z}} \mid_{z_1^+} \tag{2.140}$$

at the membrane walls.

Chapter 3

Two Membrane Point Model Neuron

In this chapter we construct solutions for the differential equations associated with the mean electrostatic potential and transverse Hankel transform mean electrostatic fluctuation potential for the two membrane model in the limit of point molecules. The two cases considered are when the fixed molecule (source point) is in the extracellular or intracellular fluid regions.

In particular we are interested in the form of the solutions (for both cases) of the transverse Hankel transform mean electrostatic fluctuation potential near the membrane wall(s). We expect from electrostatics [109] that these solutions will contain a Debye Huckel type term and image term(s) due to discontinuities in the dielectric medium. As the normal distance from a membrane wall increases the effects due to the membrane wall should become negligible due to the screening of the molecules. As a result, in the bulk of either the extracellular or intracellular fluid regions the only significant contribution to the transverse Hankel transform mean electrostatic fluctuation potential (and thus the mean electrostatic fluctuation potential) should be from the source point.

Since we are ultimately interested in calculating hydration numbers of the mobile ionic species both the small k (large ρ) and large k (small ρ) behaviour of the transverse Hankel transform mean electrostatic fluctuation potential become important in our analysis. The large k behaviour should be dominated by the distribution of molecules in the vicinity of the source whereas for the small k will include the effects due to presence of the membranes.

3.1 Mean electrostatic potential

The solution to the differential equation for the mean electrostatic potential, Eq. (2.89), in the various regions, is given by

$$\psi(z_1) = \begin{cases} A_E \exp[\kappa_E(z_1 + [L+D])] + \psi_E^B & -\infty < z_1 \leq -[L+D] \\ -A_M z_1 + B_M & -[L+D] \leq z_1 \leq -D \\ A_I \cosh[\kappa_I z_1] + \psi_I^B & -D \leq z_1 \leq D \\ A_M z_1 + B_M & D \leq z_1 \leq [L+D] \\ A_E \exp[-\kappa_E(z_1 - [L+D])] + \psi_E^B & [L+D] \leq z_1 < \infty \end{cases} . \tag{3.1}$$

Note that the solution is symmetric about $z = 0$. The constants A_E, A_M, B_M, A_I are determined using the boundary conditions at the membrane walls. The continuity condition yields

$$A_E + \psi_E^B = A_M[L+D] + B_M \ , \tag{3.2}$$

$$A_I \cosh[\kappa_I D] + \psi_I^B = A_M D + B_M \ . \tag{3.3}$$

Using the definition for the displacement vector Eq. (2.48), the other boundary condition at the membrane walls become

$$[4\pi \mathbf{P}(\mathbf{x}_1) + \mathbf{E}(\mathbf{x}_1)] \cdot \hat{\mathbf{z}} \mid_{[L+D]} + \epsilon_M A_M = 4\pi\sigma_E \ , \tag{3.4}$$

$$-\epsilon_M A_M - [4\pi \mathbf{P}(\mathbf{x}_1) + \mathbf{E}(\mathbf{x}_1)] \cdot \hat{\mathbf{z}} \mid_D = 4\pi\sigma_I \ . \tag{3.5}$$

Note we have not used the relationship between the electric field vector and the displacement vector, Eq. (2.54), thus defining the dielectric tensor, due to its inapplicability if the electric field is zero. Substituting for the explicit definition of the polarization vector Eq. (2.47), in terms of the dipole number density into the boundary conditions yields

$$4\pi\sigma_E = \int d\boldsymbol{\omega}_1 \mathbf{m}(\boldsymbol{\omega}_1) n_d^{E0} \exp\left[\beta m \cos\theta_1 A_E \kappa_E\right] + A_E \kappa_E + \epsilon_M A_M \ , \tag{3.6}$$

$$4\pi\sigma_I = -\epsilon_M A_M - \int d\boldsymbol{\omega}_1 \mathbf{m}(\boldsymbol{\omega}_1) n_d^{I0} \exp\left[-\beta m \cos\theta_1 A_I \kappa_I \sinh[\kappa_I D]\right] + A_I \kappa_I \sinh[\kappa_I D] \ . \tag{3.7}$$

The angular integral in both boundary conditions Eq. (3.6) and Eq. (3.7) are evaluated to first order in the mean electrostatic potential to yield

$$4\pi\sigma_E = \quad A_E\kappa_E\epsilon_E + \epsilon_M A_M \ , \tag{3.8}$$

$$4\pi\sigma_I = \ - \ \epsilon_M A_M + A_I\kappa_I\epsilon_I \sinh[\kappa_I D] \ . \tag{3.9}$$

Equations (3.2), (3.3), (3.8) and (3.9) can be solved for the constants A_E, A_M, B_M, A_I such that

$$A_E = \frac{1}{N}\Big[4\pi(\sigma_E+\sigma_I)\epsilon_M \cosh[\kappa_I D] + \sinh[\kappa_I D]\Big(4\pi\sigma_E L\epsilon_I\kappa_I - \epsilon_M\epsilon_I\kappa_I\Delta\psi^B\Big)\Big] \ , \tag{3.10}$$

$$A_M = -\frac{1}{N}\Big[4\pi\sigma_I\epsilon_E\kappa_E \cosh[\kappa_I D] - \epsilon_I\kappa_I \sinh[\kappa_I D]\Big(4\pi\sigma_E - \epsilon_E\kappa_E\Delta\psi^B\Big)\Big] \ , \tag{3.11}$$

$$B_M = \psi_I^B - A_M D + A_I \cosh[\kappa_I D] \ , \tag{3.12}$$

$$A_I = \frac{1}{N}\Big[4\pi(\sigma_E+\sigma_I)\epsilon_M + 4\pi\sigma_I\epsilon_E\kappa_E L - \epsilon_M\epsilon_E\kappa_E\Delta\psi^B\Big] \ , \tag{3.13}$$

where

$$N = \epsilon_E\kappa_E\epsilon_I\kappa_I L \sinh[\kappa_I D] + \epsilon_M\Big[\epsilon_E\kappa_E \cosh[\kappa_I D] + \epsilon_I\kappa_I \sinh[\kappa_I D]\Big] \ , \tag{3.14}$$

$$\Delta\psi^B = \psi_I^B - \psi_E^B \ . \tag{3.15}$$

Use of the typical values for the concentration of the molecular species (see Table 1.1) and the values from Table 3.1 (see page 65) for the surface charge density, dimension and background potential yields the following figure for the mean electrostatic potential. See Figure 3.1.

It is possible to check that the mean electrostatic potential satisfies the overall electroneutrality condition Eq. (2.55), i.e.

$$\begin{aligned} -\sigma &= \sum_k \int dz_1 e_k n_k(z_1|V) \\ &= \sum_k \int dz_1 e_k n_k^0 \exp\Big[-\beta e_k[\psi(z_1) - \psi_B]\Big] \ . \end{aligned}$$

Linearizing the exponential and substituting the explicit form for the mean electrostatic potential yields

$$-2[4\pi\sigma_E + 4\pi\sigma_I] = \quad 2\int_{-\infty}^{-[L+D]} dz_1 \Big[4\pi \sum_k e_k n_k^{E0} \exp[\beta e_k \psi_E^B] - \kappa_E^2\epsilon_E\psi_E^B\Big]$$

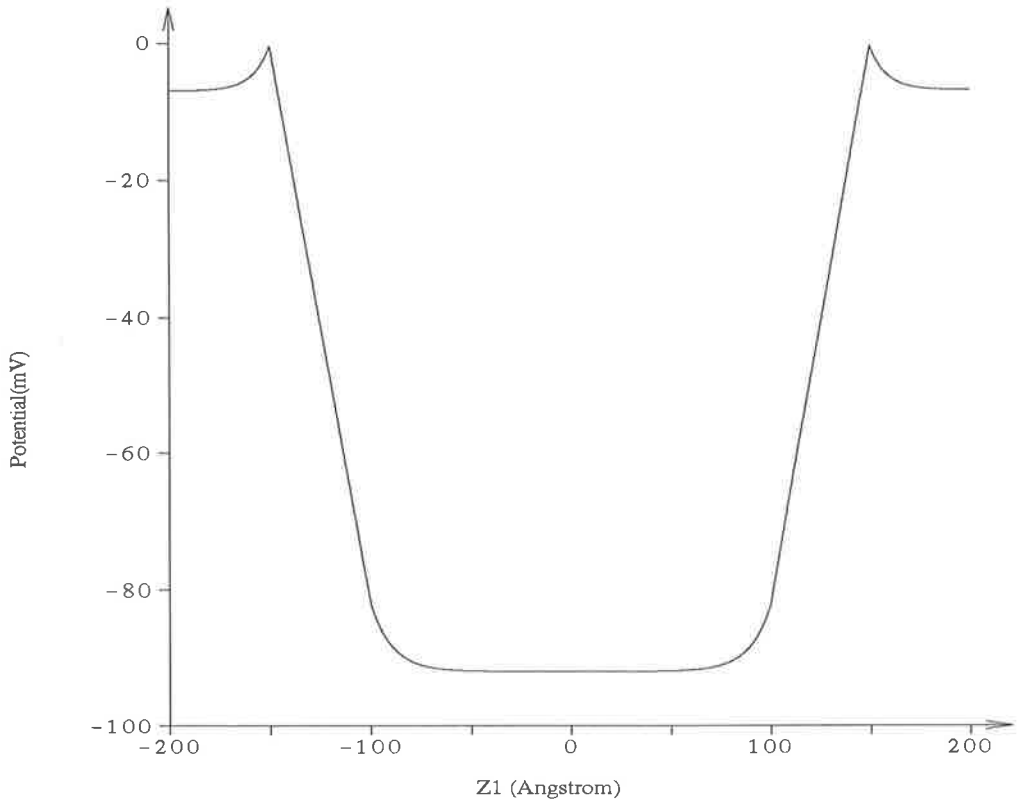

Figure 3.1: Mean electrostatic potential for a two membrane point model system.

$$
\begin{aligned}
&+ \int_{-D}^{D} dz_1 \left[4\pi \sum_k e_k n_k^{I0} \exp[\beta e_k \psi_I^B] - \kappa_I^2 \epsilon_I \psi_I^B \right] \\
&- 2\kappa_E^2 \epsilon_E \int_{-\infty}^{-[L+D]} dz_1 A_E \exp[\kappa_E (z_1 + [L+D])] \\
&- \kappa_I^2 \epsilon_I \int_{-D}^{D} dz_1 A_I \cosh[\kappa_I z_1] \ .
\end{aligned}
$$

The first two terms are equivalently zero due to the definition of the constant background potentials ψ_E^B and ψ_I^B, Eq. (2.84). The integrals in the next two terms can be evaluated and simplified to yield

$$
4\pi[\sigma_E + \sigma_I] = A_E \kappa_E \epsilon_E + A_I \kappa_I \epsilon_I \sinh[\kappa_I D] \ ,
$$

which is the result obtained from adding Eq. (3.8) and Eq. (3.9) together.

With the mean electrostatic potential determined it is now possible to obtain an explicit expression for the normal component of the dielectric tensor. The dielectric tensor can be decomposed into its normal and transverse components in the following manner

$$
\epsilon(\mathbf{x}_1) = \epsilon_T(z_1)[\mathbf{I} - \hat{\mathbf{z}}\hat{\mathbf{z}}] + \epsilon_N(z_1)\hat{\mathbf{z}}\hat{\mathbf{z}} \ . \tag{3.16}
$$

Substituting this expression into Eq. (2.54) and the explicit expressions for the electric field and polarization in regions I, III and V yields

$$
\begin{aligned}
\epsilon_N^i(z_1) &= 1 + \frac{4\pi}{[E_N^{(i)}(z_1)]^2} \frac{d}{d\beta} \left[\frac{\sinh[\beta m E_N^{(i)}(z_1)]}{\beta m E_N^{(i)}(z_1)} \right] \\
&= 1 + 4\pi \sum_{n=1}^{\infty} \frac{2n m^{2n} E_N^{(i)2n-2} \beta^{2n-1}}{(2n+1)!} \ ,
\end{aligned} \tag{3.17}
$$

where $E_N^{(i)}(z_1)$ is the component of the electric field in the direction normal to the membrane wall. See Figure 3.2.

3.1.1 One membrane limiting form

A specialized case of the one membrane model can be derived as a limiting form of the two membrane model in the following manner. Consider first the situation where there is an absence of solute and solvent molecules in the intracellular fluid region. As a result

$$
\kappa_I \ \rightarrow \ 0 \ .
$$

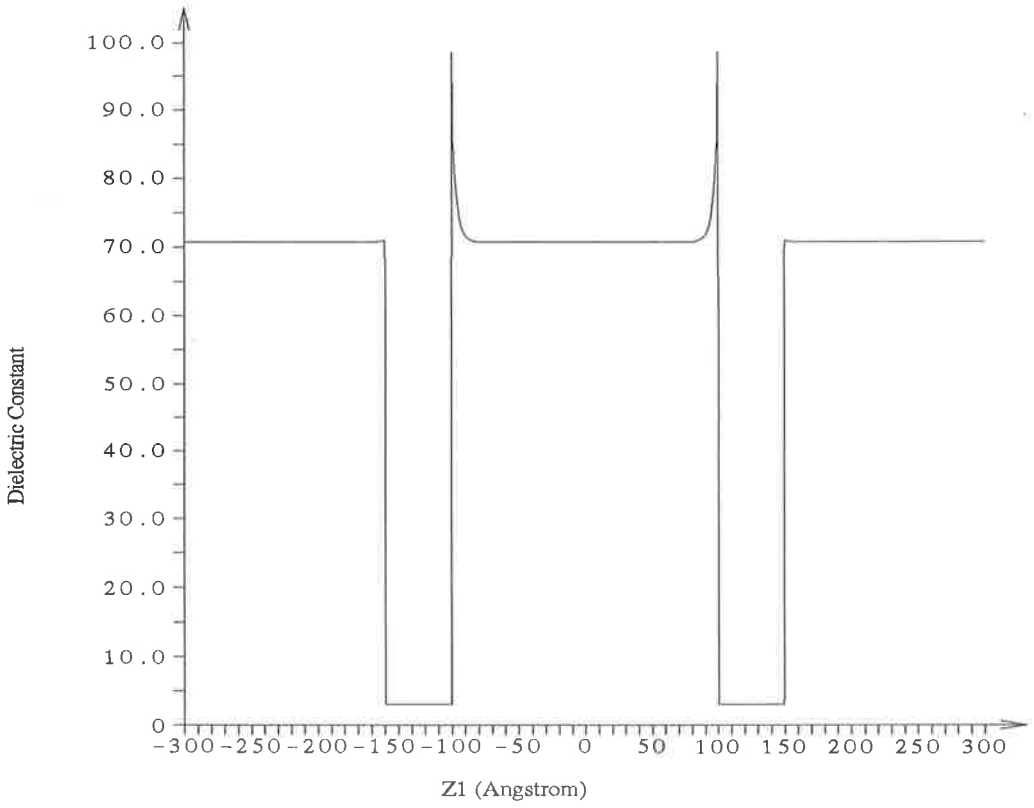

Figure 3.2: Dielectric Function

Also we require that there are no surface charges on the membrane walls adjacent to the intracellular fluid region i.e.

$$\sigma_I \to 0 \ .$$

To ensure that there is no discontinuity in the mean electrostatic potential across the membrane walls adjacent to the intracellular fluid region we set the dielectric constant in the intracellular fluid region equivalent to that of the membrane i.e.

$$\epsilon_I \to \epsilon_M \ .$$

Thus we have derived a one membrane model system with a membrane of thickness $2[L+D]$ and extracellular fluid in each of the fluid regions adjacent to the membrane.

The mean electrostatic potential in this case takes the limiting form of

$$\psi(z_1) = \begin{cases} \frac{4\pi\sigma_E}{\epsilon_E\kappa_E}\exp[\kappa_E(z_1+[L+D])]+\psi_E^B & -\infty < z_1 \le -[L+D] \\ \frac{4\pi\sigma_E}{\epsilon_E\kappa_E}+\psi_E^B & -[L+D] \le z_1 \le [L+D] \\ \frac{4\pi\sigma_E}{\epsilon_E\kappa_E}\exp[-\kappa_E(z_1-[L+D])]+\psi_E^B & [L+D] \le z_1 < \infty \end{cases} \ .$$

This result is equivalent to letting $\kappa_I \to \kappa_E$, $\epsilon_I \to \epsilon_E$, $\sigma_I \to \sigma_E$, and $\psi_I^B \to \psi_E^B$ in the solution for the mean electrostatic potential for the one membrane model system in Appendix B.

This limiting form is not only a mathematical verification of the validity of the mean electrostatic potential but is of biological interest in regards to the microtubeles in the intracellular fluid [2]. These microtubeles can be considered to be a membrane of comparable thickness to the membrane wall of the neuron and thus have similar fluid regions adjacent.

3.1.2 Two semi-infinite membrane limiting form

The two semi-infinite membrane model may be derived from the two membrane model by the following limiting process. Now we consider the situation where there is an absence of solute and solvent molecules in the extracellular fluid region i.e

$$\kappa_E \ \to \ 0 \ .$$

Next we require that there are no surface charges on the membrane walls adjacent to the extracellular fluid region i.e.

$$\sigma_E \rightarrow 0 \ .$$

To ensure that there is no discontinuity in the mean electrostatic potential across the membrane walls adjacent to the extracellular fluid region we set the dielectric constant in the extracellular fluid region equivalent to that of the membrane i.e.

$$\epsilon_E \rightarrow \epsilon_M \ .$$

The above limiting process is equivalent to letting the membrane thickness approach infinity i.e.

$$L \rightarrow \infty \ .$$

Thus we have two semi-infinite walls with the intracellular fluid contained between them. If the above limiting process is performed then the mean electrostatic potential obtained is equivalent to that of Appendix C i.e.

$$\psi(z_1) = \begin{cases} \psi_I^B + \frac{4\pi\sigma_I}{\epsilon_I\kappa_I}\coth[\kappa_I D] & -\infty < z_1 \leq -D \\ \frac{4\pi\sigma_I}{\epsilon_I\kappa_I}\left[\frac{\cosh[\kappa_I z_1]}{\sinh[\kappa_I D]}\right] + \psi_I^B & -D \leq z_1 \leq D \\ \psi_I^B + \frac{4\pi\sigma_I}{\epsilon_I\kappa_I}\coth[\kappa_I D] & D \leq z_1 < \infty \end{cases} \ .$$

3.2 Transverse Hankel transform mean electrostatic fluctuation potential

Substituting for the mean electrostatic potential in the various regions into Eq. (2.138), yields the following homogeneous differential equations for the transverse Hankel transform mean electrostatic fluctuation potential:

$$\left[\frac{d^2}{dz_1^2} - k^2 - \kappa_E^2 + \kappa_1^2\zeta_E\frac{\psi_E^B}{A_E} + \kappa_1^2\zeta_E\exp[\kappa_1(z_E + [L+D])]\right]\tilde{\psi}_E^L(z_1, z_2, \mathbf{k}) = 0 \ , \quad (3.18)$$

$$\left[\frac{d^2}{dz_1^2} - k^2\right]\tilde{\psi}_M^L(z_1, z_2, \mathbf{k}) = 0 \ , \quad (3.19)$$

$$\left[\frac{d^2}{dz_1^2} - k^2 - \kappa_I^2 + \kappa_I^2\zeta_I\frac{\psi_I^B}{A_I} + \kappa_I^2\zeta_I\cosh[\kappa_I z_1]\right]\tilde{\psi}_I(z_1, z_2, \mathbf{k}) = 0 \ , \quad (3.20)$$

$$\left[\frac{d^2}{dz_1^2} - k^2\right]\tilde{\psi}_M^R(z_1, z_2, \mathbf{k}) = 0 \ , \tag{3.21}$$

$$\left[\frac{d^2}{dz_1^2} - k^2 - \kappa_E^2 + \kappa_E^2\zeta_E\frac{\psi_E^B}{A_E} + \kappa_E^2\zeta_E \exp[-\kappa_E(z_1 - [L+D])]\right]\tilde{\psi}_E^R(z_1, z_2, \mathbf{k}) = 0 \ . \tag{3.22}$$

The differential equation in the intracellular region is a modified Mathieu differential equation which has a general solution in terms of products of Bessel or modified Bessel functions [110], given by

$$\tilde{\psi}_I = \begin{cases} (C_I + D_I)\sum_{r=-\infty}^{\infty}(-1)^r d_{2r} J_r[2\zeta_I^{\frac{1}{2}} e^{-\frac{\kappa_I z_1}{2}}] J_{r+\eta}[2\zeta_I^{\frac{1}{2}} e^{\frac{\kappa_I z_1}{2}}] \\ +(C_I - D_I)\sum_{r=-\infty}^{\infty}(-1)^r d_{2r} J_{r+\eta}[2\zeta_I^{\frac{1}{2}} e^{-\frac{\kappa_I z_1}{2}}] J_r[2\zeta_I^{\frac{1}{2}} e^{\frac{\kappa_I z_1}{2}}] & \zeta_I > 0 \\ \\ (C_I + D_I)\sum_{r=-\infty}^{\infty}(-1)^r d_{2r} I_r[2 \mid \zeta_I \mid^{\frac{1}{2}} e^{-\frac{\kappa_I z_1}{2}}] I_{r+\eta}[2 \mid \zeta_I \mid^{\frac{1}{2}} e^{\frac{\kappa_I z_1}{2}}] \\ +(C_I - D_I)\sum_{r=-\infty}^{\infty}(-1)^r d_{2r} I_{r+\eta}[2 \mid \zeta_I \mid^{\frac{1}{2}} e^{-\frac{\kappa_I z_1}{2}}] I_r[2 \mid \zeta_I \mid^{\frac{1}{2}} e^{\frac{\kappa_I z_1}{2}}] & \zeta_I < 0 \end{cases}$$

where J is the Bessel function of the first kind and I is the modified Bessel function of the first [111] and the recurrence relation for d_{2r} is given by

$$d_{2r}[4\nu_I^2 - (2r+\eta)^2] - 2\zeta_I[d_{2r+2} + d_{2r-2}] = 0 \ , \zeta_I > 0 \ ,$$

$$d_{2r}[4\nu_I^2 - (2r+\eta)^2] - 2 \mid \zeta_I \mid [d_{2r+2} + d_{2r-2}] = 0 \ , \zeta_I < 0 \ ,$$

and η is chosen such that $d_{2r} \to 0$ as $r \to \pm\infty$ to ensure convergence of the series. The method for determining η is by a numerical scheme to approximate the continued fraction form of the recurrence relation [111]. So for each value of k we must determine a value of η. Thus this form of solution is complicated and asymptotics of products of Bessel or modified Bessel functions in a series solution difficult to obtain [112]. Since the distance between the membranes is large, a simplification can be made by approximating the mean electrostatic potential between the membrane walls by

$$\psi(z_1) = \begin{cases} \frac{A_I}{2}\exp[-\kappa_I z_1] + \psi_I^B & -D \le z_1 \le 0 \\ \\ \frac{A_I}{2}\exp[\kappa_I z_1] + \psi_I^B & 0 \le z_1 \le D \end{cases} . \tag{3.23}$$

For the parameters chosen in the model, if we vary the distance between the membranes i.e. $2D$, for distances greater than $60\mathring{A}$, the difference between the approximate and

exact potential is negligible for the region within $10\mathring{A}$ of the membrane wall and has a maximum error of $\approx 4\%$ at the origin (for $2D = 60\mathring{A}$). See Figure 3.3. Thus the differential equation for the transverse Hankel transform mean electrostatic fluctuation potential can be separated into two in the following manner

$$\left[\frac{d^2}{dz_1^2} - k^2 - \kappa_I^2 + \kappa_I^2\zeta_I\frac{\psi_I^B}{A_I} + \frac{\kappa_I^2\zeta_I}{2}\exp[-\kappa_I z_1]\right]\tilde{\psi}_I^L(z_1, z_2, \mathbf{k}) = 0 \ , \tag{3.24}$$

$$\left[\frac{d^2}{dz_1^2} - k^2 - \kappa_I^2 + \kappa_I^2\zeta_I\frac{\psi_I^B}{A_I} + \frac{\kappa_I^2\zeta_I}{2}\exp[\kappa_I z_1]\right]\tilde{\psi}_I^R(z_1, z_2, \mathbf{k}) = 0 \ . \tag{3.25}$$

The homogeneous solutions to the differential equation for the transverse Hankel transform mean electrostatic fluctuation potential, in the five regions, are given by

$$\tilde{\psi}_E^L = \begin{cases} C_E^L J_{2\nu_E}\left[2\zeta_E^{\frac{1}{2}}\exp[\frac{\kappa_E(z_1+[L+D])}{2}]\right] \\ +D_E^L Y_{2\nu_E}\left[2\zeta_E^{\frac{1}{2}}\exp[\frac{\kappa_E(z_1+[L+D])}{2}]\right] & \zeta_E > 0 \\ C_E^L I_{2\nu_E}\left[2\mid\zeta_E\mid^{\frac{1}{2}}\exp[\frac{\kappa_E(z_1+[L+D])}{2}]\right] \\ +D_E^L K_{2\nu_E}\left[2\mid\zeta_E\mid^{\frac{1}{2}}\exp[\frac{\kappa_E(z_1+[L+D])}{2}]\right] & \zeta_E < 0 \end{cases} ,$$

$$\tilde{\psi}_M^L = C_M^L\exp[kz_1] + D_M^L\exp[-kz_1] \ ,$$

$$\tilde{\psi}_I^L = \begin{cases} C_I^L J_{2\nu_I}\left[\sqrt{2}\zeta_I^{\frac{1}{2}}\exp[-\frac{\kappa_I z_1}{2}]\right] \\ +D_I^L Y_{2\nu_I}\left[\sqrt{2}\zeta_I^{\frac{1}{2}}\exp[-\frac{\kappa_I z_1}{2}]\right] & \zeta_I > 0 \\ C_I^L I_{2\nu_I}\left[\sqrt{2}\mid\zeta_I\mid^{\frac{1}{2}}\exp[-\frac{\kappa_I z_1}{2}]\right] \\ +D_I^L K_{2\nu_I}\left[\sqrt{2}\mid\zeta_I\mid^{\frac{1}{2}}\exp[-\frac{\kappa_I z_1}{2}]\right] & \zeta_I < 0 \end{cases} ,$$

$$\tilde{\psi}_I^R = \begin{cases} C_I^R J_{2\nu_I}\left[\sqrt{2}\zeta_I^{\frac{1}{2}}\exp[\frac{\kappa_I z_1}{2}]\right] \\ +D_I^R Y_{2\nu_I}\left[\sqrt{2}\zeta_I^{\frac{1}{2}}\exp[\frac{\kappa_I z_1}{2}]\right] & \zeta_I > 0 \\ C_I^R I_{2\nu_I}\left[\sqrt{2}\mid\zeta_I\mid^{\frac{1}{2}}\exp[\frac{\kappa_I z_1}{2}]\right] \\ +D_I^R K_{2\nu_I}\left[\sqrt{2}\mid\zeta_I\mid^{\frac{1}{2}}\exp[\frac{\kappa_I z_1}{2}]\right] & \zeta_I < 0 \end{cases} ,$$

$$\tilde{\psi}_M^R = C_M^R\exp[kz_1] + D_M^R\exp[-kz_1] \ ,$$

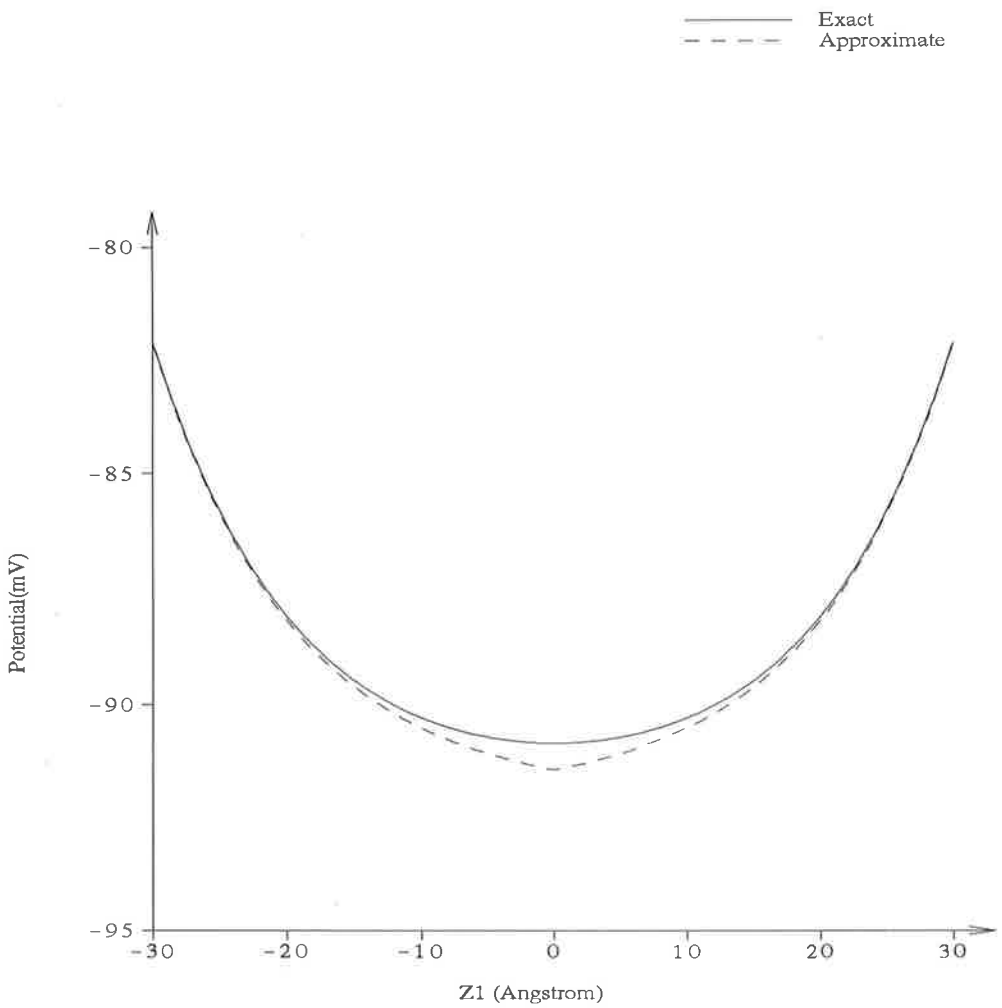

Figure 3.3: Exact and approximate mean electrostatic potential in the intracellular fluid between the membranes.

$$\tilde{\psi}_E^R = \begin{cases} C_E^R J_{2\nu_E}\left[2\zeta_E^{\frac{1}{2}}\exp[-\frac{\kappa_E(z_1-[L+D])}{2}]\right] \\ +D_E^R Y_{2\nu_E}\left[2\zeta_E^{\frac{1}{2}}\exp[-\frac{\kappa_E(z_1-[L+D])}{2}]\right] & \zeta_E > 0 \\ \\ C_E^R I_{2\nu_E}\left[2\mid\zeta_E\mid^{\frac{1}{2}}\exp[-\frac{\kappa_E(z_1-[L+D])}{2}]\right] \\ +D_E^R K_{2\nu_E}\left[2\mid\zeta_E\mid^{\frac{1}{2}}\exp[-\frac{\kappa_E(z_1-[L+D])}{2}]\right] & \zeta_E < 0 \end{cases} ,$$

where J and Y are Bessel functions of the first and second kind, I and K are modified Bessel functions of the first and second kind [111], such that

$$\nu_r^2 = \begin{cases} \frac{k^2+\kappa_r^2-\kappa_r^2\zeta_r\frac{\psi_r^B}{A_r}}{\kappa_r^2} & \zeta_r > 0 \\ \\ \frac{k^2+\kappa_r^2+\kappa_r^2|\zeta_r|\frac{\psi_r^B}{A_r}}{\kappa_r^2} & \zeta_r < 0 \end{cases} , \tag{3.26}$$

$$\zeta_r = \beta e A_r\left[\frac{\frac{1}{e}\sum_k e_k^3 n_k^{r0}}{\sum_k e_k^2 n_k^{r0}}\right] , \tag{3.27}$$

for $r = E, I$. The index parameter ν for the extracellular and intracellular fluid regions does not depend on the length parameters L and D. The parameter ζ_r, is a measure of the charge asymmetry of the ionic species in the extracellular and intracellular respectively. Note that the solutions are written in terms of Bessel functions of the first and second kind if the asymmetry is positive and in terms of modified Bessel functions of the first and second kind if the asymmetry parameter is negative. The charge asymmetries for our model neuron typically are positive both in the intracellular and extracellular fluids. See Table 3.1. It should be noted that the concentrations of the mobile ionic species used in the calculation of the various parameters are those in the resting state of a neuron. In the dynamical phase of the action potential, the concentrations can vary such that the asymmetry parameter may change sign in either or both of the fluid regions. Thus for completeness, the possible solutions for the transverse Hankel transform mean electrostatic fluctuation potential in each of the combinations for the sign of the asymmetry parameter are presented even though we are investigating the structure in the resting state.

The homogeneous differential equation associated with Eq. (2.138) can be written in

Quantity	Value
κ_I	$0.09425\mathring{A}^{-1}$
$\frac{\epsilon_I}{4\pi\epsilon_0}$	70.718
ζ_I	5.60216×10^{-5}
$\nu_I \mid_{k=0}$	2.06522
κ_E	$0.11995\mathring{A}^{-1}$
$\frac{\epsilon_E}{4\pi\epsilon_0}$	70.718
ζ_E	4.29949×10^{-2}
$\nu_E \mid_{k=0}$	1.02275

Table 3.1: Table of κ, ϵ, ζ and ν values in the extracellular and intracellular fluid regions for the two membrane point model.

the form of Schroedinger's equation in the following manner

$$-\frac{d^2\tilde{\psi}}{dz_1^2} + V_{eff}\tilde{\psi} = -k^2\tilde{\psi} \ ,$$

where

$$V_{eff} = \kappa^2 - \frac{\kappa^2\zeta}{A}\psi(z_1) \ .$$

See Figure 3.4. Since the effective potential V_{eff} is positive in the fluid regions we expect from scattering theory in quantum mechanics that no bounded solutions at $\pm\infty$ exist for real k [113]. Thus it will be possible to construct a Green's function type of solution for the transverse Hankel transform mean electrostatic fluctuation potential using the solutions to the homogeneous differential equation. This is due to the wronskian having no zeros for real k [100].

The two cases to be considered are when the fixed particle at z_2 is in region I or III. The region V case is found by the symmetry in the $x-y$ plane.

3.2.1 Case 1:$-\infty < z_2 \leq -[L+D]$

$\zeta_E > 0$

The Green's function type of solution for the transverse Hankel transform mean electrostatic fluctuation potential in region I is of the form

$$\begin{aligned}
\tilde{\psi}_E^L(z_1, z_2, \mathbf{k}) = \ & - \frac{4\pi^2}{\epsilon_E\kappa_E} Y_{2\nu_E}\left[2\zeta_E^{\frac{1}{2}}\exp[\frac{\kappa_E(z_> + [L+D])}{2}]\right] \\
& \times J_{2\nu_E}\left[2\zeta_E^{\frac{1}{2}}\exp[\frac{\kappa_E(z_< + [L+D])}{2}]\right] \\
+\Big\{\tilde{\psi}_E^L(-[L+D], z_2, \mathbf{k}) \ & + \frac{4\pi^2}{\epsilon_E\kappa_E} Y_{2\nu_E}[2\zeta_E^{\frac{1}{2}}] J_{2\nu_E}\left[2\zeta_E^{\frac{1}{2}}\exp[\frac{\kappa_E(z_2 + [L+D])}{2}]\right]\Big\} \\
& \times \frac{1}{J_{2\nu_E}[2\zeta_E^{\frac{1}{2}}]} J_{2\nu_E}\left[2\zeta_E^{\frac{1}{2}}\exp[\frac{\kappa_E(z_1 + [L+D])}{2}]\right] \ . \qquad (3.28)
\end{aligned}$$

Application of the appropriate boundary conditions at infinity and for the membrane wall located at $[L+D]$ we find

$$\begin{aligned}
D_E^R &= 0 \ , \\
\tilde{\psi}_M^R &= C_E^R\Big\{J_{2\nu_E}[2\zeta_E^{\frac{1}{2}}]\cosh[k(z_1 - [L+D])] - \frac{\epsilon_E\kappa_E\zeta_E^{\frac{1}{2}}}{k\epsilon_M} J'_{2\nu_E}[2\zeta_E^{\frac{1}{2}}]\sinh[k(z_1 - [L+D])]\Big\}.
\end{aligned}$$

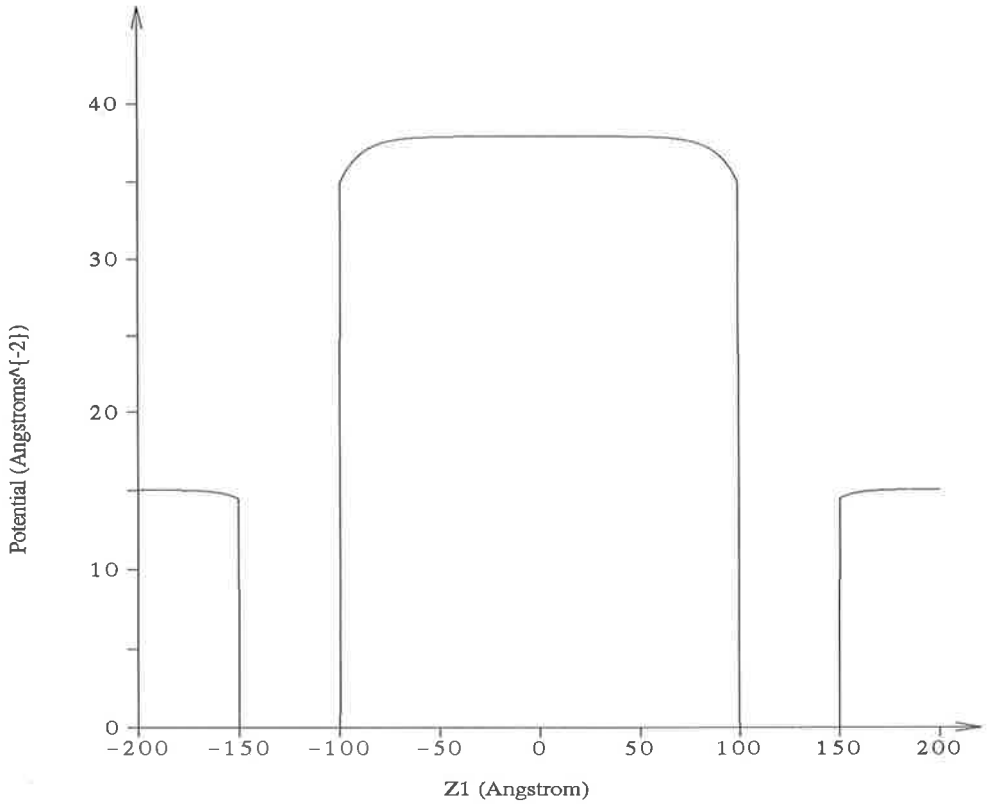

Figure 3.4: Effective Schroedinger potential of the transverse Hankel transform mean electrostatic fluctuation potential for the two membrane system.

The boundary conditions for the membrane wall located at D yield the following relations for the constants C_I^R and D_I^R i.e.

$$
\begin{aligned}
-\frac{C_I^R}{C_E^R}\frac{\epsilon_I\kappa_I}{2k\epsilon_M} &= \left\{J_{2\nu_E}[2\zeta_E^{\frac{1}{2}}]\cosh[kL] + \frac{\epsilon_E\kappa_E\zeta_E^{\frac{1}{2}}}{k\epsilon_M}J'_{2\nu_E}[2\zeta_E^{\frac{1}{2}}]\sinh[kL]\right\}S_{2\nu_I}(L,\zeta_E,D,\zeta_I)\ , \\
\frac{D_I^R}{C_E^R}\frac{\epsilon_I\kappa_I}{2k\epsilon_M} &= \left\{J_{2\nu_E}[2\zeta_E^{\frac{1}{2}}]\cosh[kL] + \frac{\epsilon_E\kappa_E\zeta_E^{\frac{1}{2}}}{k\epsilon_M}J'_{2\nu_E}[2\zeta_E^{\frac{1}{2}}]\sinh[kL]\right\}T_{2\nu_I}(L,\zeta_E,D,\zeta_I)\ ,
\end{aligned}
$$

such that

$$
S_{2\nu_I}(L,\zeta_E,D,\zeta_I) = \begin{cases}
Z_{2\nu_E}(L,\zeta_E)Y_{2\nu_I}\left[\sqrt{2}\zeta_I^{\frac{1}{2}}\exp[\frac{\kappa_I D}{2}]\right] & \\
+\frac{\epsilon_I\kappa_I\zeta_I^{\frac{1}{2}}}{k\epsilon_M\sqrt{2}}\exp[\frac{\kappa_I D}{2}]Y'_{2\nu_I}\left[\sqrt{2}\zeta_I^{\frac{1}{2}}\exp[\frac{\kappa_I D}{2}]\right] & \zeta_I > 0 \\
Z_{2\nu_E}(L,\zeta_E)K_{2\nu_I}\left[\sqrt{2}\mid\zeta_I\mid^{\frac{1}{2}}\exp[\frac{\kappa_I D}{2}]\right] & \\
+\frac{\epsilon_I\kappa_I\mid\zeta_I\mid^{\frac{1}{2}}}{k\epsilon_M\sqrt{2}}\exp[\frac{\kappa_I D}{2}]K'_{2\nu_I}\left[\sqrt{2}\mid\zeta_I\mid^{\frac{1}{2}}\exp[\frac{\kappa_I D}{2}]\right] & \zeta_I < 0
\end{cases}\ ,
$$

$$
T_{2\nu_I}(L,\zeta_E,D,\zeta_I) = \begin{cases}
Z_{2\nu_E}(L,\zeta_E)J_{2\nu_I}\left[\sqrt{2}\zeta_I^{\frac{1}{2}}\exp[\frac{\kappa_I D}{2}]\right] & \\
+\frac{\epsilon_I\kappa_I\zeta_I^{\frac{1}{2}}}{k\epsilon_M\sqrt{2}}\exp[\frac{\kappa_I D}{2}]J'_{2\nu_I}\left[\sqrt{2}\zeta_I^{\frac{1}{2}}\exp[\frac{\kappa_I D}{2}]\right] & \zeta_I > 0 \\
Z_{2\nu_E}(L,\zeta_E)I_{2\nu_I}\left[\sqrt{2}\mid\zeta_I\mid^{\frac{1}{2}}\exp[\frac{\kappa_I D}{2}]\right] & \\
+\frac{\epsilon_I\kappa_I\mid\zeta_I\mid^{\frac{1}{2}}}{k\epsilon_M\sqrt{2}}\exp[\frac{\kappa_I D}{2}]I'_{2\nu_I}\left[\sqrt{2}\mid\zeta_I\mid^{\frac{1}{2}}\exp[\frac{\kappa_I D}{2}]\right] & \zeta_I < 0
\end{cases}\ ,
$$

and

$$
Z_{2\nu_E}(L,\zeta_E) = \frac{J_{2\nu_E}[2\zeta_E^{\frac{1}{2}}]\sinh[kL] + \frac{\epsilon_E\kappa_E\zeta_E^{\frac{1}{2}}}{k\epsilon_M}J'_{2\nu_E}[2\zeta_E^{\frac{1}{2}}]\cosh[kL]}{J_{2\nu_E}[2\zeta_E^{\frac{1}{2}}]\cosh[kL] + \frac{\epsilon_E\kappa_E\zeta_E^{\frac{1}{2}}}{k\epsilon_M}J'_{2\nu_E}[2\zeta_E^{\frac{1}{2}}]\sinh[kL]}\ . \tag{3.29}
$$

At the origin, the boundary conditions yield the following relations for the constants C_I^L and D_I^L i.e.

$$
-\frac{C_I^L}{\sqrt{2}\mid\zeta_I\mid^{\frac{1}{2}}} = \begin{cases}
Y_{2\nu_I}[\sqrt{2}\zeta_I^{\frac{1}{2}}]\left[C_I^R J'_{2\nu_I}[\sqrt{2}\zeta_I^{\frac{1}{2}}] + D_I^R Y'_{2\nu_I}[\sqrt{2}\zeta_I^{\frac{1}{2}}]\right] & \\
+Y'_{2\nu_I}[\sqrt{2}\zeta_I^{\frac{1}{2}}]\left[C_I^R J_{2\nu_I}[\sqrt{2}\zeta_I^{\frac{1}{2}}] + D_I^R Y_{2\nu_I}[\sqrt{2}\zeta_I^{\frac{1}{2}}]\right. & \zeta_I > 0 \\
K_{2\nu_I}[\sqrt{2}\mid\zeta_I\mid^{\frac{1}{2}}]\left[C_I^R I'_{2\nu_I}[\sqrt{2}\mid\zeta_I\mid^{\frac{1}{2}}] + D_I^R K'_{2\nu_I}[\sqrt{2}\mid\zeta_I\mid^{\frac{1}{2}}]\right] & \\
+K'_{2\nu_I}[\sqrt{2}\mid\zeta_I\mid^{\frac{1}{2}}]\left[C_I^R I_{2\nu_I}[\sqrt{2}\mid\zeta_I\mid^{\frac{1}{2}}] + D_I^R K_{2\nu_I}[\sqrt{2}\mid\zeta_I\mid^{\frac{1}{2}}]\right] & \zeta_I < 0
\end{cases}\ ,
$$

$$\frac{D_I^L}{\sqrt{2}\mid\zeta_I\mid^{\frac{1}{2}}} = \begin{cases} J_{2\nu_I}[\sqrt{2}\zeta_I^{\frac{1}{2}}]\Big[C_I^R J'_{2\nu_I}[\sqrt{2}\zeta_I^{\frac{1}{2}}] + D_I^R Y'_{2\nu_I}[\sqrt{2}\zeta_I^{\frac{1}{2}}]\Big] \\ +J'_{2\nu_I}[\sqrt{2}\zeta_I^{\frac{1}{2}}]\Big[C_I^R J_{2\nu_I}[\sqrt{2}\zeta_I^{\frac{1}{2}}] + D_I^R Y_{2\nu_I}[\sqrt{2}\zeta_I^{\frac{1}{2}}]\Big] & \zeta_I > 0 \\ \\ I_{2\nu_I}[\sqrt{2}\mid\zeta_I\mid^{\frac{1}{2}}]\Big[C_I^R I'_{2\nu_I}[\sqrt{2}\mid\zeta_I\mid^{\frac{1}{2}}] + D_I^R K'_{2\nu_I}[\sqrt{2}\mid\zeta_I\mid^{\frac{1}{2}}]\Big] \\ +I'_{2\nu_I}[\sqrt{2}\mid\zeta_I\mid^{\frac{1}{2}}]\Big[C_I^R I_{2\nu_I}[\sqrt{2}\mid\zeta_I\mid^{\frac{1}{2}}] + D_I^R K_{2\nu_I}[\sqrt{2}\mid\zeta_I\mid^{\frac{1}{2}}]\Big] & \zeta_I < 0 \end{cases},$$

For the membrane wall located at $-D$, the boundary conditions yield

$$\tilde{\psi}_M^L = \begin{cases} \cosh[k(z_1+D)] \\ \times\Big\{C_I^L J_{2\nu_I}\Big[\sqrt{2}\zeta_I^{\frac{1}{2}}\exp[\frac{\kappa_I D}{2}]\Big] + D_I^L Y_{2\nu_I}\Big[\sqrt{2}\zeta_I^{\frac{1}{2}}\exp[\frac{\kappa_I D}{2}]\Big]\Big\} \\ -\frac{\epsilon_I\kappa_I\zeta_I^{\frac{1}{2}}}{k\epsilon_M\sqrt{2}}\exp[\frac{\kappa_I D}{2}]\sinh[k(z_1+D)] \\ \times\Big\{C_I^L J'_{2\nu_I}\Big[\sqrt{2}\zeta_I^{\frac{1}{2}}\exp[\frac{\kappa_I D}{2}]\Big] + D_I^L Y'_{2\nu_I}\Big[\sqrt{2}\zeta_I^{\frac{1}{2}}\exp[\frac{\kappa_I D}{2}]\Big]\Big\} & \zeta_I > 0 \\ \\ \cosh[k(z_1+D)] \\ \times\Big\{C_I^L I_{2\nu_I}\Big[\sqrt{2}\mid\zeta_I\mid^{\frac{1}{2}}\exp[\frac{\kappa_I D}{2}]\Big] + D_I^L K_{2\nu_I}\Big[\sqrt{2}\mid\zeta_I\mid^{\frac{1}{2}}\exp[\frac{\kappa_I D}{2}]\Big]\Big\} \\ -\frac{\epsilon_I\kappa_I\mid\zeta_I\mid^{\frac{1}{2}}}{k\epsilon_M\sqrt{2}}\exp[\frac{\kappa_I D}{2}]\sinh[k(z_1+D)] \\ \times\Big\{C_I^L I'_{2\nu_I}\Big[\sqrt{2}\mid\zeta_I\mid^{\frac{1}{2}}\exp[\frac{\kappa_I D}{2}]\Big] + D_I^L K'_{2\nu_I}\Big[\sqrt{2}\mid\zeta_I\mid^{\frac{1}{2}}\exp[\frac{\kappa_I D}{2}]\Big]\Big\} & \zeta_I < 0 \end{cases}.$$

We can now use the Green's function type of solution for the transverse Hankel transform mean electrostatic fluctuation potential in region I and apply the boundary conditions at the membrane wall located at $-[L+D]$ to solve for the constants C_E^R and $\tilde{\psi}_E^L(-[L+D], z_2, \mathbf{k})$. Thus the solution for the transverse Hankel transform mean electrostatic fluctuation potential in region I can be written in the form

$$\begin{aligned} \tilde{\psi}_E^L(z_1, z_2, \mathbf{k}) = & -\frac{4\pi^2}{\epsilon_E\kappa_E}\Big\{Y_{2\nu_E}\Big[2\zeta_E^{\frac{1}{2}}\exp[\frac{\kappa_E(z_> + [L+D])}{2}]\Big] \\ & \times J_{2\nu_E}\Big[2\zeta_E^{\frac{1}{2}}\exp[\frac{\kappa_E(z_< + [L+D])}{2}]\Big] \\ & + \bar{\Delta}_2(L,\zeta_E,D,\zeta_I)J_{2\nu_E}\Big[2\zeta_E^{\frac{1}{2}}\exp[\frac{\kappa_E(z_2 + [L+D])}{2}]\Big] \\ & \times J_{2\nu_E}\Big[2\zeta_E^{\frac{1}{2}}\exp[\frac{\kappa_E(z_1 + [L+D])}{2}]\Big]\Big\}. \end{aligned} \tag{3.30}$$

where

$$\bar{\Delta}_2 = \begin{cases} -\frac{1}{2}\left[\frac{Y_{2\nu_E}[2\zeta_E^{\frac{1}{2}}]\cosh[kL]+\frac{\epsilon_E\kappa_E\zeta_E^{\frac{1}{2}}}{k\epsilon_M}Y'_{2\nu_E}[2\zeta_E^{\frac{1}{2}}]\sinh[kL]}{J_{2\nu_E}[2\zeta_E^{\frac{1}{2}}]\cosh[kL]+\frac{\epsilon_E\kappa_E\zeta_E^{\frac{1}{2}}}{k\epsilon_M}J'_{2\nu_E}[2\zeta_E^{\frac{1}{2}}]\sinh[kL]}\right] \\ \times\left[\frac{U_{2\nu_I}J_{2\nu_I}[\sqrt{2}\zeta_I^{\frac{1}{2}}]-V_{2\nu_I}Y_{2\nu_I}[\sqrt{2}\zeta_I^{\frac{1}{2}}]}{S_{2\nu_I}J_{2\nu_I}[\sqrt{2}\zeta_I^{\frac{1}{2}}]-T_{2\nu_I}Y_{2\nu_I}[\sqrt{2}\zeta_I^{\frac{1}{2}}]}\right. \\ \left.+\frac{U_{2\nu_I}J'_{2\nu_I}[\sqrt{2}\zeta_I^{\frac{1}{2}}]-V_{2\nu_I}Y'_{2\nu_I}[\sqrt{2}\zeta_I^{\frac{1}{2}}]}{S_{2\nu_I}J'_{2\nu_I}[\sqrt{2}\zeta_I^{\frac{1}{2}}]-T_{2\nu_I}Y'_{2\nu_I}[\sqrt{2}\zeta_I^{\frac{1}{2}}]}\right] & \zeta_I > 0 \\ -\frac{1}{2}\left[\frac{Y_{2\nu_E}[2\zeta_E^{\frac{1}{2}}]\cosh[kL]+\frac{\epsilon_E\kappa_E\zeta_E^{\frac{1}{2}}}{k\epsilon_M}Y'_{2\nu_E}[2\zeta_E^{\frac{1}{2}}]\sinh[kL]}{J_{2\nu_E}[2\zeta_E^{\frac{1}{2}}]\cosh[kL]+\frac{\epsilon_E\kappa_E\zeta_E^{\frac{1}{2}}}{k\epsilon_M}J'_{2\nu_E}[2\zeta_E^{\frac{1}{2}}]\sinh[kL]}\right] \\ \times\left[\frac{U_{2\nu_I}I_{2\nu_I}[\sqrt{2}|\zeta_I|^{\frac{1}{2}}]-V_{2\nu_I}K_{2\nu_I}[\sqrt{2}|\zeta_I|^{\frac{1}{2}}]}{S_{2\nu_I}I_{2\nu_I}[\sqrt{2}|\zeta_I|^{\frac{1}{2}}]-T_{2\nu_I}K_{2\nu_I}[\sqrt{2}|\zeta_I|^{\frac{1}{2}}]}\right. \\ \left.+\frac{U_{2\nu_I}I'_{2\nu_I}[\sqrt{2}|\zeta_I|^{\frac{1}{2}}]-V_{2\nu_I}K'_{2\nu_I}[\sqrt{2}|\zeta_I|^{\frac{1}{2}}]}{S_{2\nu_I}I'_{2\nu_I}[\sqrt{2}|\zeta_I|^{\frac{1}{2}}]-T_{2\nu_I}K'_{2\nu_I}[\sqrt{2}|\zeta_I|^{\frac{1}{2}}]}\right] & \zeta_I < 0 \end{cases},$$

such that

$$U_{2\nu_I}(L,\zeta_E,D,\zeta_I) = \begin{cases} X_{2\nu_E}(L,\zeta_E)Y_{2\nu_I}\left[\sqrt{2}\zeta_I^{\frac{1}{2}}\exp[\frac{\kappa_I D}{2}]\right] \\ +\frac{\epsilon_I\kappa_I\zeta_I^{\frac{1}{2}}}{k\epsilon_M\sqrt{2}}\exp[\frac{\kappa_I D}{2}]Y'_{2\nu_I}\left[\sqrt{2}\zeta_I^{\frac{1}{2}}\exp[\frac{\kappa_I D}{2}]\right] & \zeta_I > 0 \\ X_{2\nu_E}(L,\zeta_E)K_{2\nu_I}\left[\sqrt{2}\mid\zeta_I\mid^{\frac{1}{2}}\exp[\frac{\kappa_I D}{2}]\right] \\ +\frac{\epsilon_I\kappa_I|\zeta_I|^{\frac{1}{2}}}{k\epsilon_M\sqrt{2}}\exp[\frac{\kappa_I D}{2}]K'_{2\nu_I}\left[\sqrt{2}\mid\zeta_I\mid^{\frac{1}{2}}\exp[\frac{\kappa_I D}{2}]\right] & \zeta_I < 0 \end{cases},$$

$$V_{2\nu_I}(L,\zeta_E,D,\zeta_I) = \begin{cases} X_{2\nu_E}(L,\zeta_E)J_{2\nu_I}\left[\sqrt{2}\zeta_I^{\frac{1}{2}}\exp[\frac{\kappa_I D}{2}]\right] \\ +\frac{\epsilon_I\kappa_I\zeta_I^{\frac{1}{2}}}{k\epsilon_M\sqrt{2}}\exp[\frac{\kappa_I D}{2}]J'_{2\nu_I}\left[\sqrt{2}\zeta_I^{\frac{1}{2}}\exp[\frac{\kappa_I D}{2}]\right] & \zeta_I > 0 \\ X_{2\nu_E}(L,\zeta_E)I_{2\nu_I}\left[\sqrt{2}\mid\zeta_I\mid^{\frac{1}{2}}\exp[\frac{\kappa_I D}{2}]\right] \\ +\frac{\epsilon_I\kappa_I|\zeta_I|^{\frac{1}{2}}}{k\epsilon_M\sqrt{2}}\exp[\frac{\kappa_I D}{2}]I'_{2\nu_I}\left[\sqrt{2}\mid\zeta_I\mid^{\frac{1}{2}}\exp[\frac{\kappa_I D}{2}]\right] & \zeta_I < 0 \end{cases},$$

and

$$X_{2\nu_E}(L,\zeta_E) = \frac{Y_{2\nu_E}[2\zeta_E^{\frac{1}{2}}]\sinh[kL]+\frac{\epsilon_E\kappa_E\zeta_E^{\frac{1}{2}}}{k\epsilon_M}Y'_{2\nu_E}[2\zeta_E^{\frac{1}{2}}]\cosh[kL]}{Y_{2\nu_E}[2\zeta_E^{\frac{1}{2}}]\cosh[kL]+\frac{\epsilon_E\kappa_E\zeta_E^{\frac{1}{2}}}{k\epsilon_M}Y'_{2\nu_E}[2\zeta_E^{\frac{1}{2}}]\sinh[kL]}. \tag{3.31}$$

$\zeta_E < 0$

With a similar derivation as in the $\zeta_E > 0$ case, the solution for the transverse Hankel transform mean electrostatic fluctuation potential in region I can be written in the form

$$\tilde{\psi}_E^L(z_1,z_2,\mathbf{k}) = \frac{8\pi}{\epsilon_E\kappa_E}\left\{K_{2\nu_E}\left[2\mid\zeta_E\mid^{\frac{1}{2}}\exp[\frac{\kappa_E(z_>+[L+D])}{2}]\right]\right.$$

$$
\begin{aligned}
&\times \quad I_{2\nu_E}\left[2 \mid \zeta_E \mid^{\frac{1}{2}} \exp[\frac{\kappa_E(z_< + [L+D])}{2}]\right] \\
&+ \quad \bar{\Delta}_2(L,\zeta_E,D,\zeta_I) I_{2\nu_E}\left[2 \mid \zeta_E \mid^{\frac{1}{2}} \exp[\frac{\kappa_E(z_2 + [L+D])}{2}]\right] \\
&\times \quad I_{2\nu_E}\left[2 \mid \zeta_E \mid^{\frac{1}{2}} \exp[\frac{\kappa_E(z_1 + [L+D])}{2}]\right]\Bigg\} \ . \qquad (3.32)
\end{aligned}
$$

where

$$
\bar{\Delta}_2 = \begin{cases}
-\frac{1}{2}\left[\frac{K_{2\nu_E}[2|\zeta_E|^{\frac{1}{2}}]\cosh[kL]+\frac{\epsilon_E\kappa_E|\zeta_E|^{\frac{1}{2}}}{k\epsilon_M}K'_{2\nu_E}[2|\zeta_E|^{\frac{1}{2}}]\sinh[kL]}{I_{2\nu_E}[2|\zeta_E|^{\frac{1}{2}}]\cosh[kL]+\frac{\epsilon_E\kappa_E|\zeta_E|^{\frac{1}{2}}}{k\epsilon_M}I'_{2\nu_E}[2|\zeta_E|^{\frac{1}{2}}]\sinh[kL]}\right] & \\
\times\left[\frac{U_{2\nu_I}J_{2\nu_I}[\sqrt{2}\zeta_I^{\frac{1}{2}}]-V_{2\nu_I}Y_{2\nu_I}[\sqrt{2}\zeta_I^{\frac{1}{2}}]}{S_{2\nu_I}J_{2\nu_I}[\sqrt{2}\zeta_I^{\frac{1}{2}}]-T_{2\nu_I}Y_{2\nu_I}[\sqrt{2}\zeta_I^{\frac{1}{2}}]}\right. & \\
\left.+\frac{U_{2\nu_I}J'_{2\nu_I}[\sqrt{2}\zeta_I^{\frac{1}{2}}]-V_{2\nu_I}Y'_{2\nu_I}[\sqrt{2}\zeta_I^{\frac{1}{2}}]}{S_{2\nu_I}J'_{2\nu_I}[\sqrt{2}\zeta_I^{\frac{1}{2}}]-T_{2\nu_I}Y'_{2\nu_I}[\sqrt{2}\zeta_I^{\frac{1}{2}}]}\right] & \zeta_I > 0 \\
-\frac{1}{2}\left[\frac{K_{2\nu_E}[2|\zeta_E|^{\frac{1}{2}}]\cosh[kL]+\frac{\epsilon_E\kappa_E|\zeta_E|^{\frac{1}{2}}}{k\epsilon_M}K'_{2\nu_E}[2|\zeta_E|^{\frac{1}{2}}]\sinh[kL]}{I_{2\nu_E}[2|\zeta_E|^{\frac{1}{2}}]\cosh[kL]+\frac{\epsilon_E\kappa_E|\zeta_E|^{\frac{1}{2}}}{k\epsilon_M}I'_{2\nu_E}[2|\zeta_E|^{\frac{1}{2}}]\sinh[kL]}\right] & \\
\times\left[\frac{U_{2\nu_I}I_{2\nu_I}[\sqrt{2}|\zeta_I|^{\frac{1}{2}}]-V_{2\nu_I}K_{2\nu_I}[\sqrt{2}|\zeta_I|^{\frac{1}{2}}]}{S_{2\nu_I}I_{2\nu_I}[\sqrt{2}|\zeta_I|^{\frac{1}{2}}]-T_{2\nu_I}K_{2\nu_I}[\sqrt{2}|\zeta_I|^{\frac{1}{2}}]}\right. & \\
\left.+\frac{U_{2\nu_I}I'_{2\nu_I}[\sqrt{2}|\zeta_I|^{\frac{1}{2}}]-V_{2\nu_I}K'_{2\nu_I}[\sqrt{2}|\zeta_I|^{\frac{1}{2}}]}{S_{2\nu_I}I'_{2\nu_I}[\sqrt{2}|\zeta_I|^{\frac{1}{2}}]-T_{2\nu_I}K'_{2\nu_I}[\sqrt{2}|\zeta_I|^{\frac{1}{2}}]}\right] & \zeta_I < 0
\end{cases} ,
$$

such that

$$
Z_{2\nu_E}(L,\zeta_E) = \frac{I_{2\nu_E}[2 \mid \zeta_E \mid^{\frac{1}{2}}]\sinh[kL] + \frac{\epsilon_E\kappa_E|\zeta_E|^{\frac{1}{2}}}{k\epsilon_M}I'_{2\nu_E}[2 \mid \zeta_E \mid^{\frac{1}{2}}]\cosh[kL]}{I_{2\nu_E}[2 \mid \zeta_E \mid^{\frac{1}{2}}]\cosh[kL] + \frac{\epsilon_E\kappa_E|\zeta_E|^{\frac{1}{2}}}{k\epsilon_M}I'_{2\nu_E}[2 \mid \zeta_E \mid^{\frac{1}{2}}]\sinh[kL]} \ , \qquad (3.33)
$$

$$
X_{2\nu_E}(L,\zeta_E) = \frac{K_{2\nu_E}[2 \mid \zeta_E \mid^{\frac{1}{2}}]\sinh[kL] + \frac{\epsilon_E\kappa_E|\zeta_E|^{\frac{1}{2}}}{k\epsilon_M}K'_{2\nu_E}[2 \mid \zeta_E \mid^{\frac{1}{2}}]\cosh[kL]}{K_{2\nu_E}[2 \mid \zeta_E \mid^{\frac{1}{2}}]\cosh[kL] + \frac{\epsilon_E\kappa_E|\zeta_E|^{\frac{1}{2}}}{k\epsilon_M}K'_{2\nu_E}[2 \mid \zeta_E \mid^{\frac{1}{2}}]\sinh[kL]} . \qquad (3.34)
$$

3.2.2 Asymptotic transverse Hankel transform mean electrostatic fluctuation potential

The solution for the transverse Hankel transform mean electrostatic fluctuation potential for each of the above cases for the charge asymmetry parameter ζ, is of the same form as for the one membrane system (see Appendix B) and indeed the one wall system considered by Carnie and Chan [41]. The first term will yield upon transform inversion (for all three systems) the Debye-Huckel type correlation function in the bulk solution which will be a function only of the relative position of the field and source point. The quantity $\bar{\Delta}_2(L,\zeta_E,D,\zeta_I)$ is the image term due to the dielectric boundaries of the systems. It is

important to note that the quantity $\bar{\Delta}_2(L,\zeta_E,D,\zeta_I)$ is an even function with respect to the transverse transform variable k for finite L and D. This can be seen by noting that the quantities $Z_{2\nu_E}(L,\zeta_E)$ and $Y_{2\nu_E}(L,\zeta_E)$ are odd functions of k and thus the quantities

$$\begin{aligned}
S_{2\nu_I}J_{2\nu_I}[\sqrt{2}\zeta_I^{\frac{1}{2}}] &- T_{2\nu_I}Y_{2\nu_I}[\sqrt{2}\zeta_I^{\frac{1}{2}}] \ , \\
S_{2\nu_I}J'_{2\nu_I}[\sqrt{2}\zeta_I^{\frac{1}{2}}] &- T_{2\nu_I}Y'_{2\nu_I}[\sqrt{2}\zeta_I^{\frac{1}{2}}] \ , \\
S_{2\nu_I}I_{2\nu_I}[\sqrt{2}\mid\zeta_I\mid^{\frac{1}{2}}] &- T_{2\nu_I}K_{2\nu_I}[\sqrt{2}\mid\zeta_I\mid^{\frac{1}{2}}] \ , \\
S_{2\nu_I}I'_{2\nu_I}[\sqrt{2}\mid\zeta_I\mid^{\frac{1}{2}}] &- T_{2\nu_I}K'_{2\nu_I}[\sqrt{2}\mid\zeta_I\mid^{\frac{1}{2}}] \ , \\
U_{2\nu_I}J_{2\nu_I}[\sqrt{2}\zeta_I^{\frac{1}{2}}] &- V_{2\nu_I}Y_{2\nu_I}[\sqrt{2}\zeta_I^{\frac{1}{2}}] \ , \\
U_{2\nu_I}J'_{2\nu_I}[\sqrt{2}\zeta_I^{\frac{1}{2}}] &- V_{2\nu_I}Y'_{2\nu_I}[\sqrt{2}\zeta_I^{\frac{1}{2}}] \ , \\
U_{2\nu_I}I_{2\nu_I}[\sqrt{2}\mid\zeta_I\mid^{\frac{1}{2}}] &- V_{2\nu_I}K_{2\nu_I}[\sqrt{2}\mid\zeta_I\mid^{\frac{1}{2}}] \ , \\
U_{2\nu_I}I'_{2\nu_I}[\sqrt{2}\mid\zeta_I\mid^{\frac{1}{2}}] &- V_{2\nu_I}K'_{2\nu_I}[\sqrt{2}\mid\zeta_I\mid^{\frac{1}{2}}] \ ,
\end{aligned}$$

are also odd functions of the transverse transform variable k. Since ratios of the above quantities are taken in the image term $\bar{\Delta}_2(L,\zeta_E,D,\zeta_I)$ and is therefore an even function with respect to k for finite L and D. Thus, as noted by Carnie and Chan [41], the correlation in the transverse direction is screened. The shielding in the transverse direction occurs because the charge on the opposite side of the membrane wall is able to redistribute itself, screening the potential between molecules.

As $k \to \infty$, comparison between the two membrane and one membrane system (see Appendix B) shows that both $\bar{\Delta}_2(L,\zeta_E,D,\zeta_I)$ and $\bar{\Delta}_1(2L,\zeta_E,\zeta_I)$ tend to the same limit i.e.

$$\bar{\Delta}_2 \to \bar{\Delta}_1 \to \begin{cases} \dfrac{Y_{2\nu_E}[2\zeta_E^{\frac{1}{2}}]+\frac{\epsilon_E\kappa_E\zeta_E^{\frac{1}{2}}}{k\epsilon_M}Y'_{2\nu_E}[2\zeta_E^{\frac{1}{2}}]}{J_{2\nu_E}[2\zeta_E^{\frac{1}{2}}]+\frac{\epsilon_E\kappa_E\zeta_E^{\frac{1}{2}}}{k\epsilon_M}J'_{2\nu_E}[2\zeta_E^{\frac{1}{2}}]} & \zeta_E > 0 \\ \dfrac{K_{2\nu_E}[2|\zeta_E|^{\frac{1}{2}}]+\frac{\epsilon_E\kappa_E|\zeta_E|^{\frac{1}{2}}}{k\epsilon_M}K'_{2\nu_E}[2|\zeta_E|^{\frac{1}{2}}]}{I_{2\nu_E}[2|\zeta_E|^{\frac{1}{2}}]+\frac{\epsilon_E\kappa_E|\zeta_E|^{\frac{1}{2}}}{k\epsilon_M}I'_{2\nu_E}[2|\zeta_E|^{\frac{1}{2}}]} & \zeta_E < 0 \end{cases} , \tag{3.35}$$

This is also the limit as $k \to \infty$ for $\bar{\Delta}(\zeta)$ in the one wall system [41], when $\zeta = \zeta_E$, even though $\bar{\Delta}(\zeta)$ is neither an even or odd function of k. This is not a surprising result if we consider all three quantities at the same source and field point, relative to the membrane

wall at the interface between the extracellular fluid and membrane. Since the large k behaviour describes the small ρ behaviour, a molecule experiences negligible influence from boundaries more than a Debye length away. Thus only as $k \to 0$ (large ρ behaviour) can we expect any influence from the other regions.

Also it should be noted that the large k behaviour for $\bar{\Delta}_2(L, \zeta_E, D, \zeta_I)$ has no explicit dependence on the distance between the membrane walls $2D$ and both $\bar{\Delta}_2(L, \zeta_E, D, \zeta_I)$ and $\bar{\Delta}_1(2L, \zeta_E, \zeta_I)$ have no explicit dependence on the membrane thickness. The dependence of these quantities on the parameters L and D is rather via the extracellular asymmetry parameter ζ_E. The two membrane system extracellular asymmetry parameter ζ_E, for fixed membrane thickness, has negligible dependence on the distance between the membrane walls provided the distance is large. This is certainly true for our value of $2D = 200\mathring{A}$ and is valid to the approximation breakdown distance for the intracellular mean electrostatic potential of about $60\mathring{A}$. Thus the two and one membrane systems have identical values for the extracellular asymmetry parameter ζ_E for the same values of the membrane thickness. Table 3.2 shows values of the extracellular asymmetry parameter ζ_E for various values of the membrane thickness. In the limit as $L \to \infty$, both the two and one membrane systems extracellular asymmetry parameter ζ_E approach the one wall system value given by

$$\begin{aligned} \zeta_E &= -\frac{4\pi\sigma_E\beta}{\epsilon_E\kappa_E}\left[\frac{\sum_k e_k^3 n_k^{E0}}{\sum_k e_k^2 n_k^{E0}}\right] \\ &= 0.046709 \ . \end{aligned}$$

If we assume that the ratios $\frac{2\zeta_I^{\frac{1}{2}}}{2\nu_I}\,|_{k=0}$, $\frac{2|\zeta_I|^{\frac{1}{2}}}{2\nu_I}\,|_{k=0}$, $\frac{2\zeta_E^{\frac{1}{2}}}{2\nu_E}\,|_{k=0}$ and $\frac{2|\zeta_E|^{\frac{1}{2}}}{2\nu_E}\,|_{k=0} < 1$, we can use the asymptotic forms for the Bessel and modified Bessel functions in Appendix D to show

$$Z_{2\nu_E} \to \begin{cases} \dfrac{\sinh[kL]+\frac{\epsilon_E\kappa_E\nu_E}{k\epsilon_M}\sqrt{1-\left[\frac{q_E(-[L+D])}{2\nu_E}\right]^2}\cosh[kL]\delta^-_{2\nu_E}(-[L+D])}{\cosh[kL]+\frac{\epsilon_E\kappa_E\nu_E}{k\epsilon_M}\sqrt{1-\left[\frac{q_E(-[L+D])}{2\nu_E}\right]^2}\sinh[kL]\delta^-_{2\nu_E}(-[L+D])} & \zeta_E > 0 \\ \dfrac{\sinh[kL]+\frac{\epsilon_E\kappa_E\nu_E}{k\epsilon_M}\sqrt{1+\left[\frac{q_E(-[L+D])}{2\nu_E}\right]^2}\cosh[kL]\delta^+_{2\nu_E}(-[L+D])}{\cosh[kL]+\frac{\epsilon_E\kappa_E\nu_E}{k\epsilon_M}\sqrt{1+\left[\frac{q_E(-[L+D])}{2\nu_E}\right]^2}\sinh[kL]\delta^+_{2\nu_E}(-[L+D])} & \zeta_E < 0 \end{cases} ,$$

Membrane Thickness ($\mathring{A}$)	ζ_E	ζ_I
10	0.028874	0.443978
50	0.042949	0.347285
100	0.044835	0.334335
1000	0.046558	0.322494

Table 3.2: Table of ζ_E and ζ_I values for various membrane thickness values of the one and two membrane systems.

$$X_{2\nu_E} \rightarrow \begin{cases} \dfrac{\sinh[kL]-\frac{\epsilon_E\kappa_E\nu_E}{k\epsilon_M}\sqrt{1-\left[\frac{q_E(-[L+D])}{2\nu_E}\right]^2}\cosh[kL]\delta^+_{2\nu_E}(-[L+D])}{\cosh[kL]-\frac{\epsilon_E\kappa_E\nu_E}{k\epsilon_M}\sqrt{1-\left[\frac{q_E(-[L+D])}{2\nu_E}\right]^2}\sinh[kL]\delta^+_{2\nu_E}(-[L+D])} & \zeta_E > 0 \\ \dfrac{\sinh[kL]-\frac{\epsilon_E\kappa_E\nu_E}{k\epsilon_M}\sqrt{1+\left[\frac{q_E(-[L+D])}{2\nu_E}\right]^2}\cosh[kL]\delta^-_{2\nu_E}(-[L+D])}{\cosh[kL]-\frac{\epsilon_E\kappa_E\nu_E}{k\epsilon_M}\sqrt{1+\left[\frac{q_E(-[L+D])}{2\nu_E}\right]^2}\sinh[kL]\delta^-_{2\nu_E}(-[L+D])} & \zeta_E < 0 \end{cases} ,$$

where

$$\begin{aligned} \delta^+_{2\nu_E}(z_1) &= 1+\frac{1}{2}\left[\frac{q^2_E(z_1)}{[2\nu_E]^3}\right]+O((2\nu_E)^{-4}) \ , \\ \delta^-_{2\nu_E}(z_1) &= 1-\frac{1}{2}\left[\frac{q^2_E(z_1)}{[2\nu_E]^3}\right]+O((2\nu_E)^{-4}) \ , \end{aligned}$$

such that

$$q_E(z_1) = \begin{cases} 2\zeta_E^{\frac{1}{2}}\exp\left[\frac{\kappa_E(z_1+[L+D])}{2}\right] & \zeta_E > 0 \\ 2\mid\zeta_E\mid^{\frac{1}{2}}\exp\left[\frac{\kappa_E(z_1+[L+D])}{2}\right] & \zeta_E < 0 \end{cases} .$$

Thus the quantity $\bar{\Delta}_2(L,\zeta_E,D,\zeta_I)$ has the asymptotic form of

$$\bar{\Delta}_2 \rightarrow \begin{cases} -\frac{1}{2}\dfrac{Y_{2\nu_E}[2\zeta_E^{\frac{1}{2}}]}{J_{2\nu_E}[2\zeta_E^{\frac{1}{2}}]}\dfrac{\cosh[kL]-\frac{\epsilon_E\kappa_E\nu_E}{k\epsilon_M}\sqrt{1-\left[\frac{q_E(-[L+D])}{2\nu_E}\right]^2}\sinh[kL]\delta^+_{2\nu_E}(-[L+D])}{\cosh[kL]+\frac{\epsilon_E\kappa_E\nu_E}{k\epsilon_M}\sqrt{1-\left[\frac{q_E(-[L+D])}{2\nu_E}\right]^2}\sinh[kL]\delta^-_{2\nu_E}(-[L+D])} \\ \times\left[\dfrac{X_{2\nu_E}(L,\zeta_E)+\frac{\epsilon_I\kappa_I\nu_I}{k\epsilon_M}M^+_{2\nu_I}(-D,0)}{Z_{2\nu_E}(L,\zeta_E)+\frac{\epsilon_I\kappa_I\nu_I}{k\epsilon_M}M^+_{2\nu_I}(-D,0)}+\dfrac{X_{2\nu_E}(L,\zeta_E)+\frac{\epsilon_I\kappa_I\nu_I}{k\epsilon_M}M^-_{2\nu_I}(-D,0)}{Z_{2\nu_E}(L,\zeta_E)+\frac{\epsilon_I\kappa_I\nu_I}{k\epsilon_M}M^-_{2\nu_I}(-D,0)}\right] & \zeta_E > 0 \\ -\frac{1}{2}\dfrac{K_{2\nu_E}[2|\zeta_E|^{\frac{1}{2}}]}{I_{2\nu_E}[2|\zeta_E|^{\frac{1}{2}}]}\dfrac{\cosh[kL]-\frac{\epsilon_E\kappa_E\nu_E}{k\epsilon_M}\sqrt{1+\left[\frac{q_E(-[L+D])}{2\nu_E}\right]^2}\sinh[kL]\delta^-_{2\nu_E}(-[L+D])}{\cosh[kL]+\frac{\epsilon_E\kappa_E\nu_E}{k\epsilon_M}\sqrt{1+\left[\frac{q_E(-[L+D])}{2\nu_E}\right]^2}\sinh[kL]\delta^+_{2\nu_E}(-[L+D])} \\ \times\left[\dfrac{X_{2\nu_E}(L,\zeta_E)+\frac{\epsilon_I\kappa_I\nu_I}{k\epsilon_M}M^+_{2\nu_I}(-D,0)}{Z_{2\nu_E}(L,\zeta_E)+\frac{\epsilon_I\kappa_I\nu_I}{k\epsilon_M}M^+_{2\nu_I}(-D,0)}+\dfrac{X_{2\nu_E}(L,\zeta_E)+\frac{\epsilon_I\kappa_I\nu_I}{k\epsilon_M}M^-_{2\nu_I}(-D,0)}{Z_{2\nu_E}(L,\zeta_E)+\frac{\epsilon_I\kappa_I\nu_I}{k\epsilon_M}M^-_{2\nu_I}(-D,0)}\right] & \zeta_E < 0 \end{cases} ,$$

such that

$$M^{+}_{2\nu_I}(-D,0) = \begin{cases} \sqrt{1-[\frac{q_I(-D)}{2\nu_I}]^2} \\ \times \frac{\cosh[2\nu_I\eta_{2\nu_I}(-D,0)]+\frac{1}{4}\frac{[q_I(-D)^2+q_I(0)^2]}{[2\nu_I]^3}\sinh[2\nu_I\eta_{2\nu_I}(-D,0)]}{\sinh[2\nu_I\eta_{2\nu_I}(-D,0)]-\frac{1}{4}\frac{[q_I(-D)^2-q_I(0)^2]}{[2\nu_I]^3}\cosh[2\nu_I\eta_{2\nu_I}(-D,0)]} & \zeta_I > 0 \\ \sqrt{1+[\frac{q_I(-D)}{2\nu_I}]^2} \\ \times \frac{\cosh[2\nu_I\eta_{2\nu_I}(-D,0)]-\frac{1}{4}\frac{[q_I(-D)^2+q_I(0)^2]}{[2\nu_I]^3}\sinh[2\nu_I\eta_{2\nu_I}(-D,0)]}{\sinh[2\nu_I\eta_{2\nu_I}(-D,0)]+\frac{1}{4}\frac{[q_I(-D)^2-q_I(0)^2]}{[2\nu_I]^3}\cosh[2\nu_I\eta_{2\nu_I}(-D,0)]} & \zeta_I < 0 \end{cases},$$

$$M^{-}_{2\nu_I}(-D,0) = \begin{cases} \sqrt{1-[\frac{q_I(-D)}{2\nu_I}]^2} \\ \times \frac{\sinh[2\nu_I\eta_{2\nu_I}(-D,0)]+\frac{1}{4}\frac{[q_I(-D)^2+q_I(0)^2]}{[2\nu_I]^3}\cosh[2\nu_I\eta_{2\nu_I}(-D,0)]}{\cosh[2\nu_I\eta_{2\nu_I}(-D,0)]-\frac{1}{4}\frac{[q_I(-D)^2-q_I(0)^2]}{[2\nu_I]^3}\sinh[2\nu_I\eta_{2\nu_I}(-D,0)]} & \zeta_I > 0 \\ \sqrt{1+[\frac{q_I(-D)}{2\nu_I}]^2} \\ \times \frac{\sinh[2\nu_I\eta_{2\nu_I}(-D,0)]-\frac{1}{4}\frac{[q_I(-D)^2+q_I(0)^2]}{[2\nu_I]^3}\cosh[2\nu_I\eta_{2\nu_I}(-D,0)]}{\cosh[2\nu_I\eta_{2\nu_I}(-D,0)]+\frac{1}{4}\frac{[q_I(-D)^2-q_I(0)^2]}{[2\nu_I]^3}\sinh[2\nu_I\eta_{2\nu_I}(-D,0)]} & \zeta_I < 0 \end{cases},$$

where

$$\eta_{2\nu_I}(z_1,z_2) = \begin{cases} -\frac{\kappa_I(z_1-z_2)}{2} - \frac{1}{[2\nu_I]^3}\left[\frac{q_I^2(z_1)-q_I^2(z_2)}{4}\right] + O((2\nu_I)^{-4}) & \zeta_I > 0 \\ -\frac{\kappa_I(z_1-z_2)}{2} + \frac{1}{[2\nu_I]^3}\left[\frac{q_I^2(z_1)-q_I^2(z_2)}{4}\right] + O((2\nu_I)^{-4}) & \zeta_I < 0 \end{cases},$$

$$q_I(z_1) = \begin{cases} \sqrt{2}\zeta_I^{\frac{1}{2}}\exp\left[\frac{-\kappa_I z_1}{2}\right] & \zeta_I > 0 \\ \sqrt{2}\mid\zeta_I\mid^{\frac{1}{2}}\exp\left[\frac{-\kappa_I z_1}{2}\right] & \zeta_I < 0 \end{cases}.$$

Thus the solution for the transverse Hankel transform mean electrostatic fluctuation potential in region I can be simplified to

$$\begin{aligned} \tilde{\psi}^{L}_{E}(z_1,z_2,\mathbf{k}) = & \frac{2\pi}{\epsilon_E\kappa_E\nu_E}\left[\frac{1}{1-[\frac{q_E(z_1)}{2\nu_E}]^2}\right]^{\frac{1}{4}}\left[\frac{1}{1-[\frac{q_E(z_1)}{2\nu_E}]^2}\right]^{\frac{1}{4}} \\ & \times \left\{\gamma_{2\nu_E}(z_<,z_>)\exp\left[2\nu_E\eta_{2\nu_E}(z_<,z_>)\right]\right. \\ & - \frac{1}{2}\lambda_{2\nu_E}(z_1,z_2)\exp\left[2\nu_E[\eta_{2\nu_E}(-[L+D],z_1)+\eta_{2\nu_E}(-[L+D],z_2)]\right] \\ & \times \left[\frac{\cosh[kL]-\frac{\epsilon_E\kappa_E\nu_E}{k\epsilon_M}\sqrt{1-[\frac{q_E(-[L+D])}{2\nu_E}]^2}\sinh[kL]\delta^{+}_{2\nu_E}(-[L+D])}{\cosh[kL]+\frac{\epsilon_E\kappa_E\nu_E}{k\epsilon_M}\sqrt{1-[\frac{q_E(-[L+D])}{2\nu_E}]^2}\sinh[kL]\delta^{-}_{2\nu_E}(-[L+D])}\right] \\ & \times \left[\frac{X_{2\nu_E}(L,\zeta_E)+\frac{\epsilon_I\kappa_I\nu_I}{k\epsilon_M}M^{+}_{2\nu_I}(-D,0)}{Z_{2\nu_E}(L,\zeta_E)+\frac{\epsilon_I\kappa_I\nu_I}{k\epsilon_M}M^{+}_{2\nu_I}(-D,0)}\right. \\ & \left.\left. + \frac{X_{2\nu_E}(L,\zeta_E)+\frac{\epsilon_I\kappa_I\nu_I}{k\epsilon_M}M^{-}_{2\nu_I}(-D,0)}{Z_{2\nu_E}(L,\zeta_E)+\frac{\epsilon_I\kappa_I\nu_I}{k\epsilon_M}M^{-}_{2\nu_I}(-D,0)}\right]\right\} \quad \zeta_E > 0\ , \end{aligned} \tag{3.36}$$

and

$$
\begin{aligned}
\tilde{\psi}_E^L(z_1,z_2,\mathbf{k}) = \quad & \frac{2\pi}{\epsilon_E\kappa_E\nu_E}\left[\frac{1}{1+[\frac{q_E(z_1)}{2\nu_E}]^2}\right]^{\frac{1}{4}}\left[\frac{1}{1+[\frac{q_E(z_1)}{2\nu_E}]^2}\right]^{\frac{1}{4}} \\
\times \quad & \left\{\gamma_{2\nu_E}(z_<,z_>)\exp\left[2\nu_E\eta_{2\nu_E}(z_<,z_>)\right]\right. \\
- \quad & \frac{1}{2}\lambda_{2\nu_E}(z_1,z_2)\exp\left[2\nu_E[\eta_{2\nu_E}(-[L+D],z_1)+\eta_{2\nu_E}(-[L+D],z_2)]\right] \\
\times \quad & \left[\frac{\cosh[kL]-\frac{\epsilon_E\kappa_E\nu_E}{k\epsilon_M}\sqrt{1+[\frac{q_E(-[L+D])}{2\nu_E}]^2}\sinh[kL]\delta^-_{2\nu_E}(-[L+D])}{\cosh[kL]+\frac{\epsilon_E\kappa_E\nu_E}{k\epsilon_M}\sqrt{1+[\frac{q_E(-[L+D])}{2\nu_E}]^2}\sinh[kL]\delta^+_{2\nu_E}(-[L+D])}\right] \\
\times \quad & \left[\frac{X_{2\nu_E}(L,\zeta_E)+\frac{\epsilon_I\kappa_I\nu_I}{k\epsilon_M}M_{2\nu_I}(-D,0)}{Z_{2\nu_E}(L,\zeta_E)+\frac{\epsilon_I\kappa_I\nu_I}{k\epsilon_M}M_{2\nu_I}(-D,0)}\right. \\
+ \quad & \left.\left.\frac{X_{2\nu_E}(L,\zeta_E)+\frac{\epsilon_I\kappa_I\nu_I}{k\epsilon_M}M^-_{2\nu_I}(-D,0)}{Z_{2\nu_E}(L,\zeta_E)+\frac{\epsilon_I\kappa_I\nu_I}{k\epsilon_M}M^-_{2\nu_I}(-D,0)}\right]\right\} \quad \zeta_E<0\ , \qquad (3.37)
\end{aligned}
$$

where

$$
\eta_{2\nu_E}(z_1,z_2) = \begin{cases} -\frac{\kappa_E(z_1-z_2)}{2}-\frac{1}{[2\nu_E]^2}\left[\frac{q_E^2(z_1)-q_E^2(z_2)}{4}\right]+O((2\nu_E)^{-4}) & \zeta_E>0 \\ -\frac{\kappa_E(z_1-z_2)}{2}+\frac{1}{[2\nu_E]^2}\left[\frac{q_E^2(z_1)-q_E^2(z_2)}{4}\right]+O((2\nu_E)^{-4}) & \zeta_E<0 \end{cases},
$$

$$
\gamma_{2\nu_E}(z_1,z_2) = \begin{cases} 1+\frac{1}{[2\nu_E]^3}\left[\frac{q_E^2(z_1)-q_E^2(z_2)}{4}\right]+O((2\nu_E)^{-4}) & \zeta_E>0 \\ 1-\frac{1}{[2\nu_E]^3}\left[\frac{q_E^2(z_1)-q_E^2(z_2)}{4}\right]+O((2\nu_E)^{-4}) & \zeta_E<0 \end{cases},
$$

$$
\lambda_{2\nu_E}(z_1,z_2) = \begin{cases} 1+\frac{1}{[2\nu_E]^3}\left[\frac{2q_E^2(-[L+D])-q_E^2(z_1)-q_E^2(z_2)}{4}\right]+O((2\nu_E)^{-4}) & \zeta_E>0 \\ 1-\frac{1}{[2\nu_E]^3}\left[\frac{2q_E^2(-[L+D])-q_E^2(z_1)-q_E^2(z_2)}{4}\right]+O((2\nu_E)^{-4}) & \zeta_E<0 \end{cases}.
$$

Since the above expressions for the transverse Hankel transform mean electrostatic fluctuation potential involve a considerable amount of algebra to derive and are complicated, a numerical integration of the differential equations is used to test the validity of the analytic solutions. A shooting method [114] is employed to numerical solve the differential equations for the transverse Hankel transform mean electrostatic fluctuation potential. This method solves the differential equations by starting at two boundaries and "shooting" towards an interior point using the Runge-Kutta algorithm and using iteration matches the solutions from either side. For our particular application, the shooting point is the source point. At the source point we require that the solution is continuous and has a jump discontinuity in the first derivative. To start the integration we choose boundaries

far enough away from the source point so that the solution and the first derivative are essentially zero (due to the expected exponential decay of the solutions from the source point). The distance of the boundaries from the source point is also important to ensure that there is a negligible mix of the unbounded solution with the required bounded solution.

Presented below are plots of the numerical and asymptotic transverse Hankel transform mean electrostatic fluctuation potential at the source point for specified k values. See Figures 3.5, 3.6, 3.7 and 3.8. The location of the starting boundaries for the numerical procedure decreased as the value of the transform variable k increased. For $k = 0.001\mathring{A}^{-1}$ the boundaries were located about $100\mathring{A}$ either side of the source and for $k = 1\mathring{A}^{-1}$ at about $5\mathring{A}$. This is consistent with the above discussion for large k behaviour which is determined by the region near the source point whereas the opposite is true for small k values. Thus for these values a knowledge of the differential equations for the second membrane and the extracellular region V is unnecessary. This suggests that the second membrane and thus the extracellular fluid in region V have negligible effect on the value for the transverse Hankel transform mean electrostatic fluctuation potential (and thus the mean electrostatic fluctuation potential).

As the normal distance from the membrane wall increases, the plots tend to a constant value determined by the Debye-Huckel type term in the solution i.e.

$$\tilde{\psi}_E^L(z_1, z_2, \mathbf{k}) \rightarrow \begin{cases} \frac{2\pi}{\epsilon_E \kappa_E \nu_E} \left[\frac{1}{1-\left[\frac{q_E(z_1)}{2\nu_E}\right]^2}\right]^{\frac{1}{4}} \left[\frac{1}{1-\left[\frac{q_E(z_1)}{2\nu_E}\right]^2}\right]^{\frac{1}{4}} & \zeta_E > 0 \\ \frac{2\pi}{\epsilon_E \kappa_E \nu_E} \left[\frac{1}{1+\left[\frac{q_E(z_1)}{2\nu_E}\right]^2}\right]^{\frac{1}{4}} \left[\frac{1}{1+\left[\frac{q_E(z_1)}{2\nu_E}\right]^2}\right]^{\frac{1}{4}} & \zeta_E < 0 \end{cases}$$

As the transform variable k increases this Debye-Huckel term (the field point and source point coinciding) has the form

$$\tilde{\psi}_E^L(z_1, z_2, \mathbf{k}) \rightarrow \frac{2\pi}{\epsilon_E k} \ .$$

This result is consistent with that of Carnie and Chan [41] for the constant density systems (both single and two plate) and the linearized GC density for the single plate. Again this is due to the large k behaviour being determined by the region near the source point.

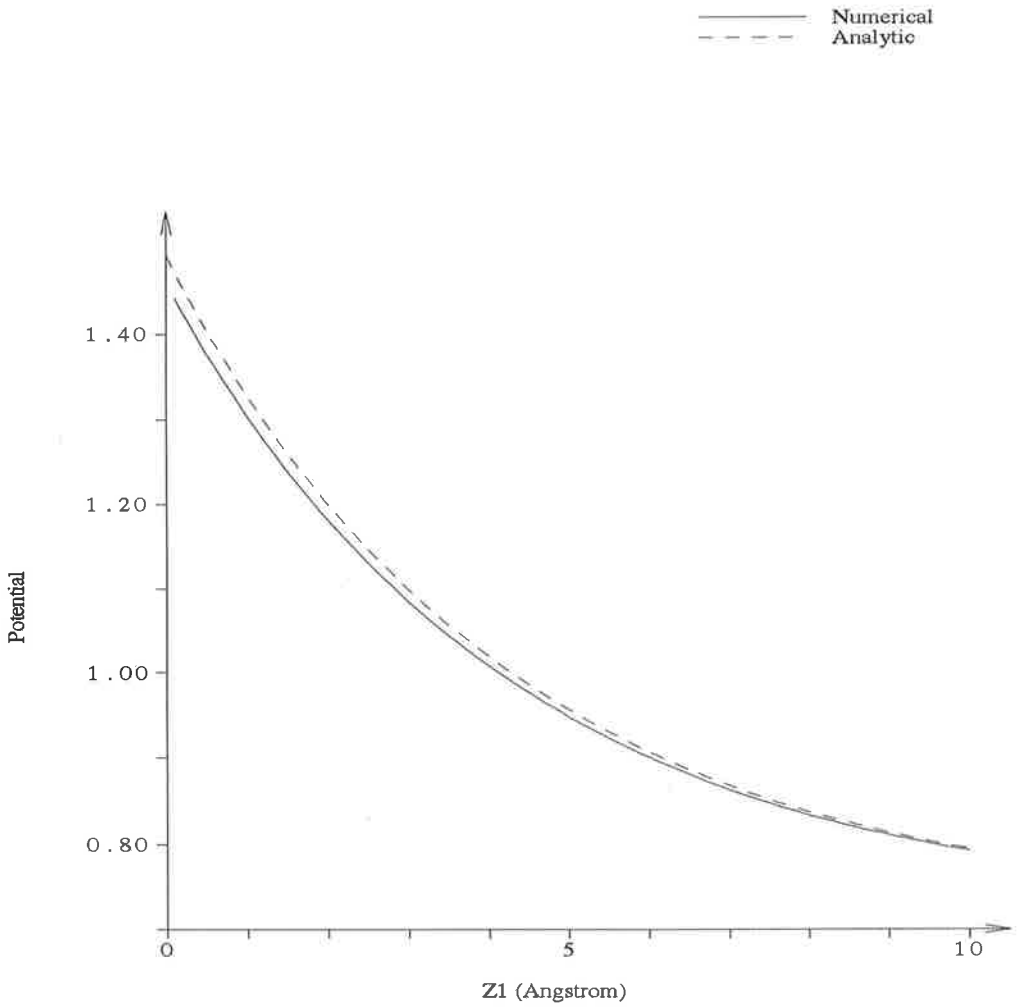

Figure 3.5: Comparison of the numerical and asymptotic solution for the transverse Hankel transform mean electrostatic fluctuation potential at the source point in the extracellular fluid of a two membrane system vs distance from the membrane wall for k=0.001.

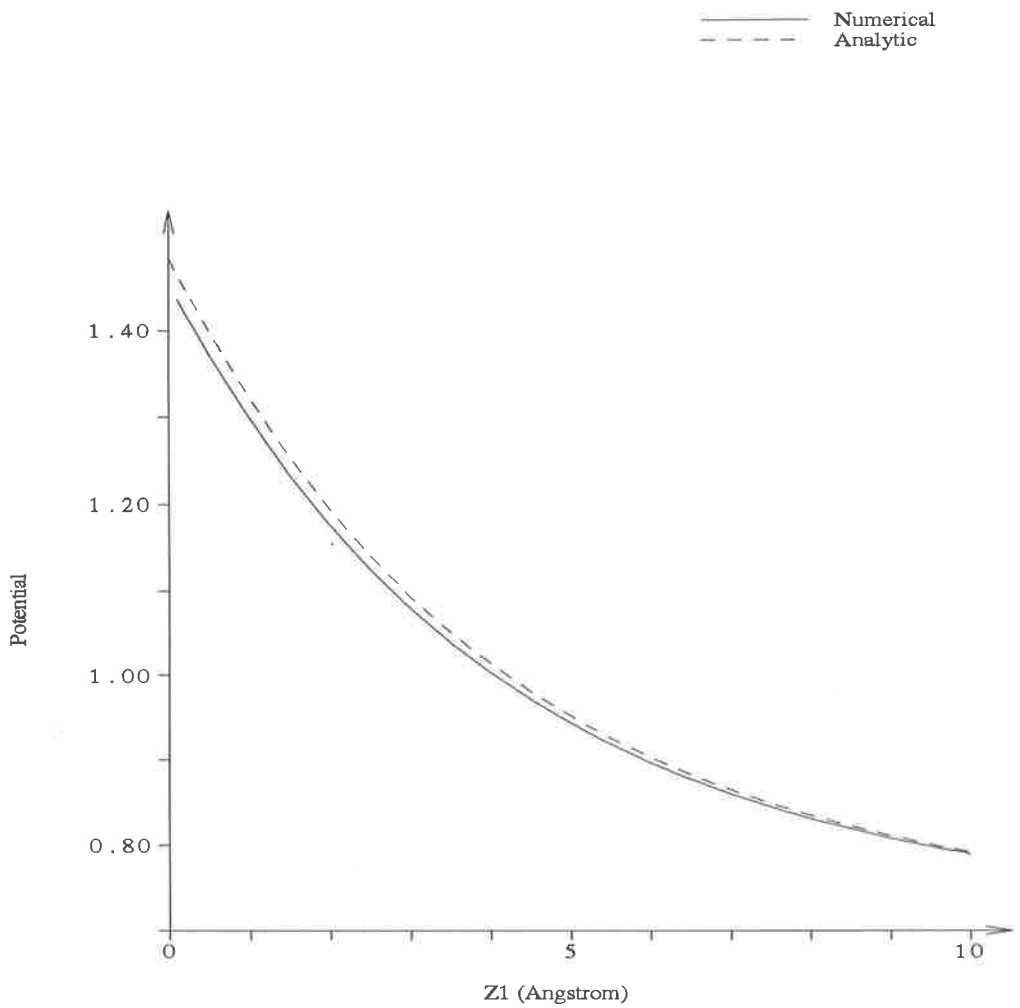

Figure 3.6: Comparison of the numerical and asymptotic solution for the transverse Hankel transform mean electrostatic fluctuation potential at the source point in the extracellular fluid of a two membrane system vs distance from the membrane wall for k=0.01.

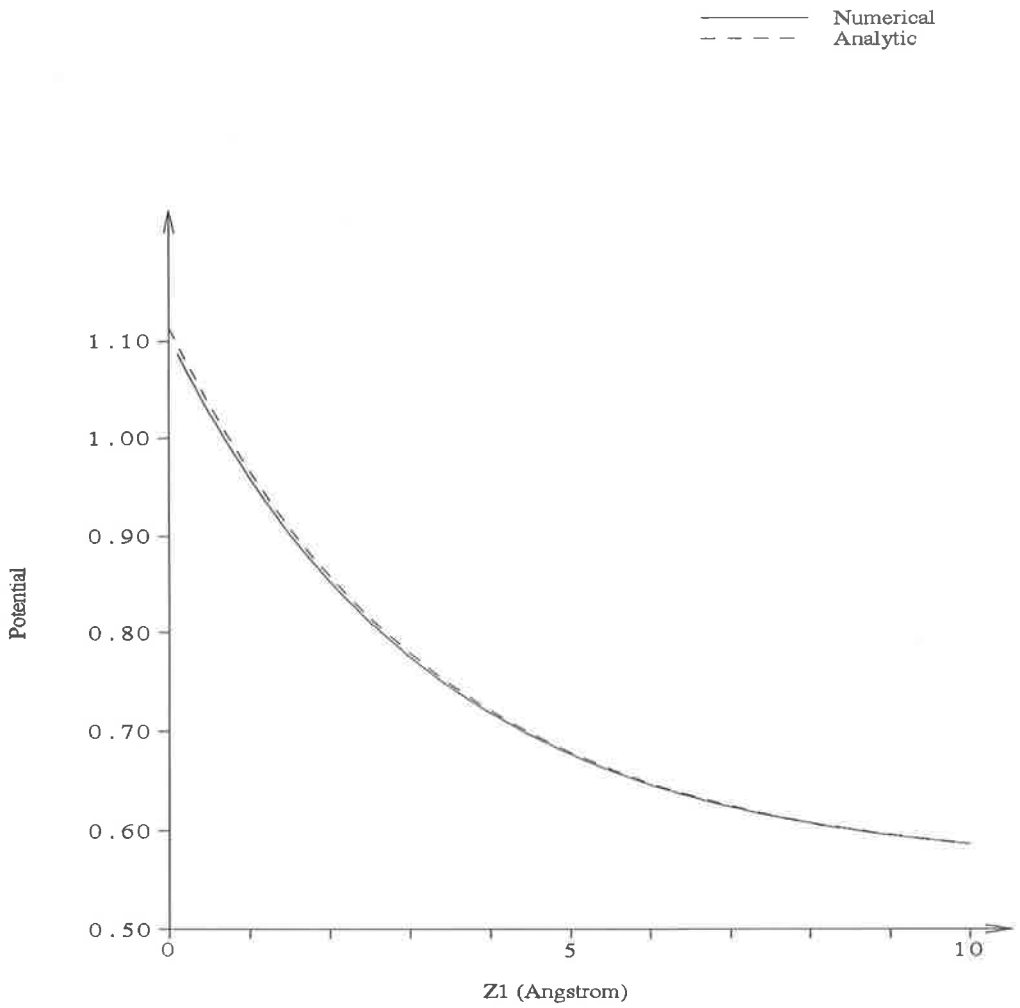

Figure 3.7: Comparison of the numerical and asymptotic solution for the transverse Hankel transform mean electrostatic fluctuation potential at the source point in the extracellular fluid of a two membrane system vs distance from the membrane wall for k=0.1.

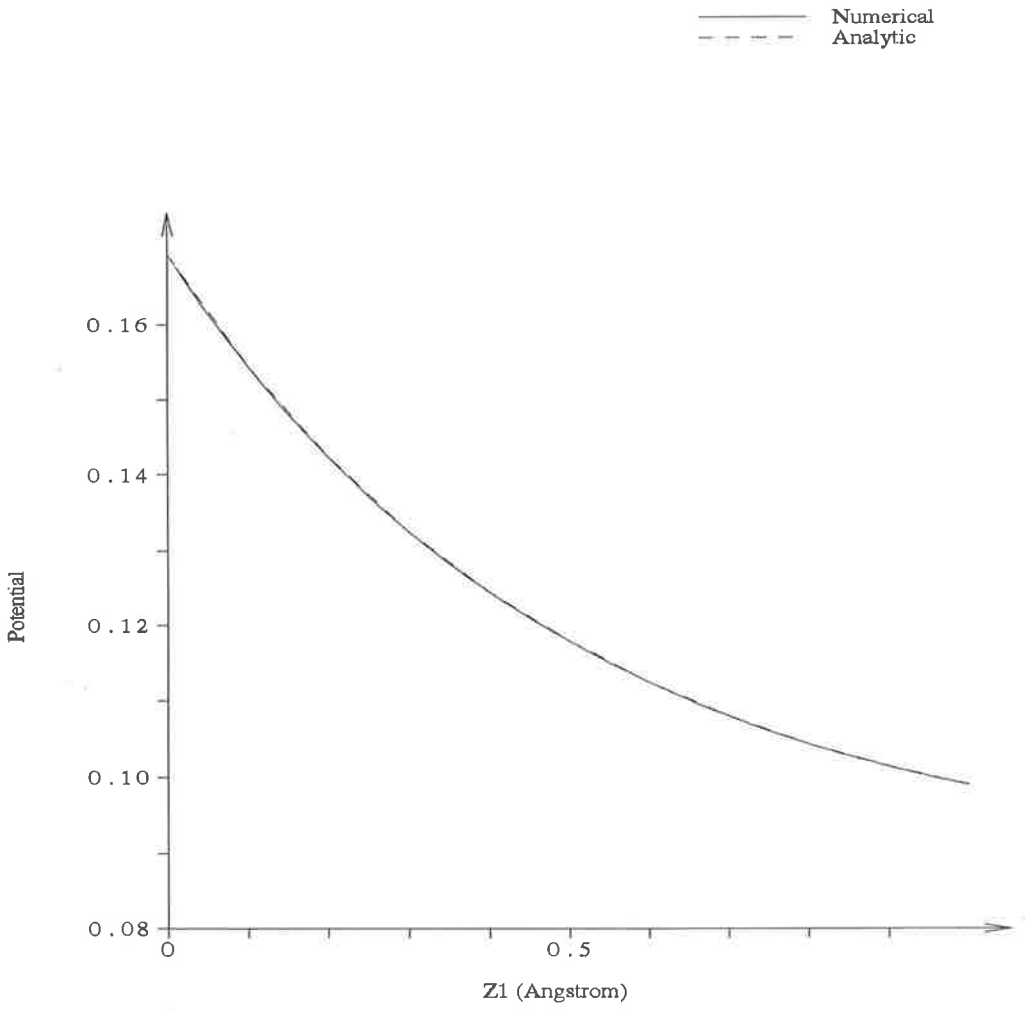

Figure 3.8: Comparison of the numerical and asymptotic solution for the transverse Hankel transform mean electrostatic fluctuation potential at the source point in the extracellular fluid of a two membrane system vs distance from the membrane wall for k=1.

The asymptotic solution for the transverse Hankel transform mean electrostatic fluctuation potential in region I is a complicated expression. A simplification can be made by noting the second membrane wall has a negligible effect on the values for the contribution from the image forces. See Figure 3.9. Thus for the purposes of performing the Hankel transform inversion we will replace $\bar{\Delta}_2(L, \zeta_E, D, \zeta_I)$ with the simpler expression for the image forces of the one membrane system $\bar{\Delta}_1(2L, \zeta_E, \zeta_I)$.

3.2.3 Limiting forms of the transverse Hankel transform mean electrostatic fluctuation potential

To obtain the one membrane limiting form (as described in Section 3.1.1) for the transverse Hankel transform mean electrostatic fluctuation potential we first take the limit as $\zeta_I \to 0$. As a result, both

$$\frac{U_{2\nu_I} J_{2\nu_I}[\sqrt{2}\zeta_I^{\frac{1}{2}}] - V_{2\nu_I} Y_{2\nu_I}[\sqrt{2}\zeta_I^{\frac{1}{2}}]}{S_{2\nu_I} J_{2\nu_I}[\sqrt{2}\zeta_I^{\frac{1}{2}}] - T_{2\nu_I} Y_{2\nu_I}[\sqrt{2}\zeta_I^{\frac{1}{2}}]}$$

and

$$\frac{U_{2\nu_I} I_{2\nu_I}[\sqrt{2} \mid \zeta_I \mid^{\frac{1}{2}}] - V_{2\nu_I} K_{2\nu_I}[\sqrt{2} \mid \zeta_I \mid^{\frac{1}{2}}]}{S_{2\nu_I} I_{2\nu_I}[\sqrt{2} \mid \zeta_I \mid^{\frac{1}{2}}] - T_{2\nu_I} K_{2\nu_I}[\sqrt{2} \mid \zeta_I \mid^{\frac{1}{2}}]}$$

tend to the same limit of

$$\frac{X_{2\nu_E} \sinh[\kappa_I \nu_I D] + \frac{\epsilon_I \kappa_I \nu_I}{k \epsilon_M} \cosh[\kappa_I \nu_I D]}{Z_{2\nu_E} \sinh[\kappa_I \nu_I D] + \frac{\epsilon_I \kappa_I \nu_I}{k \epsilon_M} \cosh[\kappa_I \nu_I D]}.$$

Also, both

$$\frac{U_{2\nu_I} J'_{2\nu_I}[\sqrt{2}\zeta_I^{\frac{1}{2}}] - V_{2\nu_I} Y'_{2\nu_I}[\sqrt{2}\zeta_I^{\frac{1}{2}}]}{S_{2\nu_I} J'_{2\nu_I}[\sqrt{2}\zeta_I^{\frac{1}{2}}] - T_{2\nu_I} Y'_{2\nu_I}[\sqrt{2}\zeta_I^{\frac{1}{2}}]}$$

and

$$\frac{U_{2\nu_I} I'_{2\nu_I}[\sqrt{2} \mid \zeta_I \mid^{\frac{1}{2}}] - V_{2\nu_I} K'_{2\nu_I}[\sqrt{2} \mid \zeta_I \mid^{\frac{1}{2}}]}{S_{2\nu_I} I'_{2\nu_I}[\sqrt{2} \mid \zeta_I \mid^{\frac{1}{2}}] - T_{2\nu_I} K'_{2\nu_I}[\sqrt{2} \mid \zeta_I \mid^{\frac{1}{2}}]}$$

tend to the same limit of

$$\frac{X_{2\nu_E} \cosh[\kappa_I \nu_I D] + \frac{\epsilon_I \kappa_I \nu_I}{k \epsilon_M} \sinh[\kappa_I \nu_I D]}{Z_{2\nu_E} \cosh[\kappa_I \nu_I D] + \frac{\epsilon_I \kappa_I \nu_I}{k \epsilon_M} \sinh[\kappa_I \nu_I D]}.$$

If we now take the limit $\kappa_I \to 0$ then the quantity $\kappa_I \nu_I \to k$. Also we set the dielectric constant of the intracellular fluid region to that of the membrane i.e. $\epsilon_I \to \epsilon_M$. Thus both

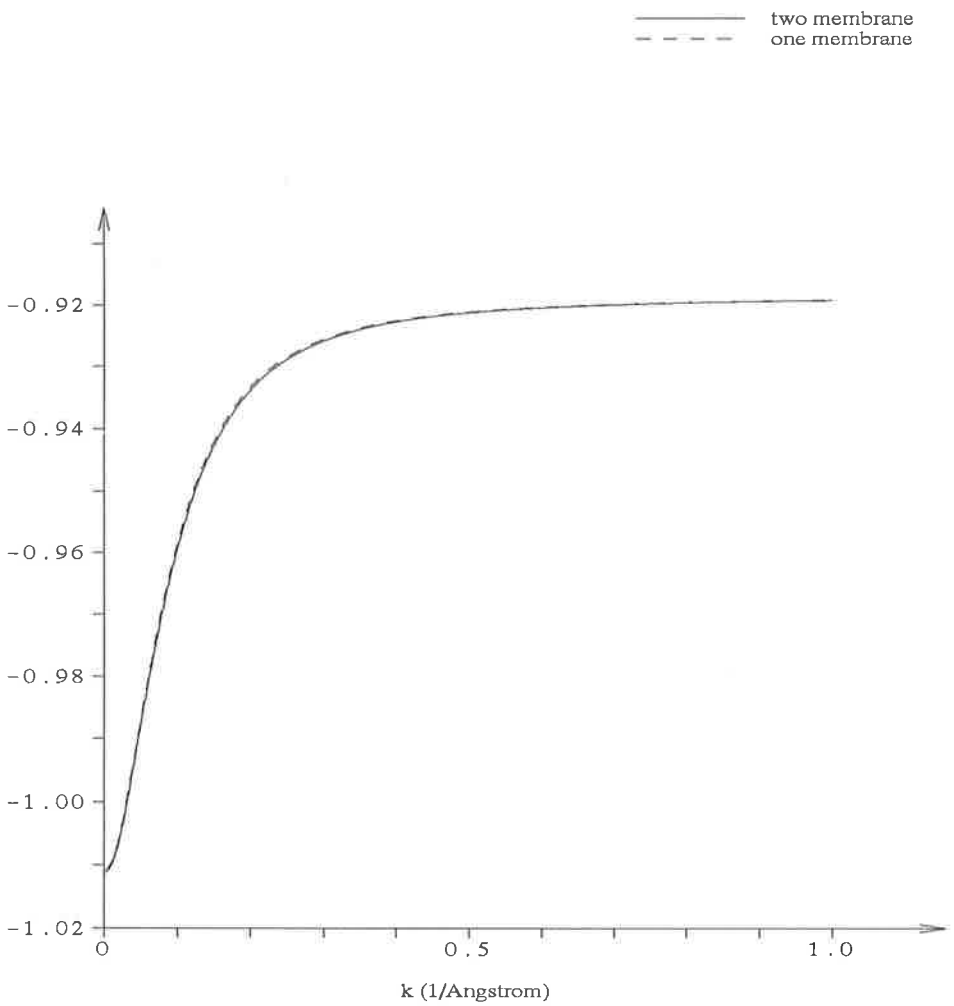

Figure 3.9: Comparison of $-\bar{\Delta}_1 \frac{J_{2\nu_E}[2\zeta_E^{\frac{1}{2}}]}{Y_{2\nu_E}[2\zeta_E^{\frac{1}{2}}]}$ and $-\bar{\Delta}_2 \frac{J_{2\nu_E}[2\zeta_E^{\frac{1}{2}}]}{Y_{2\nu_E}[2\zeta_E^{\frac{1}{2}}]}$ in the extracellular fluid vs k.

the above quantities reduce to

$$\frac{X_{2\nu_E}\sinh[\kappa_I\nu_I D]+\frac{\epsilon_I\kappa_I\nu_I}{k\epsilon_M}\cosh[\kappa_I\nu_I D]}{Z_{2\nu_E}\sinh[\kappa_I\nu_I D]+\frac{\epsilon_I\kappa_I\nu_I}{k\epsilon_M}\cosh[\kappa_I\nu_I D]}\rightarrow\frac{X_{2\nu_E}\sinh[kD]+\cosh[kD]}{Z_{2\nu_E}\sinh[kD]+\cosh[kD]}\ ,$$

$$\frac{X_{2\nu_E}\cosh[\kappa_I\nu_I D]+\frac{\epsilon_I\kappa_I\nu_I}{k\epsilon_M}\sinh[\kappa_I\nu_I D]}{Z_{2\nu_E}\cosh[\kappa_I\nu_I D]+\frac{\epsilon_I\kappa_I\nu_I}{k\epsilon_M}\sinh[\kappa_I\nu_I D]}\rightarrow\frac{X_{2\nu_E}\cosh[kD]+\sinh[kD]}{Z_{2\nu_E}\cosh[kD]+\sinh[kD]}\ .$$

Use of the definition for $\bar{\Delta}_2$ in terms of $X_{2\nu_E}$ and $Z_{2\nu_E}$, simplifies $\bar{\Delta}_2$ to

$$\bar{\Delta}_2\rightarrow\begin{cases}-\frac{1}{2}\Bigg[\dfrac{Y_{2\nu_E}[2\zeta_E^{\frac{1}{2}}]\cosh[k(L+D)]+\frac{\epsilon_E\kappa_E\zeta_E^{\frac{1}{2}}}{k\epsilon_M}Y'_{2\nu_E}\left[2|\zeta_E|^{\frac{1}{2}}\right]\sinh[k(L+D)]}{J_{2\nu_E}\left[2\zeta_E^{\frac{1}{2}}\right]\cosh[k(L+D)]+\frac{\epsilon_E\kappa_E\zeta_E^{\frac{1}{2}}}{k\epsilon_M}J'_{2\nu_E}\left[2\zeta_E^{\frac{1}{2}}\right]\sinh[k(L+D)]}\\ +\dfrac{Y_{2\nu_E}[2\zeta_E^{\frac{1}{2}}]\sinh[k(L+D)]+\frac{\epsilon_E\kappa_E\zeta_E^{\frac{1}{2}}}{k\epsilon_M}Y'_{2\nu_E}\left[2|\zeta_E|^{\frac{1}{2}}\right]\cosh[k(L+D)]}{J_{2\nu_E}\left[2\zeta_E^{\frac{1}{2}}\right]\sinh[k(L+D)]+\frac{\epsilon_E\kappa_E\zeta_E^{\frac{1}{2}}}{k\epsilon_M}J'_{2\nu_E}\left[2\zeta_E^{\frac{1}{2}}\right]\cosh[k(L+D)]}\Bigg] & \zeta_E>0\\ -\frac{1}{2}\Bigg[\dfrac{K_{2\nu_E}[2|\zeta_E|^{\frac{1}{2}}]\cosh[k(L+D)]+\frac{\epsilon_E\kappa_E|\zeta_E|^{\frac{1}{2}}}{k\epsilon_M}K'_{2\nu_E}\left[2|\zeta_E|^{\frac{1}{2}}\right]\sinh[k(L+D)]}{I_{2\nu_E}\left[2|\zeta_E|^{\frac{1}{2}}\right]\cosh[k(L+D)]+\frac{\epsilon_E\kappa_E|\zeta_E|^{\frac{1}{2}}}{k\epsilon_M}I'_{2\nu_E}\left[2|\zeta_E|^{\frac{1}{2}}\right]\sinh[k(L+D)]}\\ +\dfrac{K_{2\nu_E}[2|\zeta_E|^{\frac{1}{2}}]\sinh[k(L+D)]+\frac{\epsilon_E\kappa_E|\zeta_E|^{\frac{1}{2}}}{k\epsilon_M}K'_{2\nu_E}\left[2|\zeta_E|^{\frac{1}{2}}\right]\cosh[k(L+D)]}{I_{2\nu_E}\left[2|\zeta_E|^{\frac{1}{2}}\right]\sinh[k(L+D)]+\frac{\epsilon_E\kappa_E|\zeta_E|^{\frac{1}{2}}}{k\epsilon_M}I'_{2\nu_E}\left[2|\zeta_E|^{\frac{1}{2}}\right]\cosh[k(L+D)]}\Bigg] & \zeta_E<0\end{cases}$$

After some algebra, the above expression for $\bar{\Delta}_2$ further reduces to

$$\bar{\Delta}_2=\begin{cases}-\Bigg[\dfrac{Y_{2\nu_E}[2\zeta_E^{\frac{1}{2}}]Z_{2\nu_E}(2[L+D],\zeta_E)+\frac{\epsilon_E\kappa_E\zeta_E^{\frac{1}{2}}}{k\epsilon_M}Y'_{2\nu_E}[2\zeta_E^{\frac{1}{2}}]}{J_{2\nu_E}[2\zeta_E^{\frac{1}{2}}]Z_{2\nu_E}(2[L+D],\zeta_E)+\frac{\epsilon_E\kappa_E\zeta_E^{\frac{1}{2}}}{k\epsilon_M}J'_{2\nu_E}[2\zeta_E^{\frac{1}{2}}]}\Bigg] & \zeta_E>0\\ -\Bigg[\dfrac{K_{2\nu_E}[2|\zeta_E|^{\frac{1}{2}}]Z_{2\nu_E}(2[L+D],\zeta_E)+\frac{\epsilon_E\kappa_E|\zeta_E|^{\frac{1}{2}}}{k\epsilon_M}K'_{2\nu_E}[2|\zeta_E|^{\frac{1}{2}}]}{I_{2\nu_E}[2|\zeta_E|^{\frac{1}{2}}]Z_{2\nu_E}(2[L+D],\zeta_E)+\frac{\epsilon_E\kappa_E|\zeta_E|^{\frac{1}{2}}}{k\epsilon_M}I'_{2\nu_E}[2|\zeta_E|^{\frac{1}{2}}]}\Bigg] & \zeta_E<0\end{cases}$$

Comparison of this limiting form for $\bar{\Delta}_2(L,\zeta_E,D,\zeta_I)$ with the one membrane case $\bar{\Delta}_1(2L,\zeta_E,\zeta_I)$, see Appendix B Eq. (B.14), shows that this limiting form is equivalent to a one membrane model system with a membrane of thickness $2[L+D]$ and extracellular fluid in each of the fluid regions adjacent to the membrane.

Another two limiting cases of the system occur when the membranes are perfect insulators (i.e. $\epsilon_M=0$) or perfect conductors (i.e. $\epsilon_M=\infty$). Thus

$$\bar{\Delta}_2\ \rightarrow\begin{cases}-\dfrac{Y_{2\nu_E}[2\zeta_E^{\frac{1}{2}}]}{J_{2\nu_E}[2\zeta_E^{\frac{1}{2}}]} & \zeta_E>0\\ -\dfrac{K_{2\nu_E}[2|\zeta_E|^{\frac{1}{2}}]}{I_{2\nu_E}[2|\zeta_E|^{\frac{1}{2}}]} & \zeta_E<0\end{cases}\qquad\text{as }\epsilon_M\rightarrow\infty\ ,$$

$$\bar{\Delta}_2 \;\rightarrow\; \begin{cases} \dfrac{Y'_{2\nu_E}[2\zeta_E^{\frac{1}{2}}]}{J'_{2\nu_E}[2\zeta_E^{\frac{1}{2}}]} & \zeta_E > 0 \\ \dfrac{K'_{2\nu_E}[2|\zeta_E|^{\frac{1}{2}}]}{I'_{2\nu_E}[2|\zeta_E|^{\frac{1}{2}}]} & \zeta_E < 0 \end{cases} \quad \text{as } \epsilon_M \rightarrow 0 \ .$$

These limiting forms approach the same value as in the one membrane model (see Appendix B) and that of the one membrane wall model considered by Carnie and Chan [41].

3.2.4 Case 2:$-D \leq z_2 \leq D$

The Green's function type of solution for the transverse Hankel transform mean electrostatic fluctuation potential in region III is constructed using the functions $u(z_1)$ and $v(z_1)$ defined by

$$u(z_1) \;=\; \begin{cases} J_{2\nu_I}\left[\sqrt{2}\zeta_I^{\frac{1}{2}}\exp[-\frac{\kappa_I z_1}{2}]\right] Y_{2\nu_I}\left[\sqrt{2}\zeta_I^{\frac{1}{2}}\exp[\frac{\kappa_I D}{2}]\right] \\ -Y_{2\nu_I}\left[\sqrt{2}\zeta_I^{\frac{1}{2}}\exp[-\frac{\kappa_I z_1}{2}]\right] J_{2\nu_I}\left[\sqrt{2}\zeta_I^{\frac{1}{2}}\exp[\frac{\kappa_I D}{2}]\right] & \zeta_I > 0 \\ \\ I_{2\nu_I}\left[\sqrt{2}\mid\zeta_I\mid^{\frac{1}{2}}\exp[-\frac{\kappa_I z_1}{2}]\right] K_{2\nu_I}\left[\sqrt{2}\mid\zeta_I\mid^{\frac{1}{2}}\exp[\frac{\kappa_I D}{2}]\right] \\ -K_{2\nu_I}\left[\sqrt{2}\mid\zeta_I\mid^{\frac{1}{2}}\exp[-\frac{\kappa_I z_1}{2}]\right] I_{2\nu_I}\left[\sqrt{2}\mid\zeta_I\mid^{\frac{1}{2}}\exp[\frac{\kappa_I D}{2}]\right] & \zeta_I < 0 \end{cases} ,$$

$$v(z_1) \;=\; \begin{cases} J_{2\nu_I}\left[\sqrt{2}\zeta_I^{\frac{1}{2}}\exp[-\frac{\kappa_I z_1}{2}]\right] Y_{2\nu_I}[\sqrt{2}\zeta_I^{\frac{1}{2}}] \\ -Y_{2\nu_I}\left[\sqrt{2}\zeta_I^{\frac{1}{2}}\exp[-\frac{\kappa_I z_1}{2}]\right] J_{2\nu_I}[\sqrt{2}\zeta_I^{\frac{1}{2}}] & \zeta_I > 0 \\ \\ I_{2\nu_I}\left[\sqrt{2}\mid\zeta_I\mid^{\frac{1}{2}}\exp[-\frac{\kappa_I z_1}{2}]\right] K_{2\nu_I}[\sqrt{2}\mid\zeta_I\mid^{\frac{1}{2}}] \\ -K_{2\nu_I}\left[\sqrt{2}\mid\zeta_I\mid^{\frac{1}{2}}\exp[-\frac{\kappa_I z_1}{2}]\right] I_{2\nu_I}[\sqrt{2}\mid\zeta_I\mid^{\frac{1}{2}}] & \zeta_I < 0 \end{cases} ,$$

such that

$$u(-D) = v(0) = 0 \ .$$

Thus the Green's function type of solution for the transverse Hankel transform mean electrostatic fluctuation potential in region III is of the form

$$\tilde{\psi}_I^L(z_1, z_2, \mathbf{k}) = -\frac{4\pi}{\epsilon_I}\frac{u(z_<)v(z_>)}{W(u,v)} + \frac{\tilde{\psi}_M^L(-D, z_2, \mathbf{k})}{v(-D)}v(z_1) + \frac{\tilde{\psi}_I^R(0, z_2, \mathbf{k})}{u(0)}u(z_1) \ , \qquad (3.38)$$

where W is the wronskian of the solutions $u(z_1)$ and $v(z_1)$ and is given by

$$W(u,v) = \begin{cases} \frac{\kappa_I}{\pi} u(0) = -\frac{\kappa_I}{\pi} v(-D) & \zeta_I > 0 \\ -\frac{\kappa_I}{2} u(0) = \frac{\kappa_I}{2} v(-D) & \zeta_I < 0 \end{cases} . \tag{3.39}$$

Application of the appropriate boundary conditions at $\pm\infty$ and at the membrane walls located at $\pm[L+D]$ yields

$$D_E^R = 0 ,$$

$$\tilde{\psi}_M^R(z_1,z_2,\mathbf{k}) = \begin{cases} C_E^R \Big\{ J_{2\nu_E}[2\zeta_E^{\frac{1}{2}}] \cosh[k(z_1-[L+D])] \\ -\frac{\epsilon_E \kappa_E \zeta_E^{\frac{1}{2}}}{k\epsilon_M} J'_{2\nu_E}[2\zeta_E^{\frac{1}{2}}] \sinh[k(z_1-[L+D])] \Big\} & \zeta_E > 0 \\ C_E^R \Big\{ I_{2\nu_E}[2 \mid \zeta_E \mid^{\frac{1}{2}}] \cosh[k(z_1-[L+D])] \\ -\frac{\epsilon_E \kappa_E |\zeta_E|^{\frac{1}{2}}}{k\epsilon_M} I'_{2\nu_E}[2 \mid \zeta_E \mid^{\frac{1}{2}}] \sinh[k(z_1-[L+D])] \Big\} & \zeta_E < 0 \end{cases} ,$$

$$D_E^L = 0 ,$$

$$\tilde{\psi}_M^L(z_1,z_2,\mathbf{k}) = \begin{cases} C_E^L \Big\{ J_{2\nu_E}[2\zeta_E^{\frac{1}{2}}] \cosh[k(z_1+[L+D])] \\ +\frac{\epsilon_E \kappa_E \zeta_E^{\frac{1}{2}}}{k\epsilon_M} J'_{2\nu_E}[2\zeta_E^{\frac{1}{2}}] \sinh[k(z_1+[L+D])] \Big\} & \zeta_E > 0 \\ C_E^L \Big\{ I_{2\nu_E}[2 \mid \zeta_E \mid^{\frac{1}{2}}] \cosh[k(z_1+[L+D])] \\ +\frac{\epsilon_E \kappa_E |\zeta_E|^{\frac{1}{2}}}{k\epsilon_M} I'_{2\nu_E}[2 \mid \zeta_E \mid^{\frac{1}{2}}] \sinh[k(z_1+[L+D])] \Big\} & \zeta_E < 0 \end{cases} .$$

Then the application of the boundary conditions at the membrane wall located at D yields expressions for the constants C_I^R and D_I^R in terms of the constant C_E^R i.e.

$$-\frac{C_I^R}{C_E^R}\frac{\epsilon_I \kappa_I}{2k\epsilon_M} = \begin{cases} \Big\{ J_{2\nu_E}[2\zeta_E^{\frac{1}{2}}] \cosh[kL] \\ +\frac{\epsilon_E \kappa_E \zeta_E^{\frac{1}{2}}}{k\epsilon_M} J'_{2\nu_E}[2\zeta_E^{\frac{1}{2}}] \sinh[kL] \Big\} S_{2\nu_I}(L,\zeta_E,D,\zeta_I) & \zeta_E > 0 \\ \Big\{ I_{2\nu_E}[2 \mid \zeta_E \mid^{\frac{1}{2}}] \cosh[kL] \\ +\frac{\epsilon_E \kappa_E |\zeta_E|^{\frac{1}{2}}}{k\epsilon_M} I'_{2\nu_E}[2 \mid \zeta_E \mid^{\frac{1}{2}}] \sinh[kL] \Big\} S_{2\nu_I}(L,\zeta_E,D,\zeta_I) & \zeta_E < 0 \end{cases} ,$$

$$\frac{D_I^R}{C_E^R}\frac{\epsilon_I\kappa_I}{2k\epsilon_M} = \begin{cases} \Big\{ J_{2\nu_E}[2\zeta_E^{\frac{1}{2}}]\cosh[kL] & \\ +\frac{\epsilon_E\kappa_E\zeta_E^{\frac{1}{2}}}{k\epsilon_M} J'_{2\nu_E}[2\zeta_E^{\frac{1}{2}}]\sinh[kL]\Big\} T_{2\nu_I}(L,\zeta_E,D,\zeta_I) & \zeta_E > 0 \\ \Big\{ I_{2\nu_E}[2\mid\zeta_E\mid^{\frac{1}{2}}]\cosh[kL] & \\ +\frac{\epsilon_E\kappa_E\mid\zeta_E\mid^{\frac{1}{2}}}{k\epsilon_M} I'_{2\nu_E}[2\mid\zeta_E\mid^{\frac{1}{2}}]\sinh[kL]\Big\} T_{2\nu_I}(L,\zeta_E,D,\zeta_I) & \zeta_E < 0 \end{cases} ,$$

where $S_{2\nu_I}(L,\zeta_E,D,\zeta_I)$ and $T_{2\nu_I}(L,\zeta_E,D,\zeta_I)$ have the same definitions as in Section 3.2.1.

At the origin and the membrane wall located at $-D$, application of the boundary conditions yields the following set of equations

$$\begin{aligned} \epsilon_M\tilde{\psi}_M^{L'}(-D,z_2,\mathbf{k}) = & - \frac{4\pi}{W(u,v)}u'(-D)v(z_2) + \epsilon_I\frac{\tilde{\psi}_M^L(-D,z_2,\mathbf{k})}{v(-D)}v'(-D) \\ & + \epsilon_I\frac{\tilde{\psi}_I^R(0,z_2,\mathbf{k})}{u(0)}u'(-D) , \end{aligned} \tag{3.40}$$

$$\begin{aligned} \epsilon_I\tilde{\psi}_I^{R'}(0,z_2,\mathbf{k}) = & - \frac{4\pi}{W(u,v)}v'(0)u(z_2) + \epsilon_I\frac{\tilde{\psi}_M^L(-D,z_2,\mathbf{k})}{v(-D)}v'(0) \\ & + \epsilon_I\frac{\tilde{\psi}_I^R(0,z_2,\mathbf{k})}{u(0)}u'(0) , \end{aligned} \tag{3.41}$$

to solve for the constants $\tilde{\psi}_M^L(-D,z_2,\mathbf{k})$ and $\tilde{\psi}_I^R(0,z_2,\mathbf{k})$, such that

$$\tilde{\psi}_M^L(-D,z_2,\mathbf{k}) = \frac{4\pi}{\epsilon_I W(u,v)}v(-D)u(z_2) - \sqrt{2}\kappa_I\mid\zeta_I\mid^{\frac{1}{2}}\frac{v(-D)}{v'(0)}\tilde{\psi}_R^I(0,z_2,\mathbf{k}) ,$$

$$\tilde{\psi}_I^R(0,z_2,\mathbf{k}) = \begin{cases} \frac{4\pi}{\epsilon_I W(u,v)}\left[\frac{1}{\sqrt{2}\epsilon_I\kappa_I\zeta_I^{\frac{1}{2}}}\right]\frac{1}{S_{2\nu_I}J'_{2\nu_I}[\sqrt{2}\zeta_I^{\frac{1}{2}}]-T_{2\nu_I}Y'_{2\nu_I}[\sqrt{2}\zeta_I^{\frac{1}{2}}]} & \\ \times\Big\{\frac{\epsilon_I}{k\epsilon_M}u'(-D)v'(0)v(z_2) & \\ -v'(0)\Big[S_{2\nu_I}J_{2\nu_I}[\sqrt{2}\zeta_I^{\frac{1}{2}}] - T_{2\nu_I}Y_{2\nu_I}[\sqrt{2}\zeta_I^{\frac{1}{2}}]\Big]u(z_2)\Big\} & \zeta_I > 0 \\ \frac{4\pi}{\epsilon_I W(u,v)}\left[\frac{1}{\sqrt{2}\epsilon_I\kappa_I\mid\zeta_I\mid^{\frac{1}{2}}}\right]\frac{1}{S_{2\nu_I}I'_{2\nu_I}[\sqrt{2}\mid\zeta_I\mid^{\frac{1}{2}}]-T_{2\nu_I}K'_{2\nu_I}[\sqrt{2}\mid\zeta_I\mid^{\frac{1}{2}}]} & \\ \times\Big\{\frac{\epsilon_I}{k\epsilon_M}u'(-D)v'(0)v(z_2) & \\ -v'(0)\Big[S_{2\nu_I}I_{2\nu_I}[\sqrt{2}\mid\zeta_I\mid^{\frac{1}{2}}] - T_{2\nu_I}K_{2\nu_I}[\sqrt{2}\mid\zeta_I\mid^{\frac{1}{2}}]\Big]u(z_2)\Big\} & \zeta_I < 0 \end{cases} .$$

These results for the constants $\tilde{\psi}_M^L(-D,z_2,\mathbf{k})$ and $\tilde{\psi}_I^R(0,z_2,\mathbf{k})$ are substituted into the the solution for the transverse Hankel transform mean electrostatic fluctuation potential in region III Eq. (3.38) and the solution can be written in the form

$$\tilde{\psi}_I^L(z_1,z_2,\mathbf{k}) = - \frac{4\pi}{\epsilon_I}\frac{u(z_<)v(z_>)}{W(u,v)}$$

$$
\begin{aligned}
&- \frac{4\pi}{\epsilon_I}\frac{1}{W(u,v)}\left[\frac{1}{S_{2\nu_I}J'_{2\nu_I}[\sqrt{2}\zeta_I^{\frac{1}{2}}] - T_{2\nu_I}Y'_{2\nu_I}[\sqrt{2}\zeta_I^{\frac{1}{2}}]}\right] \\
&\times \left\{\left[\frac{1}{\sqrt{2}\kappa_I\zeta_I^{\frac{1}{2}}k\epsilon_M}\right]\left[\frac{u'(-D)v'(0)}{u(0)}\right][u(z_1)v(z_2)+v(z_1)u(z_2)]\right. \\
&- \left[\frac{1}{\sqrt{2}\kappa_I\zeta_I^{\frac{1}{2}}}\right]\left[\frac{v'(0)}{u(0)}\right]\left[S_{2\nu_I}J_{2\nu_I}[\sqrt{2}\zeta_I^{\frac{1}{2}}] - T_{2\nu_I}Y_{2\nu_I}[\sqrt{2}\zeta_I^{\frac{1}{2}}]\right]u(z_1)u(z_2) \\
&- \left.\left[\frac{u'(-D)}{k\epsilon_M}\right]v(z_1)v(z_2)\right\} \quad \zeta_I > 0 \ , \qquad (3.42)
\end{aligned}
$$

and

$$
\begin{aligned}
\tilde{\psi}_I^L(z_1,z_2,\mathbf{k}) = &- \frac{4\pi}{\epsilon_I}\frac{u(z_<)v(z_>)}{W(u,v)} \\
&- \frac{4\pi}{\epsilon_I}\frac{1}{W(u,v)}\left[\frac{1}{S_{2\nu_I}I'_{2\nu_I}[\sqrt{2}\mid\zeta_I\mid^{\frac{1}{2}}] - T_{2\nu_I}K'_{2\nu_I}[\sqrt{2}\mid\zeta_I\mid^{\frac{1}{2}}]}\right] \\
&\times \left\{\left[\frac{1}{\sqrt{2}\kappa_I\mid\zeta_I\mid^{\frac{1}{2}}k\epsilon_M}\right]\left[\frac{u'(-D)v'(0)}{u(0)}\right][u(z_1)v(z_2)+v(z_1)u(z_2)]\right. \\
&- \left[\frac{1}{\sqrt{2}\kappa_I\mid\zeta_I\mid^{\frac{1}{2}}}\right]\left[\frac{v'(0)}{u(0)}\right] \\
&\times \left[S_{2\nu_I}I_{2\nu_I}[\sqrt{2}\mid\zeta_I\mid^{\frac{1}{2}}] - T_{2\nu_I}K_{2\nu_I}[\sqrt{2}\mid\zeta_I\mid^{\frac{1}{2}}]\right]u(z_1)u(z_2) \\
&- \left.\left[\frac{u'(-D)}{k\epsilon_M}\right]v(z_1)v(z_2)\right\} \quad \zeta_I < 0 \ . \qquad (3.43)
\end{aligned}
$$

By noting that the functions $u(z_1)$ and $v(z_1)$ are even functions of the transform variable k, the solutions for the transverse Hankel transform mean electrostatic fluctuation potential, Eq. (3.42) and Eq. (3.43) are also even functions of k. Thus we expect that the correlation in the transverse direction will be screened for the mean electrostatic fluctuation potential.

3.2.5 Asymptotic transverse Hankel transform mean electrostatic fluctuation potential

If we assume that the ratios $\frac{2\zeta_I^{\frac{1}{2}}}{2\nu_I}\,|_{k=0}$, $\frac{2|\zeta_I|^{\frac{1}{2}}}{2\nu_I}\,|_{k=0}$, $\frac{2\zeta_E^{\frac{1}{2}}}{2\nu_E}\,|_{k=0}$ and $\frac{2|\zeta_E|^{\frac{1}{2}}}{2\nu_E}\,|_{k=0} < 1$, use of the asymptotic forms for the Bessel and modified Bessel functions in Appendix D yields

$$u(z_1) \rightarrow \begin{cases} -\frac{1}{\pi\nu_I}\left[\frac{1}{1-\left[\frac{q_I(z_1)}{2\nu_I}\right]^2}\right]^{\frac{1}{4}}\left[\frac{1}{1-\left[\frac{q_I(-D)}{2\nu_I}\right]^2}\right]^{\frac{1}{4}} \\ \times\Big[\sinh[2\nu_I\eta_{2\nu_I}(z_1,-D)][1+O((2\nu_I)^{-4})] \\ -\frac{1}{4}\frac{[q_I(z_1)^2-q_I(-D)^2]}{[2\nu_I]^3}\cosh[2\nu_I\eta_{2\nu_I}(z_1,-D)]\Big] \quad \zeta_I > 0 \\ \\ \frac{1}{2\nu_I}\left[\frac{1}{1+\left[\frac{q_I(z_1)}{2\nu_I}\right]^2}\right]^{\frac{1}{4}}\left[\frac{1}{1+\left[\frac{q_I(-D)}{2\nu_I}\right]^2}\right]^{\frac{1}{4}} \\ \times\Big[\sinh[2\nu_I\eta_{2\nu_I}(z_1,-D)][1+O((2\nu_I)^{-4})] \\ +\frac{1}{4}\frac{[q_I(z_1)^2-q_I(-D)^2]}{[2\nu_I]^3}\cosh[2\nu_I\eta_{2\nu_I}(z_1,-D)]\Big] \quad \zeta_I < 0 \end{cases}$$

$$v(z_1) \rightarrow \begin{cases} -\frac{1}{\pi\nu_I}\left[\frac{1}{1-\left[\frac{q_I(z_1)}{2\nu_I}\right]^2}\right]^{\frac{1}{4}}\left[\frac{1}{1-\left[\frac{q_I(0)}{2\nu_I}\right]^2}\right]^{\frac{1}{4}} \\ \times\Big[\sinh[2\nu_I\eta_{2\nu_I}(z_1,0)][1+O((2\nu_I)^{-4})] \\ -\frac{1}{4}\frac{[q_I(z_1)^2-q_I(0)^2]}{[2\nu_I]^3}\cosh[2\nu_I\eta_{2\nu_I}(z_1,0)]\Big] \quad \zeta_I > 0 \\ \\ \frac{1}{2\nu_I}\left[\frac{1}{1+\left[\frac{q_I(z_1)}{2\nu_I}\right]^2}\right]^{\frac{1}{4}}\left[\frac{1}{1+\left[\frac{q_I(0)}{2\nu_I}\right]^2}\right]^{\frac{1}{4}} \\ \times\Big[\sinh[2\nu_I\eta_{2\nu_I}(z_1,0)][1+O((2\nu_I)^{-4})] \\ +\frac{1}{4}\frac{[q_I(z_1)^2-q_I(0)^2]}{[2\nu_I]^3}\cosh[2\nu_I\eta_{2\nu_I}(z_1,0)]\Big] \quad \zeta_I < 0 \end{cases}$$

where the quantities $q_I(z_1)$ and $\eta_{2\nu_I}(z_1,z_2)$ have the same definitions as in Section 3.2.1.

Thus the quantities $u(z_1)u(z_2)$, $u(z_1)v(z_2)$ and $v(z_1)v(z_2)$ have the following asymptotic forms

$$u(z_1)u(z_2) \rightarrow \begin{cases} \left[\frac{1}{\pi\nu_I}\right]^2\left[\frac{1}{1-\left[\frac{q_I(z_1)}{2\nu_I}\right]^2}\right]^{\frac{1}{4}}\left[\frac{1}{1-\left[\frac{q_I(z_2)}{2\nu_I}\right]^2}\right]^{\frac{1}{4}}\left[\frac{1}{1-\left[\frac{q_I(-D)}{2\nu_I}\right]^2}\right]^{\frac{1}{2}} \\ \times\Big[\frac{1}{2}\cosh[2\nu_I\eta_{2\nu_I}(z_1,-D)+2\nu_I\eta_{2\nu_I}(z_2,-D)] \\ -\frac{1}{2}\cosh[2\nu_I\eta_{2\nu_I}(z_1,-D)-2\nu_I\eta_{2\nu_I}(z_2,-D)]\Big] \qquad \zeta_I > 0 \\ \\ \left[\frac{1}{2\nu_I}\right]^2\left[\frac{1}{1+\left[\frac{q_I(z_1)}{2\nu_I}\right]^2}\right]^{\frac{1}{4}}\left[\frac{1}{1+\left[\frac{q_I(z_2)}{2\nu_I}\right]^2}\right]^{\frac{1}{4}}\left[\frac{1}{1+\left[\frac{q_I(-D)}{2\nu_I}\right]^2}\right]^{\frac{1}{2}} \\ \times\Big[\frac{1}{2}\cosh[2\nu_I\eta_{2\nu_I}(z_1,-D)+2\nu_I\eta_{2\nu_I}(z_2,-D)] \\ -\frac{1}{2}\cosh[2\nu_I\eta_{2\nu_I}(z_1,-D)-2\nu_I\eta_{2\nu_I}(z_2,-D)]\Big] \qquad \zeta_I < 0 \end{cases}$$

$$u(z_1)v(z_2) \rightarrow \begin{cases} \left[\frac{1}{\pi\nu_I}\right]^2\left[\frac{1}{1-\left[\frac{q_I(z_1)}{2\nu_I}\right]^2}\right]^{\frac{1}{4}}\left[\frac{1}{1-\left[\frac{q_I(z_2)}{2\nu_I}\right]^2}\right]^{\frac{1}{4}} \\ \times\left[\frac{1}{1-\left[\frac{q_I(-D)}{2\nu_I}\right]^2}\right]^{\frac{1}{4}}\left[\frac{1}{1-\left[\frac{q_I(0)}{2\nu_I}\right]^2}\right]^{\frac{1}{4}} \\ \times\left[\frac{1}{2}\cosh[2\nu_I\eta_{2\nu_I}(z_1,-D)+2\nu_I\eta_{2\nu_I}(z_2,0)]\right. \\ \left.-\frac{1}{2}\cosh[2\nu_I\eta_{2\nu_I}(z_1,-D)-2\nu_I\eta_{2\nu_I}(z_2,0)]\right] \quad \zeta_I>0 \\ \\ \left[\frac{1}{2\nu_I}\right]^2\left[\frac{1}{1+\left[\frac{q_I(z_1)}{2\nu_I}\right]^2}\right]^{\frac{1}{4}}\left[\frac{1}{1+\left[\frac{q_I(z_2)}{2\nu_I}\right]^2}\right]^{\frac{1}{4}} \\ \times\left[\frac{1}{1+\left[\frac{q_I(-D)}{2\nu_I}\right]^2}\right]^{\frac{1}{4}}\left[\frac{1}{1+\left[\frac{q_I(0)}{2\nu_I}\right]^2}\right]^{\frac{1}{4}} \\ \times\left[\frac{1}{2}\cosh[2\nu_I\eta_{2\nu_I}(z_1,-D)+2\nu_I\eta_{2\nu_I}(z_2,0)]\right. \\ \left.-\frac{1}{2}\cosh[2\nu_I\eta_{2\nu_I}(z_1,-D)-2\nu_I\eta_{2\nu_I}(z_2,0)]\right] \quad \zeta_I<0 \end{cases},$$

$$v(z_1)v(z_2) \rightarrow \begin{cases} \left[\frac{1}{\pi\nu_I}\right]^2\left[\frac{1}{1-\left[\frac{q_I(z_1)}{2\nu_I}\right]^2}\right]^{\frac{1}{4}}\left[\frac{1}{1-\left[\frac{q_I(z_2)}{2\nu_I}\right]^2}\right]^{\frac{1}{4}}\left[\frac{1}{1-\left[\frac{q_I(0)}{2\nu_I}\right]^2}\right]^{\frac{1}{2}} \\ \times\left[\frac{1}{2}\cosh[2\nu_I\eta_{2\nu_I}(z_1,0)+2\nu_I\eta_{2\nu_I}(z_2,0)]\right. \\ \left.-\frac{1}{2}\cosh[2\nu_I\eta_{2\nu_I}(z_1,0)-2\nu_I\eta_{2\nu_I}(z_2,0)]\right] \qquad \zeta_I>0 \\ \\ \left[\frac{1}{2\nu_I}\right]^2\left[\frac{1}{1+\left[\frac{q_I(z_1)}{2\nu_I}\right]^2}\right]^{\frac{1}{4}}\left[\frac{1}{1+\left[\frac{q_I(z_2)}{2\nu_I}\right]^2}\right]^{\frac{1}{4}}\left[\frac{1}{1+\left[\frac{q_I(0)}{2\nu_I}\right]^2}\right]^{\frac{1}{2}} \\ \times\left[\frac{1}{2}\cosh[2\nu_I\eta_{2\nu_I}(z_1,0)+2\nu_I\eta_{2\nu_I}(z_2,0)]\right. \\ \left.-\frac{1}{2}\cosh[2\nu_I\eta_{2\nu_I}(z_1,0)-2\nu_I\eta_{2\nu_I}(z_2,0)]\right] \qquad \zeta_I<0 \end{cases}.$$

The source term in the solution for the transverse Hankel transform mean electrostatic fluctuation potential Eq. (3.38) has the following asymptotic using the asymptotic forms for $u(z_1)$ and $v(z_1)$, i.e.

$$-\frac{4\pi}{\epsilon_I}\frac{u(z_<)v(z_>)}{W(u,v)} \rightarrow \begin{cases} \frac{2\pi}{\epsilon_I\kappa_I\nu_I}\left[\frac{1}{1-\left[\frac{q_I(z_1)}{2\nu_I}\right]^2}\right]^{\frac{1}{4}}\left[\frac{1}{1-\left[\frac{q_I(z_2)}{2\nu_I}\right]^2}\right]^{\frac{1}{4}} \\ \times\left[\frac{\cosh[\kappa_I\nu_I(z_<+z_>+D)]-\cosh[\kappa_I\nu_I(z_<-z_>+D)]}{\sinh[\kappa_I\nu_I D]}\right] \quad \zeta_I>0 \\ \\ \frac{2\pi}{\epsilon_I\kappa_I\nu_I}\left[\frac{1}{1+\left[\frac{q_I(z_1)}{2\nu_I}\right]^2}\right]^{\frac{1}{4}}\left[\frac{1}{1+\left[\frac{q_I(z_2)}{2\nu_I}\right]^2}\right]^{\frac{1}{4}} \\ \times\left[\frac{\cosh[\kappa_I\nu_I(z_<+z_>+D)]-\cosh[\kappa_I\nu_I(z_<-z_>+D)]}{\sinh[\kappa_I\nu_I D]}\right] \quad \zeta_I<0 \end{cases}.$$

Since we are mainly interested in the fluid region adjacent to the membrane wall in region III, i.e. $z_1 \approx z_2 \approx -D$, and the quantity

$$\kappa_I\nu_I D\mid_{k=0} \gg 1 \ ,$$

the source term further reduces

$$-\frac{4\pi}{\epsilon_I}\frac{u(z_<)v(z_>)}{W(u,v)} \rightarrow \begin{cases} \frac{2\pi}{\epsilon_I\kappa_I\nu_I}\left[\frac{1}{1-\left[\frac{q_I(z_1)}{2\nu_I}\right]^2}\right]^{\frac{1}{4}}\left[\frac{1}{1-\left[\frac{q_I(z_2)}{2\nu_I}\right]^2}\right]^{\frac{1}{4}} \\ \times\left[\exp[\kappa_I\nu_I(z_< - z_>)] - \exp[\kappa_I\nu_I(z_< + z_>)]\right] & \zeta_I > 0 \\ \frac{2\pi}{\epsilon_I\kappa_I\nu_I}\left[\frac{1}{1+\left[\frac{q_I(z_1)}{2\nu_I}\right]^2}\right]^{\frac{1}{4}}\left[\frac{1}{1+\left[\frac{q_I(z_2)}{2\nu_I}\right]^2}\right]^{\frac{1}{4}} \\ \times\left[\exp[\kappa_I\nu_I(z_< - z_>)] - \exp[\kappa_I\nu_I(z_< + z_>)]\right] & \zeta_I < 0 \end{cases}$$

This asymptotic form of the source term is similar to that in the solution for the source term in the extracellular fluid i.e. Eq. (3.36) and Eq. (3.37).

A similar analysis can be performed on the other terms in the solution for the transverse Hankel transform mean electrostatic fluctuation potential, Eq. (3.42) and Eq. (3.43), to determine the dependence on the source and field point provided they are near the membrane wall located at $-D$. The details of the analysis are not presented here. Rather, presented below are plots of the numerical and asymptotic transverse Hankel transform mean electrostatic fluctuation potential at the source point for specified k values. See Figures 3.10, 3.11, 3.12 and 3.13. The location of the starting boundaries for the numerical procedure decreased as the value of the transform variable k increased. This is consistent with the above discussion for large k behaviour which is determined by the region near the source point whereas the opposite is true for small k values. Thus for these values a knowledge of the differential equations for the second membrane and the extracellular region V is unnecessary provided the source point is near the membrane wall located at $-D$. This suggests that the second membrane and thus the extracellular fluid in region V have negligible effect on the value for the transverse Hankel transform mean electrostatic fluctuation potential (and thus the mean electrostatic fluctuation potential) provided the source point is near the membrane wall located at $-D$. Comparison of these plots with the corresponding k value plot for the intracellular fluid region of the one membrane point model in Appendix B, see Figures B.6, B.7, B.8 and B.9, shows excellent agreement for both the numerical and asymptotic solution. Thus, as for the extracellular fluid case, the presence of the second membrane has negligible effect in the region near the membrane wall located at $-D$.

As the normal distance from the membrane wall increases but less than D the plots tend to a constant value determined by the Debye-Huckel type term in the solution i.e.

$$\tilde{\psi}_I^L(z_1,z_2,\mathbf{k}) \rightarrow \begin{cases} \frac{2\pi}{\epsilon_I \kappa_I \nu_I}\left[\frac{1}{1-\left[\frac{q_I(z_1)}{2\nu_I}\right]^2}\right]^{\frac{1}{4}}\left[\frac{1}{1-\left[\frac{q_I(z_1)}{2\nu_I}\right]^2}\right]^{\frac{1}{4}} & \zeta_I > 0 \\ \\ \frac{2\pi}{\epsilon_I \kappa_I \nu_I}\left[\frac{1}{1+\left[\frac{q_I(z_1)}{2\nu_I}\right]^2}\right]^{\frac{1}{4}}\left[\frac{1}{1+\left[\frac{q_I(z_1)}{2\nu_I}\right]^2}\right]^{\frac{1}{4}} & \zeta_I < 0 \end{cases} .$$

As the transform variable k increases this Debye-Huckel type term (the field point and source point coinciding) has the form

$$\tilde{\psi}_I^L(z_1,z_2,\mathbf{k}) \rightarrow \frac{2\pi}{\epsilon_I k} .$$

This result is consistent with that of Carnie and Chan [41] for the constant density systems (both single and two plate) and the linearized GC density for the single plate. Again this is due to the large k behaviour being determined by the region near the source point.

3.2.6 Limiting forms of the transverse Hankel transform mean electrostatic fluctuation potential

To obtain the two semi-infinite membrane limiting form (as described in Section 3.1.2) for the transverse Hankel transform mean electrostatic fluctuation potential we take the limit as $L \rightarrow \infty$. This results in the quantity

$$Z_{2\nu_E}(L,\zeta_E) \rightarrow 1 \ ,$$

in both cases for the sign of ζ_E. Thus the solutions for the transverse Hankel transform mean electrostatic fluctuation potential Eq. (3.42) and Eq. (3.43) in both cases for the sign of ζ_I reduce to those of the two semi-infinite membrane point model of Appendix C, Eq. (C.11) and Eq. (C.12).

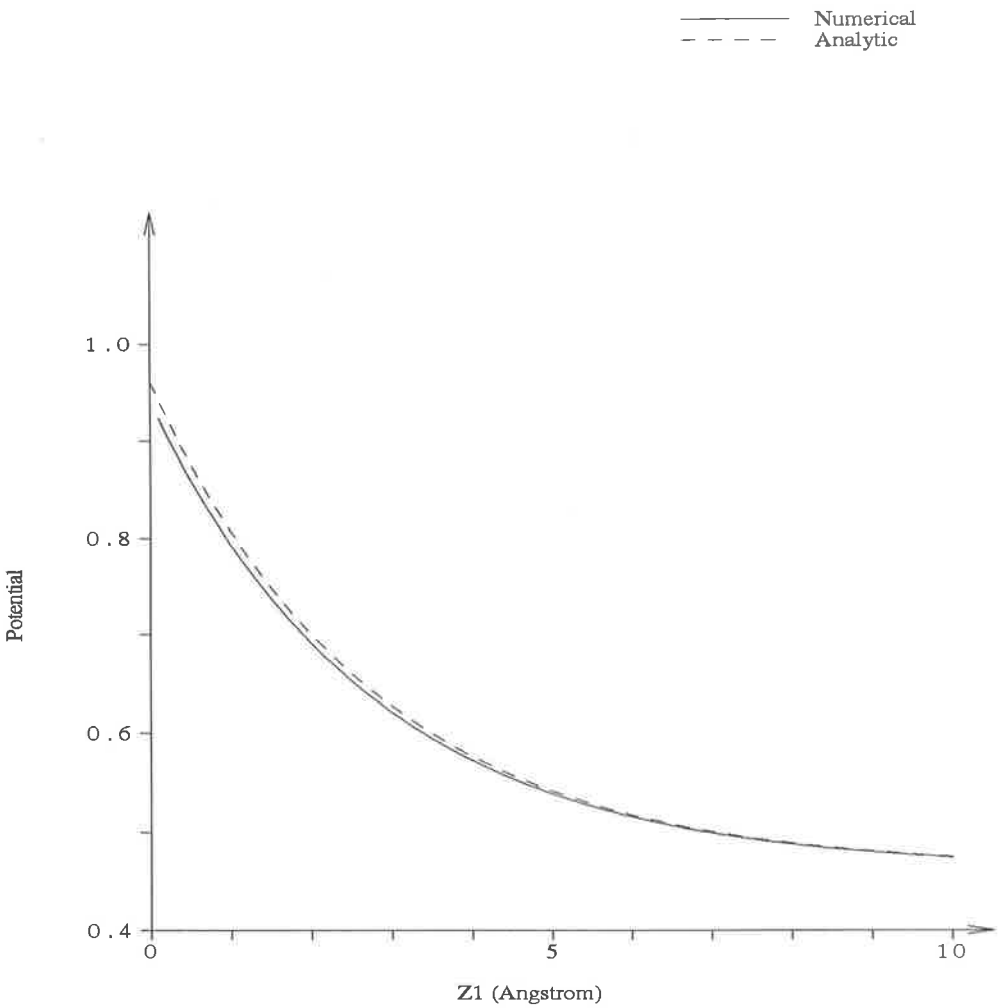

Figure 3.10: Comparison of the numerical and asymptotic solution for the transverse Hankel transform mean electrostatic fluctuation potential at the source point in the intracellular fluid of a two membrane system vs distance from the membrane wall for k=0.001.

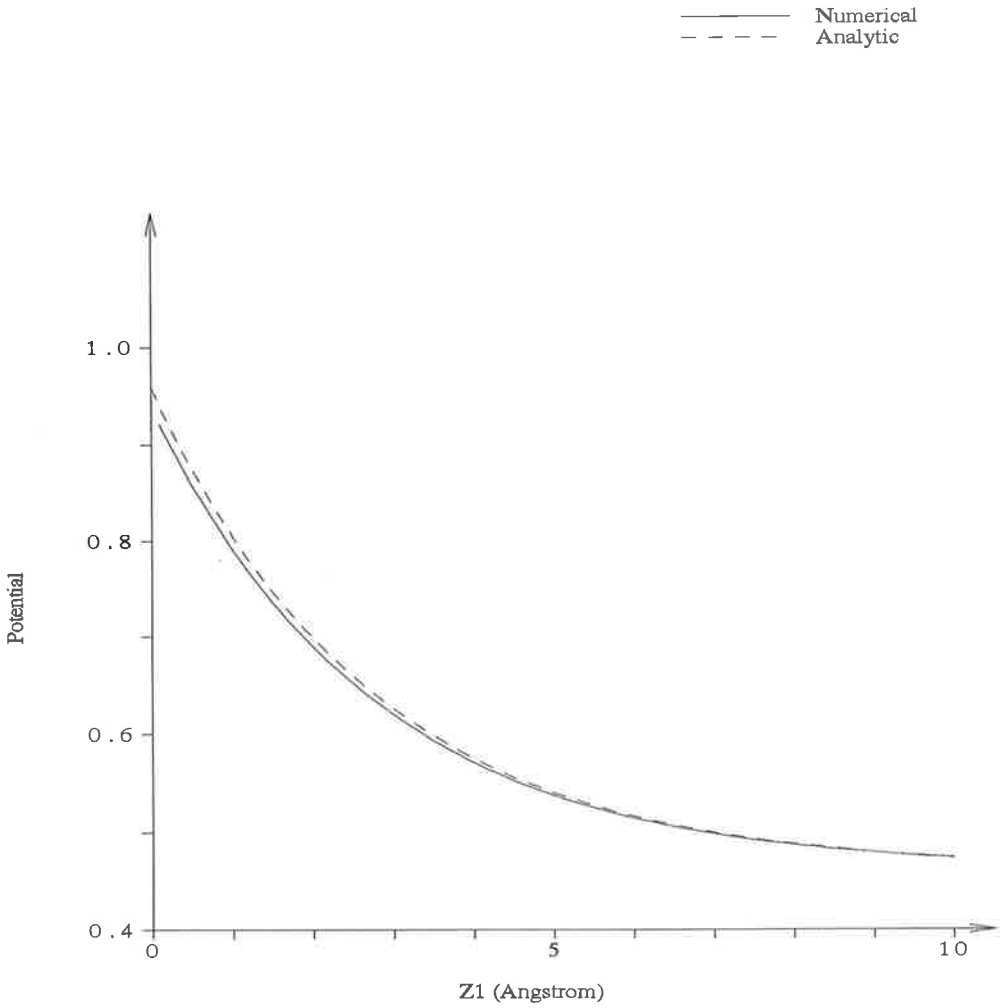

Figure 3.11: Comparison of the numerical and asymptotic solution for the transverse Hankel transform mean electrostatic fluctuation potential at the source point in the intracellular fluid of a two membrane system vs distance from the membrane wall for k=0.01.

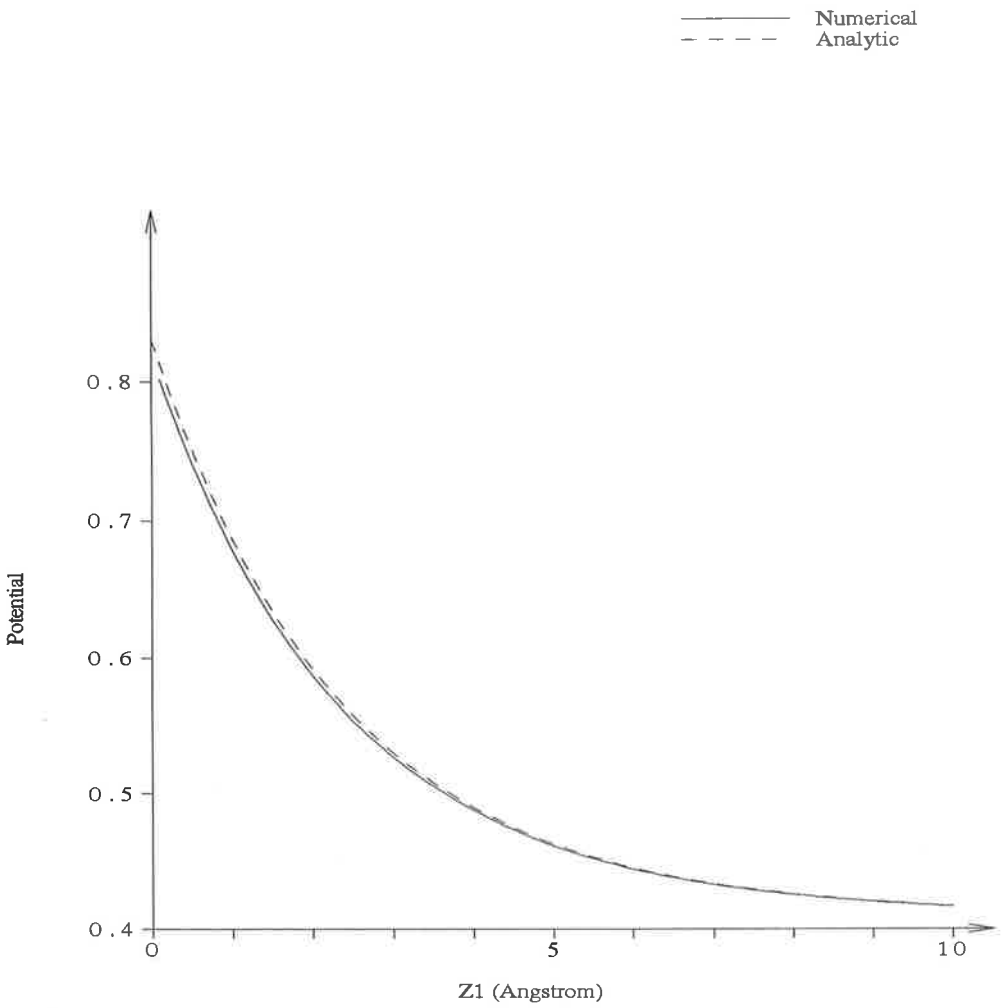

Figure 3.12: Comparison of the numerical and asymptotic solution for the transverse Hankel transform mean electrostatic fluctuation potential at the source point in the intracellular fluid of a two membrane system vs distance from the membrane wall for k=0.1.

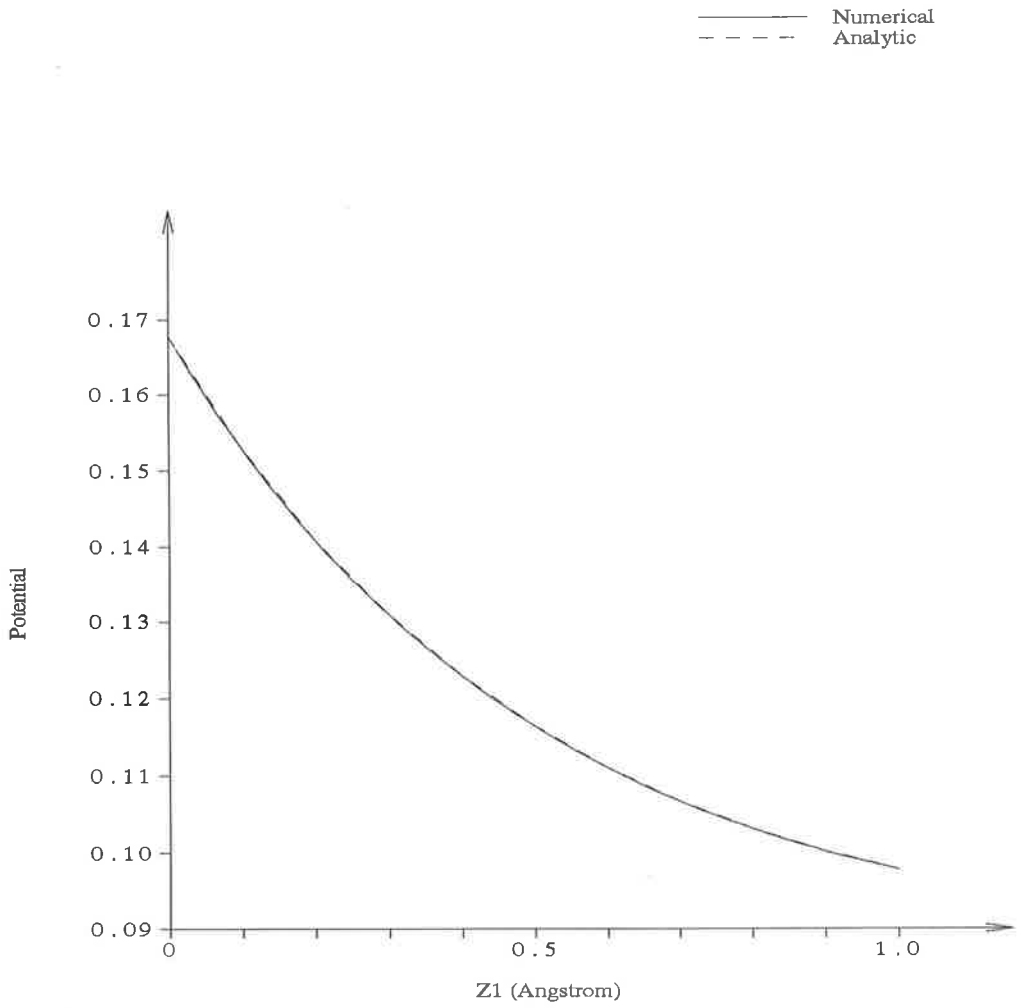

Figure 3.13: Comparison of the numerical and asymptotic solution for the transverse Hankel transform mean electrostatic fluctuation potential at the source point in the intracellular fluid of a two membrane system vs distance from the membrane wall for k=1.

Chapter 4

Ionic Hydration Numbers

In the previous chapter we constructed the solutions for the transverse Hankel transform mean electrostatic fluctuation potential for the two membrane point model for the cases when the source point is located in the extracellular and intracellular fluid regions. Comparison of these solutions with the one membrane point model solutions shows that the second membrane has a negligible effect. Thus for the determination of ionic hydration numbers we will use the one membrane point model solutions to approximate the two membrane point model solutions for the transverse Hankel transform mean electrostatic fluctuation potential.

4.1 Mean electrostatic fluctuation potential

The inverse transverse Hankel transform is defined by

$$\begin{aligned} \bar{\psi}(z_1, z_2, \boldsymbol{\rho}) &= \frac{1}{[2\pi]^2} \int d\mathbf{k} \exp[-i\mathbf{k} \cdot \boldsymbol{\rho}] \tilde{\psi}(z_1, z_2, \mathbf{k}) \\ &= \frac{1}{2\pi} \int_0^\infty dk\, k J_0(k\rho) \bar{\psi}(z_1, z_2, \mathbf{k}) \ . \end{aligned} \tag{4.1}$$

Thus this expression can be used to obtain the mean electrostatic fluctuation potential for the two cases described below.

4.1.1 Extracellular mean electrostatic fluctuation potential

In this case we are interested in the mean electrostatic fluctuation potential in the extracellular region. The transverse Hankel transform mean electrostatic fluctuation potential in the extracellular fluid region transforms to

$$\bar{\psi}_E(z_1, z_2, \boldsymbol{\rho}) = \bar{\psi}_E^{DH}(z_1, z_2, \boldsymbol{\rho}) + \bar{\psi}_E^{IM}(z_1, z_2, \boldsymbol{\rho}) \ , \tag{4.2}$$

where

$$\bar{\psi}_E^{DH}(z_1,z_2,\boldsymbol{\rho}) \;=\; \frac{1}{2\pi}\int_0^\infty dk\, kJ_0(k\rho)\tilde{\psi}_E^{DH}(z_1,z_2,\mathbf{k})\;, \tag{4.3}$$

is the Debye Huckel type term and $\tilde{\psi}_E^{DH}(z_1,z_2,\mathbf{k})$ is given by

$$\tilde{\psi}_E^{DH}(z_1,z_2,\mathbf{k}) = \begin{cases} -\frac{4\pi^2}{\epsilon_E\kappa_E}Y_{2\nu_E}\left[2\zeta_E^{\frac{1}{2}}\exp[\frac{\kappa_E(z_>+L)}{2}]\right] & \\ \times J_{2\nu_E}\left[2\zeta_E^{\frac{1}{2}}\exp[\frac{\kappa_E(z_<+L)}{2}]\right] & \zeta_E>0 \\ & \\ \frac{8\pi}{\epsilon_E\kappa_E}K_{2\nu_E}\left[2\mid\zeta_E\mid^{\frac{1}{2}}\exp[\frac{\kappa_E(z_>+L)}{2}]\right] & \\ \times I_{2\nu_E}\left[2\mid\zeta_E\mid^{\frac{1}{2}}\exp[\frac{\kappa_E(z_<+L)}{2}]\right] & \zeta_E<0 \end{cases}, \tag{4.4}$$

and

$$\bar{\psi}^{IM}(z_1,z_2,\boldsymbol{\rho}) \;=\; \frac{1}{2\pi}\int_0^\infty dk\, kJ_0(k\rho)\bar{\psi}_E^{IM}(z_1,z_2,\mathbf{k})\;, \tag{4.5}$$

is the image term due to the discontinuities in the dielectric medium across the membrane walls such that $\tilde{\psi}_E^{IM}(z_1,z_2,\mathbf{k})$ is given by

$$\tilde{\psi}_E^{IM}(z_1,z_2,\mathbf{k}) = \begin{cases} -\frac{4\pi^2}{\epsilon_E\kappa_E}\bar{\Delta}_1(2L,\zeta_E,\zeta_I)J_{2\nu_E}\left[2\zeta_E^{\frac{1}{2}}\exp[\frac{\kappa_E(z_2+L)}{2}]\right] & \\ \times J_{2\nu_E}\left[2\zeta_E^{\frac{1}{2}}\exp[\frac{\kappa_E(z_1+L)}{2}]\right] & \zeta_E>0 \\ & \\ \frac{8\pi}{\epsilon_E\kappa_E}\bar{\Delta}_1(2L,\zeta_E,\zeta_I)I_{2\nu_E}\left[2\mid\zeta_E\mid^{\frac{1}{2}}\exp[\frac{\kappa_E(z_2+L)}{2}]\right] & \\ \times I_{2\nu_E}\left[2\mid\zeta_E\mid^{\frac{1}{2}}\exp[\frac{\kappa_E(z_1+L)}{2}]\right] & \zeta_E<0 \end{cases}, \tag{4.6}$$

where

$$\bar{\Delta}_1(2L,\zeta_E,\zeta_I) = \begin{cases} -\frac{Y_{2\nu_E}[2\zeta_E^{\frac{1}{2}}]Z_{2\nu_I}(2L,\zeta_I)+\frac{\epsilon_E\kappa_E\zeta_E^{\frac{1}{2}}}{k\epsilon_M}Y'_{2\nu_E}[2\zeta_E^{\frac{1}{2}}]}{J_{2\nu_E}[2\zeta_E^{\frac{1}{2}}]Z_{2\nu_I}(2L,\zeta_I)+\frac{\epsilon_E\kappa_E\zeta_E^{\frac{1}{2}}}{k\epsilon_M}J'_{2\nu_E}[2\zeta_E^{\frac{1}{2}}]} & \zeta_E>0 \\ & \\ -\frac{K_{2\nu_E}[2|\zeta_E|^{\frac{1}{2}}]Z_{2\nu_I}(2L,\zeta_I)+\frac{\epsilon_E\kappa_E|\zeta_E|^{\frac{1}{2}}}{k\epsilon_M}K'_{2\nu_E}[2|\zeta_E|^{\frac{1}{2}}]}{I_{2\nu_E}[2|\zeta_E|^{\frac{1}{2}}]Z_{2\nu_I}(2L,\zeta_I)+\frac{\epsilon_E\kappa_E|\zeta_E|^{\frac{1}{2}}}{k\epsilon_M}I'_{2\nu_E}[2|\zeta_E|^{\frac{1}{2}}]} & \zeta_E<0 \end{cases}, \tag{4.7}$$

such that

$$Z_{2\nu_I}(L,\zeta_I) = \begin{cases} \frac{J_{2\nu_I}[2\zeta_I^{\frac{1}{2}}]\sinh[kL]+\frac{\epsilon_I\kappa_I\zeta_I^{\frac{1}{2}}}{k\epsilon_M}J'_{2\nu_I}[2\zeta_I^{\frac{1}{2}}]\cosh[kL]}{J_{2\nu_I}[2\zeta_I^{\frac{1}{2}}]\cosh[kL]+\frac{\epsilon_I\kappa_I\zeta_I^{\frac{1}{2}}}{k\epsilon_M}J'_{2\nu_I}[2\zeta_I^{\frac{1}{2}}]\sinh[kL]} & \zeta_I>0 \\ & \\ \frac{I_{2\nu_I}[2|\zeta_I|^{\frac{1}{2}}]\sinh[kL]+\frac{\epsilon_I\kappa_I|\zeta_I|^{\frac{1}{2}}}{k\epsilon_M}I'_{2\nu_I}[2|\zeta_I|^{\frac{1}{2}}]\cosh[kL]}{I_{2\nu_I}[2|\zeta_I|^{\frac{1}{2}}]\cosh[kL]+\frac{\epsilon_I\kappa_I|\zeta_I|^{\frac{1}{2}}}{k\epsilon_M}I'_{2\nu_I}[2|\zeta_I|^{\frac{1}{2}}]\sinh[kL]} & \zeta_I<0 \end{cases}. \tag{4.8}$$

The above results for the transverse Hankel transform mean electrostatic fluctuation potential for the one membrane point model are derived in Appendix B.

The transform inversion can be explicitly obtained by numerical integration for various values of the normal and transverse distance. The asymptotic form of the transverse Hankel transform mean electrostatic fluctuation potential for the one membrane point model, derived in Appendix B, is used in the intergrand for the numerical inversion. The numerical scheme employed uses Simpson's rule with an extended trapezoidal rule driver [114]. For values of the normal and transverse distance within about $2\mathring{A}$ of the source point the transform variable k (integration variable) it was necessary, to ensure convergence, to truncate the integral at value of $100\mathring{A}^{-1}$ compared with $20\mathring{A}^{-1}$ for values outside the $2\mathring{A}$ region. This is consistent with the argument presented in Chapter 3 concerning small ρ behaviour determined by the behaviour in the transform for large k.

Two plots of the extracellular mean electrostatic fluctuation potential are presented to highlight the following points. Figure 4.1 is a plot in the normal direction for various values with the source and field points in the transverse direction to the membrane coinciding i.e. $\rho = 0$. Important features are

- the skew symmetry in the potential when the source point is close to the membrane wall,
- the rapid decay (shielding) behaviour of the potential in the normal direction, and
- monotonic behaviour.

The skew symmetry is due to the image term which is a function of the normal distance of both the source and field point whereas the Debye-Huckel type term is a function of the relative normal distance between the source and field point. When the source point is further than about $5\mathring{A}$ from the membrane wall, the image term is negligible and thus the Debye-Huckel type term dominates and therefore the potential is symmetric. Figure 4.2 is a plot in the transverse direction for various source point values with the source and field points in the normal direction to the membrane coinciding i.e. $z_2 = z_1$. It should

be noted from this plot the dependence of the potential in the transverse direction on the source and field point position in the normal direction and the apparent shielding in the transverse direction. The monotonic behaviour of this solution should be contrasted against the damped oscillatory behaviour in real fluids [49]. Our neglect of the size of the molecules (i.e. setting the hard sphere diameters to zero) has caused the finite size effect in the solution for the mean electrostatic fluctuation potential (and thus the pair correlation function) to be averaged such that there is no oscillatory behaviour.

An analytic expression for the extracellular mean electrostatic fluctuation potential would be advantageous in the analysis of its dependence on the transverse and normal distance variables and for the calculation of ionic hydration numbers. Since the large k dependence determines the small distance behaviour, we take the limit as $k \to \infty$ in the asymptotic solution for the extracellular mean electrostatic fluctuation potential in the one membrane point model, see Appendix B, to yield

$$\tilde{\psi}_E^{DH}(z_1, z_2, \mathbf{k}) \rightarrow \frac{\exp[-\kappa_E \nu_E(k) \mid z_2 - z_1 \mid]}{\epsilon_E \kappa_E \nu_E(k)} , \tag{4.9}$$

$$\tilde{\psi}_E^{IM}(z_1, z_2, \mathbf{k}) \rightarrow \Delta_E \frac{\exp[\kappa_E \nu_E(k)(z_2 + z_1 + 2L)]}{\epsilon_E \kappa_E \nu_E(k)} , \tag{4.10}$$

where

$$\kappa_E \nu_E(k) = \begin{cases} \sqrt{k^2 + \kappa_E^2 - \kappa_E^2 \zeta_E \frac{\psi_E^B}{A_E}} & \zeta_E > 0 \\ \sqrt{k^2 + \kappa_E^2 + \kappa_E^2 \mid \zeta_E \mid \frac{\psi_E^B}{A_E}} & \zeta_E < 0 \end{cases} , \tag{4.11}$$

$$\Delta_E = \frac{\epsilon_E - \epsilon_M}{\epsilon_E + \epsilon_M} . \tag{4.12}$$

If we further assume that these forms are the dominant terms for the evaluation of the extracellular mean electrostatic fluctuation potential and valid for all k, then the transform inversion can be performed in closed form, see Appendix D, to yield

$$\begin{aligned} \bar{\psi}_E^{DH}(z_1, z_2, \boldsymbol{\rho}) &= \frac{1}{2\pi} \int_0^\infty dk\, k J_0(k\rho) \frac{\exp[-\kappa_E \nu_E(k) \mid z_2 - z_1 \mid]}{\epsilon_E \kappa_E \nu_E(k)} \\ &= \frac{e^{-\kappa_E \nu_E(0) r}}{\epsilon_E r} , \end{aligned} \tag{4.13}$$

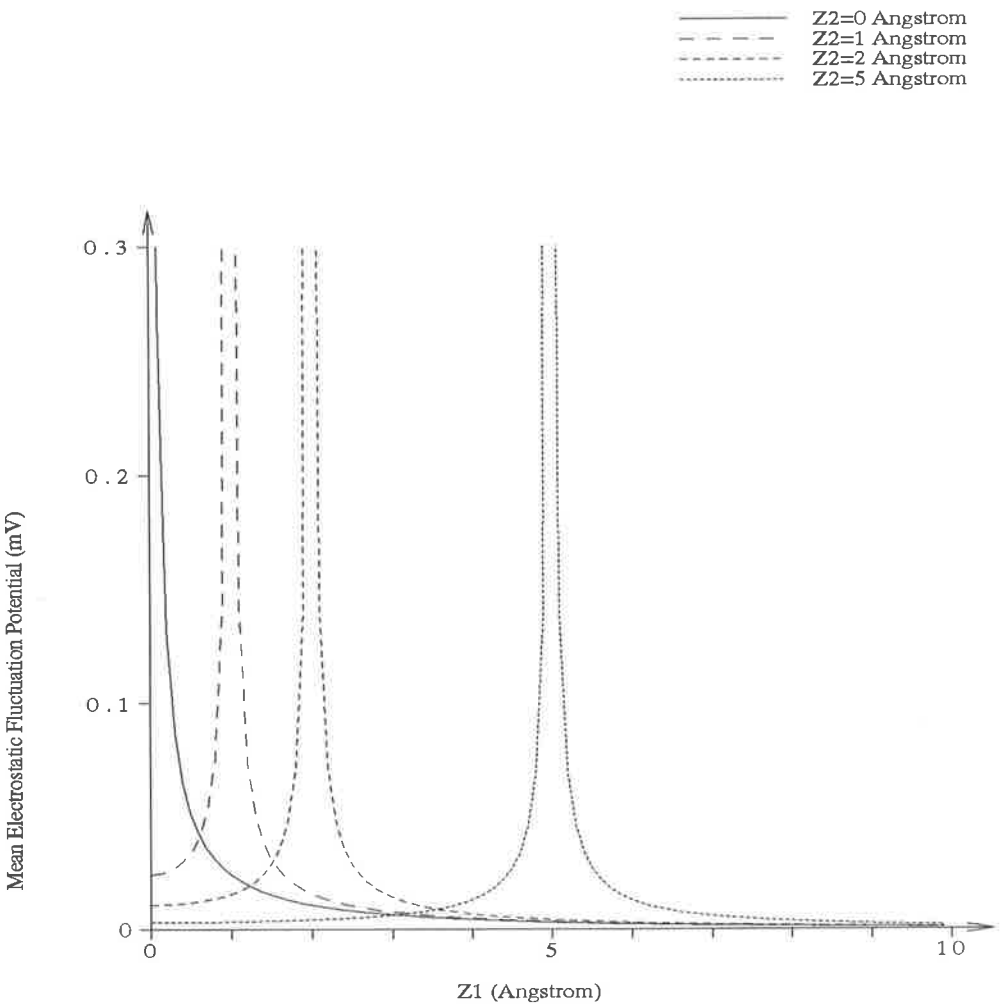

Figure 4.1: Numerical solution for the extracellular mean electrostatic fluctuation potential in the normal direction for a one membrane point model system for various values with the source and field points in the transverse direction to the membrane coinciding i.e. $\rho = 0$. Normal distances are measured from the membrane wall.

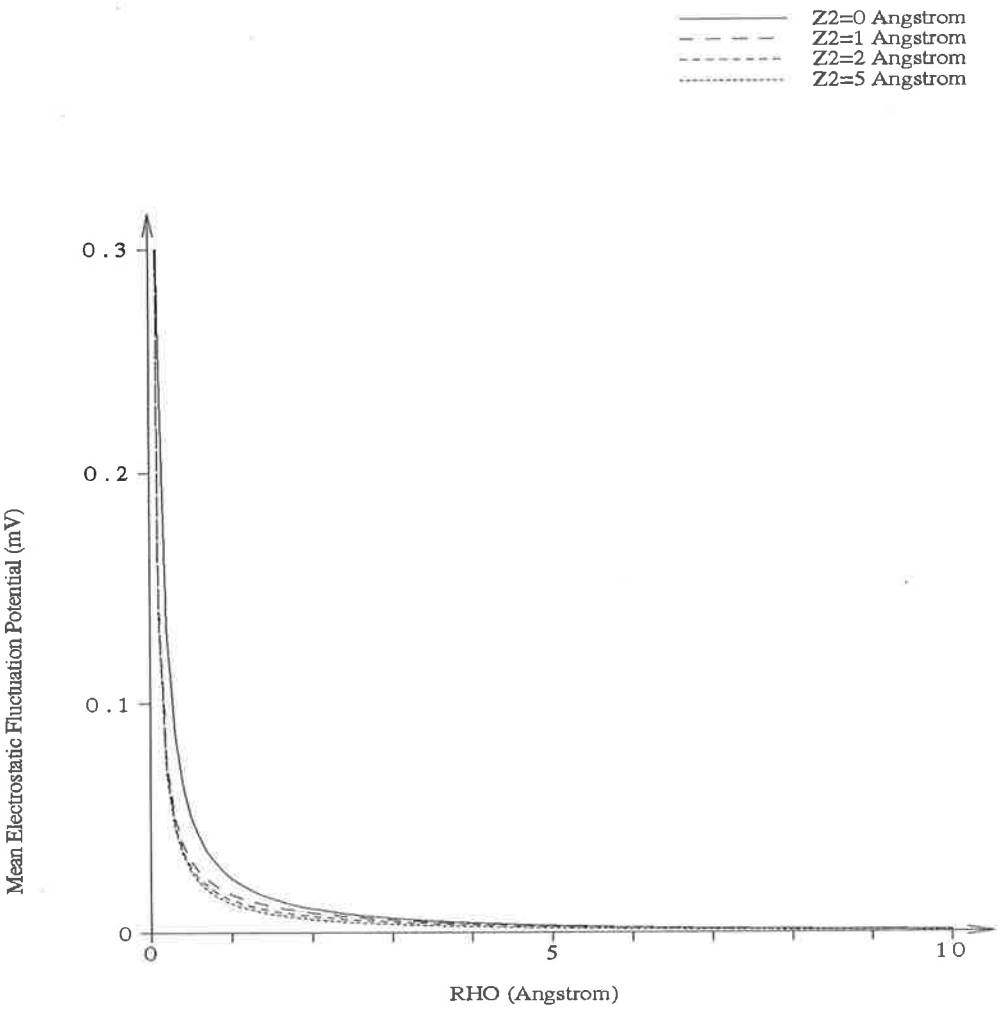

Figure 4.2: Numerical solution for the extracellular mean electrostatic fluctuation potential in the transverse direction for a one membrane point model system for various values with the source and field points in the normal direction to the membrane coinciding i.e. $z_2 = z_1$. Normal distances are measured from the membrane wall.

such that

$$r = \left[(x_2 - x_1)^2 + (y_2 - y_1)^2 + (z_2 - z_1)^2\right]^{\frac{1}{2}} ,$$

and

$$\begin{aligned} \bar{\psi}_E^{IM}(z_1, z_2, \boldsymbol{\rho}) &= \frac{1}{2\pi} \int_0^\infty dk\, k J_0(k\rho)\, \Delta_E \, \frac{\exp[\kappa_E \nu_E(k)(z_2 + z_1 + 2L)]}{\epsilon_E \kappa_E \nu_E(k)} \\ &= \Delta_E \, \frac{e^{-\kappa_E \nu_E(0) r^*}}{\epsilon_E r^*} , \end{aligned} \tag{4.14}$$

where

$$r^* = \left[(x_2 - x_1)^2 + (y_2 - y_1)^2 + (z_2 + z_1 + 2L)^2\right]^{\frac{1}{2}} .$$

Comparison of this analytic expression with the numerical solution shows negligible difference i.e. $< 1\%$. Thus the dominant behaviour for the extracellular mean electrostatic fluctuation potential is determined by the large k behaviour in the extracellular transverse Hankel transform mean electrostatic fluctuation potential.

4.1.2 Intracellular mean electrostatic fluctuation potential

The transverse Hankel transform mean electrostatic fluctuation potential equations for the one membrane point model in case of the source point in the intracellular fluid can be derived from those of extracellular fluid case by interchanging the extracellular and intracellular fluid regions.

A numerical integration of the transform inversion yields plots which are similar to those of the extracellular case in features (as discussed above). See Figure 4.3 and Figure 4.4.

A similar analysis, as discussed in the previous case, for the large k limit in the intracellular transverse Hankel transform mean electrostatic fluctuation potential and subsequent analytic inversion yields

$$\bar{\psi}_I^{DH}(z_1, z_2, \boldsymbol{\rho}) = \frac{e^{-\kappa_I \nu_I(0) r}}{\epsilon_I r} , \tag{4.15}$$

$$\bar{\psi}_I^{IM}(z_1, z_2, \boldsymbol{\rho}) = \Delta_I \, \frac{e^{-\kappa_I r^*}}{\epsilon_I r^*} , \tag{4.16}$$

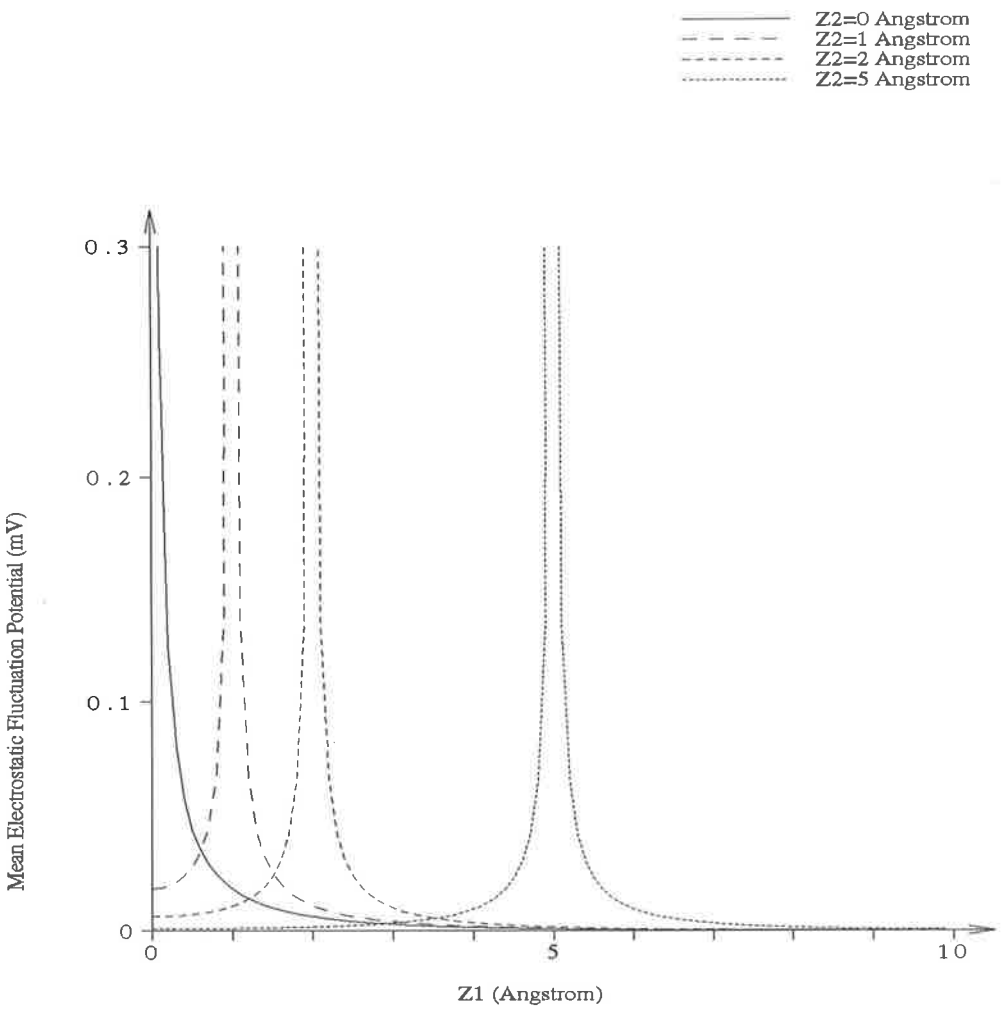

Figure 4.3: Numerical solution for the intracellular mean electrostatic fluctuation potential in the normal direction for a one membrane point model system for various values with the source and field points in the transverse direction to the membrane coinciding i.e. $\rho = 0$. Normal distances are measured from the membrane wall.

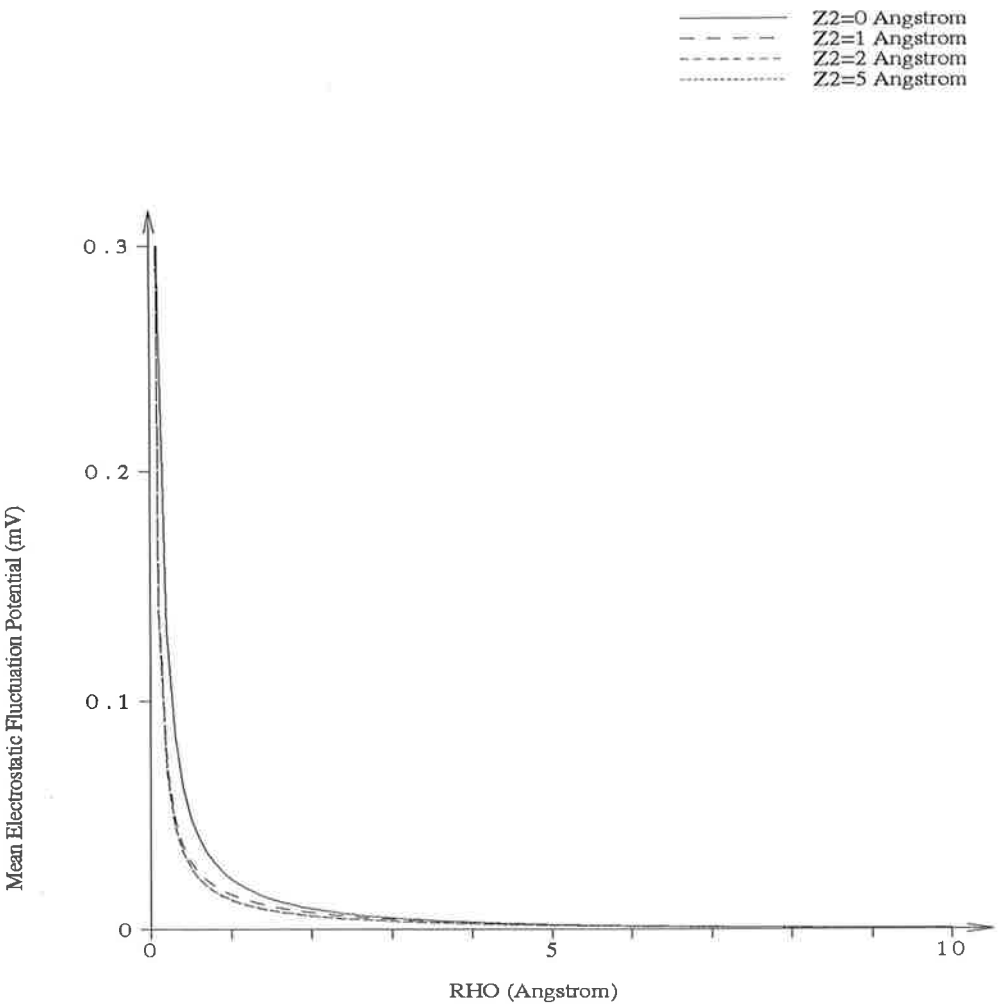

Figure 4.4: Numerical solution for the intracellular mean electrostatic fluctuation potential in the transverse direction for a one membrane point model system for various values with the source and field points in the normal direction to the membrane coinciding i.e. $z_2 = z_1$. Normal distances are measured from the membrane wall.

Quantity	Value
$\kappa_E\nu_E(0)$	$0.1227\mathring{A}^{-1}$
$\kappa_I\nu_I(0)$	$0.1946\mathring{A}^{-1}$

Table 4.1: Table of $\kappa\nu(0)$ values in the extracellular and intracellular fluid regions for the one membrane point model.

where

$$\begin{aligned}
\Delta_I &= \frac{\epsilon_I - \epsilon_M}{\epsilon_I + \epsilon_M} \ , \\
r &= \left[(x_2 - x_1)^2 + (y_2 - y_1)^2 + (z_2 - z_1)^2\right]^{\frac{1}{2}} \\
r^* &= \left[(x_2 - x_1)^2 + (y_2 - y_1)^2 + (z_2 + z_1 - 2L)^2\right]^{\frac{1}{2}} \ .
\end{aligned}$$

Comparison of this analytic expression with the numerical solution again shows negligible difference i.e. $< 1\%$. Also a comparison between the extracellular and intracellular analytic expressions shows that for the same dielectric constant in each of the fluid regions i.e. $\epsilon_E = \epsilon_I$, which is true in our model, that the parameter $\kappa_r\nu_r(0)$, which can be thought of as an "effective " inverse Debye shielding length, determines the structure in each of the fluid regions. The values of the parameter $\kappa_r\nu_r(0)$ are presented in Table 4.1. The difference in the values between the two regions is due to an order of magnitude difference in the charge asymmetry parameter ζ_r, see Table B.1. The asymmetry parameter being greater in the intracellular fluid due to the abundance of cations (Na^+, K^+, Ca^{++}) compared to the major anion Cl^-. Whereas for the extracellular fluid the asymmetry is less due to a greater balance in the amount of anions to cations. Thus the "effective" Debye shielding length in the intracellular fluid is less than that of the extracellular fluid i.e. an ion in the intracellular fluid is screened more than that of an identical ionic species in the extracellular fluid.

4.2 Calculation of ionic hydration numbers

The definition of Azzam for the ionic hydration number Eq. (1.8) has to modified to account for the orientational dependence of the dipole (water molecule). The quantity $d\mathbf{x}_2\, d\boldsymbol{\omega}_2\, n_d(\mathbf{x}_2, \boldsymbol{\omega}_2|V)\, g_{id}(\mathbf{x}_1; \mathbf{x}_2, \boldsymbol{\omega}_2|V)$ describes the number of dipoles (water molecules) in the volume region $\mathbf{x}_2$, $\mathbf{x}_2 + d\mathbf{x}_2$ with orientation in the angular region $\boldsymbol{\omega}_2$, $\boldsymbol{\omega}_2 + d\boldsymbol{\omega}_2$ given that an ionic species of the *ith* type is located at $\mathbf{x}_1$. We have to integrate this quantity over a (to be determined) region to calculate the ionic hydration number. Since the correlation functions have both a normal and transverse dependence but the mean electrostatic potential has only a dependence in the normal direction, integration over a spherical region (as in Azzam's definition) is analytically not possible in closed form. Thus a cylindrical region is chosen so as to provide an analytic expression for the ionic hydration number. The appropriate definition for the ionic hydration number is thus given by

$$n_i^H(\mathbf{x}_1) = \int_{min}^{max} d\mathbf{x}_2 \int d\boldsymbol{\omega}_2\, n_d(\mathbf{x}_2, \boldsymbol{\omega}_2|V)\, g_{id}(\mathbf{x}_1; \mathbf{x}_2, \boldsymbol{\omega}_2|V) \ . \tag{4.17}$$

The region of integration, denoted by $\int_{min}^{max} d\mathbf{x}_2$, is such that we are evaluating the number of dipoles (water molecules) contained within a cylindrical region with a region of exclusion. The region of exclusion is included (by hand) in the calculation to represent the "hard sphere" of an ion. The extremities of the region of integration are chosen to be multiples of the "effective" Debye length. This choice is physically reasonable since the interaction between the ion and any "attached" water molecules is over this length scale though it is still arbitrary compared with a choice of say two "effective" Debye lengths. Thus the region of integration has the following limits when written in terms of cylindrical co-ordinates

$$\int_{min}^{max} d\mathbf{x}_2 = 2\pi \int_{z_1 - z_{max}}^{z_1 + z_{max}} dz_2\, (z_2 - z_1) \int_{\rho_{min}}^{\rho_{max}} d\rho_2\, \rho_2 \ ,$$

where

$$\begin{aligned} \rho_{min} &= \frac{R_i}{2} \\ \rho_{max} &= \frac{1}{\kappa_E \nu_E(0)} \\ z_{max} &= \frac{1}{2\kappa_E \nu_E(0)} \end{aligned} \tag{4.18}$$

See Figure 4.5. The region of integration must be truncated in the normal direction if it extends into the membrane region since no dipoles (water molecules) can be "attached" in that region for our model.

The relationship between the ion-dipole indirect correlation function and the mean electrostatic fluctuation potential is given by Eq. (2.129) (setting molecule of type b to be a dipole) i.e.

$$h_{id}(\mathbf{x}_1;\mathbf{x}_2,\boldsymbol{\omega}_2|V) = -\beta e_i \mathbf{m}(\boldsymbol{\omega}_2)\cdot\nabla_2\bar{\psi}(\mathbf{x}_1,\mathbf{x}_2)\ . \tag{4.19}$$

Thus the ion-dipole pair correlation function is given by

$$\begin{aligned} g_{id}(\mathbf{x}_1;\mathbf{x}_2,\boldsymbol{\omega}_2|V) &= \exp[-\beta e_i \mathbf{m}(\boldsymbol{\omega}_2)\cdot\nabla_2\bar{\psi}(\mathbf{x}_1,\mathbf{x}_2)] \\ &\approx 1-\beta e_i \mathbf{m}(\boldsymbol{\omega}_2)\cdot\nabla_2\bar{\psi}(\mathbf{x}_1,\mathbf{x}_2)\ . \end{aligned} \tag{4.20}$$

Expansion to first order in the mean electrostatic potential for the dipole number density Eq. (2.88) i.e.

$$n_d(\mathbf{x}_2,\boldsymbol{\omega}_2|V) = \frac{n_d^0}{4\pi}[1-\beta\mathbf{m}(\boldsymbol{\omega}_2)\cdot\nabla_2\psi(\mathbf{x}_2)]\ , \tag{4.21}$$

and substituting for the pair correlation function Eq. (4.20) into the definition for the ionic hydration number Eq. (4.17) results in

$$\begin{aligned} n_i^H(\mathbf{x}_1) = \quad & \frac{n_d^0}{4\pi}\int_{min}^{max} d\mathbf{x}_2 \int d\boldsymbol{\omega}_2 \Big[1-\beta\mathbf{m}(\boldsymbol{\omega}_2)\cdot\nabla_2\psi(\mathbf{x}_2)\Big] \\ \times\ & \Big[1-\beta e_i \mathbf{m}(\boldsymbol{\omega}_2)\cdot\nabla_2\bar{\psi}(\mathbf{x}_1,\mathbf{x}_2)\Big]\ . \end{aligned} \tag{4.22}$$

Then performing the angular integration for the extracellular fluid case yields

$$\begin{aligned} n_i^H(\mathbf{x}_1) &= n_d^0\int_{min}^{max} d\mathbf{x}_2\Big[1+\frac{1}{3}e_i\beta^2m^2\,\frac{\partial\psi(\mathbf{x}_2)}{\partial z_2}\,\frac{\partial\bar{\psi}(\mathbf{x}_1,\mathbf{x}_2)}{\partial z_2}\Big] \\ &= n_d^0\int_{min}^{max} d\mathbf{x}_2\Big[1-\frac{1}{3}e_i\beta^2m^2\frac{A_E\kappa_E}{\epsilon_E}e^{\kappa_E(z_2+L)}\Big\{\frac{e^{-\kappa_E\nu_E(0)r}}{r}[\kappa_E\nu_E(0)+\frac{1}{r}]\frac{z_2-z_1}{r} \\ &\quad + \Delta_E\,\frac{e^{-\kappa_E\nu_E(0)r^*}}{r^*}[\kappa_E\nu_E(0)+\frac{1}{r^*}]\frac{z_2+z_1+2L}{r^*}\Big\}\Big]\ . \end{aligned} \tag{4.23}$$

The integrals involved in the above expression are of the form

$$\int_{min}^{max} d\mathbf{x}_2\,(z_2-z_1)\,e^{\kappa_E(z_2+L)}\,\frac{e^{-\kappa_E\nu_E(0)r}}{r}\,\Big[\frac{1}{r}\Big]^n\ ,$$

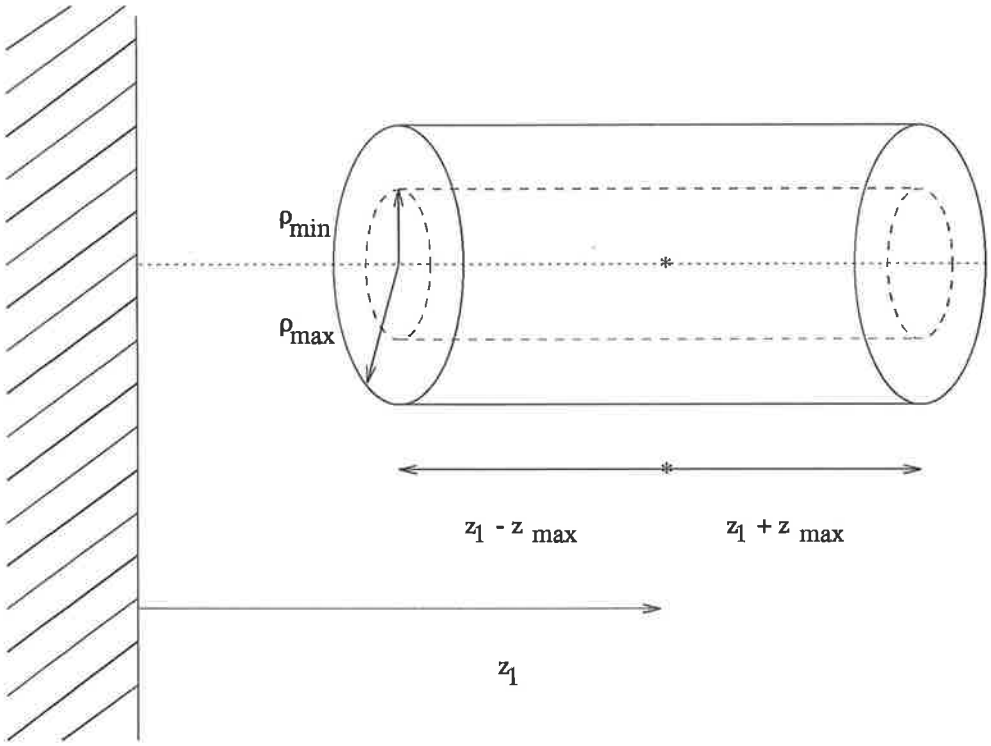

Figure 4.5: Schematic representation of the region of integration for the calculation of ionic hydration numbers.

for the Debye-Huckel term and

$$\int_{min}^{max} d\mathbf{x}_2\,(z_2+z_1+2L)\,e^{\kappa_E(z_2+L)}\;\frac{e^{-\kappa_E\nu_E(0)r^*}}{r^*}\;\left[\frac{1}{r^*}\right]^n\;,$$

for the image term, where $n=1,2$. These integrals are evaluated in Appendix D and if we now substitute those results into Eq.(4.23) we obtain

$$\begin{aligned}
n_i^H(\mathbf{x}_1) = \quad & n_d^0\pi[\rho_{max}^2-\rho_{min}^2]2z_{max} \\
- \; & n_d^0\frac{2\pi}{3}e_i\beta^2m^2\frac{A_E\kappa_E}{\epsilon_E}e^{\kappa_E(z_1+L)}\int_{-z_{max}}^{z_{max}}dy\,y\,e^{\kappa_E y} \\
\times \; & \left[\frac{e^{-\kappa_E\nu_E(0)\sqrt{\rho_{min}^2+y^2}}}{\sqrt{\rho_{min}^2+y^2}}\left\{1+O\left(\left[\frac{1}{\kappa_E\nu_E(0)\sqrt{\rho_{min}^2+y^2}}\right]^3\right)\right\}\right. \\
& \left.-\frac{e^{-\kappa_E\nu_E(0)\sqrt{\rho_{max}^2+y^2}}}{\sqrt{\rho_{max}^2+y^2}}\left\{1+O\left(\left[\frac{1}{\kappa_E\nu_E(0)\sqrt{\rho_{max}^2+y^2}}\right]^3\right)\right\}\right] \\
- \; & n_d^0\frac{2\pi}{3}e_i\beta^2m^2\frac{A_E\kappa_E}{\epsilon_E}e^{-\kappa_E(z_1+L)}\Delta_E\int_{2z_1-z_{max}+2L}^{2z_1+z_{max}+2L}dy\,y\,e^{\kappa_E y} \\
\times \; & \left[\frac{e^{-\kappa_E\nu_E(0)\sqrt{\rho_{min}^2+y^2}}}{\sqrt{\rho_{min}^2+y^2}}\left\{1+O\left(\left[\frac{1}{\kappa_I\nu_I(0)\sqrt{\rho_{min}^2+y^2}}\right]^3\right)\right\}\right. \\
& \left.-\frac{e^{-\kappa_E\nu_E(0)\sqrt{\rho_{max}^2+y^2}}}{\sqrt{\rho_{max}^2+y^2}}\left\{1+O\left(\left[\frac{1}{\kappa_I\nu_I(0)\sqrt{\rho_{max}^2+y^2}}\right]^3\right)\right\}\right]\;. \qquad (4.24)
\end{aligned}$$

A similar expression can be obtain for the ionic hydration number in the intracellular fluid region such that

$$\begin{aligned}
n_i^H(\mathbf{x}_1) = \quad & n_d^0\pi[\rho_{max}^2-\rho_{min}^2]2z_{max} \\
- \; & n_d^0\frac{2\pi}{3}e_i\beta^2m^2\frac{A_I\kappa_I}{\epsilon_I}e^{\kappa_I z_1}\int_{-z_{max}}^{z_{max}}dy\,y\,e^{\kappa_I y} \\
\times \; & \left[\frac{e^{-\kappa_I\nu_I(0)\sqrt{\rho_{min}^2+y^2}}}{\sqrt{\rho_{min}^2+y^2}}\left\{1+O\left(\left[\frac{1}{\sqrt{\rho_{min}^2+y^2}}\right]^3\right)\right\}\right. \\
& \left.-\frac{e^{-\kappa_I\nu_I(0)\sqrt{\rho_{max}^2+y^2}}}{\sqrt{\rho_{max}^2+y^2}}\left\{1+O\left(\left[\frac{1}{\sqrt{\rho_{max}^2+y^2}}\right]^3\right)\right\}\right] \\
- \; & n_d^0\frac{2\pi}{3}e_i\beta^2m^2\frac{A_I\kappa_I}{\epsilon_I}e^{-\kappa_I(z_1+L)}\Delta_I\int_{2z_1-z_{max}+2L}^{2z_1+z_{max}+2L}dy\,y\,e^{\kappa_I y} \\
\times \; & \left[\frac{e^{-\kappa_I\nu_I(0)\sqrt{\rho_{min}^2+y^2}}}{\sqrt{\rho_{min}^2+y^2}}\left\{1+O\left(\left[\frac{1}{\sqrt{\rho_{min}^2+y^2}}\right]^3\right)\right\}\right. \\
& \left.-\frac{e^{-\kappa_I\nu_I(0)\sqrt{\rho_{max}^2+y^2}}}{\sqrt{\rho_{max}^2+y^2}}\left\{1+O\left(\left[\frac{1}{\sqrt{\rho_{max}^2+y^2}}\right]^3\right)\right\}\right]\;. \qquad (4.25)
\end{aligned}$$

The ionic hydration number expression for both the extracellular and intracellular cases has the leading term $n_d^0\pi[\rho_{max}^2-\rho_{min}^2]2z_{max}$ which is independent of the charge of

the ionic species but does depend on the size of the molecule and its position relative to the membrane wall. The size of the ionic species is incorporated through the exclusion volume effect of $\pi\rho_{min}^2 2z_{max}$ and the position of the molecule through the truncation of the length of the hydration cylinder if the region extends into the membrane. Thus strictly, the quantity $2z_{max}$ for the extracellular case is given by

$$2z_{max} = \begin{cases} z_{max} \mid z_1 + L \mid & \mid z_1 + L \mid < z_{max} \\ 2z_{max} & \mid z_1 + L \mid > z_{max} \end{cases} , \tag{4.26}$$

and for the intracellular case by

$$2z_{max} = \begin{cases} z_{max} \mid z_1 - L \mid & \mid z_1 - L \mid < z_{max} \\ 2z_{max} & \mid z_1 - L \mid > z_{max} \end{cases} . \tag{4.27}$$

The truncation of the region of integration when the ionic species is within a distance of z_{max} describes the geometric effect of the exclusion of dipoles (water molecules) if the ion is close to the membrane wall. The difference between the leading term in the extracellular and intracellular fluid regions (for the same ionic species) is due to the upper limit for the region of integration in the transverse direction ρ_{max}. Since ρ_{max} is given by the "effective" Debye length, which is smaller in the intracellular fluid, the leading term behaviour is smaller in the intracellular fluid as compared with the extracellular fluid at the same relative position to the closest membrane wall and identical ionic species.

The next term in the expansion is negligible compared to the leading term ($\ll 0.1\%$) for both the extracellular and intracellular fluid regions. This is due to the term being a product of the two kinds of potential and thus a second order term. The approximations made during the thesis have been to first order in the mean electrostatic potential and thus this second order term being small is not surprising. Despite the term being negligible it does show some important qualitative features. The term shows an exponential damping in the normal direction as the distance from the membrane increases and depends on the charge of the ionic species.

Improvement of this result should be possible by starting a numerical iterative procedure with the analytic solutions for the mean electrostatic potential and the mean electrostatic fluctuation potential to obtain a better approximation for the appropriate BBGKY

hierarchy equation and then substituting this result into the potential equations. This iterative procedure is necessary due to the failure of the assumption that the potential mean electrostatic potential is small especially in the region adjacent to the membrane. Thus the non linear terms in the mean electrostatic potential are important. Also the effect of the 2 body correlations could be included in the derivation of the mean electrostatic potential equation since these contribute to the potential.

Chapter 5

Conclusion

In this thesis we proposed a model to investigate the distribution of molecules in the vicinity of the membrane of a neuron. The model neuron consisted of an electrolyte solution that was bounded by two planar membranes (of finite thickness L and separated by a distance of $2D$). Each of the membranes was modelled as a dielectric continuum with a uniform surface charge density. The concentrations of the various mobile ionic species used in the extracellular and intracellular fluid regions of the model were typical of the resting state of the neuron. The model could have been extended to consider concentrations of the mobile ionic species typically found in the dynamical phase of the action potential though the assumption of planar geometry breaks down if the Debye length becomes comparable to the radius of curvature of a neuron.

In Chapter 2 we presented a derivation of the potential formulation of the distribution functions from the BBGKY hierarchy in a similar manner to Outhwaite's derivation [75] for the PM. The resulting differential equations for the mean electrostatic potential and mean electrostatic fluctuation potential (for both the hard sphere and point molecules cases) reduced to those of Outhwaite (hard sphere [94], [95]) and Carnie and Chan (point [74]) if the condition of bulk electroneutrality was assumed. It should be noted that the differential equations for both kinds of potential were derived by truncating in the appropriate member of the BBGKY hierarchy in the higher order terms in the indirect correlation function and closing the equations with this linearized form of the BBGKY hierarchy. Thus these differential equations can be considered to be first iterates in a perturbative method for determining both the mean electrostatic potential and mean

electrostatic fluctuation potential. Further work can be pursued by using the analytic solutions to these differential equations (as derived in Chapters 3 and 4) to derive a new approximation to the n body distribution function and use these equations to close the potential equations.

In this thesis, solutions of the differential equations for both kinds of potential, in the case of hard sphere molecules, were not considered. This was due to the inherent difficulty in constructing solutions to the partial differential equation for the mean electrostatic fluctuation potential in a cylindrical geometry with a radial boundary condition across the sphere of exclusion for the generalized displacement vector $\mathbf{P}_b(\mathbf{x}_1;\mathbf{x}_2,\omega_2)$. Thus a numerical solution of this case could be explored though it is unclear how to incorporate the radial boundary condition in the numerical code.

In Chapter 3 explicit solutions for the mean electrostatic potential and the transverse Hankel transform mean electrostatic fluctuation potential for the two membrane point model system were derived. For the transverse Hankel transform mean electrostatic fluctuation potential, both cases for the position of the source point were considered. An important parameter was introduced called the charge asymmetry parameter ζ_r and its value varied from the extracellular to intracellular fluid regions. This parameter determined the type of solutions for the transverse Hankel transform mean electrostatic fluctuation potential depending on its sign in terms of Bessel functions ($\zeta > 0$) or modified Bessel functions ($\zeta < 0$). For the concentrations of the mobile ionic species used in the model, the charge asmmetry parameter was positive in both the extracellular and intracellular fluid regions. It was found that (provided the ratio of the distance between the membranes $2D$ and the Debye length is $\gg 1$) the asymmetry parameter for the two membrane case showed negligible difference to that of the one membrane case for the same membrane thickness L. Also the asymmetry parameter in the limit as $L \to \infty$ approached the value for the one wall case considered by Carnie and Chan [74].

The solution for the transverse Hankel transform mean electrostatic fluctuation potential for each of the cases for the sign of the charge asymmetry parameter ζ, when the source point was in the extracellular fluid region, was noted to be of the same form as for the one

membrane system (see Appendix B) and indeed the one wall system considered by Carnie and Chan [41]. The first term (for all three systems) was associated with a the Debye-Huckel type correlation function in the bulk solution which was a function only of the relative position of the field and source point. The other term $\bar{\Delta}_2(L,\zeta_E,D,\zeta_I)$ the image term, was due to the dielectric boundaries of the systems. The quantity $\bar{\Delta}_2(L,\zeta_E,D,\zeta_I)$ is an even function with respect to the transverse transform variable k for finite L and D. Thus, as noted by Carnie and Chan [41], the correlation in the transverse direction is screened. The shielding in the transverse direction occurs because the charge on the opposite side of the membrane wall is able to redistribute itself, screening the potential between molecules.

As $k \to \infty$, comparison between the two membrane and one membrane system (see Appendix B) showed that both $\bar{\Delta}_2(L,\zeta_E,D,\zeta_I)$ and $\bar{\Delta}_1(2L,\zeta_E,\zeta_I)$ tend to the same limit. This limit is the same as for $\bar{\Delta}(\zeta)$ in the one wall system [41], when $\zeta = \zeta_E$, even though $\bar{\Delta}(\zeta)$ is neither an even or odd function of k. This is not a surprising result if we consider all three quantities at the same source and field point, relative to the membrane wall at the interface between the extracellular fluid and membrane. Since the large k behaviour describes the small ρ behaviour, a molecule experiences negligible influence from boundaries more than a Debye length away. Also it was noted that the large k behaviour for $\bar{\Delta}_2(L,\zeta_E,D,\zeta_I)$ has no explicit dependence on the distance between the membrane walls $2D$ and both $\bar{\Delta}_2(L,\zeta_E,D,\zeta_I)$ and $\bar{\Delta}_1(2L,\zeta_E,\zeta_I)$ have no explicit dependence on the membrane thickness. The dependence of these quantities on the parameters L and D is rather via the extracellular asymmetry parameter ζ_E.

A shooting method was employed to numerically solve the differential equations for the transverse Hankel transform mean electrostatic fluctuation potential as a test of the validity of the asymptotic forms. The location of the starting boundaries for the numerical procedure decreased as the value of the transform variable k increased. This is consistent with the properties of the transform such that the large k behaviour is determined by the region near the source point whereas the opposite is true for small k values. This property of the numerical integration supported the argument that the second membrane

and thus the extracellular fluid in region V has negligible effect on the value for the transverse Hankel transform mean electrostatic fluctuation potential (and thus the mean electrostatic fluctuation potential) provided the distance $2D$ is large compared to the Debye length. A numerical procedure was also used for the case when the source point was in the intracellular fluid region and comparison with the asymptotic form showed again that the second membrane wall has negligible effect provided the distance $2D$ is large compared with the Debye length and the source point is in the vicinity of the membrane wall located at $-D$. Since the second membrane wall had negligible influence on the solution for the transverse Hankel transform mean electrostatic fluctuation potential, for both cases of the position of the source point, the simpler expression for the image forces of the one membrane system $\bar{\Delta}_1(2L, \zeta_E, \zeta_I)$ was used to perform the transform inversion.

In Chapter 4 we presented the ionic hydration number calculation for various ionic species in both the extracellular and intracellular fluid regions. An analytic expression for the mean electrostatic fluctuation potential was obtained by taking the large k limit and inverting this expression in closed form. Comparison of this analytic expression with a numerical integration of the transverse Hankel transform mean electrostatic fluctuation potential showed excellent agreement. Also a comparison between the extracellular and intracellular analytic expressions showed that for the same dielectric constant in each of the fluid regions, the parameter $\kappa\nu(0)$, which can be thought of as an "effective " inverse Debye shielding length, determines the structure in each of the fluid regions. The difference in the values between the two regions is due to an order of magnitude difference in the charge asymmetry parameter ζ. The asymmetry parameter being greater in the intracellular fluid due to the abundance of cations (Na^+, K^+, Ca^{++}) compared to the major anion Cl^-. Whereas for the extracellular fluid the asymmetry is less due to a greater balance in the amount of anions to cations. Thus the "effective" Debye shielding length in the intracellular fluid is less than that of the extracellular fluid i.e. an ion in the intracellular fluid is screened more than that of an identical ionic species in the extracellular fluid.

Our definition for the ionic hydration number took into account the orientational dependence of the dipoles as opposed to Azzam's definition. Also, due to the normal

direction dependence of the mean electrostatic potential, it was necessary to modify the region of integration to be a cylinder with an exclusion volume to obtain an analytic expression for the ionic hydration number. This analytic expression contains two terms. The leading term describes the number of dipoles in the region of integration if the number density of the dipoles takes the bulk value. The next term describes the variation from this bulk term. This term was found to be negligible compared to the leading term. Improvements should be possible by including higher order terms in the approximations made in the derivation of the defining equations for the mean electrostatic potential and mean electrostatic fluctuation potential.

Appendix A

Molecular Potentials

In this appendix we calculate the image potentials due to the discontinuity in the dielectric permittivity at the membrane walls for the two membrane system.

A.1 One body potential

The one body potentials $V_a(\mathbf{x}_1, \boldsymbol{\omega}_1)$ are written in the form

$$V_a(\mathbf{x}_1, \boldsymbol{\omega}_1) = V_a^S + V_a^E \ , \tag{A.1}$$

where V_a^S is the short range contribution to the one body potential which causes the exclusion of molecules from a region adjacent to the membrane wall. The short range potential V_a^S is given by

$$V_a^S(\mathbf{x}_1, \boldsymbol{\omega}_1) = \begin{cases} \infty & \mid z_1 \mid < \frac{R_a}{2} \\ \\ 0 & \mid z_1 \mid > \frac{R_a}{2} \end{cases} \ , \tag{A.2}$$

where z_1 is defined as the perpendicular distance from the membrane wall. The term V_a^E is the electrostatic contribution. Due to the symmetry in the model system, see Figure A.1, the displacement vector $\mathbf{D}(\mathbf{x}_1)$ satisfies

$$\mathbf{D}(\mathbf{x}_1) = D(z_1)\hat{\mathbf{z}} \ , \tag{A.3}$$

$$D(-z_1) = -D(z_1) \ . \tag{A.4}$$

At the membrane walls, we have the continuity condition of the displacement vector in the normal direction i.e.

$$\mathbf{D} \cdot \hat{\mathbf{z}} \mid_{z_1^+} - \mathbf{D} \cdot \hat{\mathbf{z}} \mid_{z_1^-} = 4\pi\sigma \ , \tag{A.5}$$

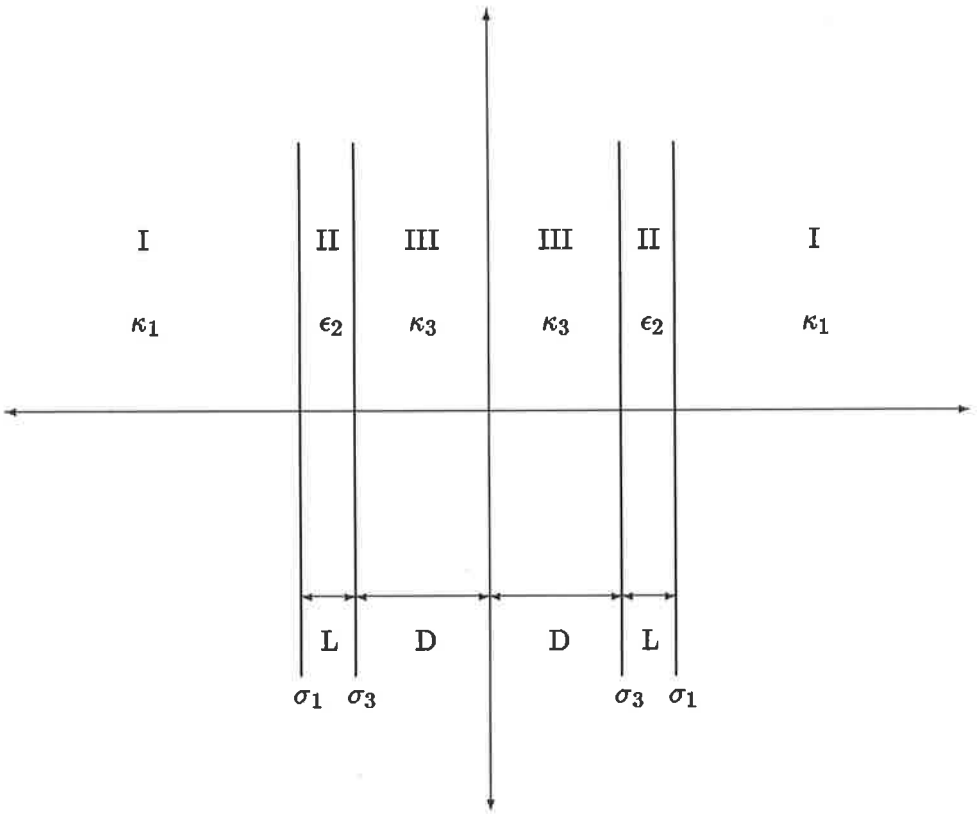

Figure A.1: Schematic representation of a two membrane model geometry showing the various regions and the associated dielectric constant, inverse Debye length and surface charge density.

where σ is the surface charge density at the membrane wall. The displacement vector is related to the electric field by

$$\mathbf{D}(\mathbf{x}_1) = \epsilon(\mathbf{x}_1) \cdot \mathbf{E}(\mathbf{x}_1) \ . \tag{A.6}$$

where $\epsilon(\mathbf{x}_1)$ is the dielectric tensor. Thus the electric field is, using the above boundary condition, given by

$$E(z_1) = \begin{cases} 0 & 0 \leq z_1 < D \\ \frac{4\pi\sigma_3}{\epsilon_2} & D < z_1 < [L+D] \\ 4\pi(\sigma_1+\sigma_3) & [L+D] < z_1 \end{cases} \ . \tag{A.7}$$

The electrostatic contribution to the one body potential, $V_a^E(\mathbf{x}_1, \boldsymbol{\omega}_1)$, is thus given by

$$V^E(\mathbf{x}_1) = \begin{cases} 4\pi(\sigma_1+\sigma_3)(z_1+[L+D]) - \frac{\sigma_3 L}{\epsilon_2} & z_1 \leq -[L+D] \\ \frac{4\pi\sigma_3}{\epsilon_2}(z_1+D) & -[L+D] \leq z_1 \leq -D \\ 0 & -D \leq z_1 \leq D \\ -\frac{4\pi\sigma_3}{\epsilon_2}(z_1-D) & D \leq z_1 \leq [L+D] \\ -4\pi(\sigma_1+\sigma_3)(z_1-[L+D]) - \frac{\sigma_3 L}{\epsilon_2} & [L+D] \leq z_1 \end{cases} \ , \tag{A.8}$$

such that

$$V_i^E(\mathbf{x}_1) = e_i V^E \ , \tag{A.9}$$

$$V_d^E(\mathbf{x}_1, \boldsymbol{\omega}_1) = \mathbf{m}(\boldsymbol{\omega}_1) \cdot \nabla_1 V^E \ . \tag{A.10}$$

A.2 Two body potential

The two body (intermolecular) potentials $\Phi_{ab}(\mathbf{x}_1, \boldsymbol{\omega}_1; \mathbf{x}_2, \boldsymbol{\omega}_2)$ are also written in the form

$$\Phi_{ab}(\mathbf{x}_1, \boldsymbol{\omega}_1; \mathbf{x}_2, \boldsymbol{\omega}_2) = \Phi_{ab}^S + \Phi_{ab}^E \ , \tag{A.11}$$

where Φ_{ab}^S is the short range contribution to the two body potential and is given by

$$\Phi_{ab}^S(\mathbf{x}_1, \boldsymbol{\omega}_1; \mathbf{x}_2, \boldsymbol{\omega}_2) = \begin{cases} \infty & r < R_{ab} \\ 0 & r > R_{ab} \end{cases} \ , \tag{A.12}$$

such that

$$R_{ab} = \frac{1}{2}(R_a + R_b) \ . \tag{A.13}$$

The other term, Φ^E_{ab}, is the electrostatic contribution which is defined by

$$\Phi^E_{ab}(\mathbf{x}_1, \boldsymbol{\omega}_1; \mathbf{x}_2, \boldsymbol{\omega}_2) = \Phi^C_{ab} + \Phi^I_{ab} \ , \tag{A.14}$$

where Φ^I_{ab} is the image potential due to the discontinuities in the dielectric tensor at the membrane walls and Φ^C_{ab} is the Coulombic contribution. The Coulombic contribution to the potential , Φ^C_{ab}, is given by

$$\text{ion-ion} \quad \Phi^C_{ij}(\mathbf{x}_1, \boldsymbol{\omega}_1; \mathbf{x}_2, \boldsymbol{\omega}_2) = \frac{e_i e_j}{r} \ , \tag{A.15}$$

$$\text{ion-dipole} \quad \Phi^C_{id}(\mathbf{x}_1, \boldsymbol{\omega}_1; \mathbf{x}_2, \boldsymbol{\omega}_2) = -e_i E_1 \frac{1}{r} \ , \tag{A.16}$$

$$\text{dipole-ion} \quad \Phi^C_{di}(\mathbf{x}_1, \boldsymbol{\omega}_1; \mathbf{x}_2, \boldsymbol{\omega}_2) = e_i E_1 \frac{1}{r} \ , \tag{A.17}$$

$$\text{dipole-dipole} \quad \Phi^C_{dd'}(\mathbf{x}_1, \boldsymbol{\omega}_1; \mathbf{x}_2, \boldsymbol{\omega}_2) = -E_1 E_1 \frac{1}{r} \ , \tag{A.18}$$

where

$$E_1 = \mathbf{m}(\boldsymbol{\omega}_1) \cdot \nabla_1 \ . \tag{A.19}$$

The dipole orientation vector $\boldsymbol{\omega}_1$ is defined by the angular co-ordinates (θ_1, ϕ_1) such that $\int d\boldsymbol{\omega}_1 = 4\pi$. $\mathbf{I}$ is the 3x3 identity tensor. The vector $\mathbf{r}$ is defined by $\mathbf{r} = \mathbf{x}_2 - \mathbf{x}_1$.

The ion-ion image potential, Φ^I_{ij}, is calculated in the following manner. We know from electrostatics [109] that the electrostatic contribution to the two body potential, Φ^E_{ij}, satisfies

$$\Phi^E_{ij} = e_i e_j \Phi^E \ , \tag{A.20}$$

$$\nabla^2_1 \Phi^E = -4\pi\delta(\mathbf{x}_2 - \mathbf{x}_1) \ , \tag{A.21}$$

since

$$\nabla^2_1 \Phi^I_{ab} = 0 \ , \tag{A.22}$$

with the boundary conditions of

$$\Phi^E \mid_{z_1^+} = \Phi^E \mid_{z_1^-} \ , \tag{A.23}$$

$$\epsilon \frac{\partial \Phi^E}{\partial z_1} \mid_{z_1^+} = \epsilon \frac{\partial \Phi^E}{\partial z_1} \mid_{z_1^-} \ , \tag{A.24}$$

at the membrane walls. Since there is cylindrical symmetry in the system due to the external potential being only a function of the perpendicular distance from the wall we can solve this problem through the use of the transverse Hankel transform. See Figure 2.2. Defining the transverse Hankel transform by

$$\begin{aligned}\tilde{\Phi}^E(z_1,z_2,\mathbf{k}) &= \int d\boldsymbol{\rho}\exp[i\mathbf{k}\cdot\boldsymbol{\rho}]\Phi^E(z_1,z_2,\boldsymbol{\rho}) \\ &= 2\pi\int_0^\infty d\rho\rho J_0(k\rho)\Phi^E(z_1,z_2,\boldsymbol{\rho}) \ , \end{aligned} \tag{A.25}$$

and the inverse transverse Fourier transform is thus given by

$$\Phi^E(z_1,z_2,\boldsymbol{\rho}) = \frac{1}{2\pi}\int_0^\infty dk k J_0(k\rho)\tilde{\Phi}^E(z_1,z_2,\mathbf{k}) \ , \tag{A.26}$$

where

$$\begin{aligned}\boldsymbol{\rho} &= (x_2-x_1, y_2-y_1) \ , \\ k &= |\,\mathbf{k}\,| \ . \end{aligned}$$

We can apply the transverse Fourier transform to Eq. (A.21) to yield

$$\left[\frac{d^2}{dz_1^2}-k^2\right]\tilde{\Phi}^E(z_1,z_2,\mathbf{k}) = -4\pi\delta(z_1-z_2) \ . \tag{A.27}$$

Equation (A.27) has to be solved in the five regions of our model. The two cases to be considered are when the fixed particle at z_2 is in region I or III. The region V case is found by the symmetry in the $x-y$ plane.

Case 1: $-\infty < z_2 \leq -[L+D]$

The differential equation for $\tilde{\Phi}^E(z_1,z_2,\mathbf{k})$, Eq. (A.27), is given by

$$\left[\frac{d^2}{dz_1^2}-k^2\right]\tilde{\Phi}^E(z_1,z_2,\mathbf{k}) = \begin{cases} -4\pi\delta(z_1-z_2) & z_1 \leq -[L+D] \\ 0 & -[L+D] \leq z_1 \leq -D \\ 0 & -D \leq z_1 \leq D \\ 0 & D \leq z_1 \leq [L+D] \\ 0 & [L+D] \leq z_1 \end{cases} \ . \tag{A.28}$$

The form of the solution to Eq. (A.28) is

$$\tilde{\Phi}^E(z_1,z_2,\mathbf{k}) = \begin{cases} \frac{2\pi}{k}e^{-k|z_1-z_2|} + B_I e^{kz_1} & z_1 \le -[L+D] \\ A_{II}e^{-kz_1} + B_{II}e^{kz_1} & -[L+D] \le z_1 \le -D \\ A_{III}e^{-kz_1} + B_{III}e^{kz_1} & -D \le z_1 \le D \\ A_{IV}e^{-kz_1} + B_{IV}e^{kz_1} & D \le z_1 \le [L+D] \\ A_V e^{-kz_1} & [L+D] \le z_1 \end{cases} . \quad \text{(A.29)}$$

Application of the boundary conditions given above, at the membrane walls, yields

$$B_I = \frac{2\pi}{k}e^{kz_2}\frac{\Delta}{R(k)}\Big[[1-e^{-2kL}][1-\Delta^2 e^{2kL}]e^{-2kD} - [1-\Delta^2 e^{-2kL}][1-e^{2kL}]e^{2kD}\Big] , \quad \text{(A.30)}$$

$$A_{II} = \frac{4\pi}{k}e^{kz_2}\frac{1}{[1+\epsilon_2]R(k)}\Big[[1-\Delta^2 e^{2kL}] - \Delta^2[1-e^{2kL}]e^{-4kD}\Big] , \quad \text{(A.31)}$$

$$B_{II} = \frac{4\pi}{k}e^{kz_2}\frac{\Delta}{[1+\epsilon_2]R(k)}\Big[[1-e^{2kL}]e^{-2kD} - [1-\Delta^2 e^{-2kL}]e^{2kD}\Big] , \quad \text{(A.32)}$$

$$A_{III} = \frac{2\pi}{k}e^{kz_2}\frac{1}{R(k)}\Big[[1-\Delta^2][1-\Delta^2 e^{-2kL}]\Big] , \quad \text{(A.33)}$$

$$B_{III} = \frac{2\pi}{k}e^{kz_2}\frac{\Delta}{R(k)}\Big[[1-\Delta^2][1-e^{-2kL}]e^{-2kD}\Big] , \quad \text{(A.34)}$$

$$A_{IV} = \frac{4\pi}{k}e^{kz_2}\frac{1}{[1+\epsilon_2]R(k)}[1-\Delta^2] , \quad \text{(A.35)}$$

$$B_{IV} = -\frac{4\pi}{k}e^{kz_2}\frac{\Delta}{[1+\epsilon_2]R(k)}\Big[[1-\Delta^2]e^{-2k[L+D]}\Big] , \quad \text{(A.36)}$$

$$A_V = \frac{4\pi}{k}e^{kz_2}\frac{1}{[1+\epsilon_2]R(k)}[1-\Delta][1-\Delta^2] , \quad \text{(A.37)}$$

where

$$R(k) = [1-\Delta^2 e^{-2kL}]^2 - \Delta^2[1-e^{-2kL}]^2 e^{-4kD} , \quad \text{(A.38)}$$

$$\Delta = \frac{1-\epsilon_2}{1+\epsilon_2} . \quad \text{(A.39)}$$

Case 2: $-D \leq z_2 \leq D$

The differential equation for $\tilde{\Phi}^E(z_1, z_2, \mathbf{k})$, Eq. (A.27), is given by

$$\left[\frac{d^2}{dz_1^2} - k^2\right]\tilde{\Phi}^E(z_1, z_2, \mathbf{k}) = \begin{cases} 0 & z_1 \leq -[L+D] \\ 0 & -[L+D] \leq z_1 \leq -D \\ -4\pi\delta(z_1 - z_2) & -D \leq z_1 \leq D \\ 0 & D \leq z_1 \leq [L+D] \\ 0 & [L+D] \leq z_1 \end{cases} . \quad \text{(A.40)}$$

The form of the solution to Eq. (A.40) is

$$\tilde{\Phi}^E(z_1, z_2, \mathbf{k}) = \begin{cases} B_I e^{kz_1} & z_1 \leq -[L+D] \\ A_{II}e^{-kz_1} + B_{II}e^{kz_1} & -[L+D] \leq z_1 \leq -D \\ \frac{2\pi}{k}e^{-k|z_1 - z_2|} & \\ \quad + A_{III}e^{-kz_1} + B_{III}e^{kz_1} & -D \leq z_1 \leq D \\ A_{IV}e^{-kz_1} + B_{IV}e^{kz_1} & D \leq z_1 \leq [L+D] \\ A_V e^{-kz_1} & [L+D] \leq z_1 \end{cases} . \quad \text{(A.41)}$$

Application of the boundary conditions given above, at the membrane walls, yields

$$B_I = -\frac{2\pi}{k}\frac{e^{2k[L+D]}}{\Delta R(k)}\Big[e^{kz_2}[R(k)-1] + e^{-kz_2}\Delta[1 - e^{-2kL} - R(k)]e^{-2kD}\Big] , \quad \text{(A.42)}$$

$$A_{II} = \frac{4\pi}{k}\frac{1}{[1+\epsilon_2][1-\Delta^2]R(k)}\Big[e^{kz_2}[R(k)-1] + e^{-kz_2}\Delta[1 - e^{-2kL} - R(k)]e^{-2kD}\Big] , \quad \text{(A.43)}$$

$$B_{II} = -\frac{4\pi}{k}\frac{e^{2k[L+D]}}{[1+\epsilon_2]\Delta[1-\Delta^2]R(k)}\Big[e^{kz_2}[R(k)-1] + e^{-kz_2}\Delta[1 - e^{-2kL} - R(k)]e^{-2kD}\Big] , \quad \text{(A.44)}$$

$$A_{III} = \frac{2\pi}{k}e^{kz_2}\frac{\Delta^2}{R(k)}\Big[[1 - \Delta^2 e^{-2kL}]e^{-2kL} + [1 - e^{-2kL}]^2 e^{-4kD}\Big] + \frac{2\pi}{k}e^{-kz_2}\frac{1}{R(k)}\Big[\Delta[1 - e^{-2kL}][1 - \Delta^2 e^{-2kL}]e^{-2kD}\Big] , \quad \text{(A.45)}$$

$$B_{III} = \frac{2\pi}{k}\frac{\Delta[1 - e^{-2kL}]e^{-2kD}}{R(k)}\Big[e^{kz_2} + e^{-kz_2}\Delta[1 - e^{-2kL}]e^{-2kD}\Big] , \quad \text{(A.46)}$$

$$A_{IV} = \frac{4\pi}{k}\frac{1}{[1+\epsilon_2]R(k)}\Big[e^{kz_2} + e^{-kz_2}\Delta[1 - e^{-2kL}]e^{-2kD}\Big] , \quad \text{(A.47)}$$

$$B_{IV} = - \frac{4\pi}{k} \frac{\Delta e^{-2k[L+D]}}{[1+\epsilon_2]R(k)} \left[e^{kz_2} + e^{-kz_2} \Delta [1 - e^{-2kL}] e^{-2kD} \right] , \tag{A.48}$$

$$A_V = \frac{4\pi}{k} \frac{[1-\Delta]}{[1+\epsilon_2]R(k)} \left[e^{kz_2} + e^{-kz_2} \Delta [1 - e^{-2kL}] e^{-2kD} \right] . \tag{A.49}$$

Thus the ion-ion image potential is given by the difference between the total electrostatic contribution calculated above using the transverse Hankel transform method and the coulombic part of the two potential. The other image potentials are calculated by applying the E_1 operator an appropriate amount of times.

Note in the limit $\sigma_1 \to 0$ and $L \to \infty$, these results reduce to those of Kjellander and Marcelja [58].

Appendix B

One Membrane Point Model Neuron

In this appendix we construct solutions for the differential equations associated with the mean electrostatic potential and mean electrostatic fluctuation potential for the one membrane model in the limit of point molecules.

B.1 Mean electrostatic potential

The solution to the differential equation for the mean electrostatic potential, Eq. (2.89), in the various regions, is given by

$$\psi(z_1) = \begin{cases} A_E \exp[\kappa_E(z_1 + L)] + \psi_E^B & -\infty < z_1 \leq -L \\ A_M z_1 + B_M & -L \leq z_1 \leq L \\ A_I \exp[-\kappa_I(z_1 - L)] + \psi_I^B & L \leq z_1 < \infty \end{cases} . \tag{B.1}$$

The constants A_E, A_M, B_M, A_I are determined from the boundary conditions at each of the membrane walls. Thus

$$A_E + \psi_E^B = -A_M L + B_M \ , \tag{B.2}$$

$$A_M L + B_M = A_I^i L + B_I^i \ , \tag{B.3}$$

$$-\epsilon_M A_M + \epsilon_E \kappa_E A_E = 4\pi\sigma_E \ , \tag{B.4}$$

$$\epsilon_I \kappa_I A_I + \epsilon_M A_M = 4\pi\sigma_I \ . \tag{B.5}$$

These equations are solved for the constants to yield

$$A_E = \frac{4\pi\epsilon_M(\sigma_E + \sigma_I) + 4\pi\sigma_E\epsilon_I\kappa_I 2L + \epsilon_M\epsilon_I\kappa_I\Delta\psi^B}{\epsilon_M(\epsilon_E\kappa_E + \epsilon_I\kappa_I) + \epsilon_E\kappa_E\epsilon_I\kappa_I 2L} \ , \tag{B.6}$$

$$A_M = -\frac{4\pi\sigma_E\epsilon_I\kappa_I - 4\pi\sigma_I\epsilon_E\kappa_E - \epsilon_E\kappa_E\epsilon_I\kappa_I\Delta\psi^B}{\epsilon_M(\epsilon_E\kappa_E + \epsilon_I\kappa_I) + \epsilon_E\kappa_E\epsilon_I\kappa_I 2L}\ , \tag{B.7}$$

$$B_M = \psi_I^B - A_M L + A_I\ , \tag{B.8}$$

$$A_I = \frac{4\pi\epsilon_M(\sigma_E + \sigma_I) + 4\pi\sigma_I\epsilon_E\kappa_E 2L - \epsilon_M\epsilon_E\kappa_E\Delta\psi^B}{\epsilon_M(\epsilon_E\kappa_E + \epsilon_I\kappa_I) + \epsilon_E\kappa_E\epsilon_I\kappa_I 2L}\ . \tag{B.9}$$

See Figure B.1. Comparison of this figure with that of the mean electrostatic potential for the two membrane point model system, Figure 3.1, shows negligible difference in the region near the membrane walls. Thus the presence of the second membrane at a distance of $2D$ has negligible effect.

B.2 Transverse Hankel transform mean electrostatic fluctuation potential

The differential equations for the transverse Hankel transform mean electrostatic fluctuation potential for the case of the source point in the extracellular region are

$$\left[\frac{d^2}{dz_1^2} - k^2 - \kappa_E^2 + \kappa_E^2\zeta_E\frac{\psi_E^B}{A_E} + \kappa_E^2\zeta_E\exp[\kappa_E(z_1+L)]\right]\tilde{\psi}_E(z_1,z_2,\mathbf{k}) = -\frac{4\pi}{\epsilon_E}\delta(z_1-z_2)\ , \tag{B.10}$$

$$\left[\frac{d^2}{dz_1^2} - k^2\right]\tilde{\psi}_M(z_1,z_2,\mathbf{k}) = 0\ , \tag{B.11}$$

$$\left[\frac{d^2}{dz_1^2} - k^2 - \kappa_I^2 + \kappa_I^2\zeta_I\frac{\psi_I^B}{A_I} + \kappa_I^2\zeta_I\exp[-\kappa_I(z_1-L)]\right]\tilde{\psi}_I(z_1,z_2,\mathbf{k}) = 0\ . \tag{B.12}$$

The solutions to the homogeneous differential equations are

$$\tilde{\psi}_E = \begin{cases} C_E J_{2\nu_E}\left[2\zeta_E^{\frac{1}{2}}\exp[\frac{\kappa_E(z_1+L)}{2}]\right] & \\ +D_E Y_{2\nu_E}\left[2\zeta_E^{\frac{1}{2}}\exp[\frac{\kappa_E(z_1+L)}{2}]\right] & \zeta_E > 0 \\ C_E I_{2\nu_E}\left[2\mid\zeta_E\mid^{\frac{1}{2}}\exp[\frac{\kappa_E(z_1+L)}{2}]\right] & \\ +D_E K_{2\nu_E}\left[2\mid\zeta_E\mid^{\frac{1}{2}}\exp[\frac{\kappa_E(z_1+L)}{2}]\right] & \zeta_E < 0 \end{cases}\ ,$$

$$\tilde{\psi}_M = C_M\exp[kz_1] + D_M\exp[-kz_1]\ ,$$

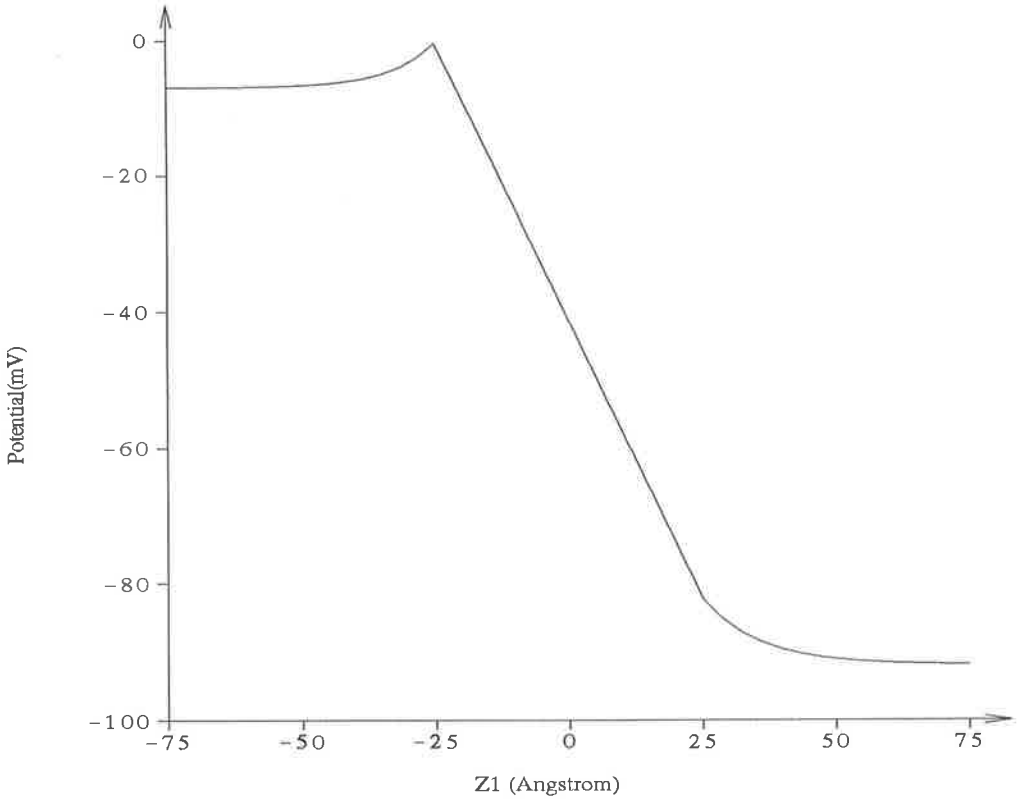

Figure B.1: Mean electrostatic potential for a one membrane point model system.

Quantity	Value
κ_I	$0.09425\mathring{A}^{-1}$
$\frac{\epsilon_I}{4\pi\epsilon_0}$	70.718
ζ_I	0.34729
$\nu_I \mid_{k=0}$	2.06522
κ_E	$0.11995\mathring{A}^{-1}$
$\frac{\epsilon_E}{4\pi\epsilon_0}$	70.718
ζ_E	4.29949×10^{-2}
$\nu_E \mid_{k=0}$	1.02275

Table B.1: Table of κ, ϵ, ζ and ν values in the extracellular and intracellular fluid regions for the one membrane point model.

$$\tilde{\psi}_I = \begin{cases} C_I J_{2\nu_I}\left[2\zeta_I^{\frac{1}{2}} \exp[-\frac{\kappa_I(z_1-L)}{2}]\right] & \\ +D_I Y_{2\nu_I}\left[2\zeta_I^{\frac{1}{2}} \exp[-\frac{\kappa_I(z_1-L)}{2}]\right] & \zeta_I > 0 \\ & \\ C_I I_{2\nu_I}\left[2 \mid \zeta_I \mid^{\frac{1}{2}} \exp[-\frac{\kappa_I(z_1-L)}{2}]\right] & \\ +D_I K_{2\nu_I}\left[2 \mid \zeta_I \mid^{\frac{1}{2}} \exp[-\frac{\kappa_I(z_1-L)}{2}]\right] & \zeta_I < 0 \end{cases},$$

Application of the appropriate boundary conditions at the membrane walls located at $\pm L$, yields the solution for the transverse Hankel transform mean electrostatic fluctuation potential in region I for the following two cases.

B.2.1 $\zeta_E > 0$

$$\tilde{\psi}_E(z_1, z_2, \mathbf{k}) = - \frac{4\pi^2}{\epsilon_E \kappa_E}\left\{ Y_{2\nu_E}\left[2\zeta_E^{\frac{1}{2}} \exp[\frac{\kappa_E(z_> + L)}{2}]\right]\right.$$

$$
\begin{aligned}
&\times \quad J_{2\nu_E}\Big[2\zeta_E^{\frac{1}{2}}\exp[\frac{\kappa_E(z_< + L)}{2}]\Big] \\
&+ \quad \bar{\Delta}_1(2L,\zeta_E,\zeta_I)J_{2\nu_E}\Big[2\zeta_E^{\frac{1}{2}}\exp[\frac{\kappa_E(z_2 + L)}{2}]\Big] \\
&\times \quad J_{2\nu_E}\Big[2\zeta_E^{\frac{1}{2}}\exp[\frac{\kappa_E(z_1 + L)}{2}]\Big]\Big\}, \qquad \text{(B.13)}
\end{aligned}
$$

where

$$
\bar{\Delta}_1(2L,\zeta_E,\zeta_I) = -\Big[\frac{Y_{2\nu_E}[2\zeta_E^{\frac{1}{2}}]Z_{2\nu_I}(2L,\zeta_I) + \frac{\epsilon_E\kappa_E\zeta_E^{\frac{1}{2}}}{k\epsilon_M}Y'_{2\nu_E}[2\zeta_E^{\frac{1}{2}}]}{J_{2\nu_E}[2\zeta_E^{\frac{1}{2}}]Z_{2\nu_I}(2L,\zeta_I) + \frac{\epsilon_E\kappa_E\zeta_E^{\frac{1}{2}}}{k\epsilon_M}J'_{2\nu_E}[2\zeta_E^{\frac{1}{2}}]}\Big], \qquad \text{(B.14)}
$$

such that

$$
Z_{2\nu_I}(L,\zeta_I) = \begin{cases} \dfrac{J_{2\nu_I}[2\zeta_I^{\frac{1}{2}}]\sinh[kL] + \frac{\epsilon_I\kappa_I\zeta_I^{\frac{1}{2}}}{k\epsilon_M}J'_{2\nu_I}[2\zeta_I^{\frac{1}{2}}]\cosh[kL]}{J_{2\nu_I}[2\zeta_I^{\frac{1}{2}}]\cosh[kL] + \frac{\epsilon_I\kappa_I\zeta_I^{\frac{1}{2}}}{k\epsilon_M}J'_{2\nu_I}[2\zeta_I^{\frac{1}{2}}]\sinh[kL]} & \zeta_I > 0 \\ \dfrac{I_{2\nu_I}[2|\zeta_I|^{\frac{1}{2}}]\sinh[kL] + \frac{\epsilon_I\kappa_I|\zeta_I|^{\frac{1}{2}}}{k\epsilon_M}I'_{2\nu_I}[2|\zeta_I|^{\frac{1}{2}}]\cosh[kL]}{I_{2\nu_I}[2|\zeta_I|^{\frac{1}{2}}]\cosh[kL] + \frac{\epsilon_I\kappa_I|\zeta_I|^{\frac{1}{2}}}{k\epsilon_M}I'_{2\nu_I}[2|\zeta_I|^{\frac{1}{2}}]\sinh[kL]} & \zeta_I < 0 \end{cases}. \qquad \text{(B.15)}
$$

B.2.2 $\zeta_E < 0$

$$
\begin{aligned}
\bar{\psi}_E(z_1,z_2,\mathbf{k}) = \quad & \frac{8\pi}{\epsilon_E\kappa_E}\Big\{K_{2\nu_E}\Big[2\mid\zeta_E\mid^{\frac{1}{2}}\exp[\frac{\kappa_E(z_> + L)}{2}]\Big] \\
&\times \quad I_{2\nu_E}\Big[2\mid\zeta_E\mid^{\frac{1}{2}}\exp[\frac{\kappa_E(z_< + L)}{2}]\Big] \\
&+ \quad \bar{\Delta}_1(2L,\zeta_E,\zeta_I)I_{2\nu_E}\Big[2\mid\zeta_E\mid^{\frac{1}{2}}\exp[\frac{\kappa_E(z_2 + L)}{2}]\Big] \\
&\times \quad I_{2\nu_E}\Big[2\mid\zeta_E\mid^{\frac{1}{2}}\exp[\frac{\kappa_E(z_1 + L)}{2}]\Big]\Big\}, \qquad \text{(B.16)}
\end{aligned}
$$

where

$$
\bar{\Delta}_1(2L,\zeta_E,\zeta_I) = -\Big[\frac{K_{2\nu_E}[2\mid\zeta_E\mid^{\frac{1}{2}}]Z_{2\nu_I}(2L,\zeta_I) + \frac{\epsilon_E\kappa_E|\zeta_E|^{\frac{1}{2}}}{k\epsilon_M}K'_{2\nu_E}[2\mid\zeta_E\mid^{\frac{1}{2}}]}{I_{2\nu_E}[2\mid\zeta_E\mid^{\frac{1}{2}}]Z_{2\nu_I}(2L,\zeta_I) + \frac{\epsilon_E\kappa_E|\zeta_E|^{\frac{1}{2}}}{k\epsilon_M}I'_{2\nu_E}[2\mid\zeta_E\mid^{\frac{1}{2}}]}\Big]. \qquad \text{(B.17)}
$$

B.2.3 Asymptotic transverse Hankel transform mean electrostatic fluctuation potential

If we assume that the ratios $\frac{2\zeta_I^{\frac{1}{2}}}{2\nu_I}\mid_{k=0}$, $\frac{2|\zeta_I|^{\frac{1}{2}}}{2\nu_I}\mid_{k=0}$, $\frac{2\zeta_E^{\frac{1}{2}}}{2\nu_E}\mid_{k=0}$ and $\frac{2|\zeta_E|^{\frac{1}{2}}}{2\nu_E}\mid_{k=0} < 1$, we can use the asymptotic forms in Appendix D to show

$$\bar{\Delta}_1 \rightarrow \begin{cases} -\frac{Y_{2\nu_E}[2\zeta_E^{\frac{1}{2}}]}{J_{2\nu_E}[2\zeta_E^{\frac{1}{2}}]}\left[\frac{Z_{2\nu_I}(2L,\zeta_I)-\frac{\epsilon_E\kappa_E\nu_E}{k\epsilon_M}\sqrt{1-\left[\frac{q_E(-L)}{\nu_E}\right]^2}\,\delta^+_{2\nu_E}(-L)}{Z_{2\nu_I}(2L,\zeta_I)+\frac{\epsilon_E\kappa_E\nu_E}{k\epsilon_M}\sqrt{1-\left[\frac{q_E(-L)}{\nu_E}\right]^2}\,\delta^-_{2\nu_E}(-L)}\right] & \zeta_E > 0 \\ -\frac{K_{2\nu_E}[2|\zeta_E|^{\frac{1}{2}}]}{I_{2\nu_E}[2|\zeta_E|^{\frac{1}{2}}]}\left[\frac{Z_{2\nu_I}(2L,\zeta_I)-\frac{\epsilon_E\kappa_E\nu_E}{k\epsilon_M}\sqrt{1+\left[\frac{q_E(-L)}{\nu_E}\right]^2}\,\delta^-_{2\nu_E}(-L)}{Z_{2\nu_I}(2L,\zeta_I)+\frac{\epsilon_E\kappa_E\nu_E}{k\epsilon_M}\sqrt{1+\left[\frac{q_E(-L)}{\nu_E}\right]^2}\,\delta^+_{2\nu_E}(-L)}\right] & \zeta_E < 0 \end{cases} \tag{B.18}$$

where

$$\begin{aligned} \delta^+_{2\nu_E}(z_1) &= 1+\frac{1}{2}\left[\frac{q_E^2(z_1)}{[2\nu_E]^3}\right]+O((2\nu_E)^{-4}) \ , \\ \delta^-_{2\nu_E}(z_1) &= 1-\frac{1}{2}\left[\frac{q_E^2(z_1)}{[2\nu_E]^3}\right]+O((2\nu_E)^{-4}) \ , \end{aligned}$$

such that

$$q_E(z_1) = \begin{cases} 2\zeta_E^{\frac{1}{2}}\exp\left[\frac{\kappa_E(z_1+L)}{2}\right] & \zeta_E > 0 \\ 2\mid\zeta_E\mid^{\frac{1}{2}}\exp\left[\frac{\kappa_E(z_1+L)}{2}\right] & \zeta_E < 0 \end{cases} \ ,$$

$$Z_{2\nu_I}(L,\zeta_I) \rightarrow \begin{cases} \frac{\sinh[kL]+\frac{\epsilon_I\kappa_I\nu_I}{k\epsilon_M}\sqrt{1-\left[\frac{q_I(L)}{\nu_I}\right]^2}\cosh[kL]\delta^-_{2\nu_I}(L)}{\cosh[kL]+\frac{\epsilon_I\kappa_I\nu_I}{k\epsilon_M}\sqrt{1-\left[\frac{q_I(L)}{\nu_I}\right]^2}\sinh[kL]\delta^-_{2\nu_I}(L)} & \zeta_I > 0 \\ \frac{\sinh[kL]+\frac{\epsilon_I\kappa_I\nu_I}{k\epsilon_M}\sqrt{1+\left[\frac{q_I(L)}{\nu_I}\right]^2}\cosh[kL]\delta^+_{2\nu_I}(L)}{\cosh[kL]+\frac{\epsilon_I\kappa_I\nu_I}{k\epsilon_M}\sqrt{1+\left[\frac{q_I(L)}{\nu_I}\right]^2}\sinh[kL]\delta^+_{2\nu_I}(L)} & \zeta_I < 0 \end{cases} \ , \tag{B.19}$$

$$\begin{aligned} \delta^+_{2\nu_I}(z_1) &= 1+\frac{1}{2}\left[\frac{q_I^2(z_1)}{[2\nu_I]^3}\right]+O((2\nu_I)^{-4}) \ , \\ \delta^-_{2\nu_I}(z_1) &= 1-\frac{1}{2}\left[\frac{q_I^2(z_1)}{[2\nu_I]^3}\right]+O((2\nu_I)^{-4}) \ , \end{aligned}$$

such that

$$q_I(z_1) = \begin{cases} 2\zeta_I^{\frac{1}{2}} \exp\left[-\frac{\kappa_I(z_1-L)}{2}\right] & \zeta_I > 0 \\ 2 \mid \zeta_I \mid^{\frac{1}{2}} \exp\left[-\frac{\kappa_E(z_1-L)}{2}\right] & \zeta_I < 0 \end{cases} ,$$

Thus the solution for the transverse Hankel transform mean electrostatic fluctuation potential in region I for large k can be simplified to

$$\begin{aligned} \tilde{\psi}_E(z_1, z_2, \mathbf{k}) = & \frac{2\pi}{\epsilon_E \kappa_E \nu_E} \left[\frac{1}{1-[\frac{q_E(z_1)}{2\nu_E}]^2}\right]^{\frac{1}{4}} \left[\frac{1}{1-[\frac{q_E(z_1)}{2\nu_E}]^2}\right]^{\frac{1}{4}} \\ & \times \left\{\gamma_{2\nu_E}(z_<, z_>) \exp\left[2\nu_E \eta_{2\nu_E}(z_<, z_>)\right]\right. \\ & - \lambda_{2\nu_E}(z_1, z_2)\left[\frac{Z_{2\nu_I}(2L, \zeta_I) - \frac{\epsilon_E \kappa_E \nu_E}{k\epsilon_M}\sqrt{1-\left[\frac{q_E(-L)}{\nu_E}\right]^2}\,\delta^+_{2\nu_E}(-L)}{Z_{2\nu_I}(2L, \zeta_I) + \frac{\epsilon_E \kappa_E \nu_E}{k\epsilon_M}\sqrt{1-\left[\frac{q_E(-L)}{\nu_E}\right]^2}\,\delta^-_{2\nu_E}(-L)}\right] \\ & \times \left.\exp\left[2\nu_E[\eta_{2\nu_E}(-L, z_1) + \eta_{2\nu_E}(-L, z_2)]\right]\right\} \quad \zeta_E > 0 , \end{aligned} \tag{B.20}$$

and

$$\begin{aligned} \tilde{\psi}_E(z_1, z_2, \mathbf{k}) = & \frac{2\pi}{\epsilon_E \kappa_E \nu_E} \left[\frac{1}{1+[\frac{q_E(z_1)}{2\nu_E}]^2}\right]^{\frac{1}{4}} \left[\frac{1}{1+[\frac{q_E(z_1)}{2\nu_E}]^2}\right]^{\frac{1}{4}} \\ & \times \left\{\gamma_{2\nu_E}(z_<, z_>) \exp\left[2\nu_E \eta_{2\nu_E}(z_<, z_>)\right]\right. \\ & - \lambda_{2\nu_E}(z_1, z_2)\left[\frac{Z_{2\nu_I}(2L, \zeta_I) - \frac{\epsilon_E \kappa_E \nu_E}{k\epsilon_M}\sqrt{1+\left[\frac{q_E(-L)}{\nu_E}\right]^2}\,\delta^-_{2\nu_E}(-L)}{Z_{2\nu_I}(2L, \zeta_I) + \frac{\epsilon_E \kappa_E \nu_E}{k\epsilon_M}\sqrt{1+\left[\frac{q_E(-L)}{\nu_E}\right]^2}\,\delta^+_{2\nu_E}(-L)}\right] \\ & \times \left.\exp\left[2\nu_E[\eta_{2\nu_E}(-L, z_1) + \eta_{2\nu_E}(-L, z_2)]\right]\right\} \quad \zeta_E < 0 , \end{aligned} \tag{B.21}$$

where

$$\eta_{2\nu_E}(z_1, z_2) = \begin{cases} -\frac{\kappa_E(z_1-z_2)}{2} - \frac{1}{[2\nu_E]^2}\left[\frac{q_E^2(z_1)-q_E^2(z_2)}{4}\right] + O((2\nu_E)^{-4}) & \zeta_E > 0 \\ -\frac{\kappa_E(z_1-z_2)}{2} + \frac{1}{[2\nu_E]^3}\left[\frac{q_E^2(z_1)-q_E^2(z_2)}{4}\right] & \zeta_E < 0 \end{cases} ,$$

$$\gamma_{2\nu_E}(z_1, z_2) = \begin{cases} 1 + \frac{1}{[2\nu_E]^3}\left[\frac{q_E^2(z_1)-q_E^2(z_2)}{4}\right] + O((2\nu_E)^{-4}) & \zeta_E > 0 \\ 1 - \frac{1}{[2\nu_E]^3}\left[\frac{q_E^2(z_1)-q_E^2(z_2)}{4}\right] + O((2\nu_E)^{-4}) & \zeta_E < 0 \end{cases} ,$$

$$\lambda_{2\nu_E}(z_1,z_2) = \begin{cases} 1+\frac{1}{[2\nu_E]^3}\left[\frac{2q_E^2(-L)-q_E^2(z_1)-q_E^2(z_2)}{4}\right]+O((2\nu_E)^{-4}) & \zeta_E>0 \\ 1-\frac{1}{[2\nu_E]^3}\left[\frac{2q_E^2(-L)-q_E^2(z_1)-q_E^2(z_2)}{4}\right]+O((2\nu_E)^{-4}) & \zeta_E<0 \end{cases} .$$

A numerical solution of the differential equations for the transverse Hankel transform mean electrostatic fluctuation potential by a shooting method [114] is used to test the validity of the asymptotic solution. The numerical and asymptotic solution for the transverse Hankel transform mean electrostatic fluctuation potential show excellent agreement for the two cases when the source point is in the extracellular or intracellular fluid regions.

For the extracellular case see Figures B.2, B.3, B.4, and B.5. As the normal distance from the membrane wall increases, the plots tend to a constant value determined by the Debye-Huckel type term in the solution i.e.

$$\tilde{\psi}_E(z_1,z_2,\mathbf{k}) \to \begin{cases} \frac{2\pi}{\epsilon_E\kappa_E\nu_E}\left[\frac{1}{1-\left[\frac{q_E(z_1)}{2\nu_E}\right]^2}\right]^{\frac{1}{4}}\left[\frac{1}{1-\left[\frac{q_E(z_1)}{2\nu_E}\right]^2}\right]^{\frac{1}{4}} & \zeta_E>0 \\ \frac{2\pi}{\epsilon_E\kappa_E\nu_E}\left[\frac{1}{1+\left[\frac{q_E(z_1)}{2\nu_E}\right]^2}\right]^{\frac{1}{4}}\left[\frac{1}{1+\left[\frac{q_E(z_1)}{2\nu_E}\right]^2}\right]^{\frac{1}{4}} & \zeta_E<0 \end{cases} .$$

As the transform variable k increases this Debye-Huckel term (the field point and source point coinciding) has the form

$$\tilde{\psi}_E(z_1,z_2,\mathbf{k}) \to \frac{2\pi}{\epsilon_E k} .$$

This result is consistent with that of Carnie and Chan [41] for the constant density systems (both single and two plate) and the linearized GC density for the single plate. Again this is due to the large k behaviour being determined by the region near the source point.

For the intracellular case see Figures B.6, B.7, B.8 and B.9. As the normal distance from the membrane wall increases the plots tend to a constant value determined by the Debye-Huckel type term in the solution i.e.

$$\tilde{\psi}_I(z_1,z_2,\mathbf{k}) \to \begin{cases} \frac{2\pi}{\epsilon_I\kappa_I\nu_I}\left[\frac{1}{1-\left[\frac{q_I(z_1)}{2\nu_I}\right]^2}\right]^{\frac{1}{4}}\left[\frac{1}{1-\left[\frac{q_I(z_1)}{2\nu_I}\right]^2}\right]^{\frac{1}{4}} & \zeta_I>0 \\ \frac{2\pi}{\epsilon_I\kappa_I\nu_I}\left[\frac{1}{1+\left[\frac{q_I(z_1)}{2\nu_I}\right]^2}\right]^{\frac{1}{4}}\left[\frac{1}{1+\left[\frac{q_I(z_1)}{2\nu_I}\right]^2}\right]^{\frac{1}{4}} & \zeta_I<0 \end{cases} .$$

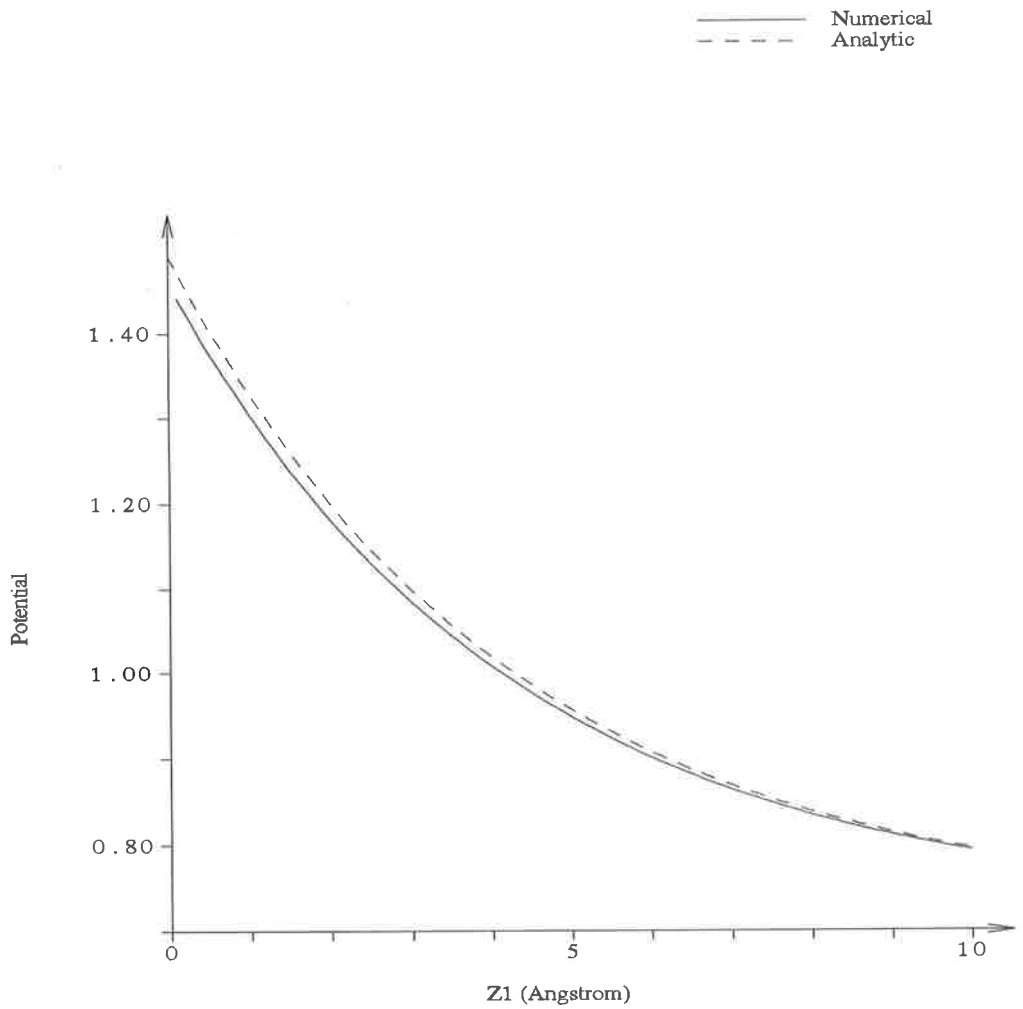

Figure B.2: Comparison of the numerical and asymptotic solution for the transverse Hankel transform mean electrostatic fluctuation potential at the source point in the extracellular fluid of a one membrane system vs distance from the membrane wall for k=0.001.

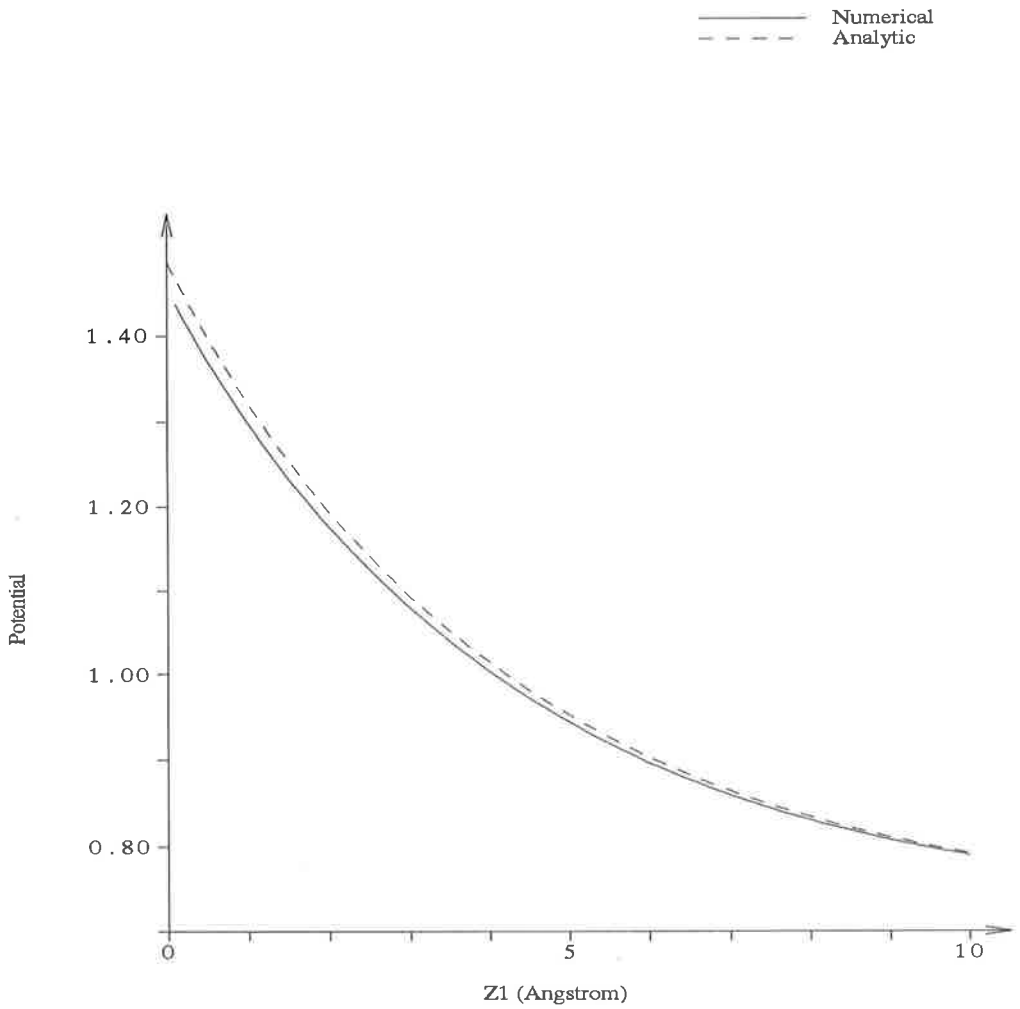

Figure B.3: Comparison of the numerical and asymptotic solution for the transverse Hankel transform mean electrostatic fluctuation potential at the source point in the extracellular fluid of a one membrane system vs distance from the membrane wall for k=0.01.

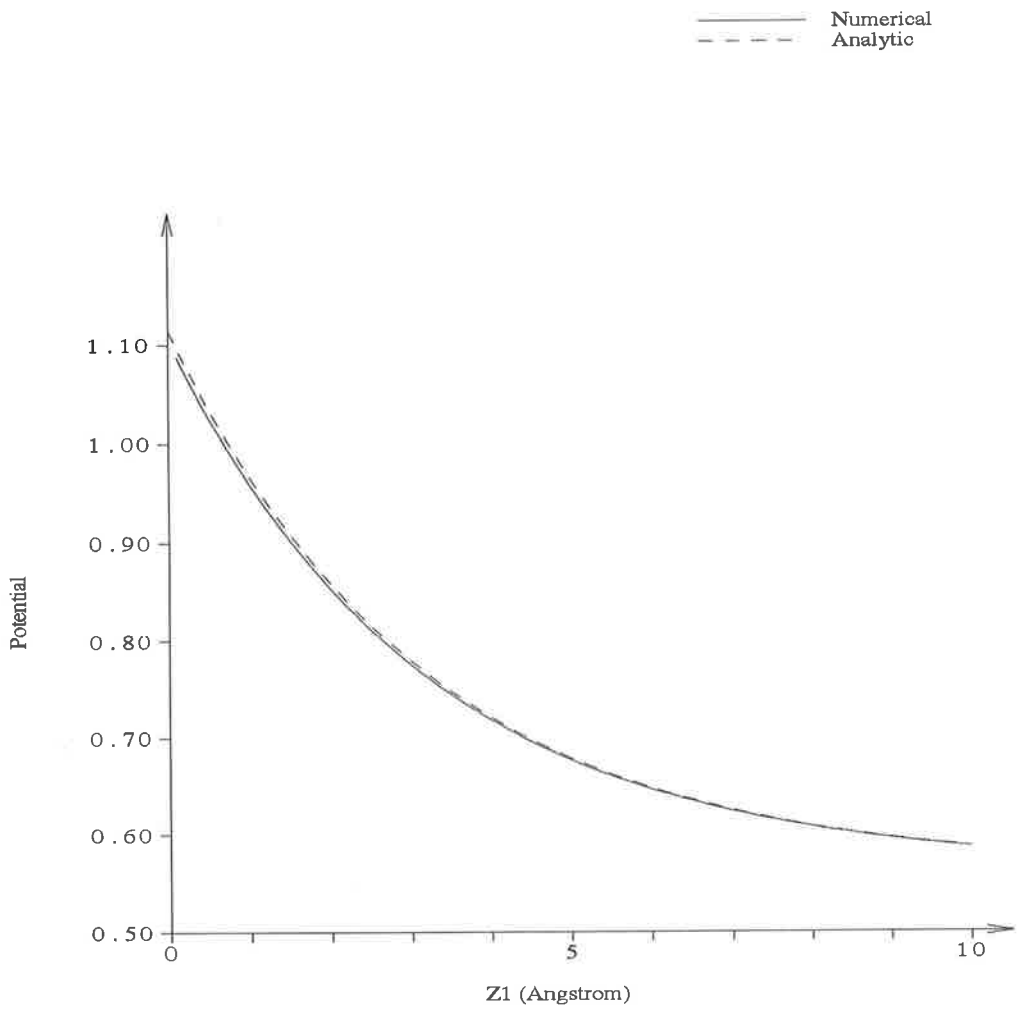

Figure B.4: Comparison of the numerical and asymptotic solution for the transverse Hankel transform mean electrostatic fluctuation potential at the source point in the extracellular fluid of a one membrane system vs distance from the membrane wall for k=0.1.

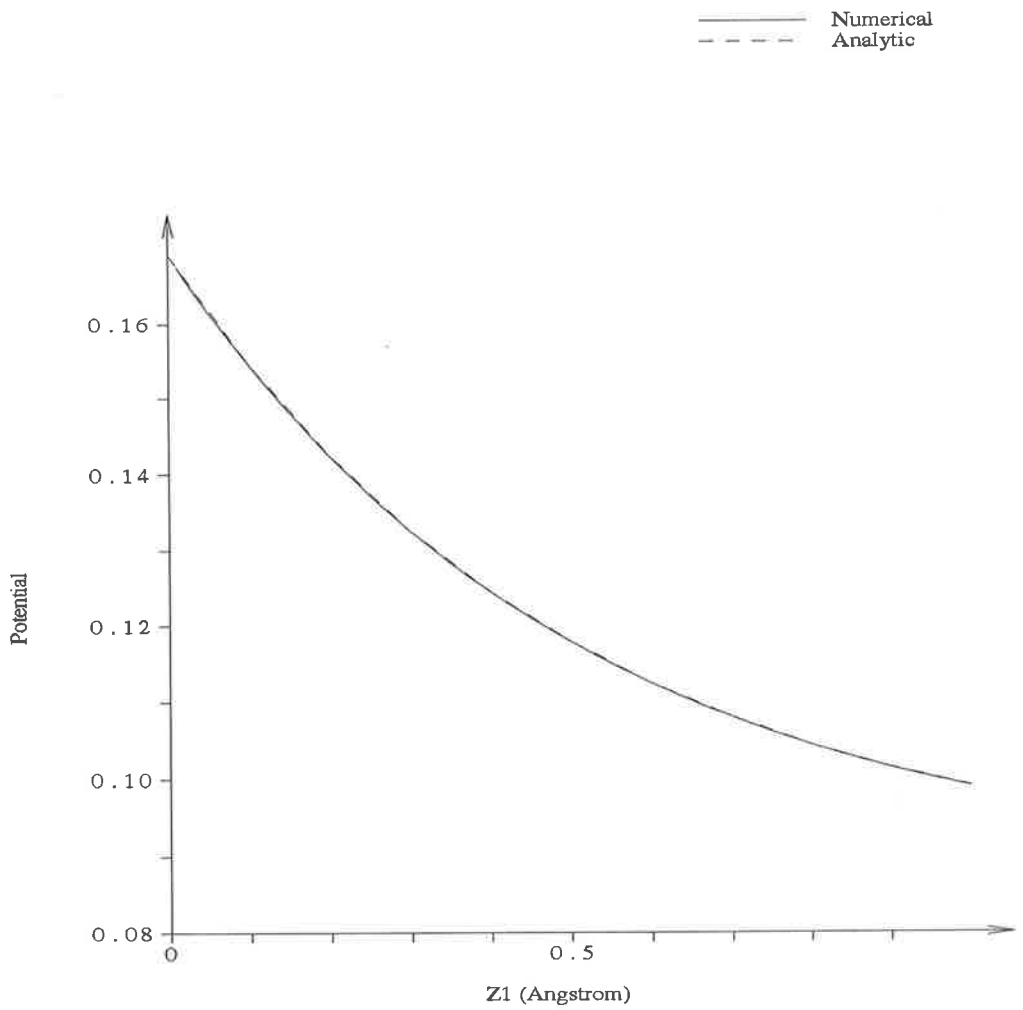

Figure B.5: Comparison of the numerical and asymptotic solution for the transverse Hankel transform mean electrostatic fluctuation potential at the source point in the extracellular fluid of a one membrane system vs distance from the membrane wall for k=1.

As the transform variable k increases this Debye-Huckel type term (the field point and source point coinciding) has the form

$$\bar{\psi}_I(z_1, z_2, \mathbf{k}) \rightarrow \frac{2\pi}{\epsilon_I k} \ .$$

This result is consistent with that of Carnie and Chan [41] for the constant density systems (both single and two plate) and the linearized GC density for the single plate. Again this is due to the large k behaviour being determined by the region near the source point.

B.2.4 Limiting forms of the transverse Hankel transform mean electrostatic fluctuation potential

The limiting form of the one membrane wall model [41] can be obtained from the one membrane model in the following manner. Consider the situation where there is an absence of solute and solvent molecules in the intracellular region. As a result

$$\begin{aligned} \zeta_I &\rightarrow 0 \ , \\ \kappa_I &\rightarrow 0 \ . \end{aligned}$$

Thus the quantity

$$Z_{2\nu_I}(2L, \zeta_I) \rightarrow 1 \ ,$$

and therefore

$$\bar{\Delta}_1(2L, \zeta_E, \zeta_I) = \begin{cases} -\left[\dfrac{Y_{2\nu_E}[2\zeta_E^{\frac{1}{2}}] + \frac{\epsilon_E \kappa_E \zeta_E^{\frac{1}{2}}}{k\epsilon_M} Y'_{2\nu_E}[2\zeta_E^{\frac{1}{2}}]}{J_{2\nu_E}[2\zeta_E^{\frac{1}{2}}] + \frac{\epsilon_E \kappa_E \zeta_E^{\frac{1}{2}}}{k\epsilon_M} J'_{2\nu_E}[2\zeta_E^{\frac{1}{2}}]}\right] & \zeta_E > 0 \\ -\left[\dfrac{K_{2\nu_E}[2|\zeta_E|^{\frac{1}{2}}] + \frac{\epsilon_E \kappa_E |\zeta_E|^{\frac{1}{2}}}{k\epsilon_M} K'_{2\nu_E}[2|\zeta_E|^{\frac{1}{2}}]}{I_{2\nu_E}[2|\zeta_E|^{\frac{1}{2}}] + \frac{\epsilon_E \kappa_E |\zeta_E|^{\frac{1}{2}}}{k\epsilon_M} I'_{2\nu_E}[2|\zeta_E|^{\frac{1}{2}}]}\right] & \zeta_E < 0 \end{cases} .$$

This limiting form is equivalent to the solution obtained by Carnie and Chan [41] for the one membrane wall model.

Other limiting cases of the system occur when the membrane is a perfect insulator (i.e. $\epsilon_M = 0$) or perfect conductor (i.e. $\epsilon_M = \infty$).

$$\bar{\Delta}_1 \rightarrow \begin{cases} -\dfrac{Y_{2\nu_E}[2\zeta_E^{\frac{1}{2}}]}{J_{2\nu_E}[2\zeta_E^{\frac{1}{2}}]} & \zeta_E > 0 \\ -\dfrac{K_{2\nu_E}[2|\zeta_E|^{\frac{1}{2}}]}{I_{2\nu_E}[2|\zeta_E|^{\frac{1}{2}}]} & \zeta_E < 0 \end{cases} \quad \text{as } \epsilon_M \rightarrow \infty \ ,$$

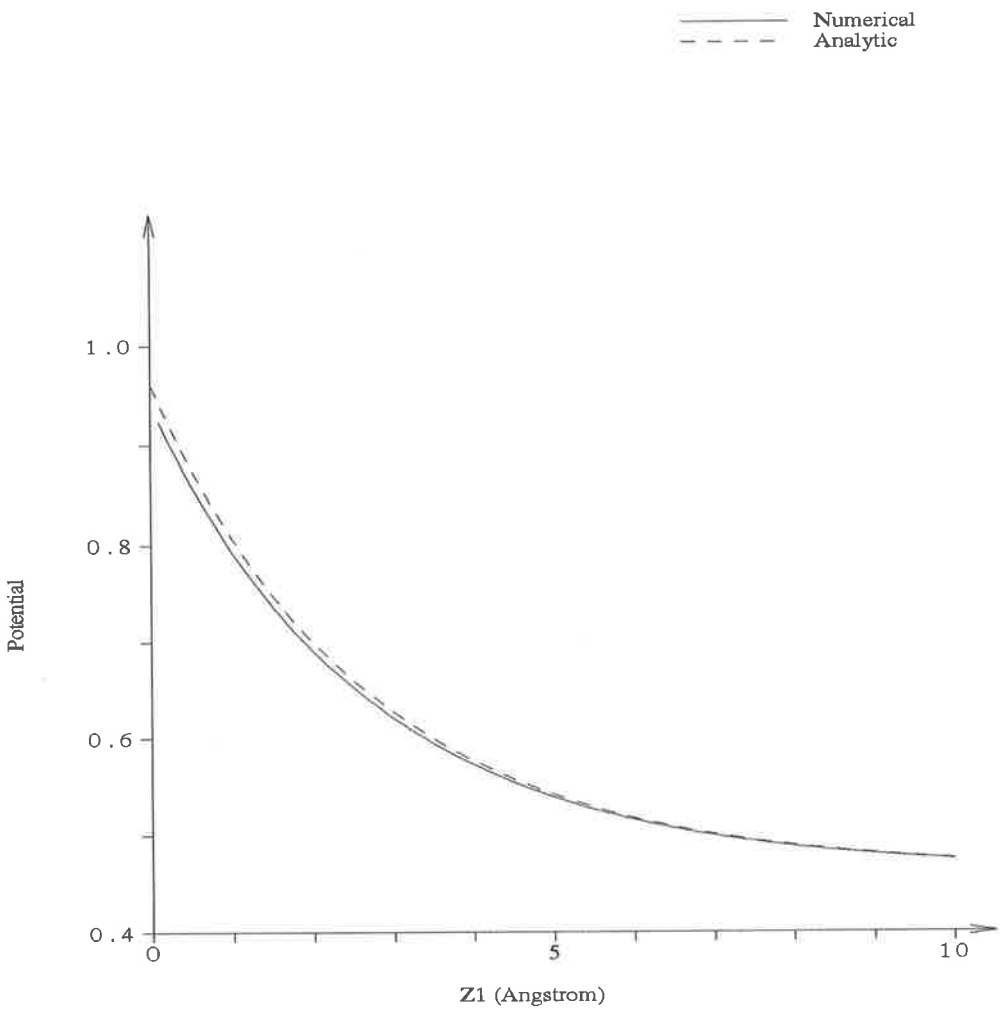

Figure B.6: Comparison of the numerical and asymptotic solution for the transverse Hankel transform mean electrostatic fluctuation potential at the source point in the intracellular fluid of a one membrane system vs distance from the membrane wall for k=0.001.

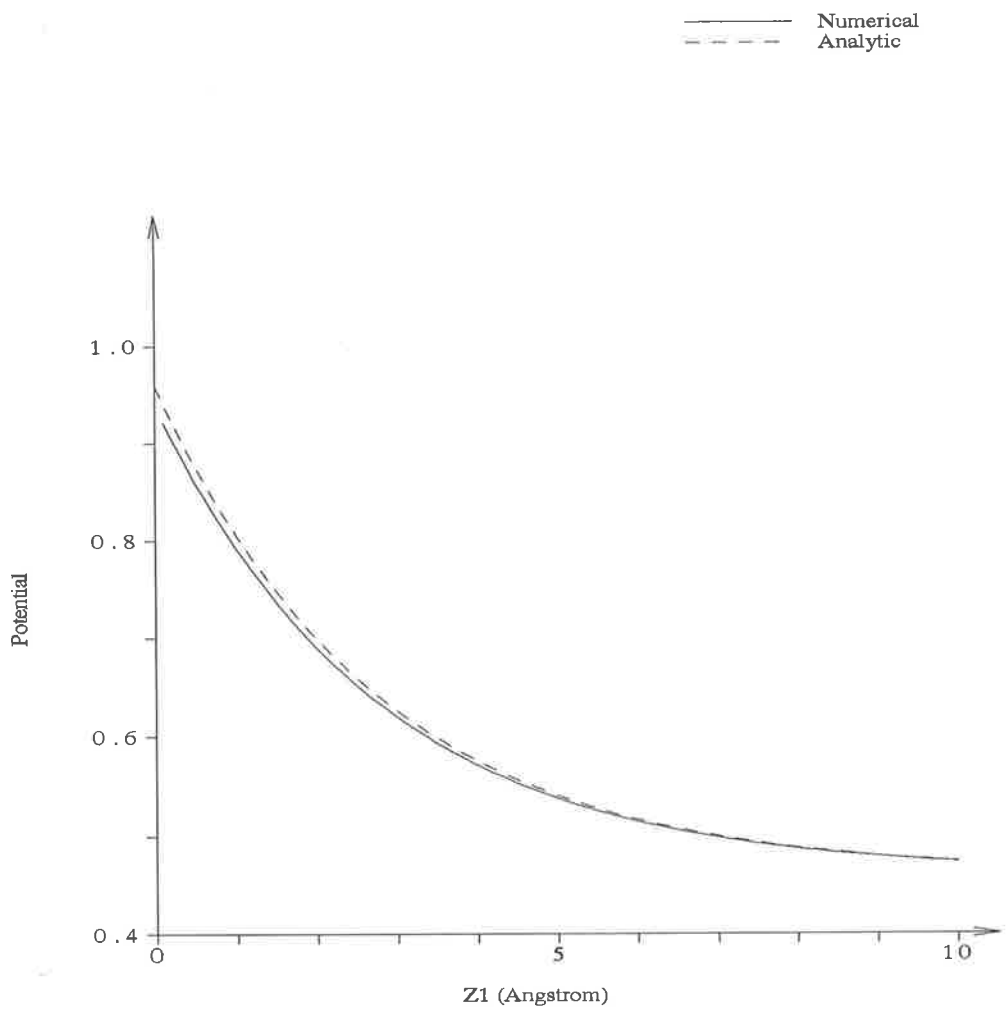

Figure B.7: Comparison of the numerical and asymptotic solution for the transverse Hankel transform mean electrostatic fluctuation potential at the source point in the intracellular fluid of a one membrane system vs distance from the membrane wall for k=0.01.

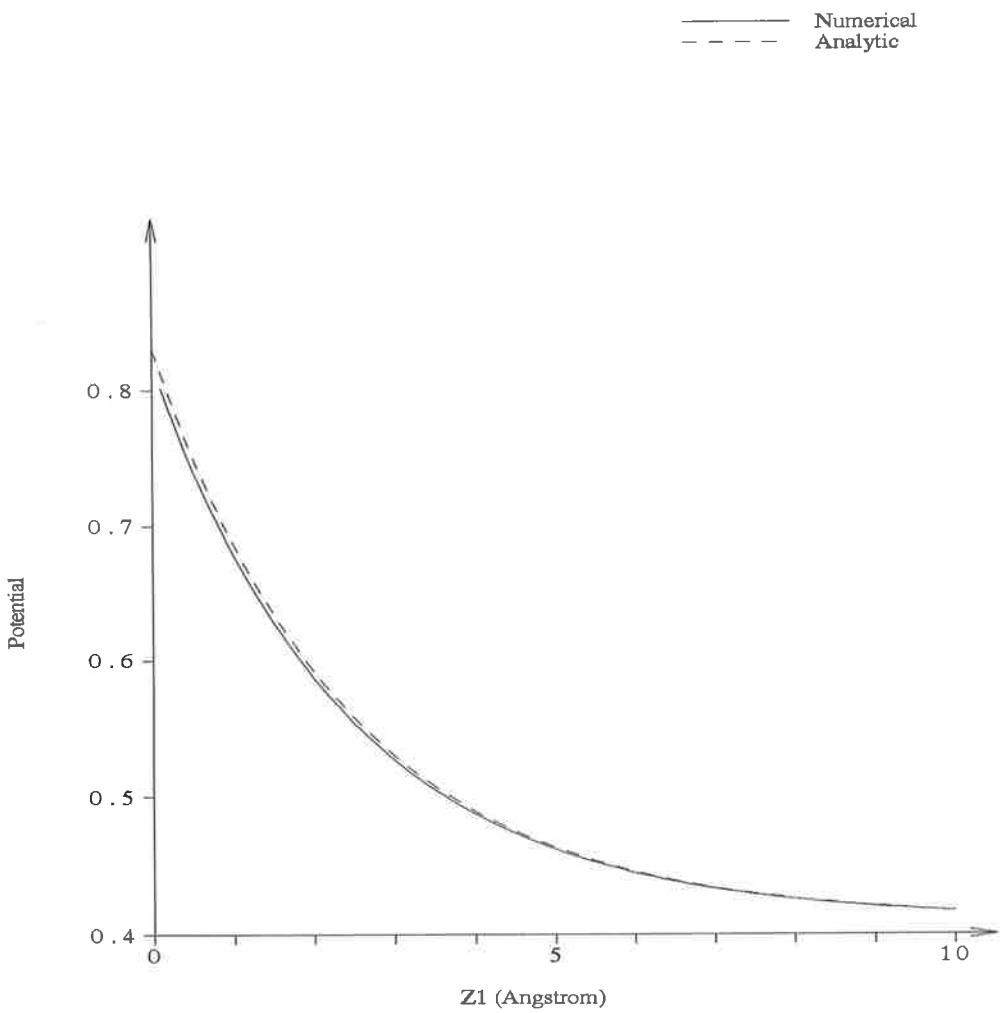

Figure B.8: Comparison of the numerical and asymptotic solution for the transverse Hankel transform mean electrostatic fluctuation potential at the source point in the intracellular fluid of a one membrane system vs distance from the membrane wall for k=0.1.

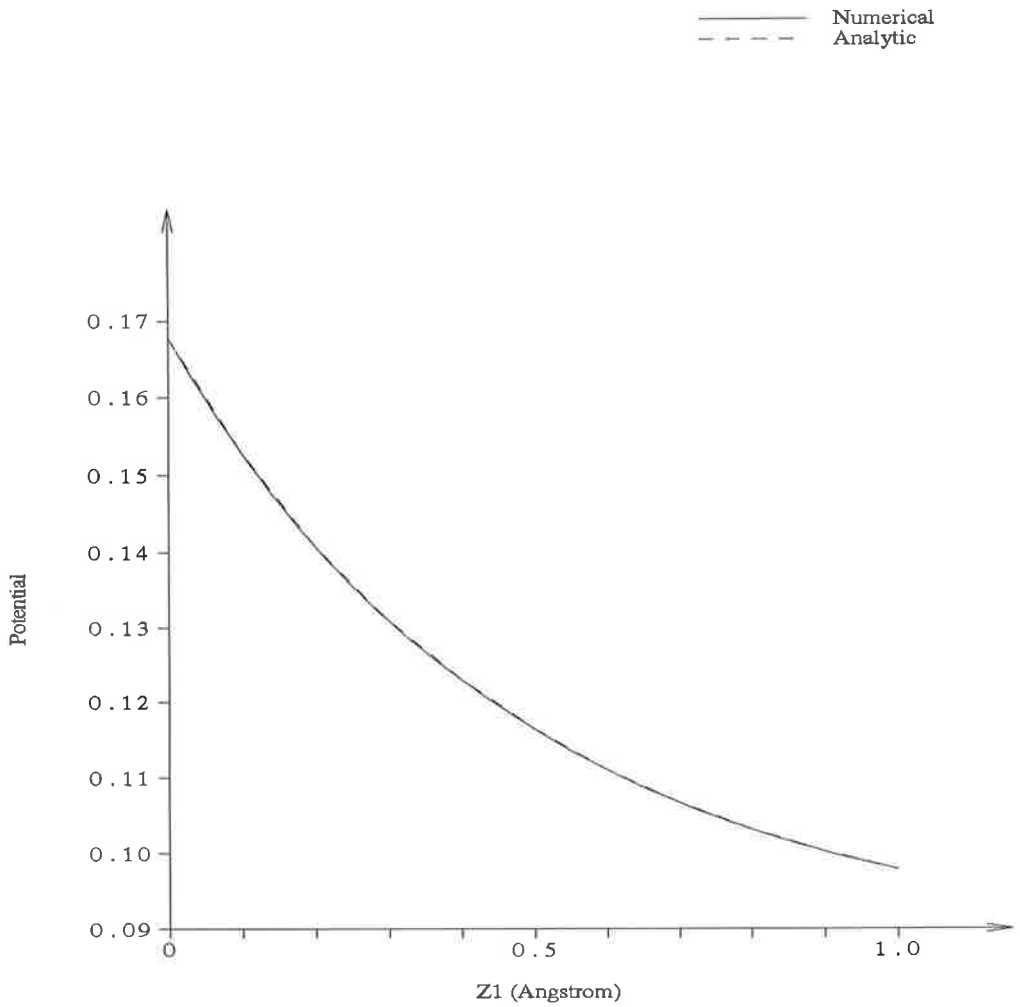

Figure B.9: Comparison of the numerical and asymptotic solution for the transverse Hankel transform mean electrostatic fluctuation potential at the source point in the intracellular fluid of a one membrane system vs distance from the membrane wall for k=1.

$$\bar{\Delta}_1 \;\rightarrow\; \begin{cases} \dfrac{Y'_{2\nu_E}[2\zeta_E^{\frac{1}{2}}]}{J'_{2\nu_E}[2\zeta_E^{\frac{1}{2}}]} & \zeta_E > 0 \\ \dfrac{K'_{2\nu_E}[2|\zeta_E|^{\frac{1}{2}}]}{I'_{2\nu_E}[2|\zeta_E|^{\frac{1}{2}}]} & \zeta_E < 0 \end{cases} \quad \text{as } \epsilon_M \rightarrow 0 \ .$$

Appendix C

Two Semi-infinite Membrane Point Model Neuron

C.1 Mean electrostatic potential

The solution to the differential equation for the mean electrostatic potential, Eq. (2.89), in the various regions, is given by

$$\psi(z_1) = \begin{cases} A_M & -\infty < z_1 \leq -D \\ A_I \cosh[\kappa_I z_1] + \psi_I^B & -D \leq z_1 \leq D \\ A_M & D \leq z_1 < \infty \end{cases} . \tag{C.1}$$

The constants A_M and A_I are determined by the application of the boundary conditions at the membrane walls located at $\pm D$ such that

$$A_M = \psi_I^B + \frac{4\pi\sigma_I}{\epsilon_I \kappa_I} \coth[\kappa_I D] , \tag{C.2}$$

$$A_I = \frac{4\pi\sigma_I}{\epsilon_I \kappa_I} \left[\frac{1}{\sinh[\kappa_I D]} \right] . \tag{C.3}$$

See Figure C.1. Comparison of this figure with that of the mean electrostatic potential for the two membrane point model system, Figure 3.1, shows negligible difference in the values of the potential. This shows that the membrane thickness can be considered as infinite (compared with the value of L) for the investigation of the mean electrostatic potential between the membranes.

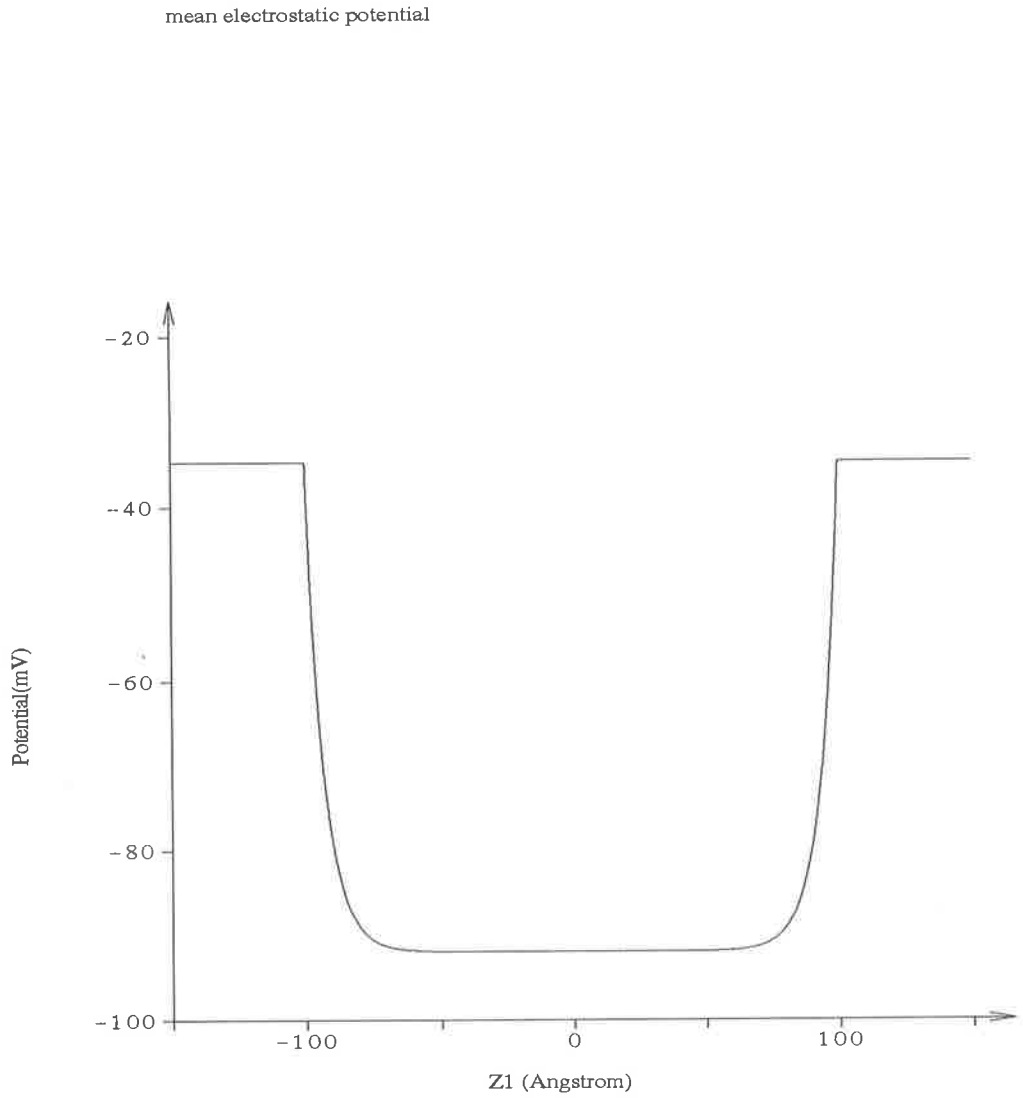

Figure C.1: Mean electrostatic potential for a two semi-infinite membrane point model system.

C.2 Transverse Hankel transform mean electrostatic fluctuation potential

The differential equations for the transverse Hankel transform mean electrostatic fluctuation potential for the two semi-infinite membrane wall system are

$$\left[\frac{d^2}{dz_1^2} - k^2\right]\tilde{\psi}_L(z_1, z_2, \mathbf{k}) = 0 \ , \tag{C.4}$$

$$\left[\frac{d^2}{dz_1^2} - k^2 - \kappa_I^2 + \kappa_I^2\zeta_I\frac{\psi_I^B}{A_I} + \frac{\kappa_I^2\zeta_I}{2}\exp[-\kappa_I z_1]\right]\tilde{\psi}_I^L(z_1, z_2, \mathbf{k}) = -\frac{4\pi}{\epsilon_I}\delta(z_1 - z_2) \ , \tag{C.5}$$

$$\left[\frac{d^2}{dz_1^2} - k^2 - \kappa_I^2 + \kappa_I^2\zeta_I\frac{\psi_I^B}{A_I} + \frac{\kappa_I^2\zeta_I}{2}\exp[\kappa_I z_1]\right]\tilde{\psi}_I^R(z_1, z_2, \mathbf{k}) = 0 \ , \tag{C.6}$$

$$\left[\frac{d^2}{dz_1^2} - k^2\right]\tilde{\psi}_R(z_1, z_2, \mathbf{k}) = 0 \ . \tag{C.7}$$

The solutions to the homogeneous differential equations are

$$\tilde{\psi}_L = C_L \exp[k(z_1 + D)] \ ,$$

$$\tilde{\psi}_I^L = \begin{cases} C_I^L J_{2\nu_I}\left[\sqrt{2}\zeta_I^{\frac{1}{2}}\exp[-\frac{\kappa_I z_1}{2}]\right] \\ +D_I^L Y_{2\nu_I}\left[\sqrt{2}\zeta_I^{\frac{1}{2}}\exp[-\frac{\kappa_I z_1}{2}]\right] & \zeta_I > 0 \\ C_I^L I_{2\nu_I}\left[\sqrt{2}\mid\zeta_I\mid^{\frac{1}{2}}\exp[-\frac{\kappa_I z_1}{2}]\right] \\ +D_I^L K_{2\nu_I}\left[\sqrt{2}\mid\zeta_I\mid^{\frac{1}{2}}\exp[-\frac{\kappa_I z_1}{2}]\right] & \zeta_I < 0 \end{cases} ,$$

$$\tilde{\psi}_I^R = \begin{cases} C_I^R J_{2\nu_I}\left[\sqrt{2}\zeta_I^{\frac{1}{2}}\exp[\frac{\kappa_I z_1}{2}]\right] \\ +D_I^R Y_{2\nu_I}\left[\sqrt{2}\zeta_I^{\frac{1}{2}}\exp[\frac{\kappa_I z_1}{2}]\right] & \zeta_I > 0 \\ C_I^R I_{2\nu_I}\left[\sqrt{2}\mid\zeta_I\mid^{\frac{1}{2}}\exp[\frac{\kappa_I z_1}{2}]\right] \\ +D_I^R K_{2\nu_I}\left[\sqrt{2}\mid\zeta_I\mid^{\frac{1}{2}}\exp[\frac{\kappa_I z_1}{2}]\right] & \zeta_I < 0 \end{cases} ,$$

$$\tilde{\psi}_R = C_R \exp[-k(z_1 - D)] \ .$$

The Green's function type of solution for the transverse Hankel transform mean electrostatic fluctuation potential is constructed in exactly the same manner as for the two membrane system with the source point in the intracellular fluid using the functions $u(z_1)$

and $v(z_1)$ as defined in Section 3.2.4. Thus the solution for the transverse Hankel transform mean electrostatic fluctuation potential is constructed in region III is of the form

$$\tilde{\psi}_I^L(z_1,z_2,\mathbf{k}) = -\frac{4\pi}{\epsilon_I}\frac{u(z_<)v(z_>)}{W(u,v)} + \frac{\tilde{\psi}_L(-D,z_2,\mathbf{k})}{v(-D)}v(z_1) + \frac{\tilde{\psi}_I^R(0,z_2,\mathbf{k})}{u(0)}u(z_1) \ . \qquad \text{(C.8)}$$

At the origin and the membrane wall located at $-D$, application of the boundary conditions yield the following set of equations

$$\begin{aligned}\epsilon_M\tilde{\psi}_L^{'}(-D,z_2,\mathbf{k}) = \ &- \ \frac{4\pi}{W(u,v)}u^{'}(-D)v(z_2) + \epsilon_I\frac{\tilde{\psi}_L(-D,z_2,\mathbf{k})}{v(-D)}v^{'}(-D) \\ &+ \ \epsilon_I\frac{\tilde{\psi}_I^R(0,z_2,\mathbf{k})}{u(0)}u^{'}(-D) \ , \qquad \text{(C.9)}\\ \epsilon_I\tilde{\psi}_I^{R'}(0,z_2,\mathbf{k}) = \ &- \ \frac{4\pi}{W(u,v)}v^{'}(0)u(z_2) + \epsilon_I\frac{\tilde{\psi}_L(-D,z_2,\mathbf{k})}{v(-D)}v^{'}(0) \\ &+ \ \epsilon_I\frac{\tilde{\psi}_I^R(0,z_2,\mathbf{k})}{u(0)}u^{'}(0) \ , \qquad \text{(C.10)}\end{aligned}$$

to solve for the constants $\tilde{\psi}_L(-D,z_2,\mathbf{k})$ and $\tilde{\psi}_I^R(0,z_2,\mathbf{k})$, to yield

$$\tilde{\psi}_L(-D,z_2,\mathbf{k}) = \frac{4\pi}{\epsilon_I W(u,v)}v(-D)u(z_2) - \sqrt{2}\kappa_I \mid \zeta_I \mid^{\frac{1}{2}} \frac{v(-D)}{v^{'}(0)}\tilde{\psi}_R^I(0,z_2,\mathbf{k}) \ ,$$

and

$$\tilde{\psi}_I^R(0,z_2,\mathbf{k}) = \begin{cases} \frac{4\pi}{\epsilon_I W(u,v)}\left[\frac{1}{\sqrt{2}\epsilon_I\kappa_I\zeta_I^{\frac{1}{2}}}\right]\frac{1}{S_{2\nu_I}J^{'}_{2\nu_I}[\sqrt{2}\zeta_I^{\frac{1}{2}}]-T_{2\nu_I}Y^{'}_{2\nu_I}[\sqrt{2}\zeta_I^{\frac{1}{2}}]} \\ \times\left\{\frac{\epsilon_I}{k\epsilon_M}u^{'}(-D)v^{'}(0)v(z_2)\right. \\ \left.-v^{'}(0)\left[S_{2\nu_I}J_{2\nu_I}[\sqrt{2}\zeta_I^{\frac{1}{2}}]-T_{2\nu_I}Y_{2\nu_I}[\sqrt{2}\zeta_I^{\frac{1}{2}}]\right]u(z_2)\right\} & \zeta_I > 0 \\ \frac{4\pi}{\epsilon_I W(u,v)}\left[\frac{1}{\sqrt{2}\epsilon_I\kappa_I|\zeta_I|^{\frac{1}{2}}}\right]\frac{1}{S_{2\nu_I}I^{'}_{2\nu_I}[\sqrt{2}|\zeta_I|^{\frac{1}{2}}]-T_{2\nu_I}K^{'}_{2\nu_I}[\sqrt{2}|\zeta_I|^{\frac{1}{2}}]} \\ \times\left\{\frac{\epsilon_I}{k\epsilon_M}u^{'}(-D)v^{'}(0)v(z_2)\right. \\ \left.-v^{'}(0)\left[S_{2\nu_I}I_{2\nu_I}[\sqrt{2}\mid\zeta_I\mid^{\frac{1}{2}}]-T_{2\nu_I}K_{2\nu_I}[\sqrt{2}\mid\zeta_I\mid^{\frac{1}{2}}]\right]u(z_2)\right\} & \zeta_I < 0 \end{cases}$$

These results for the constants $\tilde{\psi}_L(-D,z_2,\mathbf{k})$ and $\tilde{\psi}_I^R(0,z_2,\mathbf{k})$ are substituted into the the solution for the transverse Hankel transform mean electrostatic fluctuation potential in region III Eq. (C.8) and the solution can be written in the form

$$\begin{aligned}\tilde{\psi}_I^L(z_1,z_2,\mathbf{k}) = \ &- \ \frac{4\pi}{\epsilon_I}\frac{u(z_<)v(z_>)}{W(u,v)} \\ &- \ \frac{4\pi}{\epsilon_I}\frac{1}{W(u,v)}\left[\frac{1}{S_{2\nu_I}J^{'}_{2\nu_I}[\sqrt{2}\zeta_I^{\frac{1}{2}}]-T_{2\nu_I}Y^{'}_{2\nu_I}[\sqrt{2}\zeta_I^{\frac{1}{2}}]}\right]\end{aligned}$$

$$
\begin{aligned}
&\times \left\{\left[\frac{1}{\sqrt{2}\kappa_I\zeta_I^{\frac{1}{2}}k\epsilon_M}\right]\left[\frac{u'(-D)v'(0)}{u(0)}\right][u(z_1)v(z_2)+v(z_1)u(z_2)]\right.\\
&- \left[\frac{1}{\sqrt{2}\kappa_I\zeta_I^{\frac{1}{2}}}\right]\left[\frac{v'(0)}{u(0)}\right]\left[S_{2\nu_I}J_{2\nu_I}[\sqrt{2}\zeta_I^{\frac{1}{2}}]-T_{2\nu_I}Y_{2\nu_I}[\sqrt{2}\zeta_I^{\frac{1}{2}}]\right]u(z_1)u(z_2)\\
&\left.- \left[\frac{u'(-D)}{k\epsilon_M}\right]v(z_1)v(z_2)\right\} \quad \zeta_I>0\ , \qquad \text{(C.11)}
\end{aligned}
$$

and

$$
\begin{aligned}
\tilde{\psi}_I^L(z_1,z_2,\mathbf{k}) = &- \frac{4\pi}{\epsilon_I}\frac{u(z_<)v(z_>)}{W(u,v)}\\
&- \frac{4\pi}{\epsilon_I}\frac{1}{W(u,v)}\left[\frac{1}{S_{2\nu_I}I'_{2\nu_I}[\sqrt{2}\mid\zeta_I\mid^{\frac{1}{2}}]-T_{2\nu_I}K'_{2\nu_I}[\sqrt{2}\mid\zeta_I\mid^{\frac{1}{2}}]}\right]\\
&\times \left\{\left[\frac{1}{\sqrt{2}\kappa_I\mid\zeta_I\mid^{\frac{1}{2}}k\epsilon_M}\right]\left[\frac{u'(-D)v'(0)}{u(0)}\right][u(z_1)v(z_2)+v(z_1)u(z_2)]\right.\\
&- \left[\frac{1}{\sqrt{2}\kappa_I\mid\zeta_I\mid^{\frac{1}{2}}}\right]\left[\frac{v'(0)}{u(0)}\right]\\
&\times \left[S_{2\nu_I}I_{2\nu_I}[\sqrt{2}\mid\zeta_I\mid^{\frac{1}{2}}]-T_{2\nu_I}K_{2\nu_I}[\sqrt{2}\mid\zeta_I\mid^{\frac{1}{2}}]\right]u(z_1)u(z_2)\\
&\left.- \left[\frac{u'(-D)}{k\epsilon_M}\right]v(z_1)v(z_2)\right\} \quad \zeta_I<0\ , \qquad \text{(C.12)}
\end{aligned}
$$

where

$$
S_{2\nu_I}(D,\zeta_I) = \begin{cases}
Y_{2\nu_I}\left[\sqrt{2}\zeta_I^{\frac{1}{2}}\exp[\frac{\kappa_I D}{2}]\right] & \\
+\frac{\epsilon_I\kappa_I\zeta_I^{\frac{1}{2}}}{k\epsilon_M\sqrt{2}}\exp[\frac{\kappa_I D}{2}]Y'_{2\nu_I}\left[\sqrt{2}\zeta_I^{\frac{1}{2}}\exp[\frac{\kappa_I D}{2}]\right] & \zeta_I>0\\
K_{2\nu_I}\left[\sqrt{2}\mid\zeta_I\mid^{\frac{1}{2}}\exp[\frac{\kappa_I D}{2}]\right] & \\
+\frac{\epsilon_I\kappa_I\mid\zeta_I\mid^{\frac{1}{2}}}{k\epsilon_M\sqrt{2}}\exp[\frac{\kappa_I D}{2}]K'_{2\nu_I}\left[\sqrt{2}\mid\zeta_I\mid^{\frac{1}{2}}\exp[\frac{\kappa_I D}{2}]\right] & \zeta_I<0
\end{cases},
$$

$$
T_{2\nu_I}(D,\zeta_I) = \begin{cases}
J_{2\nu_I}\left[\sqrt{2}\zeta_I^{\frac{1}{2}}\exp[\frac{\kappa_I D}{2}]\right] & \\
+\frac{\epsilon_I\kappa_I\zeta_I^{\frac{1}{2}}}{k\epsilon_M\sqrt{2}}\exp[\frac{\kappa_I D}{2}]J'_{2\nu_I}\left[\sqrt{2}\zeta_I^{\frac{1}{2}}\exp[\frac{\kappa_I D}{2}]\right] & \zeta_I>0\\
I_{2\nu_I}\left[\sqrt{2}\mid\zeta_I\mid^{\frac{1}{2}}\exp[\frac{\kappa_I D}{2}]\right] & \\
+\frac{\epsilon_I\kappa_I\mid\zeta_I\mid^{\frac{1}{2}}}{k\epsilon_M\sqrt{2}}\exp[\frac{\kappa_I D}{2}]I'_{2\nu_I}\left[\sqrt{2}\mid\zeta_I\mid^{\frac{1}{2}}\exp[\frac{\kappa_I D}{2}]\right] & \zeta_I<0
\end{cases}.
$$

Appendix D

Mathematical Identities

D.1 Bessel functions

The asymptotic expansions presented below can be found in [112], [111]. The subsequent expansions in inverse powers of ν have been derived from the uniform asymptotic expansions.

D.1.1 Uniform asymptotic expansions for large order

$$J_\nu(\nu \mathrm{sech}\alpha) \approx \frac{\exp[\nu(\tanh\alpha - \alpha)]}{\sqrt{2\pi\nu\tanh\alpha}}\left[1 + \sum_{s=1}^{\infty}\frac{U_s(\coth\alpha)}{\nu^s}\right] \tag{D.1}$$

$$Y_\nu(\nu \mathrm{sech}\alpha) \approx -\frac{\exp[-\nu(\tanh\alpha - \alpha)]}{\sqrt{\frac{1}{2}\pi\nu\tanh\alpha}}\left[1 + \sum_{s=1}^{\infty}(-1)^s\frac{U_s(\coth\alpha)}{\nu^s}\right] \tag{D.2}$$

where

$$U_{s+1}(p) = \frac{1}{2}p^2(1-p^2)U_s'(p) + \frac{1}{8}\int_0^p (1-5q^2)U_s(q)dq \tag{D.3}$$

Also

$$J_\nu'(\nu \mathrm{sech}\alpha) \approx \sqrt{\frac{\sinh 2\alpha}{4\pi\nu}}\exp[\nu(\tanh\alpha - \alpha)]\left[1 + \sum_{s=1}^{\infty}\frac{V_s(\coth\alpha)}{\nu^s}\right] \tag{D.4}$$

$$Y_\nu'(\nu \mathrm{sech}\alpha) \approx \sqrt{\frac{\sinh 2\alpha}{\pi\nu}}\exp[-\nu(\tanh\alpha - \alpha)]\left[1 + \sum_{s=1}^{\infty}(-1)^s\frac{V_s(\coth\alpha)}{\nu^s}\right] \tag{D.5}$$

where

$$V_s(p) = U_s(p) - \frac{1}{2}p(1-p^2)U_{s-1}(p) - p^2(1-p^2)U_{s-1}'(p) \tag{D.6}$$

Setting $\mathrm{sech}\alpha = \frac{z}{\nu}$ and expanding the series in brackets in inverse powers of ν yields

$$1 + \sum_{s=1}^{\infty}\frac{U_s(p)}{\nu^s} = 1 - \frac{1}{12}\frac{1}{\nu} + \frac{1}{288}\frac{1}{\nu^2} + \frac{1}{\nu^3}\left[\frac{139}{51840} - \frac{z^2}{4}\right] - \frac{1}{\nu^4}\left[\frac{571}{2488320} - \frac{13}{48}z^2\right]$$

$$+ \quad O(\nu^{-5}) \tag{D.7}$$

$$1+\sum_{s=1}^{\infty}(-1)^s\frac{U_s(p)}{\nu^s} = \quad 1+\frac{1}{12}\frac{1}{\nu}+\frac{1}{288}\frac{1}{\nu^2}-\frac{1}{\nu^3}\left[\frac{139}{51840}-\frac{z^2}{4}\right]-\frac{1}{\nu^4}\left[\frac{571}{2488320}-\frac{13}{48}z^2\right]$$

$$+ \quad O(\nu^{-5}) \tag{D.8}$$

$$1+\sum_{s=1}^{\infty}\frac{V_s(p)}{\nu^s} = \quad 1-\frac{1}{12}\frac{1}{\nu}+\frac{1}{288}\frac{1}{\nu^2}+\frac{1}{\nu^3}\left[\frac{139}{51840}+\frac{z^2}{4}\right]-\frac{1}{\nu^4}\left[\frac{571}{2488320}+\frac{13}{48}z^2\right]$$

$$+ \quad O(\nu^{-5}) \tag{D.9}$$

$$1+\sum_{s=1}^{\infty}(-1)^s\frac{V_s(p)}{\nu^s} = \quad 1+\frac{1}{12}\frac{1}{\nu}+\frac{1}{288}\frac{1}{\nu^2}-\frac{1}{\nu^3}\left[\frac{139}{51840}+\frac{z^2}{4}\right]-\frac{1}{\nu^4}\left[\frac{571}{2488320}+\frac{13}{48}z^2\right]$$

$$+ \quad O(\nu^{-5}) \tag{D.10}$$

D.1.2 Small argument expansions

When ν is fixed and $z \to 0$

$$J_\nu(z) \quad \to \quad \frac{1}{\Gamma(\nu+1)}\left[\frac{z}{2}\right]^\nu \tag{D.11}$$

$$Y_\nu(z) \quad \to \quad -\frac{1}{\pi}\Gamma(\nu)\left[\frac{z}{2}\right]^{-\nu} \tag{D.12}$$

D.2 Modified Bessel functions

D.2.1 Uniform asymptotic expansions for large order

$$I_\nu(\nu z) \quad = \quad \frac{\exp[\nu\gamma]}{\sqrt{2\pi\nu}(1+z^2)^{\frac{1}{4}}}\left[1+\sum_{s=1}^{\infty}\frac{U_s(p)}{\nu^s}\right] \tag{D.13}$$

$$K_\nu(\nu z) \quad = \quad \sqrt{\frac{\pi}{2\nu}}\frac{\exp[-\nu\gamma]}{(1+z^2)^{\frac{1}{4}}}\left[1+\sum_{s=1}^{\infty}(-1)^s\frac{U_s(p)}{\nu^s}\right] \tag{D.14}$$

$$I'_\nu(\nu z) \quad = \quad (1+z^2)^{\frac{1}{4}}\frac{\exp[\nu\gamma]}{z\sqrt{2\pi\nu}}\left[1+\sum_{s=1}^{\infty}\frac{V_s(p)}{\nu^s}\right] \tag{D.15}$$

$$K'_\nu(\nu z) \quad = \quad -\sqrt{\frac{\pi}{2\nu}}\frac{(1+z^2)^{\frac{1}{4}}\exp[-\nu\gamma]}{z}\left[1+\sum_{s=1}^{\infty}(-1)^s\frac{V_s(p)}{\nu^s}\right] \tag{D.16}$$

where

$$\gamma \quad = \quad (1+z^2)^{\frac{1}{2}}+\ln\left[\frac{z}{1+(1+z^2)^{\frac{1}{2}}}\right] \tag{D.17}$$

$$p \quad = \quad (1+z^2)^{-\frac{1}{2}} \tag{D.18}$$

Setting $z \to \frac{z}{\nu}$ and expanding the series in brackets in inverse powers of ν yields

$$1+\sum_{s=1}^{\infty}\frac{U_s(p)}{\nu^s} = \quad 1-\frac{1}{12}\frac{1}{\nu}+\frac{1}{288}\frac{1}{\nu^2}+\frac{1}{\nu^3}\left[\frac{139}{51840}+\frac{z^2}{4}\right]-\frac{1}{\nu^4}\left[\frac{571}{2488320}+\frac{13}{48}z^2\right]$$

$$+ \quad O(\nu^{-5}) \tag{D.19}$$

$$1+\sum_{s=1}^{\infty}(-1)^s\frac{U_s(p)}{\nu^s} = 1+\frac{1}{12}\frac{1}{\nu}+\frac{1}{288}\frac{1}{\nu^2}-\frac{1}{\nu^3}\left[\frac{139}{51840}+\frac{z^2}{4}\right]-\frac{1}{\nu^4}\left[\frac{571}{2488320}+\frac{13}{48}z^2\right]$$
$$+ \quad O(\nu^{-5}) \tag{D.20}$$

$$1+\sum_{s=1}^{\infty}\frac{V_s(p)}{\nu^s} = 1-\frac{1}{12}\frac{1}{\nu}+\frac{1}{288}\frac{1}{\nu^2}+\frac{1}{\nu^3}\left[\frac{139}{51840}-\frac{z^2}{4}\right]-\frac{1}{\nu^4}\left[\frac{571}{2488320}-\frac{13}{48}z^2\right]$$
$$+ \quad O(\nu^{-5}) \tag{D.21}$$

$$1+\sum_{s=1}^{\infty}(-1)^s\frac{V_s(p)}{\nu^s} = 1+\frac{1}{12}\frac{1}{\nu}+\frac{1}{288}\frac{1}{\nu^2}-\frac{1}{\nu^3}\left[\frac{139}{51840}-\frac{z^2}{4}\right]-\frac{1}{\nu^4}\left[\frac{571}{2488320}-\frac{13}{48}z^2\right]$$
$$+ \quad O(\nu^{-5}) \tag{D.22}$$

D.2.2 Small argument expansions

When ν is fixed and $z \to 0$

$$I_\nu(z) \;\to\; \frac{1}{\Gamma(\nu+1)}\left[\frac{z}{2}\right]^\nu \tag{D.23}$$

$$K_\nu(z) \;\to\; \frac{1}{2}\Gamma(\nu)\left[\frac{z}{2}\right]^{-\nu} \tag{D.24}$$

D.3 Bessel integrals

$$\begin{aligned}\int d^3k\frac{e^{i\mathbf{k}\cdot\mathbf{r}}}{k^2+\alpha^2} &= \int_0^{2\pi}d\phi\int_0^{\pi}d\theta\,\theta\int_0^{\infty}dk\,k^2\,\frac{e^{ikr\cos\theta}}{k^2+\alpha^2}\\ &= 2\pi^2\frac{e^{-\alpha\sqrt{\rho^2+z^2}}}{\sqrt{\rho^2+z^2}}\\ &= \int_0^{2\pi}d\theta\int_0^{\infty}dk\,k\int_{-\infty}^{\infty}dk_3\,\frac{e^{i\beta k_3}e^{ik\rho\cos\theta}}{k_3^2+k^2+\alpha^2}\\ &= 2\pi^2\int_0^{\infty}dk k J_0(k\rho)\,\frac{e^{-z\sqrt{k^2+\alpha^2}}}{\sqrt{k^2+\alpha^2}}\end{aligned} \tag{D.25}$$

where

$$r=\sqrt{\rho^2+z^2}$$

D.4 Exponential integral

D.4.1 Definition

$$\begin{aligned}E_n(z) &= \int_1^{\infty}dt\,\frac{e^{-zt}}{t^n}\\ &= z^{n-1}\int_z^{\infty}dx\,\frac{e^{-x}}{x^n}\end{aligned} \tag{D.26}$$

D.4.2 Asymptotic expansion

$$E_n(z) \approx \frac{e^{-z}}{z}\left[1 - \frac{n}{z} + \frac{n(n+1)}{z^2} - \frac{n(n+1)(n+2)}{z^3} + \ldots\right] \tag{D.27}$$

D.5 Hydration integrals

Debye-Huckel term

$$\begin{aligned}
&\int_{min}^{max} d\mathbf{x}_2\,(z_2 - z_1)\,e^{\kappa_E(z_2+L)}\,\frac{e^{-\kappa_E\nu_E(0)r}}{r}\,\left[\frac{1}{r}\right]^n \\
= \quad & 2\pi\int_{z_1-z_{max}}^{z_1+z_{max}} dz_2\,(z_2 - z_1)\,e^{\kappa_E(z_2+L)} \\
\times \quad & \int_{\rho_{min}}^{\rho_{max}} d\rho_2\,\rho_2\,\frac{e^{-\kappa_E\nu_E(0)\sqrt{\rho_2^2+(z_2-z_1)^2}}}{\sqrt{\rho_2^2+(z_2-z_1)^2}}\left[\frac{1}{\sqrt{\rho_2^2+(z_2-z_1)^2}}\right]^n \\
= \quad & 2\pi[\kappa_E\nu_E(0)]^{n-1}\int_{z_1-z_{max}}^{z_1+z_{max}} dz_2\,(z_2 - z_1)\,e^{\kappa_E(z_2+L)} \\
\times \quad & \int_{\kappa_E\nu_E(0)\sqrt{\rho_{min}^2+(z_2-z_1)^2}}^{\kappa_E\nu_E(0)\sqrt{\rho_{max}^2+(z_2-z_1)^2}} dx\,\frac{e^{-x}}{x^n} \\
= \quad & 2\pi[\kappa_E\nu_E(0)]^{n-1}\int_{z_1-z_{max}}^{z_1+z_{max}} dz_2\,(z_2 - z_1)\,e^{\kappa_E(z_2+L)} \\
\times \quad & \left\{\frac{E_n\left(\kappa_E\nu_E(0)\sqrt{\rho_{min}^2+(z_2-z_1)^2}\right)}{\left[\sqrt{\rho_{min}^2+(z_2-z_1)^2}\right]^{n-1}} - \frac{E_n\left(\kappa_E\nu_E(0)\sqrt{\rho_{max}^2+(z_2-z_1)^2}\right)}{\left[\sqrt{\rho_{max}^2+(z_2-z_1)^2}\right]^{n-1}}\right\},
\end{aligned} \tag{D.28}$$

and the image term

$$\begin{aligned}
&\int_{min}^{max} d\mathbf{x}_2\,(z_2 + z_1 + 2L)\,e^{\kappa_E(z_2+L)}\,\frac{e^{-\kappa_E\nu_E(0)r^*}}{r^*}\,\left[\frac{1}{r^*}\right]^n \\
= \quad & 2\pi[\kappa_E\nu_E(0)]^{n-1}\int_{z_1-z_{max}}^{z_1+z_{max}} dz_2\,(z_2 + z_1 + 2L)\,e^{\kappa_E(z_2+L)} \\
\times \quad & \left\{\frac{E_n\left(\kappa_E\nu_E(0)\sqrt{\rho_{min}^2+(z_2+z_1+2L)^2}\right)}{\left[\sqrt{\rho_{min}^2+(z_2+z_1+2L)^2}\right]^{n-1}}\right. \\
& \left. - \frac{E_n\left(\kappa_E\nu_E(0)\sqrt{\rho_{max}^2+(z_2+z_1+2L)^2}\right)}{\left[\sqrt{\rho_{max}^2+(z_2+z_1+2L)^2}\right]^{n-1}}\right\}.
\end{aligned} \tag{D.29}$$

Substitution of the asymptotic expansion for $E_n(z)$, into these expressions such that the Debye-Huckel term has integrals of the form

$$2\pi[\kappa_E\nu_E(0)]^{n-1}\int_{z_1-z_{max}}^{z_1+z_{max}} dz_2\,(z_2 - z_1)\,e^{\kappa_E(z_2+L)}$$

$$\times \quad \frac{e^{-\kappa_E \nu_E(0)\sqrt{\rho^2+(z_2-z_1)^2}}}{\sqrt{\rho^2+(z_2-z_1)^2}} \left[\frac{1}{\sqrt{\rho^2+(z_2-z_1)^2}}\right]^m$$

$$= \quad 2\pi[\kappa_E \nu_E(0)]^{n-1} e^{\kappa_E(z_1+L)} \int_{-z_{max}}^{z_{max}} dy\, y\, e^{\kappa_E y}$$

$$\times \quad \frac{e^{-\kappa_E \nu_E(0)\sqrt{\rho^2+y^2}}}{\sqrt{\rho^2+y^2}} \left[\frac{1}{\sqrt{\rho^2+y^2}}\right]^m ,$$

and the image term

$$2\pi[\kappa_E \nu_E(0)]^{n-1} \int_{z_1-z_{max}}^{z_1+z_{max}} dz_2\, (z_2-z_1)\, e^{\kappa_E(z_2+L)}$$

$$\times \quad \frac{e^{-\kappa_E \nu_E(0)\sqrt{\rho^2+(z_2+z_1+2L)^2}}}{\sqrt{\rho^2+(z_2+z_1+2L)^2}} \left[\frac{1}{\sqrt{\rho^2+(z_2+z_1+2L)^2}}\right]^m$$

$$= \quad 2\pi[\kappa_E \nu_E(0)]^{n-1} e^{-\kappa_E(z_1+L)} \int_{2z_1-z_{max}+2L}^{2z_1+z_{max}+2L} dy\, y\, e^{\kappa_E y}$$

$$\times \quad \frac{e^{-\kappa_E \nu_E(0)\sqrt{\rho^2+y^2}}}{\sqrt{\rho^2+y^2}} \left[\frac{1}{\sqrt{\rho^2+y^2}}\right]^m .$$

Bibliography

[1] A. Guyton. *Textbook of Medical Physiology.* W.B. Saunders, Philadelphia, 1991.

[2] S.W. Kuffler, J.G. Nicholls, and A.R. Martin. *From Neuron to Brain.* Sinauer Associates, Sunderland,Mass., 1984.

[3] S. McLaughlin. The electrostatics properties of membranes. *Ann. Rev. of Biophysics and Biophysical Chem.*, 18:113, 1989.

[4] S. McLaughlin. Electrostatic potentials at membrane-solution interfaces. In F. Bronner and A. Kleinseller, editors, *Current Topics in Membranes and Transport Vol 9.* Academic Press, 1977.

[5] M.C. Mackey. Ion transport through biological membranes. In S. Levin, editor, *Lecture Notes in Biomathematics Vol 7.* Springer-Verlag, 1975.

[6] B. Hille. *Ionic Channels of Excitable Membranes.* Sinauer Associates Inc, Massachusetts, 1984.

[7] B.E. Conway. *Ionic Hydration in Chemistry and Biophysics.* Elsevier Scientific Pub. Co., Amsterdam, 1981.

[8] A.L. Hodgkin and A.F. Huxley. Currents carried by sodium and potassium ions through the membrane of the giant axon of *loligo. J. Physiol.*, 116:449, 1952.

[9] A.L. Hodgkin and A.F. Huxley. The components of the membrane conductance in the giant axon of *loligo. J. Physiol.*, 116:473, 1952.

[10] A.L. Hodgkin and A.F. Huxley. The dual effect of membrane potential on sodium conductance in the giant axon of *loligo. J. Physiol.*, 116:497, 1952.

[11] A.L. Hodgkin and A.F. Huxley. A quantitative description of membrane current and its application to conduction and excitation in nerves. *J. Physiol.*, 117:500, 1952.

[12] H.S. Green and T. Triffet. Extracellular fields within the cortex. *J. Theor. Biol.*, 115:43, 1985.

[13] T. Triffet and H.S. Green. Calcium dynamics at a plastic synapse in *aplysia*. *J. Theor. Biol.*, 100:645, 1983.

[14] H.S. Green and T. Triffet. Ionic currents in the Debye layers of the neural membrane and their relation to elementary learning processes. *Math. Modelling*, 3:161, 1982.

[15] H.S. Green and T. Triffet. Non-linear ion dynamics and the application to neurophysiology. In A.R. Bednarek and L. Cesari, editors, *Dynamical Systems II.* Academic Press, 1982.

[16] H.S. Green and T. Triffet. Mathematical modelling of nervous systems. *Math. Modelling*, 1:41, 1980.

[17] T. Triffet and H.S. Green. Information and energy flow in a simple nervous system. *J. Theor. Biol.*, 86:3, 1980.

[18] T. Triffet and H.S. Green. I. An electrochemical model of the brain: General theory and the single neuron. *J. Biol. Phys.*, 3:53, 1975.

[19] H.S. Green and T. Triffet. II. An electrochemical model of the brain: Collective behaviour, irreversibility and information. *J. Biol. Phys.*, 3:77, 1975.

[20] S. Vaccaro and H.S. Green. Ionic processes in excitable membranes. *J. Theor. Biol.*, 81:771, 1979.

[21] S.R. Vaccaro. *Ion Transport through Excitable Membranes.* PhD thesis, University of Adelaide, Australia, 1979.

[22] J.F. Sherwood and T. Triffet. Synaptic connectivity in a dynamical brain model. In X.J.R. Avula, editor, *First International Conference on Mathematical Modeling Vol. II.* University of Missouri-Rolla, 1977.

[23] D. Agin. Some comments on the Hodgkin-Huxley equations. *J. Theo. Biol.*, 5:161, 1963.

[24] V.S. Vaidhyanathan and H.M. Phillips. Molecular theory of nerve potentials. *J. Theo. Biol.*, 21:331, 1968.

[25] D. Agin. Electroneutrality and electrodiffusion in the squid axon. *Proc. Nat. Acad. Sci.*, 57:1232, 1967.

[26] R.A. Arndt, J.D. Bond, and L.D. Roper. Electroneutral approximate solutions of steady-state electrodiffusion equations for a simple membrane. *J. Theo. Biol.*, 34:265, 1972.

[27] K.S. Cole. *Membranes, Ions and Impulses.* Uni. California Press, Berkeley, 1968.

[28] R.J. Hunter. *Foundations of Colloid Science. Vol. 1.* Oxford University Press, Oxford, 1987.

[29] G.A. Martynov and R.R. Salem. The dense part of the electrical double layer: Molecular or electronic capacitor? *Adv. Colloid Interface Sci.*, 22:229, 1985.

[30] G.A. Martynov and R.R. Salem. Electrical double layer at a metal-dilute electrolyte solution interface. In G. Berthier, M.J.S. Dewar, and et al, editors, *Lecture Notes in Chemistry Vol 33.* Springer-Verlag, 1983.

[31] J.O'M Bockris and A.K.N. Reddy. *Modern Electrochemistry Vol 2.* Plenum Press, New York, 1970.

[32] H.L. von Helmholtz. *Weid. Ann.*, 7:337, 1879.

[33] M Gouy. Constitution of the electric charge at the surface of an electrolyte. *J. Phys.(Paris)*, 9:457, 1910.

[34] D.L. Chapman. A contribution to the theory of electrocapillarity. *Phil. Mag.*, 25:475, 1913.

[35] P. Debye and E. Huckel. *Phys. Zeits.*, 24:185, 1923.

[36] C. Wagner. The surface tension of dilute solutions of electrolytes. *Phys. Z.*, 25:474, 1924.

[37] L Onsager and N.N.T. Samaras. The surface tension of Debye-Huckel electrolytes. *J. Chem. Phys.*, 2:528, 1934.

[38] O. Stern. *Z. Elektrochem.*, 30:508, 1924.

[39] D.C. Grahame. The electrical double layer and the theory of electrocapillarity. *Chem. Rev.*, 41:441, 1947.

[40] F.P. Buff and F.H. Stillinger. Surface tension of ionic solutions. *J. Chem. Phys.*, 25:312, 1956.

[41] S.L. Carnie and G.M. Torrie. The statistical mechanics of the electrical double layer. *Adv. Chem. Phys.*, 56:141, 1984.

[42] B. Jancovici. Classical Coulomb systems near a plane wall. I. *J. Stat. Phys.*, 28:43, 1982.

[43] B. Jancovici. Classical Coulomb systems near a plane wall. II. *J. Stat. Phys.*, 29:263, 1982.

[44] G.M. Torrie and J.P. Valleau. Electrical Double Layers. I. Monte Carlo study of an uniformly charged surface. *J. Chem. Phys.*, 73:5807, 1980.

[45] G.M. Torrie, J.P. Valleau, and G.N. Patey. Electrical Double Layers. II. Monte Carlo and HNC studies of image effects. *J. Chem. Phys.*, 76:4615, 1982.

[46] S.W. DeLeeuw, J.W. Perram, and E.R. Smih. Computer simulation of the static dielectric constant of systems with permanent electric dipoles. *Ann. Rev. Phys. Chem.*, 37:245, 1986.

[47] J.M. Caillol, D. Levesque, and J.J. Weis. Monte Carlo simulation of an ion-dipole mixture: A convergence study. *Mol. Phys.*, 69:199, 1990.

[48] J.M. Caillol, D. Levesque, J.J. Weis, P.G. Kusalik, and G.N. Patey. A comparison between computer simulations and theoretical results for ionic solutions. *Mol. Phys.*, 62:461, 1987.

[49] C.G. Gray and K.E. Gubbins. *Theory of Molecular Fluids Vol. 1.* Oxford Press, New York, 1984.

[50] P. Fries and G.N. Patey. The solution of the HNC approximation for fluids of non-spherical particles.A general method with application to dipolar hard-spheres. *J. Chem. Phys.*, 82:492, 1985.

[51] L.S. Ornstein and F. Zernicke. Accidental deviations of density and opalescence at the critical point of a single substance. *Proc. Acad. Sci. Amst.*, 17:793, 1914.

[52] N.N. Bogolyubov. *J. Phys. URSS*, 10:257, 1946.

[53] M. Born and H.S. Green. A general kinetic theory of liquids I: The molecular distribution functions. *Proc. Roy. Soc. London A*, 188:10, 1946.

[54] J.G. Kirkwood. Statistical mechanics of fluid mixtures. *J. Chem. Phys.*, 3:300, 1935.

[55] J. Yvon. La Theorie Statistique des Fluides et l'equation d'Etat. *Actualities Scientifique et Industrielles*, 203, 1935.

[56] S.L. Carnie. Hypernetted-chain theories of the primitive model double layer theory. A last look at binary symmetric electrolytes. *Mol. Phys.*, 54:509, 1985.

[57] R. Kjellander and S. Marcelja. Correlation and image charge effects in electrical double layers. *Chem. Phys. Lett.*, 112:49, 1984. Errata. ibid., 114:124, 1985.

[58] R. Kjellander and S. Marcelja. Inhomogeneous Coulomb fluids with image interactions between planar surfaces. I. *J. Chem. Phys.*, 82:2122, 1985.

[59] R. Kjellander and S. Marcelja. Interaction of charged surfaces in electrolyte solutions. *Chem. Phys. Lett.*, 127:402, 1986.

[60] R. Kjellander and S. Marcelja. Double layer interaction in the primitive model and the corresponding Poisson-Boltzmann description. *J. Phys. Chem.*, 90:1230, 1986.

[61] R. Kjellander and S. Marcelja. Electolyte solutions between uncharged walls. *Chem. Phys. Lett.*, 142:485, 1987.

[62] R. Kjellander. Inhomogeneous Coulomb fluids with image interactions between planar surfaces. II. On the anisotropic hypernetted chain approximation. *J. Chem. Phys.*, 88:7129, 1988.

[63] R. Kjellander and S. Marcelja. Inhomogeneous Coulomb fluids with image interactions between planar surfaces. III. Distribution functions. *J. Chem. Phys.*, 88:7138, 1988.

[64] T.L. Croxton and D.A. McQuarrie. Numerical solution of the BGY equation for the restricted primitive model of ionic solutions. *J. Phys. Chem.*, 83:1840, 1979.

[65] T.L. Croxton and D.A. McQuarrie. A theory of the electrical double layer through the BGY equation. *Chem. Phys. Lett.*, 68:489, 1979.

[66] S. Levine and C.W. Outhwaite. Comparison of theories of the aqueous electric double layer at a charged plane interface. *J. Chem. Soc. Faraday Trans. II*, 74:1670, 1978.

[67] L.B. Bhuiyan, C.W. Outhwaite, and S. Levine. Numerical solution of a modified Poisson-Boltzmann equation in electrical double layer theory. *Chem. Phys. Lett.*, 66:321, 1979.

[68] C.W. Outhwaite, L.B. Bhuiyan, and S. Levine. Theory of the electrical double layer using a modified Poisson Boltzmann equation. *J. Chem. Soc. Faraday Trans. II*, 76:1388, 1980.

[69] S. Levine, C.W. Outhwaite, and L.B. Bhuiyan. Statistical mechanical theories of the electrical double layer. *J. Electroanal. Chem.*, 123:105, 1981.

[70] L.B. Bhuiyan, C.W. Outhwaite, and S. Levine. Numerical solution of a modified Poisson-Boltzmann equation for 1 : 2 and 2 : 1 electrolytes in the diffuse layer. *Mol. Phys.*, 42:1271, 1981.

[71] C.W. Outhwaite, L.B. Bhuiyan, and S. Levine. Variation of the diffuse layer potential drop with surface charge in the modified Poisson-Boltzmann theory. *Chem. Phys. Lett.*, 78:413, 1981.

[72] C.W. Outhwaite and L.B. Bhuiyan. A further treatment of the exclusion volume term in the modified Poisson Boltzmann theory of the electrical double layer. *J. Chem. Soc. Faraday Trans. II*, 78:775, 1982.

[73] C.W. Outhwaite and L.B. Bhuiyan. An improved modified Poisson Boltzmann equation in electrical double layer theory. *J. Chem. Soc. Faraday Trans. II*, 79:707, 1983.

[74] S.L. Carnie and D.Y.C. Chan. Correlations in inhomogeneous coulomb systems. *Mol. Phys.*, 51:1047, 1984.

[75] C.W. Outhwaite. Modified Poisson-Boltzmann equation in electric double layer theory based on the Bogoliubov-Born-Green-Yvon intergral equations. *J. Chem. Soc. Faraday Trans. II*, 74:1214, 1978.

[76] J.W. Perram and M.N. Barber. Coulomb Green's functions at diffuse interfaces. *Mol. Phys.*, 28:131, 1974.

[77] F.P. Buff and N.S. Goel. Electrostatics of diffuse anisotropic interfaces. I. Planar layer model. *J. Chem. Phys.*, 51:4983, 1969.

[78] F.P. Buff and N.S. Goel. Electrostatics of diffuse anisotropic interfaces. II. Effects of long-range diffuseness. *J. Chem. Phys.*, 51:5363, 1969.

[79] F.P. Buff and N.S. Goel. Image potentials for multipoles embedded in a cavity and their applications to the surface tension of aqueous solutions of amino acids. *J. Chem. Phys.*, 56:2405, 1972.

[80] J.R. Clay. Electrostatics of diffuse anisotropic interfaces. III. Point charge and dipole image potentials for air-water and metal-water interfaces. *J. Chem. Phys.*, 56:4245, 1972.

[81] L. Blum. Structure of the electrical double layer. *Adv. Chem. Phys.*, 78:171, 1990.

[82] S. Trasatti. In J.O'M Bockris and B.E. Conway, editors, *Modern Aspects of Electrochemistry Vol 13.* Plenum Press, 1979.

[83] W.R. Fawcett. Molecular models for solvent structure at polarizable interfaces. *Isr. J. Chem.*, 18:3, 1979.

[84] J.C. Rasaiah, D.J. Isbister, and G. Stell. Nonlinear effects in polar fluids: A molecular theory of electrostriction. *J. Chem. Phys.*, 75:4707, 1981.

[85] J.C. Rasaiah, D.J. Isbister, and G. Stell. Electrostriction and dipolar ordering at an electrified wall. *Chem. Phys. Lett.*, 79:189, 1981.

[86] D.J. Isbister and B.C. Freasier. Adsorption of dipolar hard-spheres onto a smooth, hard wall in the presence of an electric field. *J. Stat. Phys.*, 20:331, 1979.

[87] J.M. Eggebrecht, D.J. Isbister, and J.C. Rasaiah. The adsorption of dipoles at a wall in the presence of an electric field: The RLHNC approximation. *J. Chem. Phys.*, 73:3980, 1980.

[88] G.M. Torrie, P.G. Kusalik, and G.N. Patey. Molecular solvent model for an electrical double layer: Reference Hypernetted-Chain RHNC results for solvent structure at a charged surface. *J. Chem. Phys.*, 88:7826, 1988.

[89] G.M. Torrie, P.G. Kusalik, and G.N. Patey. Molecular solvent model for an electrical double layer: Reference Hypernetted-Chain Results for ion behaviour at infinite dilution. *J. Chem. Phys.*, 89:3285, 1988.

[90] G.M. Torrie, P.G. Kusalik, and G.N. Patey. Molecular solvent model for an electrical double layer: Reference Hypernetted Chain results for potassium chloride solutions. *J. Chem. Phys.*, 90:4513, 1989.

[91] G.M. Torrie, P.G. Kusalik, and G.N. Patey. Theory of the electrical double layer: Ion size effects in a molecular solvent. *J. Chem. Phys.*, 91:6368, 1989.

[92] C.W. Outhwaite. The electric double layer capacitance for a hard sphere ion-dipole electrolyte in the mean field approximation. *Chem. Phys. Lett.*, 76:619, 1980.

[93] C.W. Outhwaite. A preliminary treatment of solute and solvent interactions in the diffuse part of the electrical double layer. *Can. J. Chem*, 59:1854, 1981.

[94] C.W. Outhwaite. Towards a mean electrostatic potential treatment of an ion-dipole mixture or a dipolar system next to a plane wall. *Mol. Phys.*, 48:599, 1983.

[95] C.W. Outhwaite. Image effects for point ions in a molecular solvent next to a plane wall. *Mol. Phys.*, 63:77, 1988.

[96] J.O'M Bockris and A.K.N. Reddy. *Modern Electrochemistry Vol 1.* Plenum Press, New York, 1970.

[97] A.M. Azzam. *Can. J. Chem.*, 38:933, 1960.

[98] D.Y.C. Chan, D.J. Mitchell, and B.W. Ninham. A model of solvent structure around ions. *J. Chem. Phys.*, 70:2946, 1979.

[99] S.L. Carnie and D.Y.C. Chan. The structure of electrolytes at charged surfaces :Ion-dipole mixtures. *J. Chem. Phys.*, 73:2949, 1980.

[100] I. Stakgold. *Green's Functions and Boundary Value Problems.* Wiley Interscience, New York, 1979.

[101] R.G. Storer. *Irreversible Processes in Fluids and Plasmas.* PhD thesis, University of Adelaide, Australia, 1963.

[102] H.S. Green and R.B. Leipnik. *Sources of Plasma Physics Vol 1.* Wolters-Noordhoff, Groningen, 1970.

[103] E.P. Wigner. *Phys. Rev.*, 40:789, 1932.

[104] J.K. Percus. The pair distribution function in classical statistical mechanics. In H.L. Frisch and J.L. Lebowitz, editors, *The Equilibrium Theory of Classical Fluids.* Benjamin Press, New York, 1964.

[105] J.P. Hansen and I.R. McDonald. *Theory of Simple Liquids.* Academic Press, London, 1976.

[106] S. Sarman. *Correlation Functions and Solvation Forces in Thin Liquid Films.* PhD thesis, Royal Institute of Technology, Sweden, 1990.

[107] A.L. Loeb. An interionic attraction theory applied to the diffuse double layer around colloid particles. *J. Colloid Sci.*, 6:75, 1951.

[108] B. Davies. *Integral Transforms and their Applications.* Springer Verlag, New York, 1978.

[109] J.D. Jackson. *Classical Electrodynamics.* John Wiley and Sons, New York, 1975.

[110] N.W. McLachlan. *Theory and Application of Mathieu Functions.* Oxford University Press, London, 1947.

[111] M. Abramowitz and I.A. Stegun. *Handbook of Mathematical Functions.* Dover, New York, 1970.

[112] G.N. Watson. *A Treatise on the Theory of Bessel functions.* Cambridge, Cambridge, 1922.

[113] R. Newton. *Scattering Theory of Waves and Particles.* McGraw-Hill, New York, 1966.

[114] W.H. Press, B.P. Flannery, S.A. Teukolsky, and W.T. Vetterling. *Numerical Recipes.* Cambridge University Press, Cambridge, 1989.